2007

Channel, spectrum, and waveform awareness in OFDM-based cognitive radio systems

Tevfik Yücek
University of South Florida

Channel, Spectrum, and Waveform Awareness in OFDM-Based Cognitive Radio Systems

by

Tevfik Yücek

A dissertation submitted in partial fulfillment
of the requirements for the degree of
Doctor of Philosophy
Department of Electrical Engineering
College of Engineering
University of South Florida

Major Professor: Hüseyin Arslan, Ph.D.
Havish Koorapaty, Ph.D.
Miguel A. Labrador, Ph.D.
Wilfrido A. Moreno Ph.D.
Thomas M. Weller, Ph.D.

Date of Approval:
July 16, 2007

Keywords: Wireless communications, multi-carrier transmission, spectrum sensing, adaptation, parameter estimation

DEDICATION

To my parents and grand parents.

ACKNOWLEDGEMENTS

The foremost, I would like to thank my advisor, Dr. Hüseyin Arslan for his guidance and encouragement throughout the course of this dissertation. Learning from him has been a very fruitful and enjoyable experience. The discussions we had concerning the research often led to new ideas, taking research to new directions with successful results.

I wish to thank Dr. Havish Koorapaty, Dr. Miguel A. Labrador, Dr. Wilfrido A. Moreno, and Dr. Thomas M. Weller for serving in my committee, for their valuable time, feedback and suggestions; and to Dr. Dmitry B. Goldgof for chairing my defense. Dr. Paris Wiley, Dr. Elias K. Stefanakos, Gayla Montgomery, Irene Wiley, Maria Du, Becky Brenner, and Norma Paz from the Electrical Engineering administration and staff definitely deserve many thanks for helping out in numerous issues over the past years.

I owe a lot to the people of Logus Broadband Wireless Solutions Inc. who financially supported my work for the majority of Ph.D. duration. I've also spent two summer semesters during my Ph.D. as an intern at Logus. I would especially like to thank to Francis E. Retnasothie for providing me the opportunity to work at Logus on some real research projects. I enjoyed working with Logus team.

I would like to thank a lot to my colleagues at USF. I am grateful to my roommate Dr. İsmail Güvenç with whom I stayed with for the first two years of my Ph.D., and to my friends at wireless communications and signal processing (WCSP) group; Hasari Çelebi, Serhan Yarkan, Hisham A. Mahmoud, Mustafa E. Şahin, Sadia Ahmed, Kemal Özdemir and others. We shared many things together, including long group meetings, conference travels, and fruitful discussions; I wish all of you the best in your future careers and lives.

My deepest gratitude goes to my wife for her encouragement and patience. You were there to share joys and disappointments, and to provide hope and motivation at times I started losing them. I know that it was very difficult to be the wife of a Ph.D. student, and I will always remember your understanding and support.

Last but by no means least, I would like to thank my parents and to my dear grand parents, for whom this dissertation is dedicated, for their continued support, encouragement and sacrifice throughout the years, and I will be forever indebted to them for all that they have done.

TABLE OF CONTENTS

LIST OF TABLES

LIST OF FIGURES

CHANNEL, SPECTRUM, AND WAVEFORM AWARENESS IN OFDM-BASED COGNITIVE RADIO SYSTEMS

Tevfik Yücek

ABSTRACT

The radio spectrum is becoming increasingly congested everyday with emerging technologies and with the increasing number of wireless devices. Considering the limited bandwidth availability, accommodating the demand for higher capacity and data rates is a challenging task, requiring innovative technologies that can offer new ways of exploiting the available radio spectrum. *Cognitive radio* arises to be a tempting solution to the spectral crowding problem by introducing the notion of opportunistic spectrum usage. Because of its attractive features, orthogonal frequency division multiplexing (OFDM) has been successfully used in numerous wireless standards and technologies. We believe that OFDM will play an important role in realizing the cognitive radio concept as well by providing a proven, scalable, and adaptive technology for air interface.

The goal of this dissertation is to identify and address some of the challenges that arise from the introduction of cognitive radio. Specifically, we propose methods for obtaining awareness about channel, spectrum, and waveform in OFDM-based cognitive radio systems in this dissertation. Parameter estimation for enabling adaptation, spectrum sensing, and OFDM system identification are the three main topics discussed.

OFDM technique is investigated as a candidate for cognitive radio systems. Cognitive radio features and requirements are discussed in detail, and OFDM's ability to satisfy these requirements is explained. In addition, we identify the challenges that arise from employing OFDM technology in cognitive radio. Algorithms for estimating various channel related parameters are presented. These parameters are vital for enabling adaptive system design, which is a key requirement for cognitive radio. We develop methods for estimating root-mean-square (RMS) delay spread, Doppler spread, and noise variance. The spectrum opportunity and spectrum sensing concepts are re-evaluated by

considering different dimensions of the spectrum which is known as multi-dimensional spectrum space. Spectrum sensing problem in a multi-dimensional space is addressed by developing a new sensing algorithm termed as partial match filtering (PMF). Cognitive radios are expected to recognize different wireless networks and have capability of communicating with them. Algorithms for identification of multi-carrier transmissions are developed. Within the same work, methods for blindly detecting transmission parameters of an OFDM based system are developed. Blind detection is also very helpful in reducing system signaling overhead in the case of adaptive transmission where transmission parameters are changed depending on the environmental characteristics or spectrum availability.

CHAPTER 1

INTRODUCTION

As wireless communication systems are making the transition from wireless telephony to interactive Internet data and multi-media types of applications, the desire for higher data rate transmission is increasing tremendously. As more and more devices go wireless, future technologies will face spectral crowding and coexistence of wireless devices will be a major issue. Considering the limited bandwidth availability, accommodating the demand for higher capacity and data rates is a challenging task, requiring innovative technologies that can offer new ways of exploiting the available radio spectrum.[1] *Cognitive radio* offers a solution to the spectral crowding problem by introducing the opportunistic usage of frequency bands that are not heavily occupied by licensed users [3]. It is a new concept in wireless communications which aims to have more adaptive and aware communication devices which can make better use of available natural resources [4].

Even though there is no agreement on the formal definition, and hence capabilities, of cognitive radio as of now, the concept has evolved recently to include various meanings in several contexts [5]. One main aspect of it is related to autonomously exploiting locally unused spectrum to provide new paths to spectrum access. Other aspects include interoperability across several networks; roaming across borders while being able to stay in compliance with local regulations; adapting the system, transmission, and reception parameters without user intervention; and having the ability to understand and follow actions and choices taken by their users to become more responsive over time. Cognitive radios can be used as a secondary system on top of current allocation of users which are called primary (or licensed) users. In this case, secondary (cognitive) users need to detect the unused spectrum in order to be able to exploit it. Moreover, the radio should be able to shape its waveform so as to exploit only the unused part of the spectrum.

[1] The term "spectrum" refers to the multi-dimensional radio space in this dissertation and it should not be confused with the general term that only refers to the frequency dimension. A more detailed definition for this term is presented in Chapter 6.

In order to understand the importance of cognitive radio technology within the wireless research community, it is sufficient to have a look at the conferences and special issues organized on cognitive radio. Within the last couple of years, there have been numerous conferences specifically on cognitive radio and dynamic spectrum access,[2] not to mention the various workshops and sessions on cognitive radio in many communications related conferences. Moreover, many of the prestigious journals have prepared special issues on cognitive radio.[3] There have also been standardization activities for cognitive radio: IEEE 802.22 and IEEE Standards Coordinating Committee 41[4] (Dynamic Spectrum Access Networks), and 4 books have been published (or are in press) on cognitive radio only within the last two years. These facts underline the significant interest of the wireless research community in cognitive radio technology.

In this introductory chapter, a brief introduction to orthogonal frequency division multiplexing (OFDM) technology is given and OFDM based cognitive radio is explained. Then, an outline of the dissertation is presented.

1.1 OFDM Technology

OFDM is a multicarrier modulation technique that can overcome many problems that arise from high bit rate communications, the biggest of which is time dispersion. In OFDM, carrier frequencies are chosen in such a way that there is no influence of other carriers when detecting the information in a particular carrier as long as the orthogonality between the carriers is maintained. The data bearing symbol stream is split into several lower rate streams and these streams are transmitted on different carriers. Since this splitting increases the symbol period by the number of non-overlapping carriers (subcarriers), multipath echoes affect only a small portion of the neighboring symbols. Remaining inter-symbol interference (ISI) is removed by cyclically extending the OFDM symbol. The length of the cyclic extension should be at least as long as the maximum excess delay (MED) of the channel. This way, OFDM reduces the effect of multipath channels encountered with high data

[2]To count few; IEEE Dynamic Spectrum Access Networks Conference DySPAN (November 2005, April 2007), International Conference on Cognitive Radio Oriented Wireless Networks and Communications (June 2007, July 2008), and so on.

[3]To count few; IEEE Journal on Selected Areas in Communications Special Issue on Adaptive, Spectrum Agile and Cognitive Wireless Networks (February 2006), Wireless Communications and Mobile Computing Journal: Special Issue on Cognitive Radio, Software Defined Radio, and Adaptive Wireless System (May 2006), IEEE Communications Magazine Feature Topic on Cognitive Radios for Dynamic Spectrum Access (October 2006), Special Issue of Elsevier Computer Networks on Cognitive Wireless Networks (December 2006), Special Issue of IEEE Journal on Selected Areas in Communications on Cognitive Radio, Theory and Applications (March 2007), The European Association for Signal Processing (EURASIP) Journal on Wireless Communications and Networking Special Issue on Cognitive Radio and Dynamic Spectrum Sharing Systems (June 2007), and so on.

[4]Formerly IEEE 1900 Standards Committee on Next Generation Radio and Spectrum Management.

rates and avoids the need for complex equalizers. Other advantages of OFDM include high spectral efficiency, robustness against narrow-band interference (NBI), scalability, and easy implementation by fast Fourier transforms (FFTs). OFDM is used as the modulation method for digital audio broadcasting (DAB) [6] and terrestrial digital video broadcasting (DVB-T) [7] in Europe, and in asymmetric digital subscriber line (ADSL) [8]. The wireless local area network (WLAN) [9–11], and wireless metropolitan area network (WMAN) standards [12] use OFDM as their physical layer transmission technique as well. OFDM is also a strong candidate for IEEE wireless personal area network (WPAN) standard [13], for fourth generation (4G) cellular systems (see *e.g.* [14]), and finally wireless regional area network (WRAN) standard which is known as cognitive radio standard [15].

1.2 OFDM-Based Cognitive Radio

Application of OFDM to cognitive radio brings about new aspects and challenges to system design. The cognitive OFDM conceptual model considered in this dissertation is shown in Fig. 1.1.[5] Cognitive engine is responsible for making the intelligent decisions and configuring the radio and physical layer (PHY) parameters. Spectral opportunities are identified by the decision unit based on the information from policy engine as well as local and network spectrum sensing data.

Policy engine provides information to the cognitive engine concerning the current policies to be considered by the system depending on the location of the system. This ensures that cognitive radio does not use illegal waveforms or breach any policies. On the other hand, local spectrum sensing unit processes the spectrum information and identifies licensed users accessing to spectrum and their signal specifications such as their bandwidth and power level. It also detects spectrum opportunities that can be exploited by cognitive radio. Once the required information is available, decision unit can make a conclusion on the best course of action for the system. The decision includes choosing the appropriate channel coding, modulation, operation frequencies, and bandwidth. At this stage, OFDM technology gets the upper hand over other similar transmission technologies with its adaptive features and great flexibility. By only changing the configuration parameters of OFDM (see Table 2.2 for some example parameters) and radio, the cognitive system can communicate with various radio access technologies in the environment, or it can optimize the transmission depending on the environmental characteristics. The radio circuit is divided into digital part (digital IF, analog to digital converter (ADC), and digital to analog converter (DAC)) and analog part (software tunable

[5]Some OFDM functions are skipped or simplified for the sake of brevity.

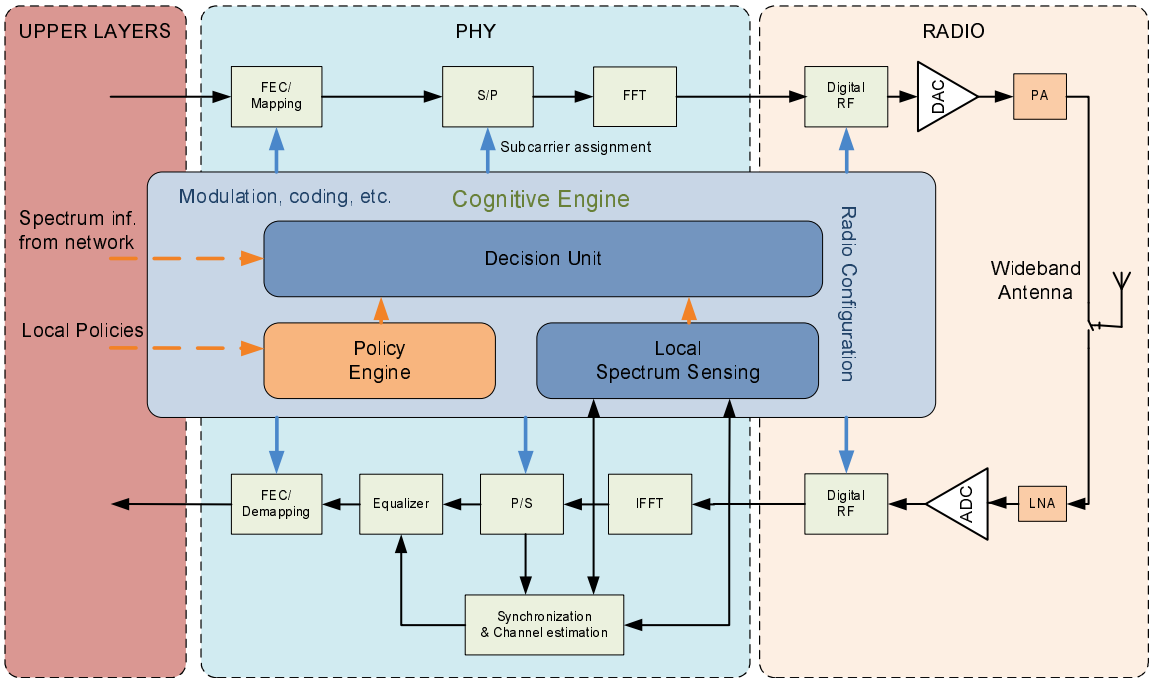

Figure 1.1 OFDM-based cognitive radio system block diagram. All of the layers can interact with the cognitive engine. OFDM parameters and radio are configured by the cognitive engine.

analog radio). Both parts are reconfigurable by the cognitive engine to increase the flexibility of the system. This includes controlling the operating frequency, bandwidth, filters, and mixers. Even antenna parameters, *e.g.* number of antennas and beam forming, can be configured to improve the system performance.

1.3 Awareness in Cognitive Radio

One of the most important elements of the cognitive radio concept is the ability to measure, sense, learn, and be aware of parameters related to the radio channel characteristics, availability of spectrum and power, interference and noise temperature, radio's operational environments, user requirements and applications, available networks (infrastructures) and nodes, local policies and other operating restrictions. A list of key types of awareness in cognitive radio is given in [16]. Main types of awareness include location awareness, geographical environment awareness, RF environment awareness, waveform awareness, mobility and trajectory awareness, power supply and energy efficiency awareness, regulation awareness, policy awareness, capabilities awareness, language awareness, mission awareness, spectrum awareness, priority awareness, past experience awareness, network

awareness [16]. Acquiring some of these awareness types related to physical layer is the main topic of this dissertation. Specifically, RF environment (channel) awareness, spectrum awareness, and waveform awareness are considered. Having the capability of acquiring these awareness enables adaptation and helps realizing cognitive radio concept. Furthermore, opportunistic spectrum access can be implemented as the major requirement of spectrum awareness is achieved using developed algorithms.

1.4 Dissertation Outline

In this dissertation, based on the preliminary discussion in the previous sections, we try to identify and address certain challenges related to physical layer awareness. Following the introduction (Chapter 1), the outline of this dissertation consists of four parts:

1. Detailed study of cognitive OFDM systems (Chapter 2).
2. Estimation of critical channel parameters for enabling adaptation (Chapters 3 – 5)
3. Spectrum sensing for dynamic spectrum access in cognitive radio (Chapters 6 and 7)
4. OFDM system identification and secure OFDM transmission for cognitive radio applications (Chapters 8 and 9)

The first part given above expands on the current chapter and provides detailed information about OFDM technology and cognitive radio. The last three parts contain the main contribution of the dissertation and include original research results. The conceptual relationship among these parts is illustrated in Fig. 1.2. As shown in this figure, the goal of this dissertation is to develop algorithms that enable the *awareness* capability of cognitive radio. While doing this, we consider an OFDM-based physical layer technology.

We start by investigating the requirements of cognitive radio and how OFDM fulfills these requirements in Chapter 2. Challenges that arise from employing OFDM in cognitive radio systems are identified and cognitive properties of some OFDM-based wireless standards are discussed in the same chapter.

In designing mobile wireless systems, the variation of radio channel characteristics needs to be taken into account. Traditional designs build head-room so that the mobile subscribers at the worst-case channel conditions can still maintain the communication. This would translate to lower data

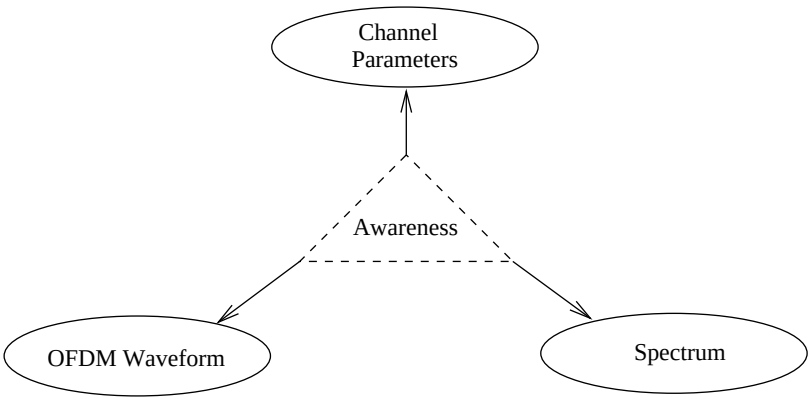

Figure 1.2 The three elements that are studied in this dissertation.

rates and inefficient usage of the available resources such as power and spectrum. While this ensures reliable communications from the services and consumer points of view, scarce resources are not exploited efficiently, yielding a sub-optimal communications system. Therefore, recently, adaptation of wireless communications systems has gained a strong momentum and the new generation wireless standards are designed to be more aware of the variations and characteristics of the channel. This is what cognitive radio aims and these new standards include cognitive radio features. In terms of adapting the transmission parameters, OFDM offers many possibilities. Adapting the transmit power, cyclic prefix (CP) size, modulation and coding, and the number of sub-carriers are some of these transmission parameters.[6] In addition to adaptation over each symbol (as in the case of single carrier systems), OFDM also offers adaptation of the parameters for each carrier or over a small group of carriers. In other words, adaptation can be done independently over narrower bands rather than employing adaptation over the whole transmission band. Similarly, reception of an OFDM signal can bring about several new designs and approaches for adaptive receiver. An overview of commonly used adaptation techniques in multi-carrier systems and their applications for wireless mobile radio systems are discussed in [17]. Many of these adaptation techniques require measurement (or estimate) of the related channel parameters. The three main channel related parameters are root-mean-squared (RMS) delay spread, Doppler spread and noise variance.[7] We discuss estimation of these three parameters and propose new algorithms in Chapters 3, 4, and 5, respectively. With the knowledge of these parameters, cognitive radio can obtain an environmental awareness.

[6] Please see Section 2.3.1.1 for more details.

[7] In coherent wireless systems, signal-to-noise ratio (SNR) can be calculated once the noise variance is estimated using the knowledge of channel frequency response (CFR).

One important task in realizing cognitive radio is characterization of the spectrum, or in other words, spectrum sensing. Cognitive radio devices should be able to identify the unused spectrum in a fast and efficient way to provide new ways to access spectrum. Spectrum sensing includes multi-dimensional awareness about the interference temperature and existence of primary users in these dimensions. A detailed survey of the spectrum sensing methods for cognitive radio applications is given in Chapter 6. In Chapter 7, a new spectrum sensing method based on the feature extraction of primary users' signals is presented. Proposed method makes use of the *a priori* information about the characteristics of primary users operating in a specific band and geographic location. Successful application of the proposed algorithm enables dynamic spectrum access and helps to solve the spectral crowding problem.

Cognitive radios are expected to recognize different wireless networks and have capability of communicating with them. Multi-carrier techniques, specifically OFDM, are commonly used in modern communications systems. Some examples include IEEE 802.11a/g based WLAN and IEEE 802.16 based WMAN systems. For identification of active transmissions, signals can be classified as single-carrier and multi-carrier first. Hence, the size of candidate set can be reduced. Moreover, transmission parameters of an OFDM based system can be detected blindly if the system is not known to cognitive radio bringing in waveform awareness. Maximum-likelihood (ML) estimation is used to identify the OFDM waveform and estimate its crucial parameters in Chapter 8. Furthermore, we develop estimation of signal parameters via rotational invariance techniques (ESPRIT)-based algorithm for identifying active subcarriers in the case of a cognitive radio scenario. In Chapter 9, we propose new algorithms for achieving transmission-level security in OFDM systems for preventing detection of OFDM parameters blindly. Hence, in a sense, Chapter 8 and Chapter 9 are opposite of each other.

Performances of different algorithms and techniques discussed above are analyzed with closed form expressions and/or simulations. In the rest of this chapter, we provide more details regarding the content of these upcoming individual chapters and our contributions in each chapter.

1.4.1 Chapter 2: OFDM for Cognitive Radio: Merits and Challenges

In this chapter, cognitive radio systems and their requirements of the physical layer are discussed and OFDM technique is investigated as a candidate transmission technology for cognitive radio. In addition, the challenges that arise from employing OFDM in cognitive radio systems are identified.

The cognitive properties of some OFDM-based wireless standards are discussed in order to indicate the trend towards a more cognitive radio.[8]

1.4.2 Chapter 3: Time Dispersion and Delay Spread Estimation for Adaptive OFDM Systems

In this chapter, algorithms for estimating the time dispersion (frequency selectivity) of the channel, which use the frequency domain channel estimates or the frequency domain received signal, are proposed. The proposed algorithms estimate the power delay profile (PDP) from which the two important dispersion parameters, namely RMS delay spread and MED of the channel, are estimated. It is shown that synchronization errors bias the performance of the estimators based on the channel correlation, and this bias is removed by obtaining the PDP using the magnitude of channel estimates. Moreover, Cramér-Rao lower bound (CRLB) for estimation of RMS delay spread is derived and performances of the proposed algorithms are compared against this theoretical limit.[9]

1.4.3 Chapter 4: Doppler Spread Estimation for Wireless OFDM Systems

In this chapter, we present a method for estimating the Doppler spread in mobile OFDM systems. The estimation is based on finding the autocorrelation function of time domain channel estimates over several OFDM symbols. In OFDM systems, channel estimation is popularly performed in frequency domain. Channel frequency response estimates are affected by noise and inter-carrier interference (ICI). As a result, Doppler estimates based on frequency domain channel estimates are affected significantly. We show that usage of channel estimates in time domain can greatly improve the performance of Doppler estimates. The channel impulse response (CIR) can be obtained by taking inverse discrete Fourier transform (IDFT) of the CFR. Consequently, the proposed method reduces processing time and memory usage. Computer simulations support our claim for a broad range of Doppler spread and SNR values in Rayleigh fading channels.[10]

1.4.4 Chapter 5: MMSE Noise Plus Interference Power Estimation in Adaptive OFDM Systems

Noise variance and SNR are important parameters for adaptive OFDM systems since they serve as a standard measure of signal quality. Conventional algorithms assume that noise statistics remain constant over the OFDM frequency band, and thereby average the instantaneous noise samples to

[8] Certain parts of the content in this chapter are published in [18], and are submitted to [19].
[9] Certain parts of the content in this chapter are published in [20–22], and are submitted to [23].
[10] Certain parts of the content in this chapter are published in [24].

get a single estimate. In reality, noise is often made up of white Gaussian noise along with correlated colored noise that affects the OFDM spectrum unevenly. This chapter proposes a minimum mean-square error (MMSE) filtering technique to estimate the noise power that takes into account the variation of the noise statistics across the OFDM sub-carrier index as well as across OFDM symbols. The proposed method provides many local estimates that allow tracking of the variation of noise statistics in frequency and time. The MMSE filter coefficients are obtained from mean-squared-error (MSE) expression, which can be calculated using noise statistics. Evaluation of the performance with computer simulations shows that the proposed method tracks the local statistics of noise more efficiently than conventional methods.[11]

1.4.5 Chapter 6: Spectrum Sensing for Cognitive Radio Applications

In this chapter, a survey of spectrum sensing methodologies for cognitive radio is presented. Various aspects of spectrum sensing problem are studied from cognitive radio perspective. Challenges associated with spectrum sensing is given and enabling spectrum sensing methods are reviewed. The chapter explains cooperative sensing concept and its various forms. External sensing algorithms and other alternative sensing methods are discussed. Furthermore, statistical modeling of network traffic and utilization of these models for prediction of primary user behavior is studied. Hardware perspective of sensing problem is discussed and multi-dimensional spectrum sensing concept is explained. Finally, sensing features of some current wireless standards are given.[12]

1.4.6 Chapter 7: Spectrum Sensing for Cognitive Radio Using Partial Match Filtering

In this chapter, a new spectrum sensing method is introduced where primary users are identified by matching the features extracted from the received signal to the *a priori* information about primary users' transmission characteristics. By identifying active primary users, multi-dimensional spectrum awareness is obtained. Furthermore, application of proposed algorithm to energy detector based sensing methods is presented as a case study.[13]

[11] Certain parts of the content in this chapter are published in [25–27], and a patent application is filed with US Patent office [28].

[12] Certain parts of the content in this chapter are published in [29], and are submitted to [30].

[13] Certain parts of the content in this chapter are published in [31], and are submitted to [32]. In addition, a patent application is filed with US Patent office [33].

1.4.7 Chapter 8: OFDM Signal Identification and Transmission Parameter Estimation for Cognitive Radio Applications

Methods for identification of OFDM signals and estimation of fundamental OFDM parameters are developed in this chapter. Detected transmissions are classified as single-carrier or multi-carrier. In the case of multi-carrier transmission, OFDM symbol duration, CP length, number and frequencies of subcarriers, and nominal bandwidth are estimated blindly using characteristics of OFDM transmission. For estimation of symbol duration and CP length, cyclostationarity of OFDM signaling is explored by using a suboptimal maximum likelihood (ML) estimator. Active subcarriers are estimated by employing a modified version of ESPRIT method. The proposed algorithms can be used in cognitive radio for identifying various OFDM-based transmissions and for electronic surveillance to detect illegal or enemy signals. In addition, in the case of adaptive subcarrier selection in a cognitive radio scenario, the receiver can blindly identify deactivated subcarriers without the need for signaling.[14]

1.4.8 Chapter 9: Feature Suppression for Physical-Layer Security in OFDM Systems

OFDM symbols carry redundancy due to the cyclic extension employed for providing immunity to multipath distortion. This redundancy can be used for blindly detecting the transmission parameters as well as achieving synchronization to transmitted signal as discussed in Chapter 8. This chapter proposes transmission-level techniques for suppressing physical-layer features of OFDM waveform. Hence, a covert, secure and reliable transmission based on OFDM technique can be achieved. We analyze the effectiveness of the proposed methods by investigating the cyclic autocorrelation function (CAF) of the OFDM waveforms.[15]

1.4.9 Other Work Done

Apart from the work discussed above, there are some other works that did not get into this dissertation.[16] During my internship at Logus wireless, I have worked significantly on base station (BS) design for fixed and mobile Worldwide Interoperability for Microwave Access (WiMAX).[17] I

[14] Certain parts of the content in this chapter are published in [34], and are submitted to [35].

[15] Certain parts of the content in this chapter are submitted to [36], and a patent application is filed with US Patent office [37].

[16] There are few different reasons for not including these in the dissertation. In some other work, I am not the main author, and/or my contribution is rather minor. Also, I want to keep the integrity of the manuscript and have the topics in a good flow.

[17] I have worked on design and very high-speed integrated circuits hardware description language (VHDL) implementation of PHY algorithms [38, 39].

have also worked on carrier frequency offset compensation for orthogonal frequency division multiple access (OFDMA) systems, *e.g.* mobile WiMAX.[18]

1.5 Notation

Throughout this dissertation, the following notation is followed. Bold upper letters denote matrices and bold lower letters denote column vectors; $(\cdot)^T$ denotes transpose; $(\cdot)^H$ denotes Hermitian operation; $\star$ denotes convolution operation; $\boldsymbol{I}$ is the identity matrix; $\delta(\cdot)$ is the Kronecker delta function; $\lfloor \cdot \rfloor$ denotes the largest integer less then or equal to input argument, and $E[\cdot]$ denotes expectation.

[18]The outcome of this research is published in [40, 41]

CHAPTER 2

OFDM FOR COGNITIVE RADIO: MERITS AND CHALLENGES

2.1 Introduction

Spectrum measurements show that wide ranges of the spectrum are rarely used most of the time while other bands are heavily used. However, those unused portions of the spectrum are licensed and thus cannot be utilized by users other than the license owners. Hence, there is a need for a novel technology that can benefit from these opportunities. Cognitive radio is a promising concept that offers solution to spectral crowding problem by introducing the opportunistic usage of frequency bands that are not heavily occupied by licensed users [3]. It can be defined as an intelligent wireless system that is aware of its surrounding environment through sensing and measurements; a system that uses its gained experience to plan future actions and adapt to improve the overall communication quality and meet user needs. One main aspect of cognitive radio is its ability to exploit unused spectrum to provide new ways of communication. Hence, cognitive radio should have ability to sense and be aware of its operational environment, and dynamically adjust its radio operating parameters accordingly. For cognitive radio to achieve this objective, the physical layer (PHY) needs to be highly flexible and adaptable. A special case of multicarrier transmission known as orthogonal frequency division multiplexing (OFDM) is one of the most widely used technologies in current wireless communications systems and it has the potential of fulfilling the aforementioned requirements of cognitive radios inherently or with minor changes. By dividing the spectrum into subbands that are modulated with orthogonal subcarriers, OFDM removes the need for equalizers and thus reduces the complexity of the receiver. Because of its attractive features, OFDM has been successfully used in numerous wireless technologies including wireless local area network (WLAN), wireless metropolitan area network (WMAN), and the European terrestrial digital video broadcasting (DVB-T). It is believed that OFDM will also play an important role in realizing cognitive radio concept by providing a proven, scalable and adaptive technology for air interface. In this chapter, the application of OFDM

to cognitive radio is discussed. We identify the advantages of OFDM over other technologies and provide challenges associated with its application to cognitive radio.

2.2 A Basic OFDM System Model

In this section, basic principles of OFDM technology is introduced. A basic system model is given, common components for OFDM based systems are explained, and a simple OFDM transceiver design is presented. Important impairments in OFDM systems are mathematically analyzed.

The discrete Fourier transform (DFT) of a discrete sequence $f(n)$ of length N, $F(k)$, is defined as [42]

$$F(k) = \frac{1}{N} \sum_{n=0}^{N-1} f(n) e^{-j\frac{2\pi kn}{N}}, \tag{2.1}$$

and inverse discrete Fourier transform (IDFT) is defined as

$$f(n) = \sum_{k=0}^{N-1} F(k) e^{j\frac{2\pi kn}{N}}. \tag{2.2}$$

OFDM converts serial data stream into parallel blocks of size N, and uses IDFT to obtain time-domain signal. Time-domain OFDM symbol can be calculated as

$$\begin{aligned} x_m(n) &= IDFT\{X_m(k)\} && (2.3) \\ &= \sum_{k=0}^{N-1} X_m(k) e^{j2\pi nk/N} \qquad -N_G \le n \le N-1, && (2.4) \end{aligned}$$

where $X_m(k)$ is the symbol transmitted on the kth subcarrier of mth OFDM symbol and N is the number of sub-carriers. Symbols are obtained from the data bits using an M-ary modulation, *e.g.* binary phase shift keying (BPSK), quadrature amplitude modulation (QAM), *etc.* Time domain signal is cyclically extended N_G samples to avoid inter-symbol interference (ISI) from previous symbol (see next section). Transmitted signal can be obtained by concatenating OFDM symbols as

$$x(n) = \sum_{m=-\infty}^{\infty} x_m(n - m(N + N_G)) \tag{2.5}$$

The symbols $X_m(k)$ are interpreted as frequency domain signal and samples $x(n)$ are interpreted as time domain signal. Applying the central limit theorem, while assuming that N is sufficiently large, $x(n)$ can be shown to have zero-mean complex-valued Gaussian distribution. Power spectrum

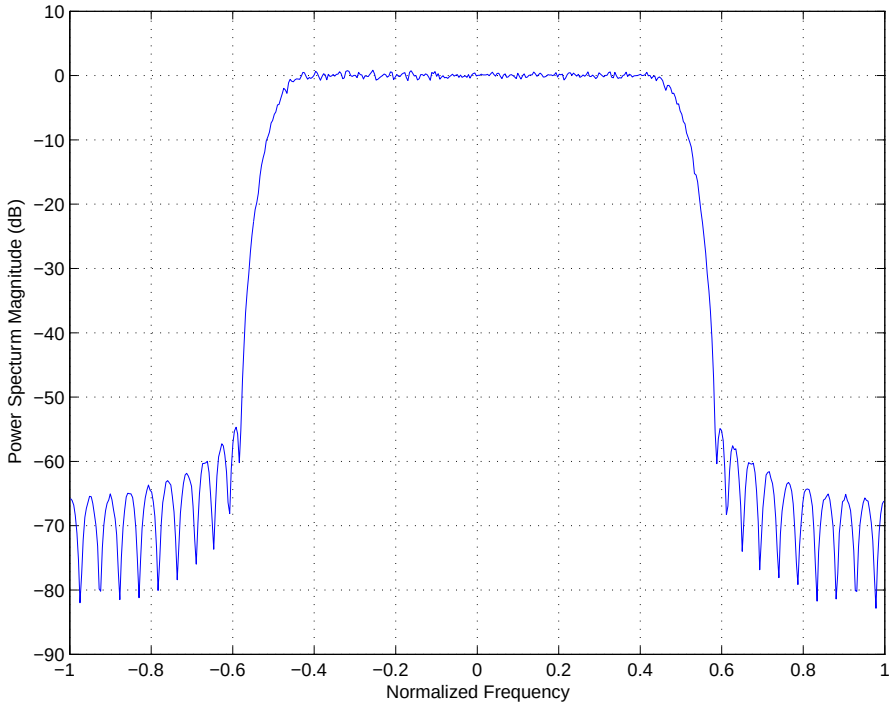

Figure 2.1 Power spectrum density of transmitted time domain OFDM signal.

of OFDM signal with 64 sub-carriers is shown in Fig. 2.1. Symbols are mapped using quadrature phase shift keying (QPSK) modulation.

The sub-carriers at the end sides of the spectrum are usually set to zero in order to simplify the spectrum shaping requirements at the transmitter, *e.g.* IEEE 802.11a. These subcarriers are used as frequency guard band and referred as *virtual carriers* or *null subcarriers* in literature [43]. To avoid difficulties in D/A and A/D converter offsets, and to avoid DC offset, the subcarrier falling at DC is not used as well. The power spectrum for such a system is shown in Fig. 2.2. Number of sub-carriers that are set to zero at the sides of the spectrum is 11.

2.2.1 Cyclic Extension of OFDM Symbols

Time domain OFDM signal is cyclically extended to mitigate the effect of time dispersion. The length of cyclic prefix (CP) has to exceed the maximum excess delay of the channel in order to avoid ISI [44, 45]. Basic idea of cyclic extension is to replicate part of the OFDM time-domain symbol from back to the front to create a guard period. This is shown in the Fig. 2.3. This figure also shows how cyclic prefix prevents the ISI. As can be seen from the figure, as long as maximum excess delay

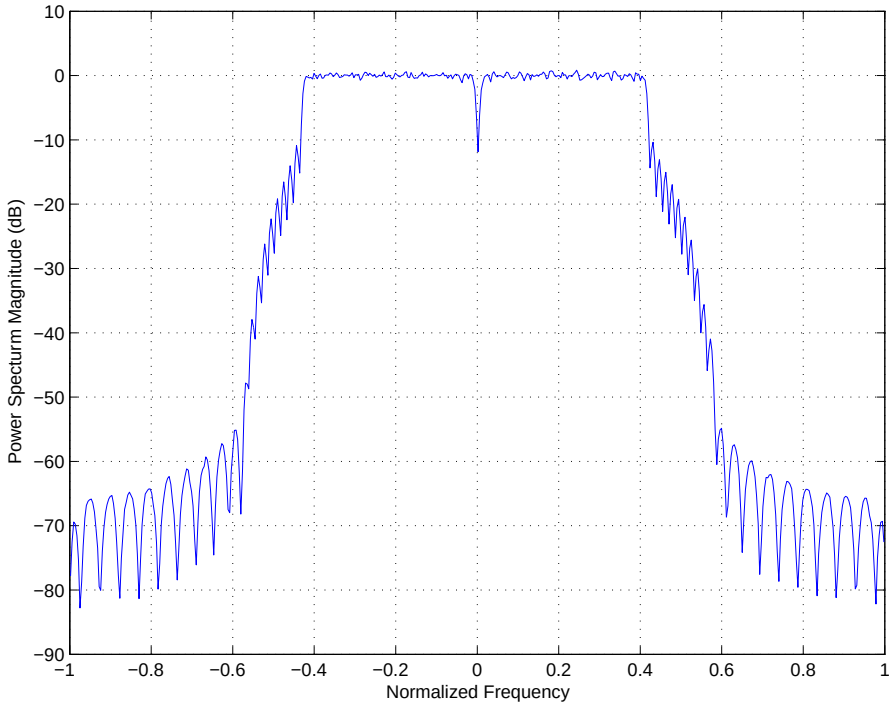

Figure 2.2 Power spectrum density of OFDM signal when the subcarriers at the sides of the spectrum and at DC is set to zero.

(τ_{max}) is smaller than the length of the cyclic extension T_G, the distorted part of the signal stays within the guard interval, which is removed later at the transmitter. Hence, ISI is prevented at the expense of spectral efficiency loss.

The ratio of the guard interval to the useful symbol duration is application dependent. If this ratio is large, the overhead increases causing a decrease in the system throughput. A *cyclic* prefix is used for the guard time for the following reasons;

1. To maintain the receiver time synchronization; since a long silence can cause synchronization to be lost.

2. To convert the linear convolution of the signal and channel to a circular convolution and thereby causing the DFT of the circularly convolved signal and channel to simply be the product of their respective DFTs.

3. It is easy to implement in digital signal processors (DSPs) and field-programmable gate arrays (FPGAs).

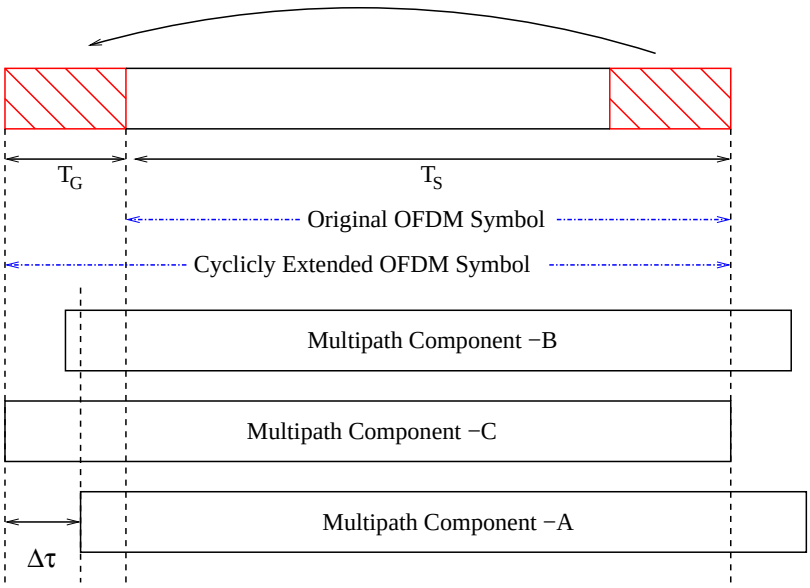

Figure 2.3 Illustration of cyclic prefix extension.

2.2.2 Wireless Channel

In wireless communication systems, information is transmitted to a receiver through a radio channel. Transmitted signals are typically reflected, diffracted, and scattered, arriving at the receiver along multiple paths with different delays, amplitudes, and phases as illustrated in Fig. 2.4. Multipath propagation affects the signal significantly, corrupting the signal and often placing limitations on the performance of the system.

Depending on the transmission bandwidth (or symbol duration) and the type of the environment that the communication takes place, multipath can cause various problems. When relative time delays are small compared to the transmitted symbol period, different "images" of the *same* symbol arrive at the same time, adding either constructively or destructively. The overall effect is a random fading channel response. When the relative path delays are on the order of a symbol period or more, then images of *different symbols* arrive at the same time. For example, when a particular symbol arrives at the receiver along one path, the previous symbol is arriving along another, delayed path. This is analogous to an acoustic echo and results in a more complicated channel response, which is often referred as time dispersive channel (or frequency selective channel). For example, in office buildings, the average delay spread is around 50 ns and maximum delay spread is around 300 ns in 5 GHz band. Therefore, if the transmitted symbol duration is less than the maximum excess delay (MED) of the channel, the dispersion causes ISI. Traditionally, in single carrier systems, ISI is

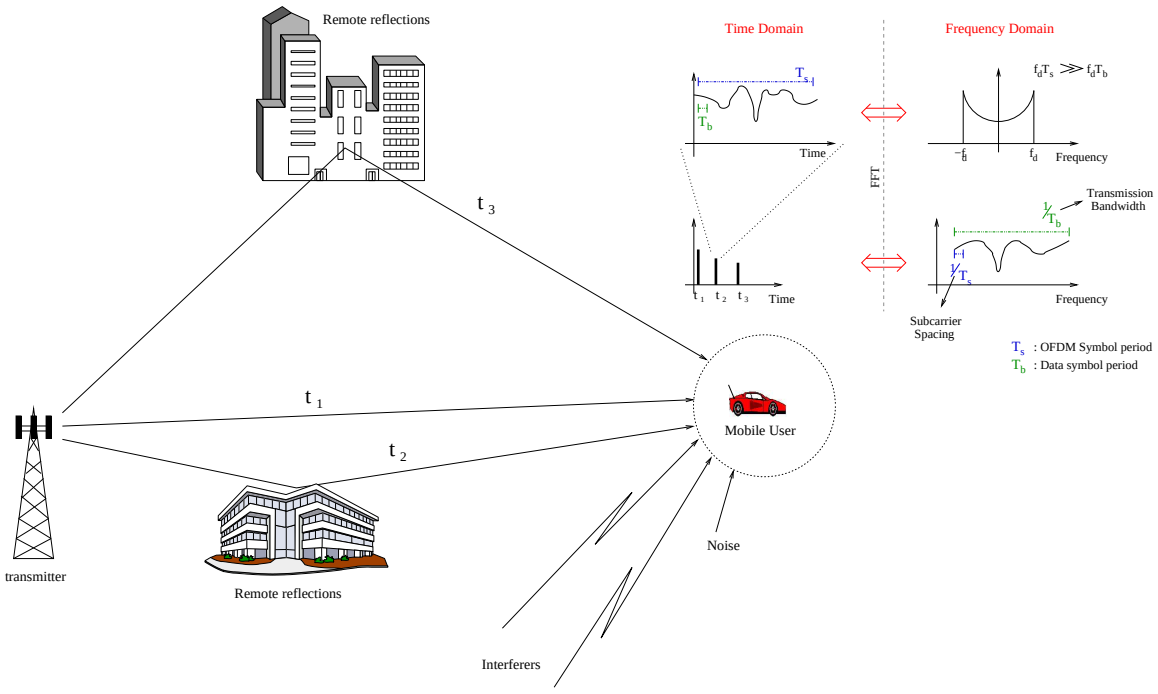

Figure 2.4 Illustration of some of the effects of radio channel: Local scatterers cause fading; remote reflectors cause multipath and time dispersion, leading to ISI; mobility of user or scatterers cause time varying channel, leading to frequency dispersion (Doppler spread); reuse of frequencies, adjacent carriers etc. cause interference.

handled by equalizers. For example, in the popular global system for mobile communications (GSM) cellular receivers, 3-5 tap equalizers are used to handle the ISI due to channel and filter effects. As the demand for higher and higher data rates increase, the transmission bandwidth to accommodate this high data rates also increases. Hence, the transmitted symbol duration (which is about the inverse of the transmission bandwidth) decreases as well. As a result, for a given environment, the amount of dispersion and equalizer complexity increases dramatically. Multi-carrier transmission and OFDM solves this problem, by dividing the wide frequency band into narrower bands.

The channel response can change rapidly with time due to the mobility of the transmitter, the receiver, or the scattering objects. This phenomenon causes spectral broadening which is also referred as Doppler spread. Doppler spread affects the signal differently depending on the transmission bandwidth. As the transmission bandwidth increases, the relative broadening of the channel with respect to the transmission bandwidth is insignificant. In other words, the time variation within the transmission of a symbol is negligible. This brings about a common trade-off between high mobility and high data rate. An example two-dimensional channel response is shown in Fig. 2.5.

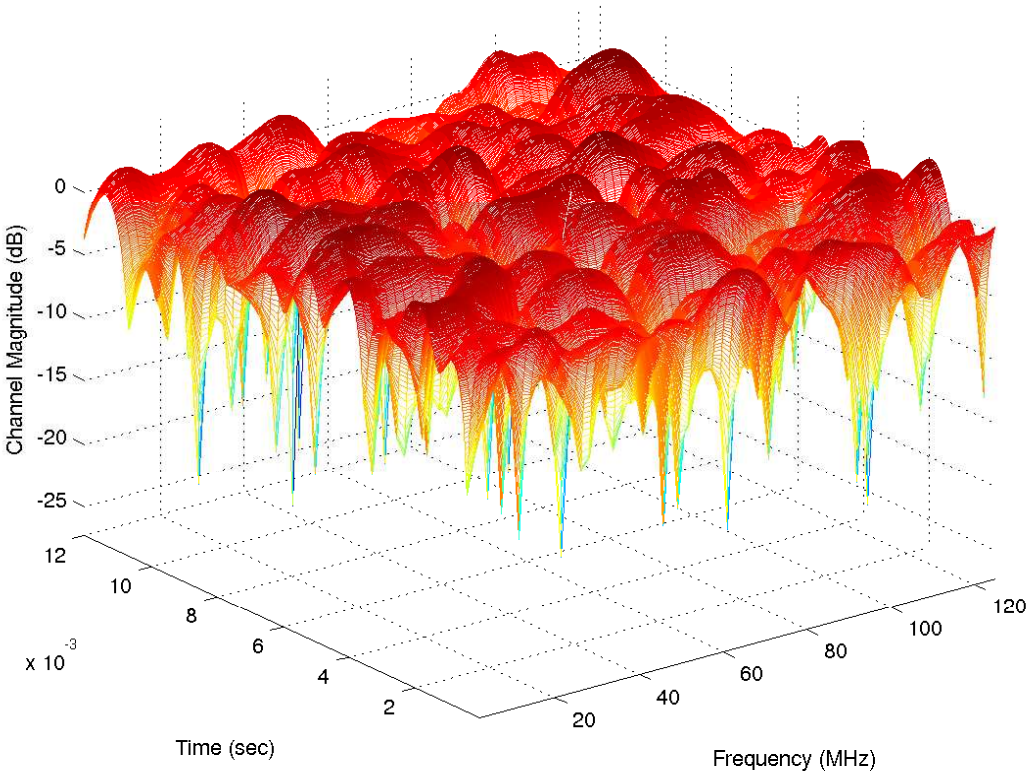

Figure 2.5 An example 2-dimensional channel response: An exponential PDP with RMS delay spread of 16μs is used, mobile speed is assumed to be 100km/h, and the center frequency was 5.2GHz. Channel taps are obtained using modified Jakes' model [1].

An exponential power delay profile (PDP) with root-mean-squared (RMS) delay spread of 16 μs is used and mobile speed is assumed to be 100 km/h. Channel taps are obtained using modified Jakes' model [1].

Channel equalizers are usually used to compensate multipath effects. Equalizers can considerably increase the system complexity as their complexity increases exponentially with the number of channel paths. In OFDM system, however, the need for equalizers can be avoided by careful system design. To avoid ISI, symbol duration is extended by adding a guard band to the beginning of each symbol as explained before. If we define the delay spread (or multipath spread) of the channel as the delay between the first and last received paths over the channel[1], the CP should be longer than that delay. On the other hand, frequency selective fading is avoided by decreasing the subcarrier spacing or consequently increasing the number of subcarriers. We define the channel coherence bandwidth as the bandwidth over which the channel could be considered flat. Since OFDM signal can be

[1]See Chapter 3 for more details on delay spread and how to estimate it.

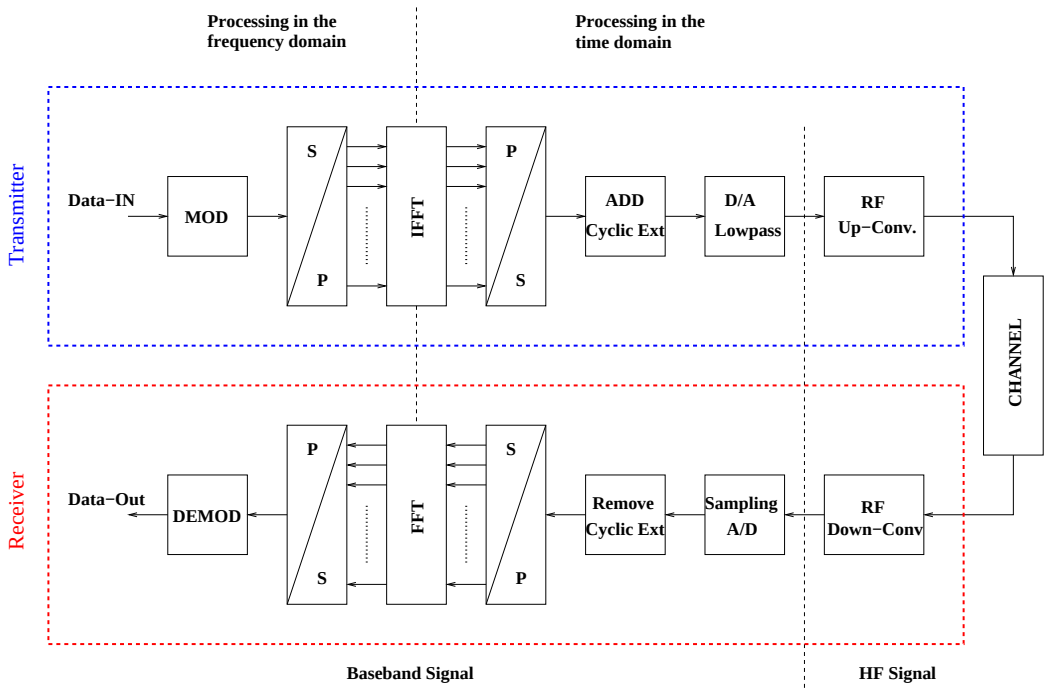

Figure 2.6 Block diagram of an OFDM transceiver.

considered as group of narrowband signals, by increasing the number of subcarriers, the bandwidth of each subcarrier (subcarrier spacing) becomes narrower. When the subcarrier spacing is set to be less than coherence bandwidth of the channel, each subcarrier is going to be affected by a flat channel and thus no channel equalization is needed.

2.2.3 A Simple System

A block diagram of a basic OFDM system is given in Fig. 2.6. Usually raw data is coded and interleaved before modulation. In a multipath fading channel, all subcarriers have different attenuations. Some subcarriers may even be completely lost because of deep fades. Therefore, the overall bit-error-rate (BER) may be largely dominated by a few subcarriers with the smallest amplitudes. To avoid this problem, channel coding and interleaving can be used. By using coding, errors can be corrected up to a certain level depending on the code rate and type, and the channel. Interleaving is applied to randomize the occurrence of bit errors.

Coded and interleaved data is then be mapped to the constellation points to obtain data symbols. These steps are represented by the first block of Fig. 2.6. The serial data symbols are then converted to parallel and inverse fast Fourier transform (IFFT) is applied to these parallel blocks to obtain

the time domain OFDM symbols. Later, these samples are cyclically extended as explained in Section 2.2.1, converted to analog signal and up-converted to radio frequencies (RF) frequencies using mixers. The signal is then amplified by using a power amplifier (PA) and transmitted through antennas.

In the receiver side, the received signal is passed through a band-pass noise rejection filter and downconverted to baseband. After frequency and time synchronization, cyclic prefix is removed and the signal is transformed to the frequency domain using fast Fourier transform (FFT) operation. Finally, the symbols are demodulated, deinterleaved and decoded to obtain the transmitted information bits.

2.2.4 OFDM Impairments

This section gives the main impairments that exist in OFDM systems with underlying mathematical details. For simplicity, the symbol index is dropped in this section without loss of generality.

2.2.4.1 Frequency Offset

Frequency offset is a critical factor in OFDM system design. It results in inter-carrier interference (ICI) and degrades the orthogonality of sub-carriers. Frequency errors tend to occur from two main sources. These are local oscillator errors and common Doppler shift due to mobility. Any difference between transmitter and receiver local oscillators results in a frequency offset. This offset is usually compensated for by using adaptive frequency correction (AFC), however, any residual (uncompensated) error results in a degraded system performance.

The characteristics of ICI are similar to Gaussian noise, hence it leads to degradation of the signal-to-noise ratio (SNR). The amount of degradation is proportional to the fractional frequency offset which is equal to ratio of frequency offset to carrier spacing.

Frequency offset can be estimated by different methods *e.g.* using pilot symbols, the statistical redundancy in the received signal, or transmitted training sequences. In [46], a frequency offset estimator which uses the repeated structure of training signal is given. The average phase difference between the first and second part of the long training sequences is calculated and then normalized to obtain the frequency offset.

Assume that we have the symbols $X(k)$ to be transmitted using an OFDM system. These symbols are transformed to the time domain using IDFT as shown earlier in (2.4). This baseband signal is

then up-converted to RF frequencies and transmitted over the wireless channel. In the receiver, the received signal is down-converted to baseband. But, due to the frequency mismatch between the transmitter and receiver, the received signal has a frequency offset. This signal is denoted as $y(n)$. Frequency offset is added to the OFDM symbol in the receiver. Finally, to recover the data symbols, DFT is applied to the OFDM symbol taking the signal back to frequency domain. Let $Y(k)$ denote the recovered data symbols. This process is shown below.

$$X(k) \xrightarrow{IDFT} x(n) \xrightarrow{frequency\ offset} y(n) \xrightarrow{DFT} Y(k).$$

Let us apply the above operations to $X(k)$ in order to get $Y(k)$. First find $x(n)$ using (2.2)

$$\begin{aligned} x(n) &= IDFT\{X(k)\} && (2.6)\\ &= \sum_{k=0}^{N-1} X(k) e^{j\frac{2\pi kn}{N}}. && (2.7) \end{aligned}$$

The effect of frequency offset on $x(n)$ is a phase shift of $2\pi\epsilon n/N$, where ϵ is the normalized frequency offset. Therefore;

$$\begin{aligned} y(n) &= x(n) e^{j\frac{2\pi\epsilon n}{N}} && (2.8)\\ &= \sum_{k=0}^{N-1} X(k) e^{j\frac{2\pi kn}{N}} e^{j\frac{2\pi\epsilon n}{N}} && (2.9)\\ &= \sum_{k=0}^{N-1} X(k) e^{j\frac{2\pi n}{N}(k+\epsilon)}. && (2.10) \end{aligned}$$

Finally, we need to apply DFT to $y(n)$ for recovering the symbols

$$\begin{aligned} Y(k) &= DFT(\ y(n)\ ) && (2.11)\\ &= \frac{1}{N} \sum_{n=0}^{N-1} \left\{ \sum_{m=0}^{N-1} X(m) e^{j\frac{2\pi n}{N}(m+\epsilon)} \right\} e^{-j\frac{2\pi kn}{N}} && (2.12)\\ &= \frac{1}{N} \sum_{n=0}^{N-1} \sum_{m=0}^{N-1} X(m) e^{j\frac{2\pi n}{N}(m-k+\epsilon)} && (2.13)\\ &= \frac{1}{N} \sum_{m=0}^{N-1} X(m) \left\{ \sum_{n=0}^{N-1} e^{j\frac{2\pi n}{N}(m-k+\epsilon)} \right\}. && (2.14) \end{aligned}$$

The term within the curly braces can be calculated using geometric series expansion, $S_n \equiv \sum_{k=0}^{n} r^k = \frac{1-r^{n+1}}{1-r}$. Using this expansion we have

$$
\begin{aligned}
Y(k) &= \frac{1}{N}\sum_{m=0}^{N-1} X(m)\left\{\sum_{n=0}^{N-1} e^{j\frac{2\pi n}{N}(m-k+\epsilon)}\right\} && (2.15)\\
&= \frac{1}{N}\sum_{m=0}^{N-1} X(m)\frac{1-e^{j2\pi(m-k+\epsilon)}}{1-e^{j\frac{2\pi(m-k+\epsilon)}{N}}} && (2.16)\\
&= \frac{1}{N}\sum_{m=0}^{N-1} X(m)\frac{e^{j\pi(m-k+\epsilon)}(e^{-j\pi(m-k+\epsilon)}-e^{j\pi(m-k+\epsilon)})}{e^{j\frac{\pi(m-k+\epsilon)}{N}}(e^{-j\frac{\pi(m-k+\epsilon)}{N}}-e^{j\frac{\pi(m-k+\epsilon)}{N}})} && (2.17)\\
&= \frac{1}{N}\sum_{m=0}^{N-1} X(m)\frac{e^{j\pi(m-k+\epsilon)}}{e^{j\frac{\pi(m-k+\epsilon)}{N}}}\frac{-2j\sin(\pi(m-k+\epsilon))}{-2j\sin(\frac{\pi(m-k+\epsilon)}{N})} && (2.18)\\
&\approx \sum_{m=0}^{N-1} X(m)e^{j\pi(m-k+\epsilon)\frac{N-1}{N}}\frac{sin(\pi(m-k+\epsilon))}{\pi(m-k+\epsilon)} && (2.19)\\
&\approx \sum_{m=0}^{N-1} X(m)\frac{sin(\pi(m-k+\epsilon))}{\pi(m-k+\epsilon)}e^{j\pi(m-k+\epsilon)}. && (2.20)
\end{aligned}
$$

In the above derivation we used the fact that $\sin(x) \approx x$ for small x values, and $\frac{N-1}{N} \approx 1$ for large values of N. These approximations are reasonable since usually N is a large integer.

We can now relate the received symbols to the transmitted symbols using (2.20). But we first define

$$S_F(m,k) = \frac{sin(\pi(m-k+\epsilon))}{\pi(m-k+\epsilon)}e^{j\pi(m-k+\epsilon)}.$$

Therefore;

$$
\begin{aligned}
Y(k) &= \sum_{m=0}^{N-1} X(m)S_F(m,k) && (2.21)\\
&= X(k)S_F(k,k) + \sum_{m=0,m\neq k}^{N-1} X(m)S_F(m,k). && (2.22)
\end{aligned}
$$

The first term in (2.22) is equal to the originally transmitted symbol shifted by a constant term that corresponds to ϵ. This term $S_F(k,k)$ introduces a phase shift of $\pi\epsilon$ and an attenuation of $\sin(\pi\epsilon)/\pi\epsilon$ in magnitude. Actually, this term only depends on the value of offset ϵ but not carrier index k, so the effect of frequency offset on each sub-carrier is the same. The second term in (2.22) represents the interference from other sub-carriers which is a dual to ISI in time domain due to timing offset and it is known as ICI.

2.2.4.2 Time-Varying Channel

Another channel effect that should be considered in OFDM system design is mobility. For fixed communication systems, the channel can be considered constant over time. However, if either transmitter or receiver is mobile, channel is going to vary over time resulting in fast fading of the received signal. Coherence time of the channel is defined as the time over which the channel is considered constant. To avoid fast fading effect, OFDM symbol time is chosen to be shorter than the coherence time of the channel. In the frequency domain, mobility results in frequency spread of the signal which dependents on the operating frequency and the relative speed between the transmitter and receiver, also know as Doppler spread [47]. Doppler spread of OFDM signals results in ICI which can be reduced by increasing the subcarrier spacing [48]. Assuming an L-tap symbol-spaced time-varying channel, the time domain received OFDM signal can be obtained by convolving the transmitted signal with channel impulse response (CIR) $h_l(n)$ as

$$y(n) = \sum_{l=0}^{L-1} h_l(n)x(n-l) \qquad 0 \leq n \leq N-1 \ . \tag{2.23}$$

By taking FFT of (2.23) and ignoring the channel noise for the moment, frequency domain received symbols can be obtained as

$$\begin{aligned}
Y(k) &= \frac{1}{N}\sum_{n=0}^{N-1} y(n)e^{-j\frac{2\pi kn}{N}} && (2.24)\\
&= \frac{1}{N}\sum_{n=0}^{N-1}\left[\sum_{l=0}^{L-1} h_l(n)x(n-l)\right]e^{-j\frac{2\pi kn}{N}} && (2.25)\\
&= \frac{1}{N}\sum_{n=0}^{N-1}\left[\sum_{l=0}^{L-1} h_l(n)\left(\sum_{m=0}^{N-1} X(m)e^{j\frac{2\pi m(n-l)}{N}}\right)\right]e^{-j\frac{2\pi kn}{N}} && (2.26)\\
&= \sum_{m=0}^{N-1} X(m)\left\{\sum_{l=0}^{L-1}\underbrace{\left(\frac{1}{N}\sum_{n=0}^{N-1} h_l(n)e^{j\frac{2\pi n(m-k)}{N}}\right)}_{H_l(m-k)}e^{-j\frac{2\pi ml}{N}}\right\} \ . && (2.27)
\end{aligned}$$

Note that when $h_l(n) = h_l$, *i.e.* when the channel is constant over the OFDM symbol, $H_l(m-k) = h_l$ and there is no ICI.

Let us define the interference matrix due to channel variation as a matrix with elements given by

$$S_C(m,k) = \frac{1}{N}\sum_{l=0}^{L-1}\sum_{n=0}^{N-1} h_l(n) e^{\frac{j2\pi n(m-k)}{N}} e^{-\frac{j2\pi ml}{N}} \quad . \tag{2.28}$$

Note that (2.28) also includes the effect of frequency selective channel. Therefore,

$$\begin{aligned} Y(k) &= \sum_{m=0}^{N-1} X(m) \left\{ \frac{1}{N}\sum_{l=0}^{L-1}\sum_{n=0}^{N-1} h_l(n) e^{\frac{j2\pi n(m-k)}{N}} e^{-\frac{j2\pi ml}{N}} \right\} && (2.29)\\ &= \sum_{m=0}^{N-1} X(m) S_C(m,k) && (2.30)\\ &= X(k)S_C(k,k) + \sum_{m=0, m\neq k}^{N-1} X(m) S_C(m,k). && (2.31) \end{aligned}$$

As in (2.22), the second term in (2.31) represents the interference between the subcarriers. while the first term is equal to the originally transmitted symbol multiplied by $S_C(k,k)$ which, in this case, depends on the carrier index. This term can be re-written as

$$\begin{aligned} S_C(k,k) &= \frac{1}{N}\sum_{l=0}^{L-1}\sum_{n=0}^{N-1} h_l(n) e^{\frac{j2\pi n(k-k)}{N}} e^{-\frac{j2\pi kl}{N}} && (2.32)\\ &= \sum_{l=0}^{L-1} \left(\frac{1}{N}\sum_{n=0}^{N-1} h_l(n) \right) e^{-\frac{j2\pi kl}{N}} \quad . && (2.33) \end{aligned}$$

The term in the parentheses is just an arithmetic average of the varying CIR taps within an OFDM symbol. Hence, the whole expression is Fourier transform of the average CIR which gives the frequency domain channel, *i.e* a transmitted symbol is multiplied with the value of frequency domain channel at that sub-carrier.

2.2.4.3 Phase Noise

Phase noise is introduced by local oscillator in any receiver and can be interpreted as a parasitic phase modulation in the oscillator's signal. It can be modeled as a zero mean random variable [49]. If we assume the channel is flat and the signal is only effected by phase noise $\phi(n)$ at the receiver, the received time domain signal can be written as

$$r(n) = x(n)e^{j\phi(n)}. \tag{2.34}$$

When phase offset is assumed to be small $e^{j\phi(n)} \approx 1 + j\phi(n)$, and the recovered symbols have the form

$$\hat{X}_k \approx X(k) + \frac{j}{N}\sum_{r=0}^{N-1} X(r)\sum_{n=0}^{N-1}\phi(n)e^{j(2\pi/N)(r-k)n} \tag{2.35}$$

$$\approx X(k) + \underbrace{jX(k)\frac{1}{N}\sum_{n=0}^{N-1}\phi(n)}_{jX(k)\Phi} + \underbrace{\frac{j}{N}\sum_{r=0,r\neq k}^{N-1} X(r)\sum_{n=0}^{N-1}\phi(n)e^{j(2\pi/N)(r-k)n}}_{ICI\ term}. \tag{2.36}$$

In (2.36), the second term represents a common error added to every subcarrier that is proportional to its value multiplied by a complex number $j\Phi$, *i.e.* a rotation of the constellation. This rotation is the same for all subcarriers, so it can be corrected by using a phase rotation equal to the average of the phase noise,

$$\Phi = \frac{1}{N}\sum_{n=0}^{N-1}\phi(n). \tag{2.37}$$

The last term in (2.36) represents the leakage from neighboring subcarriers to the useful signal of each subcarrier, *i.e.*, ICI. This term can not be corrected, since both phase offset $\phi(n)$ and input data sequence $X(k)$ are random. Therefore it causes SNR degradation of the overall system. The only way to reduce interference due to the phase noise is to improve the performance of the oscillator, with associated cost increase [50].

A more detailed study of the effects of phase noise on OFDM system can be found in [50–53].

2.2.4.4 Receiver Timing Errors

The effect of sampling time offset in OFDM is the rotation of symbols. This rotation can be folded into the channel estimate and corrected easily. This section derives the amount of rotation assuming a small timing offset.[2]

As in the frequency offset case, we are going to relate the transmitted and recovered data symbols with respect to time offset. Let us use the same notation used in frequency offset case, represent transmitted symbols by $X(k)$, and represent the baseband equivalent of the time domain signal by $x_b(n)$. To prevent confusion, the impaired signals are represented with a *tilde* this time, so $\tilde{x}_b(n)$ represents the baseband signal with time offset and $\tilde{X}[k]$ represents the recovered symbols.

[2]Timing offset is assumed to be smaller than the unused part of the cyclic prefix.

Therefore, new OFDM process chain can be as follows;

$$X(k) \xrightarrow{IDFT} x_b(n) \xrightarrow{timing\ error} \tilde{x}_b(n) \xrightarrow{DFT} \tilde{X}(k)$$

The formula for $x_b(n)$ is already derived, and is given in (2.7). Timing error is caused by sampling the received signal at a wrong time. So $\tilde{x}_b(n)$ is nothing but the shifted version of $x_b(n)$ in time domain. Hence, in the case of a timing error of θ it can be written as

$$\begin{aligned} \tilde{x}_b(n) &= x_b(n \pm \theta) && (2.38) \\ &= \sum_{k=0}^{N-1} X(k) e^{j\frac{2\pi k}{N}(n\pm\theta)}. && (2.39) \end{aligned}$$

Here the sign of θ depends on whether sampling is performed before or after the correct time instant. Assuming θ to be positive, we use a minus sign hereafter. Now $\tilde{X}(k)$ can be calculated using $\tilde{x}_b(n)$ by DFT as

$$\begin{aligned} \tilde{X}(k) &= \frac{1}{N}\sum_{n=0}^{N-1}\left\{\sum_{m=0}^{N-1} X(m) e^{j\frac{2\pi m}{N}(n-\theta)}\right\} e^{-j\frac{2\pi kn}{N}} && (2.40) \\ &= \frac{1}{N}\sum_{n=0}^{N-1}\left\{\sum_{m=0}^{N-1} X(m) e^{j\frac{2\pi n}{N}(m-k)} e^{-j\frac{2\pi m\theta}{N}}\right\} && (2.41) \\ &= \frac{1}{N}\sum_{m=0}^{N-1}\underbrace{\left\{\sum_{n=0}^{N-1} X(m) e^{j\frac{2\pi n}{N}(m-k)}\right\}}_{N\Delta(m-k)} e^{-j\frac{2\pi m\theta}{N}} && (2.42) \\ &= \sum_{m=0}^{N-1} X(m)\Delta(m-k) e^{-j\frac{2\pi m\theta}{N}} && (2.43) \\ &= X(k) e^{j\frac{2\pi k\theta}{N}}. && (2.44) \end{aligned}$$

Equation 2.44 shows that a timing offset of θ causes only a rotation on the recovered data symbols. The value of the recovered symbol depends only on the transmitted data, but not the neighboring carriers. As a result, timing error does not destroy the orthogonality of carriers and the effect of timing error is a phase rotation which linearly changes with carrier order. Therefore, timing synchronization is not a very serious problem in OFDM based systems. Unless otherwise stated, perfect timing synchronization is assumed in the rest of this thesis.

2.2.4.5 Additive Noise

In addition to the distortions due to channel, additive noise is introduced to the transmitted signal due to wireless channel and impairments in the hardware of the receivers and transmitters. The main sources of noise are thermal background noise, electrical noise in the receiver amplifiers, and interference. In addition to this, noise can also be generated internal to the communications system as a result of ISI, ICI, and inter-modulation distortion (IMD) [54]. The noise decrease SNR resulting in an increase in the BER. The total effective noise at the receiver of an OFDM system can be modeled as additive white Gaussian noise (AWGN). AWGN has a uniform spectral density (making it white), and a Gaussian probability distribution. Additive noise is assumed to be white throughout this dissertation except Chapter 5 where this assumption is removed. Time and frequency domain noise samples are represented by $w_m(n)$ and $W_m(k)$ respectively where m is the OFDM symbol index and is dropped in some chapters for simplicity. The variance of noise is assumed to be σ_w^2.

2.2.4.6 Peak-to-Average Power Ratio

One of the major drawbacks of OFDM is its high peak-to-average-power ratio (PAPR). Superposition of a large number of subcarrier signals results in a power density with Rayleigh distribution which has large fluctuations. OFDM transmitters therefore require power amplifiers with large linear range of operation which are expensive and inefficient. Any amplifier non-linearity causes signal distortion and inter-modulation products resulting in unwanted out-of-band power and higher BER [55]. Moreover, digital to analog converters (DACs) and analog to digital converters (ADCs) are also required to have a wide dynamic range which increases complexity.

Discrete-time PAPR of mth OFDM symbol x_m is defined as [56]

$$PAPR_m = \max_{0 \le n \le N-1} \frac{|x_m(n)|^2}{E\{|x_m(n)|^2\}}. \tag{2.45}$$

Although PAPR is moderately high for OFDM, high magnitude peaks occur relatively rarely and most of the transmitted power is concentrated in signals of low amplitude, *e.g.* maximum $PAPR$ for an OFDM system with 32 carriers and QPSK modulation is observed statistically only once in 3.7 million years if the duration of an OFDM symbol is $100\,\mu$s [57]. Therefore, statistical distribution of the PAPR should also be taken into account in addition to PAPR value only.

Applying the central limit theorem, while assuming that N is sufficiently large, $x(n)$ is zero-mean complex-valued near Gaussian distributed random variable for all modulation options. Therefore, PAPR is independent of modulation used.

One way to avoid non-linear distortion is to operate the amplifier in its linear region. Unfortunately such solution is not power efficient and thus not suitable for battery operated wireless communication applications. Minimizing the PAPR before power amplifier allows a higher average power to be transmitted for a fixed peak power, improving the overall signal to noise ratio at the receiver. It is therefore important to minimize the PAPR. In the rest of this thesis, the distortion of the signal due to non-linear effects is ignored. In the literature, different approaches are used to reduce PAPR of OFDM signals (see [58] and references therein). Some of these include clipping [59], scrambling [60], coding [61], phase optimization [56], tone reservation [62] and tone injection.

2.2.5 Multiple-Accessing With OFDM

In this section, a single user system model is represented, where the available channel is used by a single user. Note that OFDM by itself is not a multi-access technique. However, it can be combined with existing multiple accessing methods to allow multiple users to access to the available channel. Please refer to Section 2.3.5 for more information.

2.3 Why OFDM is a Good Fit for Cognitive Radio

The underlying sensing and spectrum shaping capabilities together with flexibility and adaptiveness make OFDM probably the best candidate for cognitive radio systems. In the following, we present some of the requirements for cognitive radios and explain how OFDM can fulfill these requirements. A summary of these requirements and OFDM's strength in addressing them are presented in Table 2.1.

2.3.1 Adapting to Environment

Adaptivity is one of the key requirements for a cognitive radio [63]. By combining the measured information (awareness) with the knowledge of current system abilities and limitations, cognitive radio can adapt waveforms to interoperate with other friendly communication devices, choose the most appropriate communications channel or network for transmission, allocate appropriate frequency to

Table 2.1 OFDM cognitive radio.

Cognitive Radio Requirements	**OFDM's Strength**
Spectrum sensing	Inherent FFT operation of OFDM eases spectrum sensing in frequency domain.
Efficient Spectrum Utilization	Waveform can easily be shaped by simply turning off some subcarriers where primary users exist.
Adaptation/Scalability	OFDM systems can be adapted to different transmission environments and available resources. Some parameters include: FFT size, subcarrier spacing, CP size, modulation, coding, and subcarrier powers.
Advanced Antenna Techniques	MIMO techniques are commonly used with OFDM mainly because of the reduced equalizer complexity. OFDM also supports smart antennas.
Interoperability	With WLAN (IEEE 802.11), WMAN (IEEE 802.16). WRAN (IEEE 802.22), WPAN (IEEE 802.15.3a) all using OFDM as their physical layer techniques, interoperability becomes easier compared to other technologies.
Multiple accessing and spectral allocation	Support for multiuser access is already inherited in the system design by assigning groups of subcarriers to different users (OFDMA).
NBI Immunity	NBI affect only some subcarriers in OFDM systems. These subcarriers can be simply turned off.

transmit in an open area of spectrum, adapt the waveform to compensate for channel fading, and null an interfering signal [64].

The adaptivity in OFDM systems can be divided into two groups [65]: algorithm-selection level adaptivity and algorithm-parameter level adaptivity. In classical wireless systems, usually parameters of the algorithms, e.g. coding rate, have been adapted in order to optimize the transmission. However, in cognitive OFDM systems, algorithm type, e.g. channel coding method, can also be adapted in order to achieve interoperability with other systems and/or to further optimize the transmission. To achieve such adaptivity, a fully configurable hardware platform would be needed.

OFDM offers a great flexibility in this regard as the number of parameters for adaptation is quite large [17]. The transmission parameters that can be changed based on the spectrum awareness include bandwidth, FFT size, filters, windows, modulation, transmit power, and active subcarriers used for transmission. Moreover, the parameters that can be adapted depending on the characteristics of the environment in order to optimize the transmission include cyclic prefix size, coding rate/type, modulation type, interleaving method, pilot patterns, preambles/midambles, duplexing

method. In the next section, a detailed explanation of some of these adaptation techniques is discussed.

2.3.1.1 Adaptation Techniques in Multi-Carrier Systems

In this section, some of the popular adaptation techniques that are suitable for multi-carrier systems are discussed. Adaptation of the link between the transmitter and receiver depending on the variation of the channel, adaptation of the system and transmission parameters depending on the user and channel requirements, and adaptation of the multi-carrier signal are discussed briefly.

Link Adaptation: Link adaptation plays an important role in wireless communication systems because of the dynamic nature of the channel. Link adaptation ensures that the signal at the receiver side is in a form that can be processed and detected properly. It leads to efficient utilization of the resources including the bandwidth and power, as well as making sure that the communication is maintained to satisfy a desired service quality. The cost function can be multi-dimensional. Also, the number of factors that affect the link quality can be more than one. Among these factors power control, variable coding and modulation are very popular.

Adaptive modulation and coding provide a framework to adjust modulation level and forward error correction (FEC) coding rate depending on the link quality. Higher order modulations allow more bits to be transmitted for a given symbol rate. On the other hand, they are less power efficient, requiring higher energy per bit for a given BER. Therefore, higher order modulations should be used only when the link quality is high, as they are less robust to channel impairments. Similarly, strong FEC and interleaving provide robustness against channel impairments at the expense of lower data rate and spectral efficiency. As a result, by properly adapting the coding and modulation depending on the link quality, the average throughput can be maximized, which makes it very attractive for wireless packet data communication. Note that for mobile users, the instantaneous data rates vary depending on the link quality.

Without power control, adaptive coding and modulation increase the variation of throughput among users such that users with good link quality always have high throughput, but users with bad link quality always have low throughput [66]. On the other hand, power control tries to equalize the link quality of the users so that all the receivers have a constant signal-to-interference ratio (SIR). This allows reducing the interference from other sources while making sure that each user gets just

enough power to be able to detect what is being transmitted by the desired transmitter. If the transmitter sends more power for a specific user, the user benefits from it by having a better link quality, but the level of interference for the other users increases accordingly. On the other hand, if the user does not receive enough power, a reliable link cannot be established. In order to establish a reliable link while minimizing interference to other users, the transmitter should continuously control the transmitted power level. From a user perspective, power control ensures a constant service quality across the network, and such adaptation is suitable for real time audio and video communication applications. Power control can be combined with adaptive coding and modulation scheme to achieve both benefits for better resource utilization [67].

In OFDM systems, it is also possible to adapt the modulation and power for each subcarrier individually. Note that since the bandwidths of OFDM systems are much larger than the coherence bandwidth of the channel, different carriers experience different signal-to-interference-plus-noise ratio (SINR). Therefore, the modulation level or the power on different carriers can be changed depending on the link quality observed at that carrier [68].

Transmitting different modulation on each carrier requires a large overhead for signaling. Therefore, approaches that group the neighboring carriers into subsets and use the same modulation in each group of carriers are preferred. This is called subband adaptive OFDM and illustrated in Fig. 2.7. The signaling can also be avoided in time division duplexing (TDD) systems under certain assumptions. Unlike frequency division duplexing (FDD) systems, where the channel on the downlink and uplink are different, in TDD systems, using the assumption of the reciprocal and slow varying channel, the transmitter and receiver can be assumed to experience the same channel response. Therefore, this might eliminate the need for signaling of the channel state information to the transmitter if the channel estimates are used as the link quality measures. However, the receiver still needs to know which modulation is used at the transmitter for each group. Blind modulation detection techniques can be used for this purpose [69, 70] as there is enough *a priori* information to estimate the modulation type. Note that although the channels could be the same, the interferences observed in transmitter and receiver are not necessarily the same because the interferer may be physically closer to transmitter or receiver.

Even though adaptive power control has a long and rich history for wireless communication systems, the adaptive coding and modulation recently become popular due to the increased interest for high data rate communications, and they are becoming an integral part of most of the new gen-

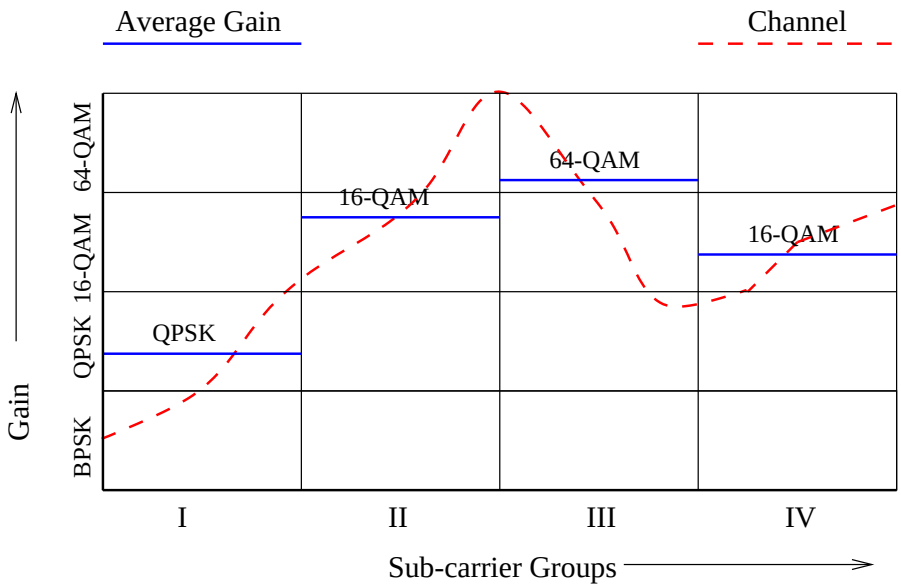

Figure 2.7 Modulation mode selection based on channel quality in subband adaptive OFDM systems.

eration standards. Adaptive modulation and coding are employed for WLAN and WMAN systems successfully. Both systems use OFDM as their transmission technique. IEEE 802.11a physical layer, for example, allow four different modulation options (BPSK, QPSK, 16-QAM, and 64-QAM) with different coding rates. The coding rates are obtained with different puncturing patterns to a mother convolutional code, resulting in 8 different modulation/coding options [10]. Therefore, a data rate ranging from 6 to 54 Mbit/s can be obtained by using various modes. BPSK, QPSK, and 16-QAM are used as mandatory modulation formats, whereas 64-QAM is an optional mode.

Adaptation with Multiple Antennas: Adaptive antennas and adaptive beam forming techniques have also been studied extensively to increase the capacity and/or to improve the performance of wireless communication systems [71]. The adaptive antenna systems shape the radiation pattern in such a way that the information is transmitted (for example, from a base station) directly to the mobile user in narrow beams. This reduces the probability of another user experiencing interference in the network, resulting in improved link quality, which can also be translated into increased network capacity. Although, adaptive beam forming is an excellent way to utilize multiple antenna systems to enhance the link quality, recently different flavors of the usage of multi-antenna systems have gained significant interest. Space-time processing and multiple-input multiple-output (MIMO) antenna systems are some new developments that allow further usage of multiple antenna systems in

wireless communications. Adaptive implementation of these technologies is important for successful and efficient integration of them into wireless communication systems.

Combining adaptive antennas with OFDM for operation in a faded delay-spread channel is discussed in [72]. In this adaptive beamforming algorithm, a short training process first updates the weight vector and then a decision-directed technique is used for updating the weight vector. It has been demonstrated that this algorithm is able to extract desired signals while suppressing co-channel interferers.

MIMO and multi-antenna systems bring about a new dimension to wireless channel. It can provide huge capacity and/or improved performance gains by exploiting spatial selectivity of the channel. However, these gains, in reality, depend heavily on the statistical properties of the channel and the correlations between antenna elements. One of the factors that affects the antenna correlation is the characteristics of the scattering environment. Therefore, optimal way of using multiple antenna systems depends on the situation awareness. If the transmitter knows the instantaneous channel gains (the MIMO channel matrix), it can adapt the transmission to maximize the capacity of MIMO system [73, 74]. Similarly, the instantaneous antenna correlation values can be exploited to adapt the transmission. In many cases, estimation of the perfect instantaneous channel state and antenna correlation information, and feeding this information back to the transmitter might not be possible. This is the case especially when the mobility is high. Instead, other parameter measures like partial (statistical) channel information, average channel selectivity or angular spread would be useful for adapting the transmitter and receiver. Advanced signal processing techniques to calculate these partial channel and correlation information are needed.

In MIMO-OFDM, the SNR not only varies over time and frequency but also depends on a number of parameters including the way the transmitted signals are mapped and weighed onto the transmit antennas, the processing technique used at the receiver, and the antenna polarization and propagation parameters such as mutual coupling between antennas [75]. Space-time adaptation aims to choose the best way of combining antennas either through space-time coding approach, beamforming or using the BLAST architecture. Those approaches can be coupled with adaptation of OFDM parameters, e.g., on each OFDM subcarrier, adaptive space-time coding, beamforming along with adaptive power and bit loading schemes can be employed yielding a space-time frequency adaptation scenario. The process can be generalized for multiuser MIMO-OFDM systems.

Adaptive Cyclic Prefix Size: The CP provides multipath immunity and tolerance to symbol time synchronization errors. In order to remove the distortion due to multipath, the length of the CP should be larger than the maximum excess delay of the channel. On the other hand, large CP size reduces the transmission efficiency because of the redundancy that it introduces. Conventional OFDM system uses fixed-length cyclic prefix to combat the ISI caused by multipath fading. This may cause considerable performance degradation when the CP length is less than the channel delay spread [44, 76]. On the other hand it may decrease the system power and spectral efficiency when it is much larger.

The CP length can be changed adaptively depending on the channel conditions, specifically maximum excess delay of the channel. Adaptive CP is studied in [48, 77]. In the proposed algorithms the CP length is varied according to the current delay spread of the channel and the length information is conveyed to the receiver by signaling. This adaptation requires the knowledge of the maximum excess delay of the channel, estimation of which is studied in Chapter 3.

Adaptive Interleaving: Interleaving is a method that is used in communication systems to randomize the bursty channel errors. This can greatly improve the performance of channel coding which works better when the errors do not occur in bursty fashion. In OFDM, interleaving can be achieved in both time and frequency. Time interleaving is similar to the single carrier systems. Frequency interleaving is achieved by changing the order of symbols in frequency domain. Interleaving pattern is another parameter that can be changed adaptively to obtain better shuffling of the symbols in time and frequency domain. Symbols can be rearranged according to instantaneous channel state information (CSI) of the OFDM subcarriers so as to minimize the BER after decoding. This approach is proposed in [78] and its performance is analyzed in [79] by finding bounds on the system BER.

Adaptive Subcarrier Spacing: Subcarrier spacing, or number of subcarriers for a given bandwidth, is one of the most critical OFDM parameters. Subcarrier spacing can be changed adaptively depending on the Doppler spread, delay spread, and SNR of the channel. As subcarrier spacing increase, ICI effect decreases as the spacing between subcarriers becomes larger compared to the Doppler shift. The raw BER performance of an OFDM system is shown in Fig. 2.8 as a function of FFT size. A center frequency of 5.8 GHz, transmission bandwidth of 3.5 MHz, and mobile speed of 100 km/h are used in this figure. Note that since the bandwidth is fixed, x-axis can be interpreted as decreasing

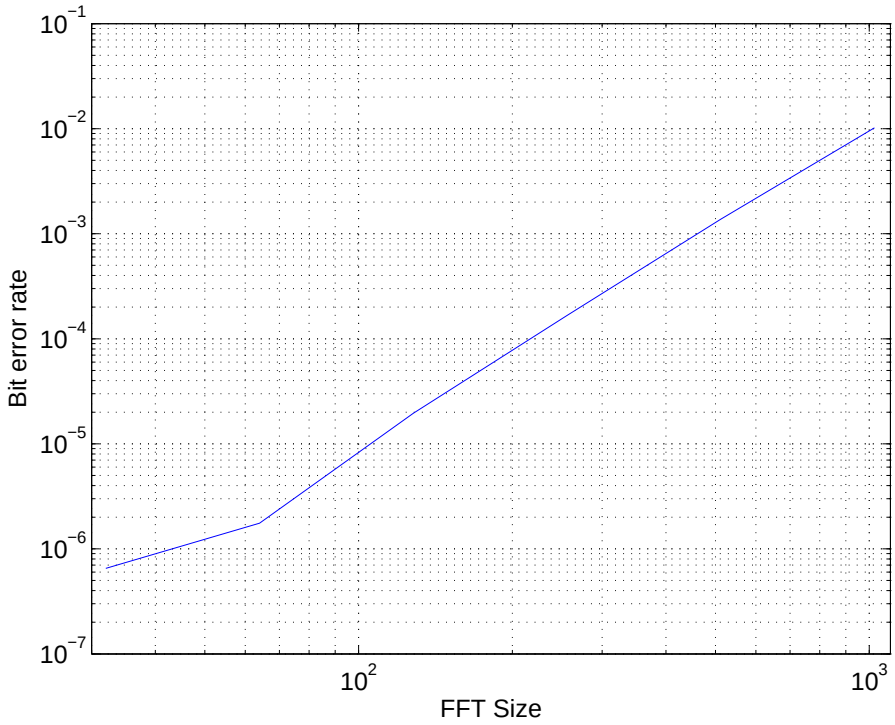

Figure 2.8 Bit error rate of an OFDM system in time-varying channel as a function of FFT size. The transmission bandwidth is 3.5 MHz, the center frequency is 5.8 GHz and the mobile speed is 100 km/h.

subcarrier spacing. Large subcarrier sizes cause higher PAPR and the receiver becomes less immune to the frequency synchronization errors as the number of subcarriers increases.

While increasing subcarrier spacing cures the ICI problem, it means shorter symbol duration. Therefore, the relative size of required CP becomes larger, decreasing bandwidth efficiency. The effect of number of subcarriers on the system performance is investigated in [80]. The optimum number of subcarriers is found to be increasing with delay spread and the coherence time. The calculation of optimum subcarrier spacing for different channel conditions is studied in [48] by simulation and analytically in [81].

Using variable FFT sizes is proposed for IEEE 802.16e standard to implement scalable OFDMA (see [82] and references therein) in which a constant subcarrier spacing is obtained by changing the FFT size and system bandwidth. Doppler spread knowledge can be used for selecting the optimum subcarrier spacing adaptively. Estimation of Doppler spread is discussed in Chapter 4.

Adaptive Pilot Pattern: Pilot symbols can be inserted into the transmitted symbol stream regularly. These symbols can be used to find the channel values at their corresponding locations and these estimates can be filtered or interpolated to calculate the estimates of the channel parameters at other locations [83]. The rate of insertion of pilots in frequency and time direction (from OFDM symbol to OFDM symbol) can not be set arbitrarily. It depends on the variation of the channel parameters in time and frequency. It should be noted that an optimum pilot allocation is a trade-off between wasted energy in unnecessary pilot symbols, the fading process not being sampled sufficiently, and the spectral efficiency of the system. Hence, an optimum pilot allocation for a given channel might not be optimal for another channel as the fading process is different.

Some other important elements for pilot arrangements can be the allocation of power to the pilots with respect to the data symbols, the transmitted modulation for the pilot tones *etc.* In most cases, the power for pilot tones and data symbols are equally distributed, however, it does not have to be uniform. For example, the channel estimation accuracy can be improved by transmitting more power at the pilot tones compared to the data symbols. Yet, this reduces the SNR over the data transmission for a given total power.

It is clear from the above discussion about the pilot allocation that a better system performance can be obtained when the system is adaptive [84–87]. In this case, the information about the channel statistics becomes very critical. The pilot allocation in the frequency direction requires the delay spread estimation, whereas the one in time direction requires Doppler spread estimation. If these estimates are available, then a pilot scheme using relatively less pilots but still providing an acceptable performance can be utilized. If this information is not available, then the pilot scheme can be designed based on the worst channel condition, *i.e.* the maximum expected delay spread and mobile speed. In [88], the pilot patterns are chosen adaptively based on the prediction of the channel estimation error at the receiver. The transmitter tries to guarantee the minimum required SNR by using the minimum number of pilot subcarriers. Adaptation is performed over a block of OFDM symbols.

2.3.1.2 Adaptation in Mobile OFDM Systems

OFDM is a suitable solution for high data rate transmission because of its immunity to the time dispersion of the channel. However, frequency dispersion, or time-varying channel introduces another

problem as OFDM systems loose their orthogonality when the channel varies over the OFDM symbol time, *i.e.* when the Doppler spread is a significant portion of the subcarrier spacing [89].

The output of IFFT at the receiver can be obtained as (2.31). The second term in the right hand size of (2.31) is the power leakage from the neighboring subcarriers and it is called ICI. When there is no time variation in channel during a block period, *e.g.* $h_l(n) = h_l$, the resulting ICI is zero.

For a fixed total bandwidth, the ICI contribution increases as the number of subcarriers increases. This happens since the OFDM symbol period increases and hence the variation of channel within the symbol duration. Analysis of the effects of Doppler spread for OFDM systems is given in [47,90,91]. Tight and general bounds for ICI due to Doppler spread are found in [92]. The ICI power is reported to be linearly proportional with the square of maximum Doppler frequency and symbol duration ($f_D T_S$). In other words, the ratio between the maximum Doppler frequency and subcarrier spacing determines the effect of ICI.

While increasing the subcarrier spacing may decrease the ICI, it increases the energy loss due to the cyclic prefix extension of OFDM systems. Hence the optimum window size is a function of frequency and time selectivity of the channel. This trade-off is shown in Fig. 2.9. The BER performance of an OFDM system with 3.5 MHz bandwidth operating at 5.8 GHz center frequency is shown for different FFT sizes and CP lengths. The SNR of the system is 30dB and mobile speed is 100 km/h. As opposed to the Fig. 2.8, the affect of energy loss due to CP is taken into consideration in this figure. However, the length of the CP is chosen larger than the delay spread of the channel in order to only show the affect of CP and FFT sizes. As this figure shows the subcarrier spacing (or FFT size) that gives optimum performance is a function of the delay spread and Doppler spreads of the channel.

Transmitter adaptation can be used to overcome the mobility problem. The subcarrier spacing can be changed depending on the Doppler and delay spread of the channel in order to reduce ICI while keeping the bandwidth usage maximum. Calculation of the optimum subcarrier spacing in doubly dispersive channels is investigated in [48, 81]. The ICI problem can also be solved using advanced receiver algorithms such as frequency domain equalization or interference cancellation. However, these algorithms are computationally complex and they can only eliminate some of the disturbance due to ICI.

Another factor that needs to be considered in mobile OFDM systems is the estimation of fast varying channel. When the training symbols transmitted before the data symbols are used for

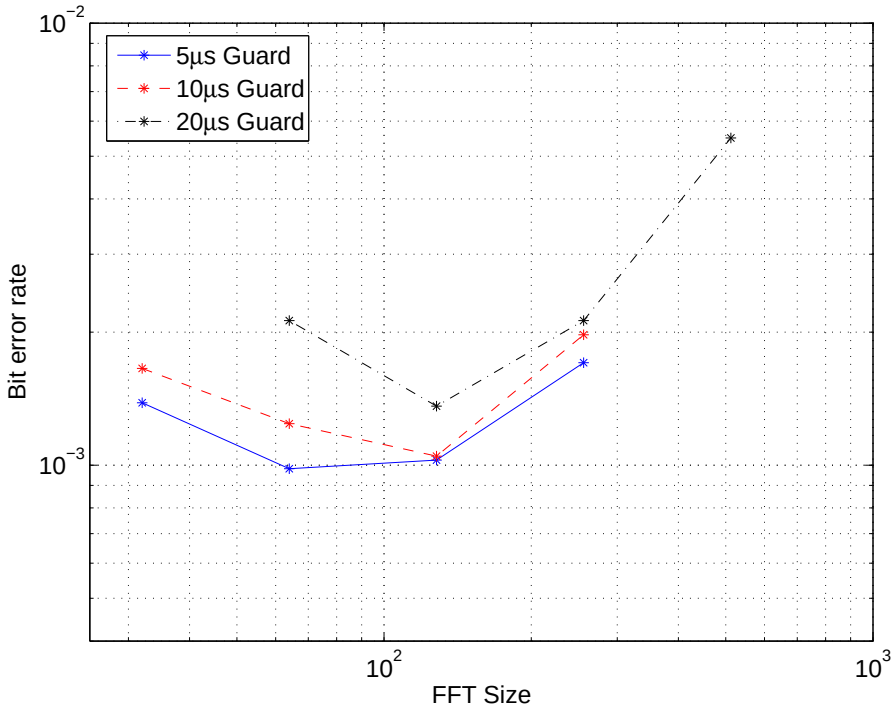

Figure 2.9 Bit error rate of an OFDM system in time-varying channel as a function of FFT size and guard interval length. The transmission bandwidth is 3.5 MHz, the center frequency is 5.8 GHz, the mobile speed is 100 km/h and SNR is 30 dB.

estimation, an error floor for time-varying channels is introduced. To overcome this problem, pilot subcarriers or midambles can be used [93].

2.3.2 Spectrum Sensing and Awareness

Cognitive radio should be able to scan the spectrum and measure different channel characteristics such as power availability, interference, and noise temperature [94]. In addition, the system should be able to identify different users' signals in the spectrum and also identify if they are either licensed or rental users. These abilities allow cognitive radio system to identify unused parts of the spectrum and spectral opportunities.

However, since for a rental system it is important not to interfere with other licensed systems using the spectrum, other measures should be taken to guarantee an interference-free communication between rental users. One approach is to share the spectrum sensing information between multiple cognitive radio devices to decrease or even eliminate the probability of interference with licensed

users [95]. On the other hand, more sophisticated algorithms can be used for sensing the spectrum (see Chapter 6 and 7).

While the efficiency of the spectrum sensing and analyzing process is important for a successful implementation of cognitive radio, the processing time can be even more important. The periodicity of spectrum sensing should be short enough to allow for detection of new spectrum opportunities and, at the same time, to detect licensed users accessing the previously-identified-as-unused parts of the spectrum. On the other hand, if spectrum sensing is done so frequently, the overhead of sharing such information increases reducing the spectrum efficiency of the whole system not to mention the increase in system complexity. In OFDM systems, conversion from time domain to frequency domain is achieved inherently by using DFT. Hence, all the points in the time-frequency grid can be scanned without any extra hardware and computation because of the hardware reuse of FFT cores. Using the time-frequency grid, the selection of bins that are available for exploitation (spectrum holes) can be carried out using simple hypothesis testing [96]. The DFT outputs can be filtered across time and frequency dimensions to reduce the uncertainty in detection as well [26, 27]. Note that the resolution of the frequency grid is dependent on subcarrier spacing.

2.3.3 Spectrum Shaping

After a cognitive radio system scans the spectrum and identifies active licensed users and available opportunities, comes the next step: spectrum shaping. Theoretically, it is desired to allow the cognitive users to freely use available unused portions of the spectrum.

Cognitive users should be able to flexibly shape the transmitted signal spectrum. It is desired to have control over waveform parameters such as the signal bandwidth, power level, center frequency, and most of all a flexible spectrum mask. OFDM systems can provide such flexibility due to the unique nature of OFDM signaling. By disabling a set of subcarriers, the spectrum of OFDM signals can be adaptively shaped to fit into the required spectrum mask. Assuming the spectrum mask is already known to the cognitive radio system, choosing the disabled subcarriers is a relatively simple process [97].

The main parameters of an OFDM system that can be used to shape the signal spectrum are number of subcarriers, subcarrier's power, and pulse-shaping filters. Increasing the number of subcarriers for a fixed bandwidth allows the OFDM system to have a higher resolution in the frequency

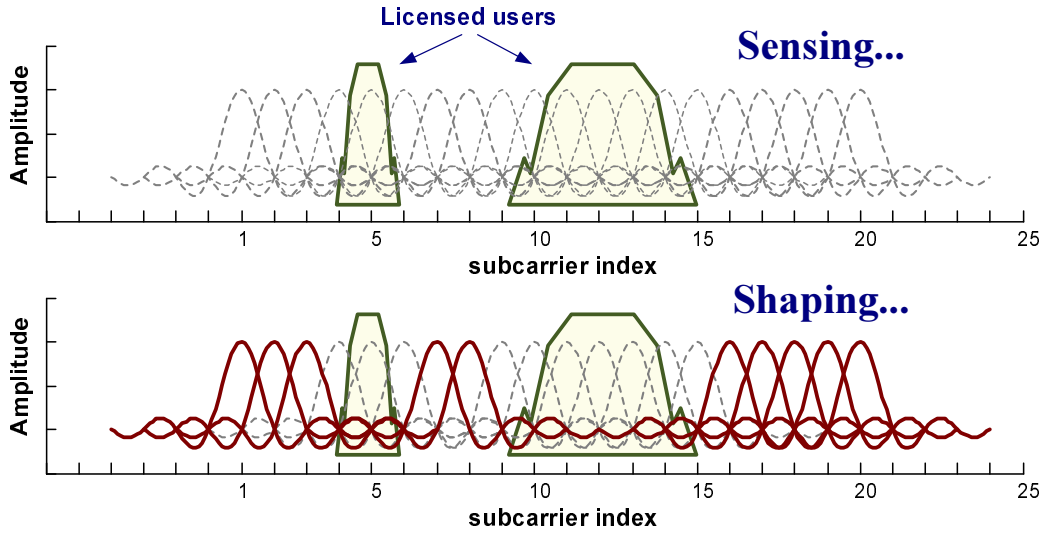

Figure 2.10 Spectrum sensing and shaping using OFDM.

domain. However, this results in increasing the complexity of the FFT operations and thus increasing the overall system complexity.

Subcarrier power can be used to shape the signal into the desired mask. One reason to assign subcarriers different powers is to better fit into the channel response [98]. For example, subcarriers with higher SNR values can be assigned lower power than those with lower SNR to improve the overall system BER. Another reason is to reduce the adjacent channel interference from an OFDM system by reducing the power assigned to edge subcarriers.

An example of spectrum sensing and shaping procedures in OFDM-based cognitive radio systems is illustrated in Fig. 2.10. Two licensed users are detected using the output of FFT block, and subcarriers that can cause interference to licensed user are turned off. The transmitter then uses the free parts of the spectrum for signal transmission. In addition, pulse-shaping filters can also be used to reduce the interference to adjacent bands. More discussions on reducing interference is introduced in section 2.4.5.

2.3.4 Advanced Antenna Techniques

Advanced antenna techniques are not necessarily required for cognitive radios. However, they are desirable as they provide better spectral efficiency which is the primary motivation for cognitive radio. Smart antennas and multiple-input multiple-Output (MIMO) systems can be used to exploit the spatial dimension of spectrum space (e.g. through beam forming) to improve the ef-

ficiency. In essence multi-antenna systems can help to find spectral opportunities in the spatial domain and can help to exploit these opportunities in full. The use of MIMO techniques offers several important advantages including spatial degree of freedom, increased spectral efficiency and diversity [99]. These advantages can be used to increase the spectrum utilization of the overall system. Furthermore, beamforming, diversity combining and space-time equalization can also be applied to cognitive OFDM systems. Another application of adaptive antenna techniques is the reduction of the interference in OFDM systems [100].

MIMO systems commonly employ OFDM as their transmission technique because of simple diversity combination and equalization, particularly at high data rates [101]. In MIMO-OFDM, the channel response becomes a matrix. Since each tone can be equalized independently, the complexity of space-time equalizers is avoided and signals can be processed using relatively straightforward matrix algebra. Moreover, the advantages of OFDM in multipath are preserved in MIMO-OFDM system as frequency selectivity caused by multipath increases the capacity.

2.3.5 Multiple Accessing and Spectral Allocation

The resources available to a cognitive system have to be shared among users. Several techniques can be used to achieve such tasks. OFDM supports the well-known multiple accessing techniques such as time division multiple access (TDMA), frequency division multiple accessing (FDMA) and carrier sense multiple accessing (CSMA). Moreover, code division multiple access (CDMA) can also be used together with OFDM for multiplexing different users, in which case the transmission is known as multi-carrier code division multiple access (MC-CDMA) or multicarrier direct spread code division multiple access (DS-CDMA) [102].

OFDMA, a special case of FDMA, has gained tremendous attention recently with its usage in mobile Worldwide Interoperability for Microwave Access (WiMAX) [82, 103]. In OFDMA, subcarriers are grouped into sets each of which is assigned to a different user. Interleaved, randomized, or clustered assignment schemes can be used for this purpose. Hence, it offers very flexible multiple accessing and spectral allocation capability for cognitive radios without any extra complexity or hardware. The allocation of subcarriers can be tailored according to the spectrum availability. The flexibility and support of OFDM systems for various multiple accessing enables the interoperability and increases the adoption of cognitive radio as well.

2.3.6 Interoperability

Another desirable feature of cognitive radio is interoperability. Interoperability can be defined as *the ability of two or more systems or components to exchange information and to use the information that has been exchanged* [104]. Since cognitive radio systems have to deal with licensed users as well as other cognitive users, the ability to detect and encode existing users' signals can expedite the adoption and improve the performance of cognitive radio systems. Furthermore, some recent unfortunate events manifested the importance of interoperability in terms of wireless communications for the first responders [105, 106]. For interoperability problems, cognitive radio will improve the disaster relief operations by developing the coordination between first responders [107,108]. For such tasks, OFDM is one of the best candidates as OFDM signaling has been successfully used in various technologies. Systems based on OFDM includes 802.11a and 802.11g Wireless LAN standards, digital audio broadcasting (DAB), DVB-T, and WiMAX. Fig. 2.11 shows some of the OFDM-based wireless technologies according to communication range. As shown in this figure, OFDM has been used in both short range and long range communication systems. Hence, a cognitive radio system employing OFDM can communicate with systems using other OFDM-based technologies with much ease. Only the knowledge of the signal parameters used by the desired users are needed (see Table 2.2). However, for such task to be successful, the cognitive radio system should be built around a software-defined radio architecture. In addition, the cognitive radio system should have all the standard-related information required to decode other signals, such as the data and pilot mapping to the frequency subcarriers, frame structure or the coding type and rate.

2.4 Challenges to Cognitive OFDM Systems

As an intelligent system with features such as awareness, adaptability and learning, cognitive radio represents the future of wireless systems with the promise of offering solutions to various communication problems as outlined in the previous section. However, with this new technology, new challenges appear, raising interesting research topics. In the considered OFDM based cognitive radio systems, the challenges can be grouped into three categories as illustrated in Fig. 2.12. The first category includes the challenges that are the unique to classical OFDM systems including PAPR, sensitivity to frequency offset and phase noise, synchronization *etc.* The second category includes problems faced by all cognitive radios such as spectrum sensing, cross layer adaptation, and interference avoidance. Our main focus in this chapter is on the third category: challenges that arise

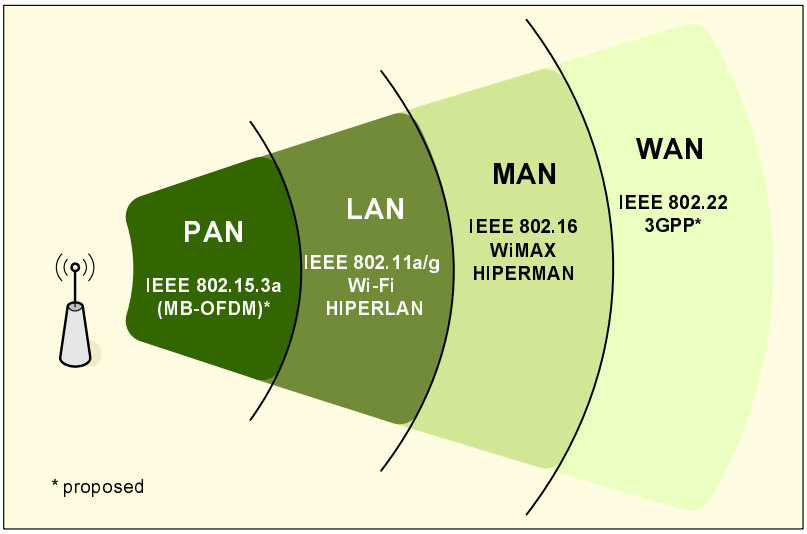

Figure 2.11 OFDM-based wireless technologies.

Table 2.2 OFDM-based wireless standards.

Standard	**IEEE 802.11(a/g)**	**IEEE 802.16(d/e)**	**IEEE 802.22**	**DVB-T**
FFT Size	64	128, 256, 512, 1024, 2048	1024, 2048, 4096	2048, 8192
CP Size [3]	1/4	1/4, 1/8, 1/16, 1/32	variable	1/4, 1/8, 1/16, 1/32
Bit per Symbol	1, 2, 4, 6	1, 2, 4, 6	2, 4, 6	2, 4, 6
Pilots	4	variable	96, 192, 384	62, 245
Bandwidth (MHz)	20	1.75 to 20	6, 7, 8	8
Multiple Accessing	CSMA	OFDMA /TDMA	OFDMA /TDMA	N/A

when OFDM technique is employed by cognitive radio systems. In the following, some challenges and approaches for solving these are given.

2.4.1 Spectrum Shaping

One of the main challenges in OFDM cognitive radio systems is spectrum shaping. In OFDM-based systems, spectrum shaping means determining the subcarriers to be used by the OFDM system while keeping the interference to and from primary users at a negligible level. Once spectrum sensing

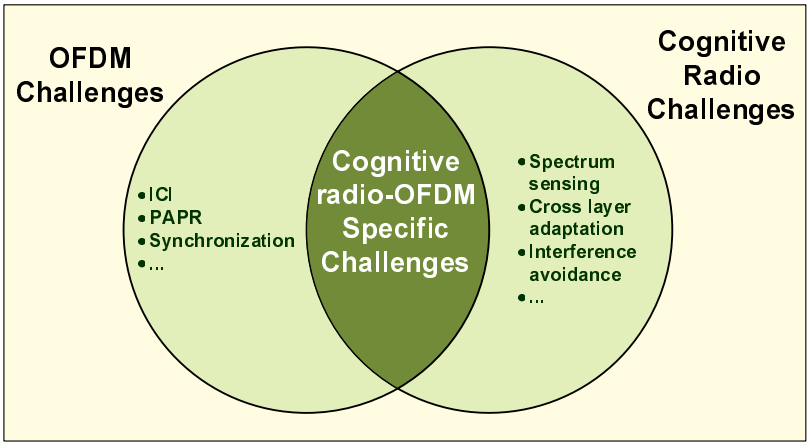

Figure 2.12 Research challenges in cognitive radio and OFDM.

information is acquired, this knowledge should be utilized to select the subcarriers to be used by the secondary/cognitive users. This problem is addressed in [109] by using energy detectors over each subcarrier. Moreover, a detection criterion is used to determine used subcarriers. Spectrum sensing is directly related to the sensing problem for spectrum hole identification. However, the cognitive radio might prefer to skip some opportunities depending on the power and network traffic requirements.

2.4.2 Effective Pruning Algorithm Design

Once the subcarriers to be used are determined, there might be many subcarriers that are deactivated. In such a case, the efficiency of FFT algorithms can be increased and/or execution time can be decreased by removing operations on input values which are zero; a process known as pruning. Designing effective pruning algorithms is important for cognitive OFDM systems for achieving higher performance. Specific implementation of pruning technique for CR-OFDM systems is discussed in [110].

2.4.3 Signaling Transmission Parameters

OFDM system can adjust its waveform by turning off some subcarriers in order to exploit the available spectrum holes (see Fig. 2.10). The receiver, however, should be informed about subcarriers that are deactivated and that are to be used. Signaling of this information should be performed carefully in order to prevent interference to primary users while keeping the bandwidth loss at minimum. Detection of those unused subcarriers can also be performed blindly as proposed in Chapter 8. One

method to reduce the overhead due to signaling is proposed in [111]. The activation/deactivation of subcarriers is performed over a block of subcarriers instead of each individual subcarrier. Hence, the signaling overhead can be reduced by a factor of each block's size. Moreover, depending on the channel quality and available resources, parameters like FFT size, CP size *etc.* can also be changed and this information should also be conveyed to the receiver.

2.4.4 Synchronization

Synchronization is another important issue that needs to be addressed in OFDM system design. With the introduction of cognitive radio, new aspects are introduced to the problem. The narrow-band interference (NBI), which can interfere with the preamble, is one of the problems [112]. Furthermore, the incomplete subcarrier set might be an issue for preambles, and pilots might fall into unused subcarriers if used. Moreover, if multiple user accessing is employed, the subcarriers can be assigned to different users. To keep the orthogonality between subcarriers and avoid interference, all users should be synchronized to the receiver. In [112], it is shown that longer preambles are needed in CR-OFDM systems as compared to conventional systems. Moreover, new preamble structures are introduced and their performance for time and frequency synchronization is investigated.

2.4.5 Mutual Interference

Mutual interference should be carefully considered when designing cognitive radio systems. The side lobes of modulated OFDM subcarriers are known to be large. As a result, there is power leakage from used subcarriers to nulled subcarriers which causes interference to the licensed users. Various methods are proposed in the literature to reduce this leakage and to enable co-existence of cognitive-OFDM systems with primary license owner systems. One method is to make the *sinc* function decay faster by windowing the time domain OFDM samples [113]. Similar techniques have already been investigated to reduce ICI and out-of-band radiation in OFDM systems [114, 115]. In [113], a raised-cosine window is applied. By changing the roll-off factor of the raised-cosine window, interference reduction of up to 6 dB has been achieved. Figs. 2.13 and 2.14 show the raised-cosine window shape for different roll-off values and corresponding power spectral densities. The drawback of this method is the reduction of system throughput due to the temporal extension of time domain signal to maintain orthogonality. Another method for reducing the interference is to adaptively deactivate the subcarriers that are adjacent to the subcarriers occupied by licensed users [113]. This

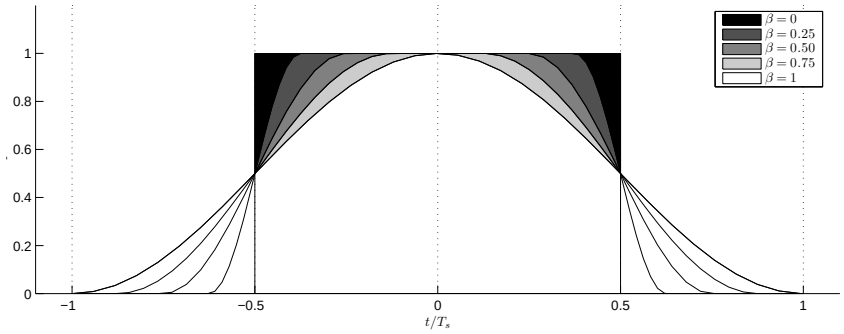

Figure 2.13 Raised cosine windowing with different rolloff (β) values.

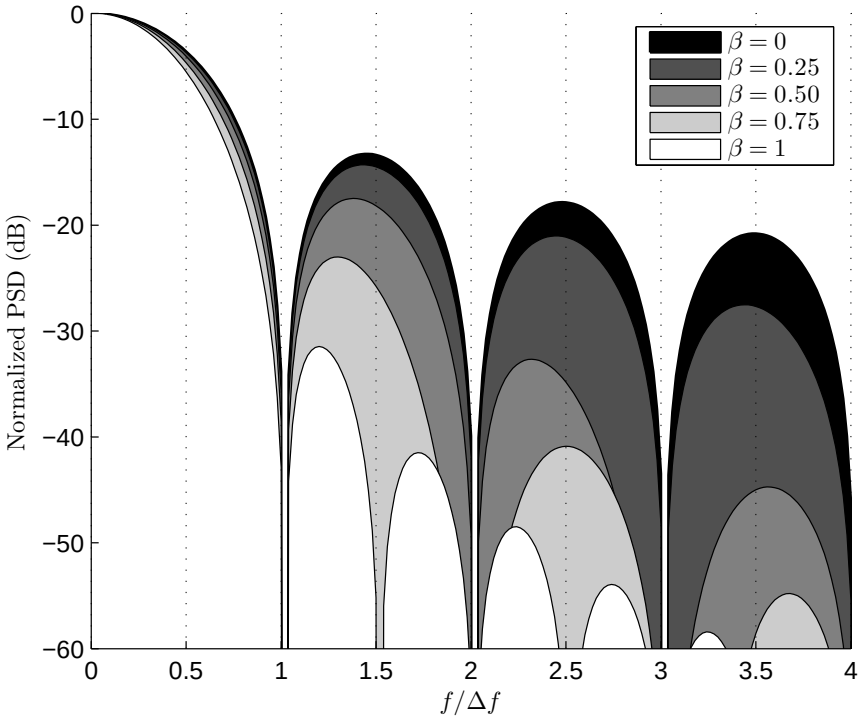

Figure 2.14 Rolloff effect on the PSD of a single OFDM subcarrier.

way the interference can be greatly reduced as most of the interference comes from the neighboring subcarriers. However, the obvious disadvantage of this method is the reduction of spectral efficiency. Instead of deactivating the neighboring subcarriers, their values can be determined actively in order to cancel the interference in the deactivated bands. This technique is proposed in [116] and [117] and referred as active interference cancellation and cancellation carriers respectively. It is shown that the performance can be improved, however, determination of the values for cancellation subcarriers is

complex as it requires optimization. One last method for reducing the interference to and from the narrowband primary users is subcarrier weighting [118,119]. In this method, the subcarrier weights are determined in such a way that the sidelobes of the transmission signal are minimized according to an optimization algorithm which allows several optimization constraints. This way, more than 10 dB reduction in the sidelobes of OFDM signal can be achieved. Note that subcarrier weighting requires constant envelope modulation such as BPSK or QPSK. Moreover, the receiver does not need to know the weighting sequence as the phase information is not changed.

In addition to the aforementioned challenges, there are other issues for practical implementation of OFDM cognitive radio systems. While cognitive radio is such a promising technology, more research is needed to build practical system with affordable complexity.

2.5 A Step Toward Cognitive-OFDM: Standards and Technologies

As cognitive radio concept is attracting more interest everyday, recently developed standards are considering more cognitive features. Dynamic frequency allocation, transmit power control (TPC), and spectrum sensing are just a few examples of features that are included in some of the current standards. These can be considered as a step toward the future implementation of a cognitive radio. It is worth to note that most of these standards consider OFDM as their choice for transmission technology (see Fig. 2.11).

2.5.1 WiMAX - IEEE 802.16

One of the technologies that are getting a fair amount of interest lately –in both academia and industry– is WiMAX. The first WiMAX standard, IEEE 802.16a [120], operates in the 10 to 66 GHz range. In this frequency range, only line-of-sight (LOS) communication is possible. The standard later evolved in 2004 to the IEEE 802.16-2004 [12]; also know as IEEE 802.16d. The IEEE 802.16-2004 standard supported the operation in the 2 to 11 GHz range allowing for a non-line-of-sight (NLOS) communications. It provides point to multipoint access for fixed subscribers. The IEEE 802.16e-2005 [103] standard updates and extends this standard to allow for mobile subscriber stations traveling at vehicular speeds. A scalable version of orthogonal frequency division multiple access (OFDMA) is introduced improving the overall system performance. While IEEE's role is to develop standards for the PHY and medium access control (MAC) layers, WiMAX forum ensures compatibility and interoperability between vendors' equipments through its certification process.

OFDMA PHY mode is probably the most interesting mode supported by WiMAX. Using OFDM signaling, OFDMA PHY mode enables a WiMAX base station (BS) to support multiple fixed or mobile users at the same time. In this mode, a BS system utilizes the available channel by dividing the available subcarriers into subchannels. A number of subchannel grouped with a number of OFDMA symbols constitutes a slot. A slot is defined as the minimum data allocation unit [12]. The slot definition shows that the system resources are being shared between users in two domains. The first dimension is frequency which is represented by the number of subchannels in each slot. The second dimension is time which is represented by number of OFDMA symbols. Fig. 2.15 shows the OFDMA signal structure used in WiMAX. Note that this figure is only for illustration purposes and thus the number of subcarriers or the slot size does not reflect the actual numbers used by the standard.

In WiMAX-based systems, users can be assigned different bandwidths, time durations, transmit power levels, and modulation orders (see Table 2.2) based on various parameters such as user carrier-to-interference-plus-noise ratio (CINR), received signal strength indicator (RSSI) or the available bandwidth. Moreover, OFDMA PHY offers multiple FFT sizes, CP sizes, and pilot allocation schemes. The FFT size can be selected as 128, 256, 512, 1024 or 2048 depending on the transmission bandwidth[4]. Similarly, the CP length can be set to 1/4, 1/8, 1/16 and 1/32 time the OFDM symbol length. The CP size can be changed depending on the various environmental characteristics. With all these adaptive features, WiMAX has the ability to adapt to various channel conditions and communication scenarios. Indeed, a WiMAX BS measures the available channel and received signal parameters, makes a plan on what the most appropriate settings for communication with current subscribers (with certain goals in mind such as maximum throughput, quality of service (QoS).) is, and executes this plan.

WiMAX standard is very rich in terms of advanced antenna techniques as well. Table 2.3 shows the MIMO features available in the mobile-WiMAX standard IEEE 802.16E-2005 [103]. Although these antenna techniques are not requirements, they are well suited to cognitive radio and useful for achieving high data rates.

The amendment to IEEE 802.16 standard IEEE 802.16h, which is currently being developed, introduces cognitive features to WiMAX. The goal is to achieve coexistence of WiMAX devices in unlicensed bands. Furthermore, methods for coexistence with primary users are also developed.

[4]This is known as scalable OFDMA. Various FFT sizes are used to keep the subcarrier spacing constant for different transmission bandwidths

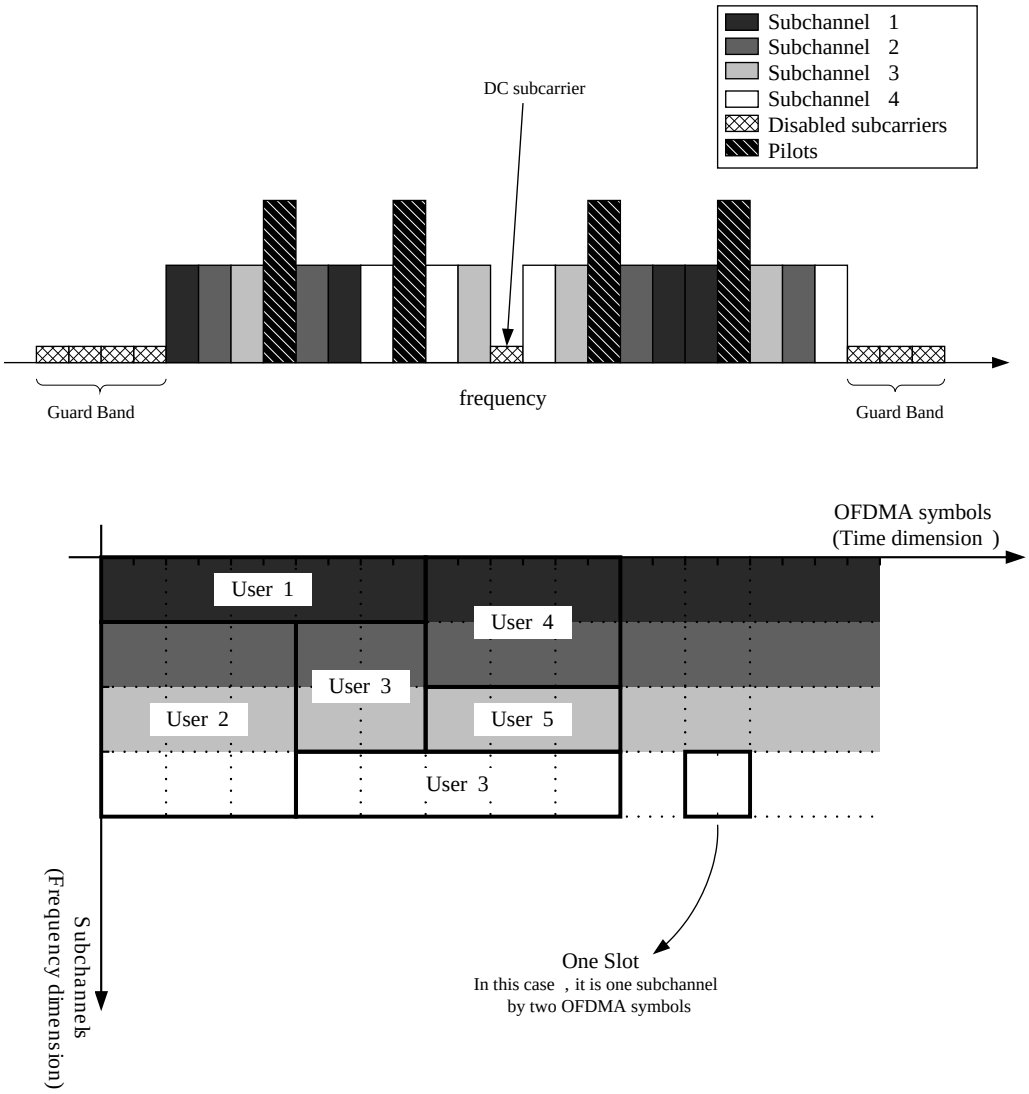

Figure 2.15 Illustration of OFDMA signal structure used in WiMAX.

2.5.2 IEEE 802.22

IEEE 802.22 standard is known as *cognitive radio standard* because of the cognitive features that it has [15]. It is designed to operate within the TV bands. However, IEEE 802.22-based systems should avoid interfering with incumbent signals. Systems should be able to sense the channel, detect incumbent signals within spectrum, and adjust their operating frequency and transmit power accordingly [121]. With features such as channel sensing, licensed users detection, dynamic frequency selection (DFS), and TPC, IEEE 802.22 can be considered as a cognitive radio standard. Even

Table 2.3 Advanced antenna features of WiMAX.

Techniques	**Details**	**Advantages**
Adaptive Antenna Systems (AAS) - Beamforming	The BS uses multiple antennas to form the beams in the direction of a subcarrier.	Extended range and increased capacity thanks to lower interference.
Space-time coding (STC)	Transmit diversity such as Alamouti code is used.	Increase in system gain through spatial diversity and reduced fade margin.
Spatial multiplexing (SM)	Independent and separately encoded data signals are transmitted over multiple antennas.	Increase in capacity (higher data rates).
Collaborative SM	Two UL users can transmit collaboratively in the same slot as if two streams are spatially multiplexed from two antennas of the same user.	Increased coverage and throughput.
Antenna selection	Any combination of antennas are selected (on-off type of selection of group of antennas from the available antennas) based on the channel feedback.	Efficient use of available power.
Antenna grouping	The BS can group multiple antennas for different carriers in different way based on the feedback from BSs. For example, if we have 3 Tx antennas, the BS can group the first two antennas in some carriers, and the last 2 antennas in some other carriers.	Maximum diversity / capacity gain.
MIMO precoding	The antenna elements are weighted with a matrix before mapping them to transmit antennas based on the feedback from SSs. This scheme is similar to a water-pouring algorithm.	Increased capacity gain.
STC sub-packet combining	In the initial transmission, the packets are transmitted in a full MIMO spatial multiplexing mode (no diversity). If the data can not be decoded correctly (CRC did not check), then the packets are sent in full STC mode (full transmit diversity mode). The receiver combines the initial data and the later data for better detection.	Provides incremental redundancy.
Frequency hopping diversity coding (FHDC)	This scheme (as for STC) transmits two complex symbols using the multiple input single output channel.	
Adaptive MIMO Switch (AMC)	STC or SM is selected adaptively to adopt channel conditions.	Optimum spectral efficiency is achieved.

though this standard is not finalized yet, it is anticipated that it will be based on OFDM transmission as well.

The main difference between WiMAX and the IEEE 802.22 standard is that the latter is mainly targeting rural and remote areas, since it is reusing TV bands. However, this gives 802.22 the upper hand in terms of range. A coverage area of up to 100 km is possible making it the first wireless regional area network (WRAN) standard. Current specifications can establish a coverage area of up to 33 km.

The 802.22 standard is designed for a fixed point-to-multipoint communication topology where the BS acts as the master mandating all the operation parameters of users with its cell. And while the users (slaves) can share sensing information with the BS through distributed sensing, it is up to the BS to change a user's transmit power, modulation, coding or operating frequency. In such topology, it is the responsibility of the service provider to ensure that users signal is causing no interference to the incumbent signals by within the coverage area. This is a crucial issue for the coexistence of the standard with the already existing TV services.

Another challenge in designing the 802.22 standard is the initialization of new users who desire to communicate with the BS. Unlike current wireless technologies, the frequency and time duration of the initialization channel is not predefined. In other words, initial users will have to scan parts (if not all) of the TV bands to find the current BS operating frequency and time. In addition, users should be able to differentiate between incumbent signals and the BS signal. This could prove to be very challenging especially if the BS is operating over a combination of multiple frequency bands.

A discussion of the aforementioned challenges and more issues related to the design of the 802.22 standard can be found in [121].

2.5.3 IEEE 802.11

The legendary WLAN standard, IEEE 802.11a/g [10,122], is amended to have cognitive features with IEEE 802.11h and IEEE 802.11k standards. IEEE 802.11h [123] is designed to allow estimation of channel characteristics and DFS, which is the ability to switch to different physical RF channels for transmit and receive activity based on channel measurements. In addition, TPC is incorporated as well, providing the system with more control over the signal range and interference level. The purpose of the IEEE 802.11h standard is to allow WLAN systems to share the 5-GHz spectrum with primary users (e.g. military radar systems).

The DFS detects devices using the same radio channel and the system switches to other radio channels if necessary avoiding interference with other existing primary users. WLAN station reports

a list of channels that it can support to an access point. When it's necessary to switch to a new channel, the access point uses this data to determine the best channel. On the other hand, TPC is used to reduce the interference from stations to other devices by controlling the power level of the transmitted signal. In addition, TPC is used to manage the power consumption of wireless devices and the range between access points and wireless devices.

On the other hand, IEEE 802.11k standard is proposed for radio resource management. The aim is to improve the traffic distribution in a WLAN. The standard defines a list of several radio parameters to be estimated by the system. While this list is limited and aimed for IEEE 802.11 standards, it is further enhanced compared to earlier standards. WLAN devices can be upgraded to support the new standard, since it is designed to be implemented in software. The standard allows access points to collect data from clients regarding access points they can hear and their signal power. After the collected data is analyzed, access points within range of a client are ordered into a list according to their signal strength, services, and encryption types supported by the client. This list is called *site report*. The access points provide the clients with the site report and thus improve the roaming decisions and increase the overall network throughput.

The access point could gather information from clients about the RF channel. For example, the access point could request the client to measure the channel noise level, or to provide the access point with information regarding the traffic load on the channel and the time duration over which the channel is occupied. Using this information, the access point can make a decision whether a certain channel is being crowded or if the channel contains high level of noise/interference.

Other features including tracking of hidden nodes and sharing clients' statistics are included in the standard. By applying both 802.11h and 802.11k standards to current 802.11-based WLAN systems, the performance and efficiency of wireless networking can be improved significantly. Adding cognitive features such as channel sensing and estimation, statistics distribution, DFS, TPC to WLAN devices will soon be possible. It is important to remember that 802.11 standards mainly use OFDM making it the signaling of choice for future technologies. Fig. 2.16 shows an illustration of the discussed current and future technologies and standards.

2.6 Conclusion

In this chapter, a general overview of cognitive radio and OFDM technology is presented. Cognitive radio is an exciting and promising effort for solving the spectrum crowding problem. On the

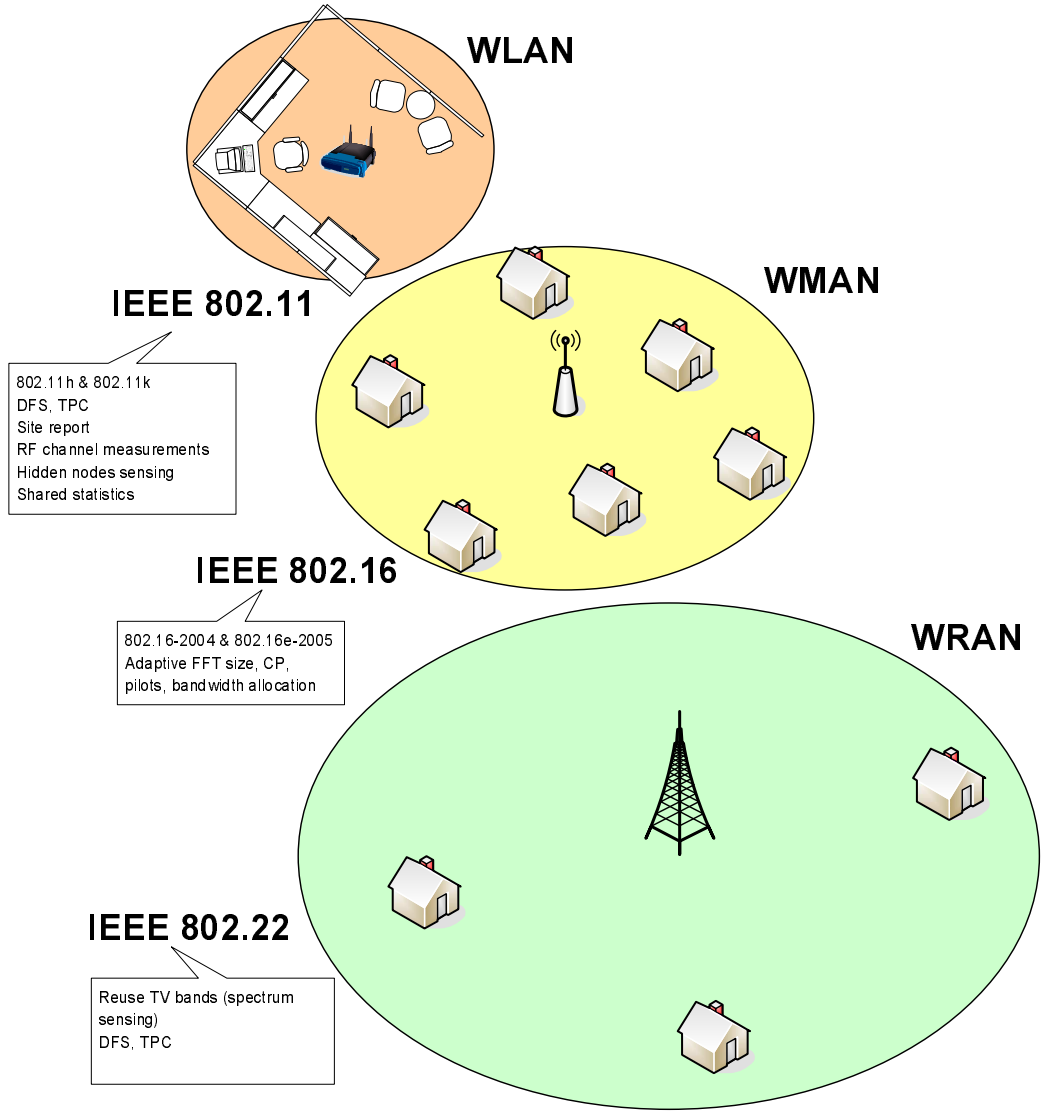

Figure 2.16 Standards and technologies developments.

other hand, OFDM technique is used in many wireless systems and proven as a reliable and effective transmission method. OFDM can be used for realizing cognitive radio concept because of its inherent capabilities that are discussed in detail in this chapter. By employing OFDM transmission in cognitive radio systems; adaptive, aware and flexible systems that can interoperate with current technologies can be realized.

CHAPTER 3

TIME DISPERSION AND DELAY SPREAD ESTIMATION FOR ADAPTIVE OFDM SYSTEMS

3.1 Introduction

OFDM has been applied for various wireless communication systems successfully in the last decade [124]. Those systems, however, should be capable of working efficiently in wide range of operating conditions, such as large range of mobile speeds, different carrier frequencies in licensed and license-exempt bands, various delay spreads, asymmetric traffic loads in downlink and uplink, and wide dynamic signal-to-noise ratio (SNR) ranges. The aforementioned reasons motivated the use of adaptive algorithms in new generation wireless communication systems [17]. Adaptation aims to optimize wireless mobile radio system performance, enhance its capacity, and utilize the available resources in an efficient manner. It is also an integral element of cognitive radio. However, adaptation requires a form of accurate parameter measurements. One key parameter in adaptation of OFDM systems is the time dispersion which provides information about the frequency selectivity of the wireless channel. Knowledge of the frequency selectivity in mobile communication systems can improve detection and help to optimize transmission.

In OFDM systems, the cyclic prefix (CP) length needs to be larger than the maximum excess delay of the channel. If this information is not available, the worst case channel condition is used for system design which makes CP a significant portion of the transmitted data. One way to increase the spectral efficiency is to adapt the length of the CP to the changing multipath conditions which requires the channel excess delay knowledge [48, 77]. Adaptive filtering for channel estimation is another area where time dispersion information of the channel is useful. A two-dimensional Wiener filter, implemented as a cascade of two one-dimensional filters, is used for channel estimation in [125]. The bandwidth of the second filter, which is in the frequency direction, is changed depending on the estimated delay spread of the channel to keep the noise low and thus to improve the channel estimation performance. Similarly, the coefficients of the frequency domain channel estimation filter

is chosen adaptively in [126] depending on the channel difference vector which is directly related to the delay spread of the channel. The information about the time dispersion of the channel can also be used for allocating the pilot symbols in frequency direction, whereas the allocation in time direction requires Doppler spread estimation. For example, the number of pilots and their spacing are adjusted depending on the delay spread knowledge in [84, 88]. Other OFDM parameters that could be changed adaptively using the knowledge of the time dispersion are OFDM symbol duration and OFDM sub-carrier bandwidth.

Characterization of the frequency selectivity of the radio channel is studied in [127,128] using level crossing rate (LCR) of the channel in frequency domain. Frequency domain LCR gives the average number of crossings per Hz at which the measured amplitude intersects a threshold level. However, LCR is very sensitive to noise which increases the number of level crossings and severely deteriorates the performance of the LCR measurements [129]. Filtering the channel frequency response (CFR) reduces the noise effect, but finding the appropriate filter parameters could be a problem. If the filter is not designed properly, one might end up smoothing the actual variation of the frequency domain channel response. Time dispersion of the channel can be estimated using the channel impulse response (CIR) estimates as well. In [84, 125], the CIR is obtained by taking the inverse discrete Fourier transform (IDFT) of the frequency domain channel estimate which is calculated at pilot locations. In [130], instantaneous root-mean-squared (RMS) delay spread is obtained by estimating the CIR in time domain. The detected symbols in the frequency domain are used to re-generate the time domain signal through IDFT and then this signal is correlated with the received signal in order to obtain the CIR. Since the detected symbols are random, they might not have good autocorrelation properties, which can be a problem especially when the number of carriers is small and SNR is low. Timing synchronization errors create a problem with the time domain estimation; if synchronization is performed independently over different frames (or symbols), the estimated CIRs should be time aligned as the timing errors will be different for each CIR estimate. Techniques exploiting the CP are proposed for delay spread estimation in [131, 132]. The change of gradient of the correlation between the CP and the last part of the OFDM symbol is used as a strategy to detect the dispersion parameters in [131]. Using the change of gradient in the correlation, the amplitude and delay of each tap is calculated and the delay spread information is extracted from this information. This method requires computationally complex optimization and the accuracy of the technique can be expected to degrade for closely spaced and weak multipath components.

In [132], the magnitude of each arriving tap and the corresponding delay are estimated from the calculated correlation. Once the delays and magnitudes are estimated, the maximum excess delay or RMS delay spread of the channel can be computed. In [20], RMS delay spread of the channel is obtained using the channel frequency correlation (CFC) without calculating the channel power delay profile (PDP). Analytical relations between the CFC and the RMS delay spread value are derived by assuming an exponentially decaying PDP. To calculate the RMS delay spread, the proposed algorithm uses the CFC estimate and the analytical relation between the RMS delay spread and the coherence bandwidth which is obtained from the CFC for a given correlation level. In [126], the adaptive filter coefficients are updated using the first derivative of frequency domain channel estimates. Note that, although the RMS delay spread value is not estimated, a directly related parameter is used, and hence, it can be considered as a simplified version of delay spread estimation using CFC.

In this chapter, time dispersion of the radio channel is estimated using frequency domain channel estimates. In OFDM systems, channel can be estimated in frequency domain easily, and this is usually the preferred method as both estimation and equalization in frequency domain are simpler than their time domain equivalents. Since the timing errors are folded into the channel estimates in frequency domain as a subcarrier-dependent phase term, the magnitudes of the channel estimates are used for delay spread estimation in order to remove the phase dependence. As a third algorithm, the magnitude of the received frequency domain signal is used when a constant envelope modulation is employed. The proposed algorithms estimate the channel PDP which is then used to extract the time dispersion parameters: RMS delay spread and maximum excess delay of the channel.

This chapter is organized as following. In Section 3.2, system model will be introduced, and the proposed algorithms will be presented in Section 3.3. Numerical results will be given in Section 3.4 and the chapter will be concluded in Section 3.5.

3.2 System Model

For the time and frequency domain OFDM symbols, the model given in Section 2.2 is used. Furthermore, the channel is assumed to be constant over an OFDM symbol, but time-varying across OFDM symbols, which is a reasonable assumption for low and medium mobility.

At the receiver, the signal is received along with noise. After time and frequency synchronization, down-sampling, and removal of CP, the simplified baseband model of the received samples can be

formulated as

$$y_m(n+\theta_m) = \sum_{l=0}^{L-1} x_m(n+\theta_m-l)h_{l,m} + w_m(n), \tag{3.1}$$

where L is the number of sample-spaced channel taps, and the time domain CIR for mth OFDM symbol, $h_{l,m}$, is given as a time-invariant linear filter. The timing error θ_m is caused by the imperfect synchronization and its statistics depends on the SNR and the synchronization algorithm used. In this case, after taking discrete Fourier transform (DFT) of the received signal $y_m(n+\theta_m)$, the samples in frequency domain can be written as[1] [133]

$$\begin{aligned} Y_m(k) &= DFT\{y_m(n+\theta_m)\} \\ &= X_m(k)H_m(k)e^{-j2\pi k\theta_m/N} + W_m(k) \quad 0 \le k \le N-1, \end{aligned} \tag{3.2}$$

where H and W are DFTs of h and w respectively. The least squares (LS) estimate of the CFR $\hat{H}_m$ can be calculated using the received signal and the knowledge of transmitted symbols as

$$\hat{H}_m(k) = \frac{Y_m(k)}{X_m(k)} \tag{3.3}$$

$$= \underbrace{H_m(k)e^{-j2\pi k\theta_m/N}}_{\tilde{H}_m(k)} + \underbrace{\frac{W_m(k)}{X_m(k)}}_{Z_m(k)}. \tag{3.4}$$

The LS channel estimation consists of the desired channel with a frequency dependent phase term due to timing errors and an additive estimation error term due to noise.

3.3 Proposed Delay Spread Estimation Algorithms

In this section, we propose algorithms for estimating the time dispersion parameters. Three methods will be given for estimating the PDP using frequency domain information. Calculation of the RMS delay spread and maximum excess delay from the estimated PDPs is also discussed in this section.

[1] It is assumed that the timing errors are small enough so there will not be any inter-symbol interference (ISI) or inter-carrier interference (ICI).

3.3.1 Channel Estimation Based Algorithm

In OFDM systems, channel estimation is usually done in frequency domain using known training symbols. Hence, the frequency domain channel estimates are usually available. Using these estimates, the instantaneous channel frequency correlation values can be calculated as

$$R_{\hat{H}}(\Delta) = E_{t,k}\left[\hat{H}_t(k)\hat{H}_t^*(k+\Delta)\right], \tag{3.5}$$

where $E_{t,k}[\cdot]$ is the expectation over training symbols t and over subcarriers k (averaging within an OFDM symbol). Assuming that the channel and noise terms are uncorrelated, the correlation given in (3.5) can be written as

$$R_{\hat{H}}(\Delta) = R_{\tilde{H}}(\Delta) + R_Z(\Delta), \tag{3.6}$$

where $R_{\tilde{H}}(\Delta)$ is the correlation of the effective channel and $R_Z(\Delta)$ is the correlation of channel estimation error. $R_Z(\Delta)$ becomes a delta function when the estimation errors at different subcarriers are uncorrelated, *i.e.* when it is white. However, as channel estimation is a filtering operation, this noise is usually colored and it creates a bias on the estimates obtained using $R_{\hat{H}}$, hence care should be taken. When the channel estimates are obtained using the LS method given in Section 3.2, however, the noise becomes white as the additive noise on the received signal $W(k)$ is assumed to be white and uncorrelated with the transmitted signal as well as the channel. In this case the correlation (3.5) can be written as

$$R_{\hat{H}}(\Delta) = R_{\tilde{H}}(\Delta) + \delta(\Delta)\sigma_z^2, \tag{3.7}$$

where σ_z^2 is the variance of channel estimation error $Z(k)$, and $\delta(\cdot)$ is the Kronecker delta function.

Using (3.4) and (3.5), the channel correlation with timing errors can be obtained as

$$R_{\tilde{H}}(\Delta) = R_H(\Delta)E_t\left[e^{j2\pi\theta_t\Delta/N}\right]. \tag{3.8}$$

The expectation in (3.8) is a function of the statistics of the estimation error θ_t which depends on channel conditions and the algorithm used for synchronization. This expectation can be written in

terms of timing error probabilities as

$$E_t\left[e^{j2\pi\theta_t\Delta/N}\right] = \sum_{\theta=\theta_{min}}^{\theta_{max}} \cos\frac{2\pi\theta\Delta}{N} P(\theta), \tag{3.9}$$

where θ_{min} and θ_{max} are the minimum and maximum synchronization values respectively. $P(\theta)$ is the probability of having the synchronization error θ and in the case of perfect synchronization it becomes a delta function, *i.e.* $P(\theta) = \delta(\theta)$. In this chapter, the timing errors are assumed to have a Gaussian distribution with zero mean and the variance of σ_θ^2 [134].

As can be seen from (3.7) and (3.8), there are two impairments that affect the correlation estimates. We first assume perfect timing synchronization and concentrate on the noise term. In a similar problem for a different context, a parabola is fitted to the lags with non-zero index for finding the value at the zero-th lag of time domain channel correlation in [135]. In this chapter, we use the same algorithm for removing the correlation term due to noise in (3.7). This algorithm consists of the following steps:

- calculate $R_{\hat{H}}(\Delta)$ for $\Delta = 1 \dots M$,
- obtain the coefficients of the parabola $\mathscr{P}(\Delta)$ using the LS method,
- substitute $\mathscr{P}(0)$ into $R_{\hat{H}}(0)$ and call it $R'_{\tilde{H}}$.

Once the effect of noise is removed, the PDP can be estimated from the CFC estimate $R'_{\tilde{H}}$ by simply applying IDFT operation as

$$P_l = IDFT\left\{R'_{\tilde{H}}(\Delta)\right\} \tag{3.10}$$

$$= \frac{1}{\sqrt{N}} \sum_{\Delta=0}^{N-1} R'_{\tilde{H}}(\Delta) e^{j2\pi\Delta l/N} \quad 0 \le l \le L-1. \tag{3.11}$$

where $P_l = E_m\left[|h_{l,m}|^2\right]$ is the lth tap of the channel PDP. As the PDP coefficients are real, the CFC exhibits a conjugate symmetry that can be used to decrease the number of correlation lags to be calculated by half.

Timing error is the other impairment that degrades the performance of the channel estimation based algorithm. Fig. 3.1 shows the correlation magnitude as a function of subcarrier separation Δ for perfect synchronization and for synchronization errors with a zero-mean Gaussian distribution and variance of $2t_s^2$, *i.e.* $\sigma_\theta^2 = 2$, where t_s is the sampling frequency. Both analytical results obtained

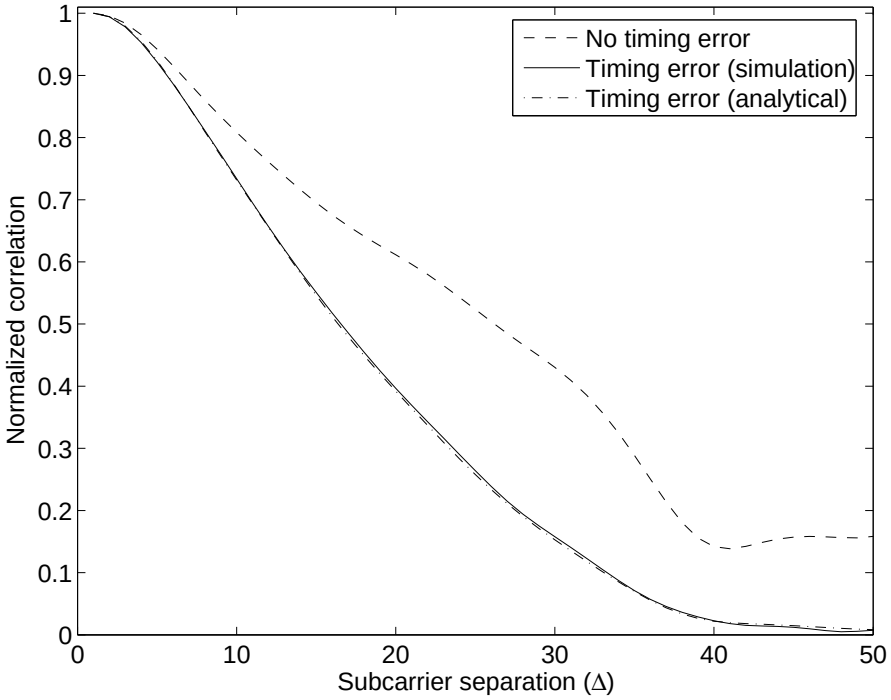

Figure 3.1 Magnitude of channel frequency correlation with perfect synchronization and with synchronization errors. Analytical (Eqn. 3.9) and simulation results are shown.

using (3.9) and simulation results are given. Although the algorithm given in this section is simple to calculate and straightforward, timing errors affect the correlation estimates and bias the time dispersion estimation as Fig. 3.1 shows. In order to remove this effect, we propose to use the magnitude square of the frequency domain channel estimates which will be discussed in the next section.

3.3.2 Channel Magnitude Based Algorithm

The correlation of the magnitude of the channel estimates can be represented as

$$R_{|\hat{H}|^2}(\Delta) = E_{t,k}\left[|\hat{H}_t(k)|^2 |\hat{H}_t(k+\Delta)|^2\right]. \tag{3.12}$$

By inserting (3.4) into (3.12), the correlation can be simplified to

$$R_{|\hat{H}|^2}(\Delta) = R_{|H|^2}(\Delta) + (1+\delta(\Delta))\left(2R_H(0)\sigma_z^2 + \sigma_z^4\right), \tag{3.13}$$

where $R_{|H|^2}(\Delta)$ is the correlation of the magnitude of true channel and it can be written as (see Appendix A for detailed derivation)

$$\begin{aligned} R_{|H|^2}(\Delta) &= E_{t,k}\left[|H_t(k)|^2|H_t(k+\Delta)|^2\right] \\ &= \frac{2}{N^2}\sum_{l=0}^{N-1}\sum_{u=0}^{N-1} P_l P_u \cos^2\frac{\pi(l-u)\Delta}{N} \qquad (3.14) \\ &= \frac{1}{N^2}\sum_{l=0}^{N-1}\sum_{u=0}^{N-1} P_l P_u \Bigg[1+\cos\frac{2\pi l\Delta}{N}\cos\frac{2\pi u\Delta}{N} \\ &\quad + \sin\frac{2\pi l\Delta}{N}\sin\frac{2\pi u\Delta}{N}\Bigg]. \qquad (3.15) \end{aligned}$$

The effect of noise on (3.13) at the first correlation lag, *i.e.* $\Delta = 0$, is two times the effect of noise on the other lags. Therefore, if the value of the first correlation lag is calculated using other lags, the overall effect of the noise can be subtracted from the correlation removing the effect of the noise. The parabola fitting algorithm described in Section 3.3.1 is used for removing the noise contribution in this method as well.

Note that the first term in the right-hand side (RHS) of (3.15) is equal to $R_{|H|^2}(0)/2$ and the second and third terms together are equal to the magnitude square of the correlation of the channel response, $R_H(\Delta)$. Using these facts, the following equality can be obtained

$$R_{|H|^2}(\Delta) - \frac{R_{|H|^2}(0)}{2} = R_H(\Delta)R_H^*(\Delta), \qquad (3.16)$$

where $R_H(\Delta)$ is the correlation of $H(k)$ as defined before. Note that the left-hand side (LHS) of this equation can be estimated using the received signal. The RHS is a multiplication, and when IDFT is applied on this term, it becomes a convolution of PDP with the flipped version of itself in time domain. This follows from the properties of DFT [42] and from the fact that the IDFT of the CFC is equal to the PDP. The resulting equation can then be written as

$$\begin{aligned} IDFT\left\{R_{|H|^2}(\Delta) - \frac{R_{|H|^2}(0)}{2}\right\} &= IDFT\left\{R_H(\Delta)R_H^*(\Delta)\right\} \qquad (3.17) \\ &= \sum_{i=0}^{L-1} P_{l-i}P_{\langle -i\rangle_N}. \qquad (3.18) \end{aligned}$$

Having the LHS of the equality calculated using the received signal, we can estimate the PDP using (3.18) and by solving the non-linear set of equations. For this purpose, least squares optimization is

used in this chapter. The number of unknowns can be limited to the number of PDP taps L. As the length of the CP is expected to be larger than the maximum excess delay, the number of unknowns is set to the length of CP. The system of equations can then be solved as the number of unknowns is smaller than the number of equations which is N.

3.3.3 Received Signal Based Algorithm

The algorithms given in the previous sections can use only the training symbols for the estimation. However, when the OFDM system employs a constant envelope modulation, the power of the received signal $Y(k)$ can be used. The received signal in the frequency domain for OFDM is given in (3.2). Using this equation, the correlation of the magnitude of the received frequency domain signal can be calculated as

$$R_{|Y|^2}(\Delta) = E_{m,k}\left[|Y_m(k)|^2 |Y_m(k+\Delta)|^2\right] \tag{3.19}$$

After expanding (3.19), the simplified version can be written as

$$R_{|Y|^2}(\Delta) = R_{|H|^2}(\Delta) R_{|X|^2}(\Delta) + (1+\delta(\Delta))\left(2R_H(0)R_X(0)\sigma_w^2 + \sigma_w^4\right). \tag{3.20}$$

For constant envelope modulations $R_{|X|^2}(\Delta) = R_X(\Delta) = 1$, and therefore (3.20) reduces to (3.13) as[2]

$$R_{|Y|^2}(\Delta) = R_{|\hat{H}|^2}(\Delta). \tag{3.21}$$

Therefore the algorithm given in Section 3.3.2 can be used for estimating PDP using $Y(k)$ instead of $\hat{H}(k)$. This enables us to use all of the received OFDM symbols which results in both noise averaging and getting better correlation estimates.

3.3.4 Estimation of RMS Delay Spread and Maximum Excess Delay

The RMS delay spread and excess delay spread (X dB) are multipath channel parameters that can be determined from a PDP. Once the PDP of the channel is estimated using the proposed methods, these parameters can be estimated using their definitions. The RMS delay spread τ_{rms} is the square root of the second central moment of the PDP and the maximum excess delay (X dB) of the PDP is defined as the time delay during which multipath energy falls to X dB below the

[2]Without loss of generality, we assume $\sigma_X^2 = 1$. Hence $\sigma_w^2 = \sigma_z^2$.

maximum value. The RMS delay spread is defined as [136]

$$\tau_{rms} = \sqrt{\frac{\sum_{l=0}^{L-1} P_l \tau_l^2}{\sum_{l}^{L-1} P_l} - \left(\frac{\sum_{l=0}^{L-1} P_l \tau_l}{\sum_{l}^{L-1} P_l} \right)^2}, \tag{3.22}$$

where $\tau_l = lt_s$ is the delay of lth multipath component. In order to decrease the effect of errors in the PDP estimation, taps with power 25 dB below the most powerful lag are set to zero. Moreover, we consider the maximum excess delay of 25 dB, *i.e.* the maximum excess delay is equal to the delay of the last non-zero tap.

The statistics of the channel might be changing in time because of the environmental changes or because of the mobility of the transmitter or receiver. In this case, the correlation estimates can be updated using an alpha tracker in order to capture this variation. For channel magnitude based algorithm, for example, the correlation values can be updated as

$$R^m_{|H|^2}(\Delta) = (1-\alpha) R_{|H_m|^2}(\Delta) + \alpha R^{m-1}_{|H|^2}(\Delta) \tag{3.23}$$

where $R_{|H_m|^2}(\Delta)$ is the correlation value obtained using mth symbol. The forgetting factor $0 \leq \alpha \leq 1$ is a design parameter and it should be selected depending on how fast the channel parameters are changing.

3.4 Numerical Results

A system similar to the OFDM mode of IEEE 802.16d [12] is used for the simulations. Total number of subcarriers is 256, out of which 200 subcarriers are used for transmitting data information and pilots. The center frequency carrier is set to zero and the outermost 55 subcarriers (27 on left and 28 on the right of the spectrum) are not used to allow for guard bands. The system bandwidth is chosen as 10 MHz and the length of the CP is set to 32 samples (the length of the guard band is 3.2 μs). For simulating the wireless channel, the Channel A of ITU-R channel model [137] for vehicular environments with high antenna is used. The relative delays and average power of each tap of this model is given in Table 3.1. The mobile speed used in the simulations[3] is 60 km/h and time-varying channel is generated according to [138]. For estimating the CFR, LS method (see Section 3.2) is used.

[3]Similar results are observed when tests at different mobile speeds are performed.

Table 3.1 Characteristics of the ITU-R "Vehicular A" channel model.

Tap	**1**	**2**	**3**	**4**	**5**	**6**
Relative delay (ns)	0	310	710	1090	1730	2510
Average power (dB)	0	-1	-9	-10	-15	-20

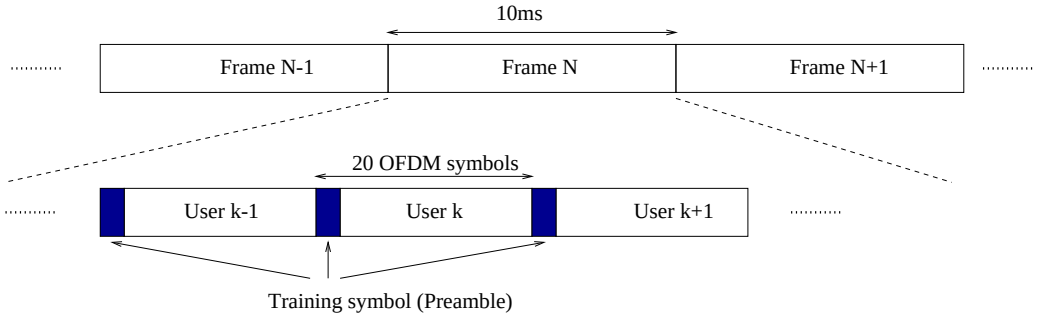

Figure 3.2 Illustration of frame structure of the system used for testing the proposed algorithms.

The estimation is assumed to be done in uplink for a user with 20 OFDM symbols in a frame with 10 ms frame duration. The frame structure of the considered system is illustrated in Fig. 3.2. In uplink, each user is assumed to have a training symbol for synchronization and channel estimation purposes. The channel estimation based algorithms use the channel estimates obtained using the training symbols while the received signal power based algorithm uses all of the 20 transmitted symbols (1 training symbol and 19 data symbols) for estimation of PDP. The first 5 non-zero correlation values are used for obtaining the parameters of the parabola which is used to remove the effect of noise on correlation estimates, *i.e.* $M = 5$.

Normalized MSE is used as a performance measure of the estimator as it reflects both the bias and the variance of the estimator. The normalized MSE of τ_{rms} is defined as $NMSE(\tau_{rms}) \triangleq E\left[(\hat{\tau}_{rms} - \tau_{rms})^2\right] / \tau_{rms}^2$ where $\hat{\tau}_{rms}$ is the estimate of τ_{rms}. Fig. 3.3 shows the normalized mean-squared-error (MSE) of the RMS delay spread as a function of the number of frames used for estimation. In this figure, perfect channel and timing information is assumed to be available and Cramér-Rao lower bound (CRLB) for the estimation (B.7) is also presented. The proposed algorithms are labeled as *Algorithm A, B,* and *C* respectively. The multipath channel components at different frames are assumed to be independent in this figure in order to show .?. The channel estimation based algorithm yields close results to the bound and the performance loss in the channel magnitude based algorithm can be explained by the information lost by not utilizing the phase information of channel estimates. Figs. 3.4 and 3.5 show the normalized MSE of the RMS delay

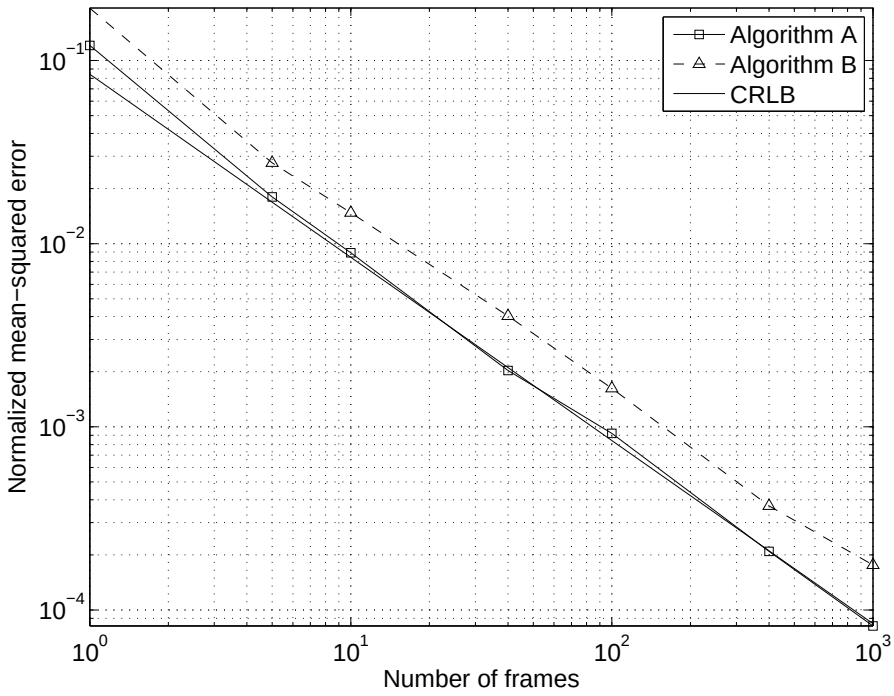

Figure 3.3 Normalized mean-square-error performances of the RMS delay spread estimators as a function of number of frames used for estimation.

spread estimation as a function of the number of frames used for estimation. Fig. 3.4 shows the case of perfect timing knowledge, while in Fig. 3.5 a timing mismatch with zero-mean Gaussian distribution and variance of $2t_s^2$ is introduced. The SNRs of the received signal for both figures are set to 10dB. Channel estimation based algorithm performs better than the other algorithms in the case of no timing errors as the phase information on the channel is also used. On the other hand, it has a large error floor when there are timing errors. The results presented in these figures show that the channel magnitude based algorithm (*Algorithm A*) and the received magnitude based algorithm (*Algorithm C*) work quite satisfactory under timing errors.

The normalized MSE as a function of SNR for 80 frames is shown in Fig. 3.6 for perfect timing synchronization. The performances of all three algorithms increase as the SNR is increasing. However, after a certain SNR level (around 10 dB), the performance does not change significantly with increasing SNR.

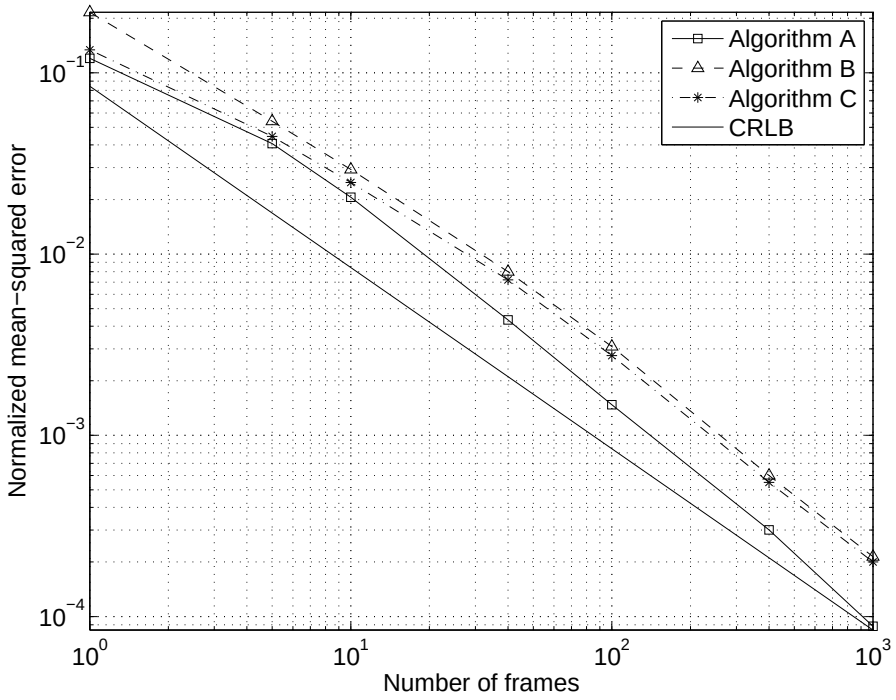

Figure 3.4 Normalized mean-square-error performances of the RMS delay spread estimators as a function of number of frames used for estimation.

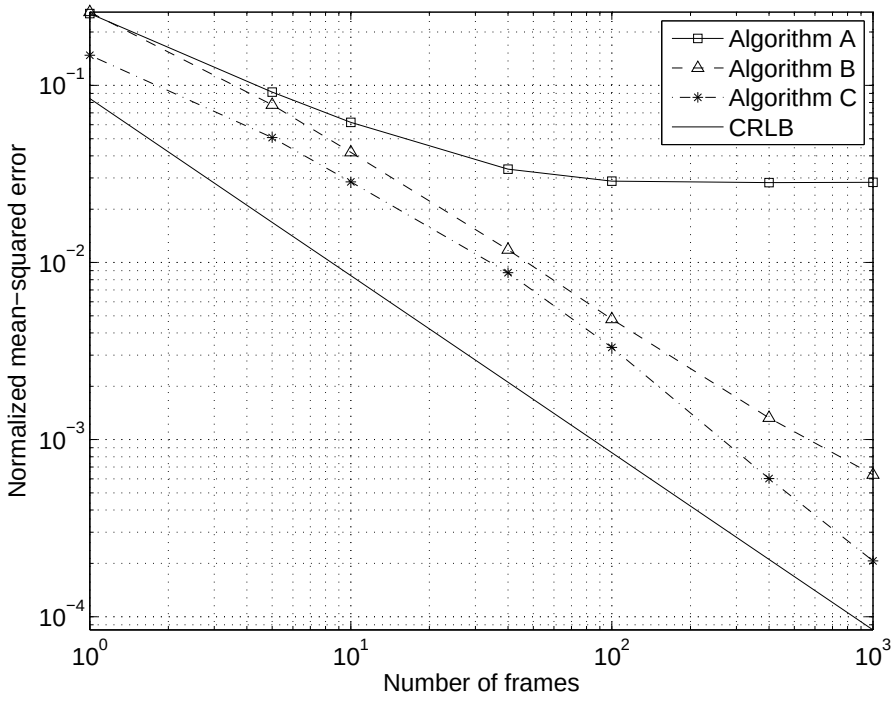

Figure 3.5 Normalized mean-square-error performances of the RMS delay spread estimators as a function of number of frames used for estimation when there are timing synchronization errors.

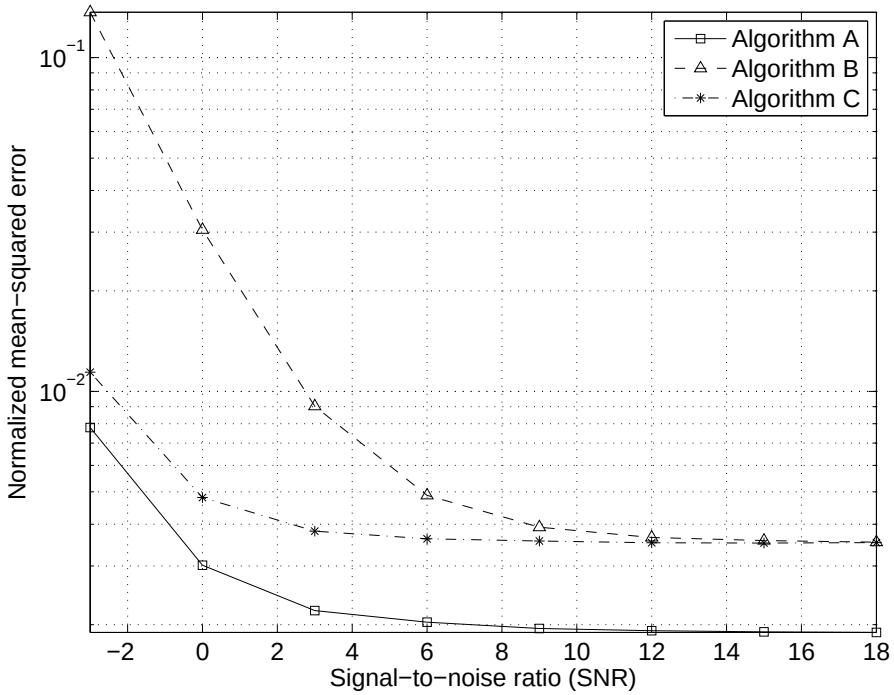

Figure 3.6 Normalized mean-square-error performances of the RMS delay spread estimators as a function of the SNR. Estimation is performed over 80 frames.

3.5 Conclusion

Delay spread estimation algorithms for OFDM systems are proposed in this chapter. The proposed algorithms estimate the PDP of the channel which is then used to calculate the dispersion parameters. It is found that timing errors cause estimation error floor if the channel frequency estimates are directly used, and this problem is overcome by using the magnitude of the channel estimates. Moreover, the channel magnitude based algorithm is extended to a method which uses the received signal power (in frequency domain) when the transmitted symbols has a constant envelope. The performances of the developed algorithms are tested using computer simulations and the channel and received signal magnitude based algorithms are shown to perform well under different scenarios. In addition, the CRLB for the RMS delay spread parameter is derived and used to validate the performance of the proposed methods.

CHAPTER 4

DOPPLER SPREAD ESTIMATION FOR WIRELESS OFDM SYSTEMS

4.1 Introduction

Because of its tremendous success in digital video broadcasting (DVB) and wireless local area networks (WLANs), orthogonal frequency division multiplexing (OFDM) is now considered for broadband wireless systems for both fixed and mobile applications such as wireless metropolitan area networks (WMANs), mobile broadband wireless access (MBWA) and proposed fourth generation (4G) cellular systems [139]. Those systems however, should be capable of working efficiently in wide range of operating conditions, such as large range of mobile subscriber station (MSS) speeds, different carrier frequencies in licensed and licensed-exempt bands, various delay spreads, asymmetric traffic loads in downlink (DL) and uplink (UL) and wide dynamic signal-to-noise ratio (SNR) ranges.

The aforementioned reasons motivated the use of adaptive algorithms in new generation wireless communication systems. Adaptation aims to optimize wireless mobile radio systems performance, enhance its capacity and utilize available resources in an efficient manner. However, adaptation requires a form of accurate parameter measurements. One key parameter in adaptation of mobile radio systems is the maximum Doppler spread. It provides information about the fading rate of the channel. Knowing Doppler spread in mobile communication systems can improve detection and help to optimize transmission at the physical layer as well as higher levels of the protocol stack [140]. Specifically, knowing Doppler spread can decrease unnecessary hand-offs, adjust interleaving lengths to reduce reception delays, update rate of power control algorithms, *etc.* In addition, in OFDM systems, if the channel varies considerably within one OFDM symbol because of high MSS mobility, orthogonality between subcarriers is lost, leading to inter-carrier interference (ICI) [89]. Doppler information can help in selection of appropriate transmission profiles that are immune to ICI and hence the overall system performance will be improved.

Various methods based on the auto-correlation function (ACF) have been used to estimate the Doppler spread f_D in single carrier systems [140]. In OFDM systems, the autocorrelation between the repeated parts of the symbol due to cyclic prefix (CP) is exploited in [141] to estimate the Doppler spread. However, adaptive OFDM systems employ a form of variable CP size selection according to the delay spread of the channel. The part of the CP that is undisturbed by the multipath channel may be small especially when the environment causes large delay spread. This will degrade estimation greatly. Moreover, the results presented shows that the algorithm is biased at low and medium Doppler values, and gives good estimates at very high velocities which are less likely to occur. The scheme is also sensitive to SNR variations. In OFDM systems, channel estimates are often obtained in frequency domain. By obtaining the ACF of a certain subcarrier over several symbols, f_D can also be estimated [142]. However, every subcarrier will have noise perturbation due to additive white Gaussian noise (AWGN) and ICI. In this chapter, we overcome this bias by performing inverse fast Fourier transform (IFFT) to the channel estimates and then using the few obtained channel taps to get f_D.

The organization of this chapter is as follows. In Section 4.2, brief system and channel models are presented. Then, the Doppler spread estimation algorithm is discussed in Section 4.3. Simulation results are presented and analyzed in Section 4.4. Finally, Section 4.5 concludes the chapter.

4.2 System and Channel Models

For the time and frequency domain OFDM symbols, the model given in Section 2.2 is used. Furthermore, we adopt the two dimensional channel model proposed by Clarke, where at a given instant, there exist L multipath components arriving at the receiver with distinct complex amplitudes, phases, Doppler shifts and delays. It was shown that with no line-of-sight (LOS) path the envelope of each path fading is modeled by Rayleigh distribution [143]. The channel is assumed to be time-variant. Consequently, during an OFDM symbol period, the discrete time channel impulse response is given by

$$h(n,\tau) = \sum_{l=1}^{L} h_l(n)\delta(n-\tau_l), \tag{4.1}$$

where τ_l is the propagation delay associated with lth path. The path gains $h_l(n)$ are zero-mean stochastic processes with normalized overall power, so that $E\left[(h_l(n))\right] = 0$ and $\sum_{l=1}^{L} E\left[\left|h_l(n)\right|^2\right] = 1$. Assuming wide-sense stationary uncorrelated scattering (WSSUS) channel model, and with uni-

formly distributed angle of arrival (AOA), the autocorrelation function of the channel impulse response (CIR) for a certain tap l is given by

$$E\left[h(n)h^*(n+\tau)\right] = J_0\left(2\pi f_D \tau\right), \tag{4.2}$$

where $J_o(.)$ is the zeroth order Bessel function of the first kind. The maximum Doppler shift f_D is determined by the mobile velocity and the wavelength. After passing through a radio channel, the mth received time-domain OFDM signal $y_m(n)$ can be written as a function of the transmitted signal, the channel transfer function, and AWGN as

$$y_m(n) = x_m(n) * h(n,\tau) + w_m(n), \quad 1 \leq n \leq N. \tag{4.3}$$

After performing the fast Fourier transform (FFT) operation at receiver, the received frequency-domain signal $Y_m(k)$ can be expressed as [144]

$$Y_m(k) = X_m(k)H_m(k) + I_m(k) + W_m(k), \tag{4.4}$$

where $H_m(k)$ is the channel transfer function at the kth subcarrier and $I_m(k)$ is the ICI term. The interference term depends on transmitted symbols and the variation of the channel over an OFDM symbol. It can be formulated as

$$I_m(k) = \sum_{u=0,\ u\neq k}^{N-1} \sum_{l=0}^{L-1} X_m(u) \frac{1}{N} \sum_{d=0}^{N-1} h_l(d) e^{j2\pi d(u-k)/N} \ . \tag{4.5}$$

Note that the interference power increases with increasing variation in the channel response, *i.e* with increasing velocity or Doppler spread.

4.3 Doppler Spread Estimation

In OFDM systems, channel estimation is usually done in frequency domain either by sending pilots on specific subcarriers or using preambles and inserting frequent mid-ambles to capture channel variations. The latter case will be considered in this chapter. The channel estimates at all subcarriers

can be obtained by dividing (4.4) by the known transmitted symbols $X_m(k)$ as

$$\hat{H}_m(k) = \frac{Y_m(k)}{X_m(k)} = H_m(k) + \frac{I_m(k)}{X_m(k)} + \frac{W_m(k)}{X_m(k)} \ . \tag{4.6}$$

The second term on the right hand side is the bias in the estimate due to ICI and can have an effect on the estimation if the Doppler frequency is relatively high. However, the ICI term depends on the signal values modulated on all the other subcarriers. Since, we are interested in the correlation of the channel estimate at kth subcarrier in time, ICI appears uncorrelated. Hence, it can be treated as additional noise. The last term in (4.6) represents the AWGN.

It is known that the channel in time domain is limited to the maximum excess delay of the channel. The data mapped into various subcarriers are zero-mean random variables. Thus ICI appears fast varying over subcarriers. The same holds true for the totally random AWGN samples in frequency domain which change very fast over OFDM subcarriers. Therefore, by transforming the frequency domain channel components, the true channel and noise components (ICI and AWGN) can be separated. When IFFT is applied to the channel frequency response (CFR), the CIR will be concentrated on the first few taps, while noise and ICI terms will be spread over all IFFT size. Fig. 4.1 illustrates this fact for a MSS with moderate vehicular speed. The average power levels of the components in the channel estimate are plotted for a uniform power delay profile (PDP).

In this chapter, we propose to use time domain channel estimation instead of frequency domain estimation in order to increase the immunity to white noise and to ICI in the channel estimation. Similar approaches are used in OFDM literature for channel estimation, and are commonly referred to as transform-domain methods [145]. In the time-domain, the first few taps can be used to estimate the Doppler spread with lower estimation error. Besides, this can allow use of less number of symbols to find the autocorrelation and so we can reduce memory usage and computation time needed for fast adaptation. By using (4.2) and following the assumptions, we can obtain the autocorrelation of a CIR tap as

$$E\left[\hat{h}(n)\hat{h}^*(n+sT_S)\right] = J_0(2\pi f_D s T_S) + \sigma_r^2 \delta(l) \tag{4.7}$$

where $\hat{h}$ is the estimate of the time domain channel taps, s is the difference in OFDM symbol number and σ_r^2 is the combined reduced variance of ICI and AWGN.

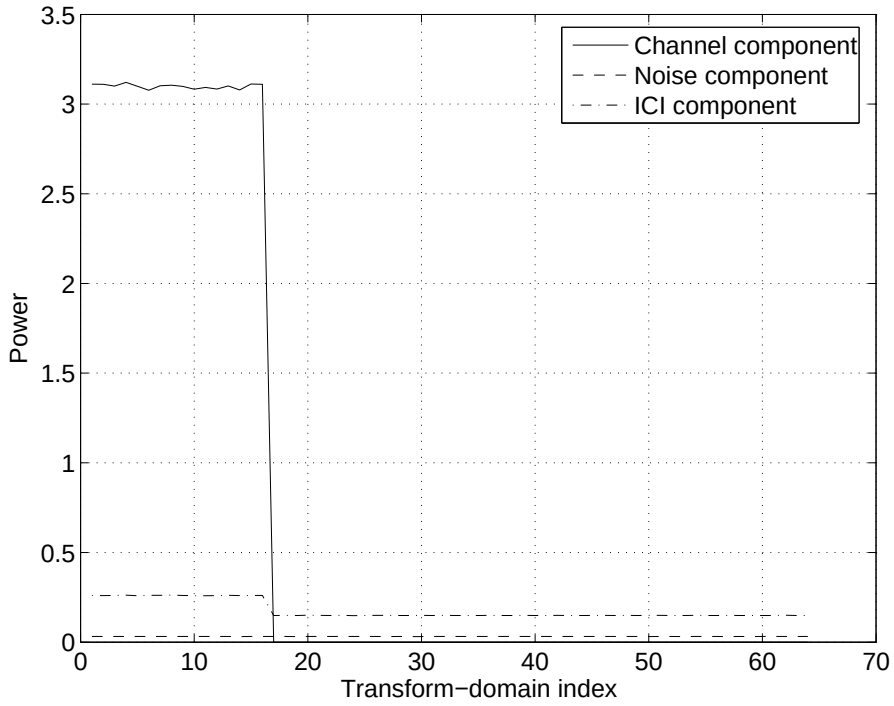

Figure 4.1 Average powers of the channel components and disturbances in time-domain.

4.3.1 Computing f_D from Auto-Correlation Function

Once the ACF is estimated, different methods can be used to calculate the Doppler spread (see references in [140]). We use a similar method to that proposed in [146] to extract f_D from the calculated ACF. In this method, the best hypothesis that minimizes the mean-squared-error (MSE) between the actual ACF and the Bessel function given by (4.2) is used. The Doppler range is divided into several bins depending on accuracy required. The ACF of few lags is then obtained and the estimate of Doppler spread which minimizes the MSE goal function is selected.

We note here that although the zero-crossing method used in [147] avoids the influence of noise on finding zero-crossing point if perfect match with Bessel function is assumed, this is unlikely to occur especially in relatively low Doppler values where the high lags are not reliable due to insufficient samples for correlation computation. The method will require very large number of symbols for ACF computation. On the contrary, here we assume use of less symbols to obtain the ACF.

4.3.2 Coherence Time Versus Doppler Spread

The coherence time of the channel t_C is the duration over which the channel characteristics can be considered as time-invariant [148]. It is of utmost importance for evaluating and adapting the techniques that try to exploit time diversity of the channel or to compensate its time selectivity [149]. Time diversity can be exploited if the separation between time slots carrying the same information exceeds the coherence time. For an OFDM transmission system, coherence time t_C has a special significance because symbol duration should be chosen to be much smaller than t_C to avoid ICI. Although, there is no specific definition for the coherence time, it is known to be inversely proportional to the maximum Doppler frequency [136], *i.e.*

$$t_C \approx \frac{1}{f_D} \ . \tag{4.8}$$

The computation of the coherence time can be easily obtained from the ACF of the available channel estimates if a certain threshold is attained within an amount of time lags. Commonly, when the time elapsed for ACF to drop to half of its maximum zero lag value, this can be regarded as a measure of the coherence time. It is obvious that our proposed method will also allow a reliable estimate of the coherence time due to its immunity to noise and ICI perturbations.

4.3.3 Complexity of Proposed Method Versus Gains

The proposed modification performs an added IFFT operation. In some cases this might be already implemented in order to perform reliable channel estimation. The added complexity of this is $O(N \log N)$. The complexity of computing ACF is $O(C^2)$, C is the number of samples used to estimate the ACF and can be regarded as the correlation length. For a fixed FFT size, by reducing C to ten folds, the proposed method will allow 100 folds complexity reduction in obtaining ACF but adds $N \log N$. As a numerical example, in [147], pilot carriers over 4096 symbols were used in a 2048 FFT size OFDM system to estimate ACF. In our proposed modification, we use only 200 symbols and even get gains in our results. Simple calculations show tremendous 350 times complexity reduction and at least 20 times reduction in processing time.

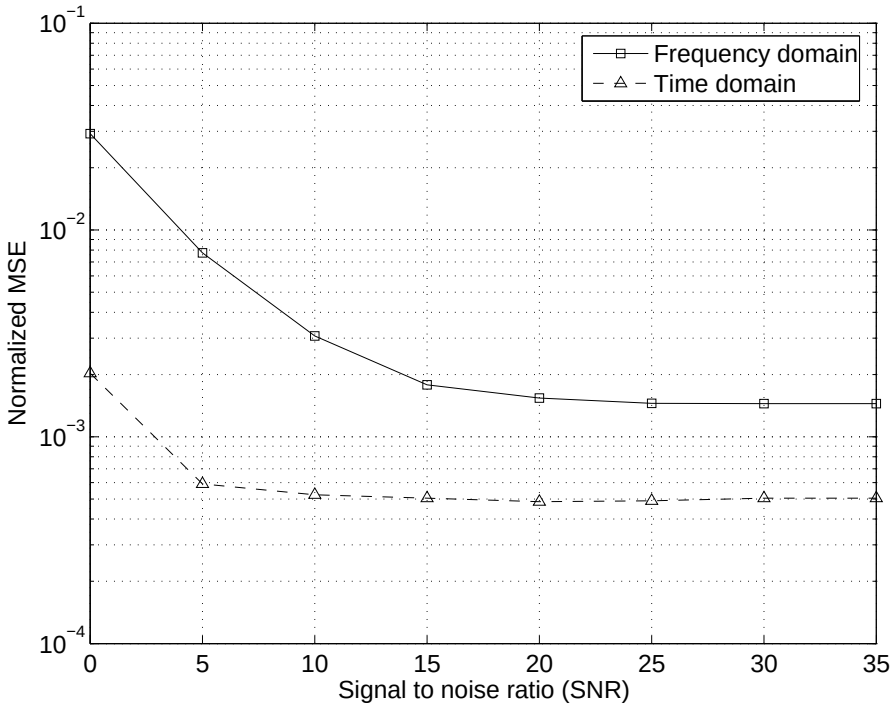

Figure 4.2 Mean squared error as a function of signal to noise ratio for a fixed Dopper spread of 300Hz.

4.4 Numerical Results

Computer simulations were performed to evaluate the performance of the proposed scheme. An OFDM system with 64 subcarriers is used for simulations. The carrier frequency is set to 3.5 GHz and CP size of 16 is used. The available channel bandwidth is 1 MHz and QPSK is used for mapping bits into data symbols. For a MSS speed of 55 mph, f_D=300 Hz. A 16-tap time-varying channel with exponentially decaying power profile, which is generated according to [138], is used in simulations.

For obtaining the Doppler values, all of the subcarriers in the CFR based method and all of the taps in the CIR method are used. The correlations from different taps are added up to obtain maximum ratio combining.

Fig. 4.2 shows the normalized mean square error (NMSE) of Doppler estimation when estimation is done using CFR and when it is done using CIR as proposed. 300 OFDM symbols are used to obtain the correlation values and the Doppler spread was 300 Hz. We can see a considerable gain achieved by the proposed method especially in low SNR (5-10 dB) conditions where the effect of noise is more visible.

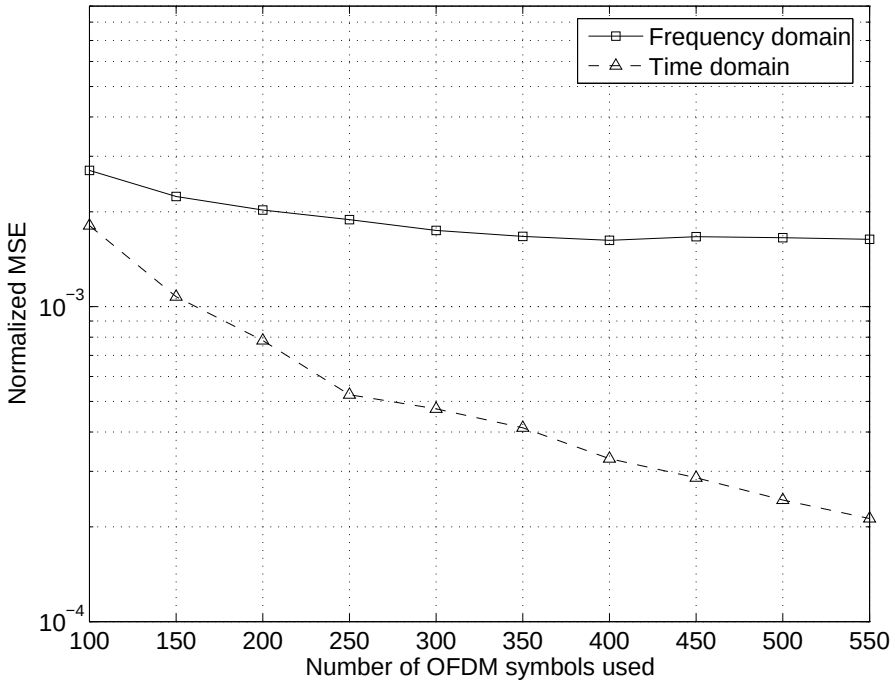

Figure 4.3 Mean squared error as a function of averaging size for fixed Dopper spread of 300Hz and SNR value of 15dB.

The NMSE versus the correlation length is shown in Fig. 4.3. The Doppler spread is fixed to 300 Hz and SNR is 15 dB. It is evident that our method reduces the correlation length to many folds less than conventional method for same estimation performance. In general, the results obtained indicate robustness of this method for Doppler spread estimation in Rayleigh fading channels.

Finally, Fig. 4.4 shows the MSE as a function of the maximum Doppler frequency for a fixed SNR of 15 dB. As this figure shows, the MSE increases for both time and frequency domain estimations with increasing Doppler frequency. This is caused by the increased ICI power due to larger Doppler frequencies.

4.5 Conclusion

In this chapter, Doppler spread estimation for mobile OFDM systems in Rayleigh fading channels is presented. Doppler spread is estimated using the time domain channel estimates instead of frequency domain channel response. By using the CIR, the effect of the noise and ICI on the frequency-domain channel is reduced. Computer simulations are carried out for comparing the

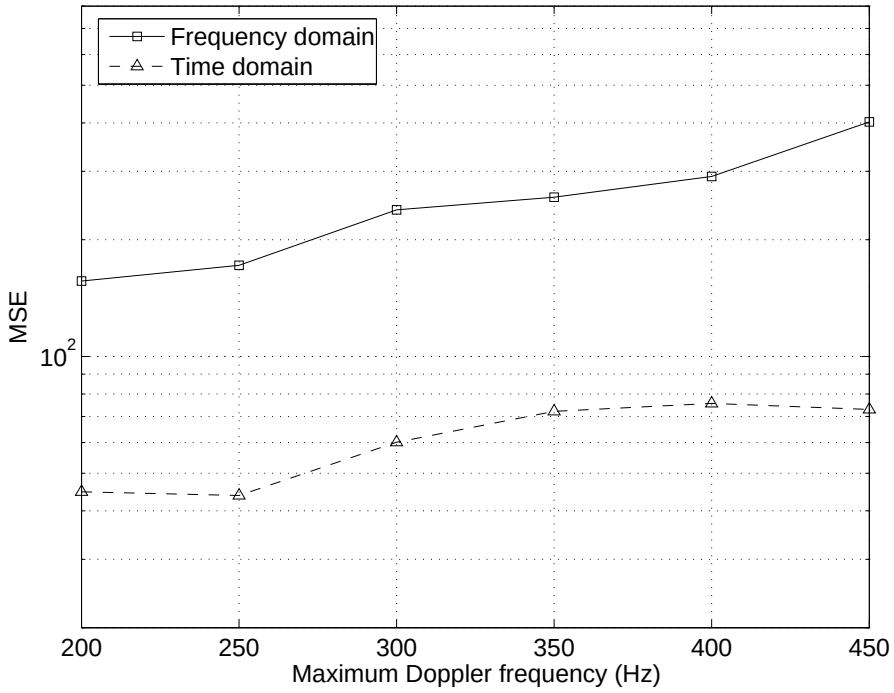

Figure 4.4 Mean squared error as a function of the maximum Doppler frequency for SNR value of 15dB.

performances of time domain and frequency domain Doppler estimation methods. Our results show the validity and the robustness of proposed scheme in wide range of operating conditions.

CHAPTER 5

MMSE NOISE PLUS INTERFERENCE POWER ESTIMATION IN ADAPTIVE OFDM SYSTEMS

5.1 Introduction

In orthogonal frequency division multiplexing (OFDM), the wide transmission spectrum is divided into narrower bands and data is transmitted in parallel on these narrow bands. Therefore, the symbol period is increased by the number of sub-carriers, decreasing the effect of inter-symbol interference (ISI). The remaining ISI effect is eliminated by cyclically extending the signal. OFDM provides effective solution to high data-rate transmission by its robustness against multi-path fading [124]. Parallel with the possible data rates, the transmission bandwidth of OFDM systems is also large. UWB-OFDM [150] and IEEE 802.16 based wireless metropolitan area networks (WMANs) [151] are examples of OFDM systems with large bandwidths. Because of these large bandwidths, noise can not be assumed to be white with flat spectrum across subcarriers.

The signal-to-noise ratio (SNR) is broadly defined as the ratio of desired signal power to noise power and has been accepted as a standard measure of signal quality for communication systems. Adaptive system design requires the estimate of SNR in order to modify the transmission parameters to make efficient use of system resources. Poor channel conditions, reflected by low SNR values, require that the transmitter modifies transmission parameters such as coding rate, modulation mode *etc.* in order to compensate for the channel and to satisfy certain application dependent constraints such as constant bit-error-rate (BER) and throughput. Dynamic system parameter adaptation requires a real-time noise power estimator for continuous channel quality monitoring and corresponding compensation in order to maximize resource utilization. In [152–154], bit loading in DMT systems is performed using the knowledge of SNR information in each subcarrier position, and adaptive bit-loading is applied to OFDM systems in [155, 156]. In these papers, SNR is assumed to be perfectly known. In [157] the effect of imperfect SNR information on adaptive bit-loading is investigated, but the errors are assumed to be caused by channel estimation and noise variance is assumed to

be constant over all subcarriers. The knowledge of SNR also provides information about the channel quality which can be used by handoff algorithms, power control, channel estimation through interpolation, and optimal soft information generation for high performance decoding algorithms.

White noise is rarely the case in practical wireless communication systems where the noise is dominated by interferences, which are often colored in nature. This is more pronounced in OFDM systems where the bandwidth is large and the noise power is not the same over all of the sub-carriers. Color of the noise is defined as the variation of its power spectral density in frequency domain. This variation of spectral content affects certain sub-carriers more than the others. Therefore, an averaged noise estimate is not the optimal technique to use. The SNR can be estimated using regularly transmitted training sequences, pilot data or data symbols (blind estimation). In this chapter, we restrict ourselves to data aided estimation. A comparison of time-domain SNR estimation techniques can be found in [158]. There are several other SNR measurement techniques which are given in [159] and references listed therein. In the literature of OFDM SNR estimation, the number of related works is limited. In conventional SNR estimation techniques, the noise is usually assumed to be white and an SNR value is calculated for all subcarriers [160–163]. In [161], channel estimation for an OFDM system with multiple transmit and receive antennas is studied. Using the intermediate signals from channel estimation, noise variance is also calculated. Pilots are used for estimation and only one noise variance is estimated for the whole subcarrier range. In [162], the noise variance (assumed to be constant for each subcarrier) is estimated by finding the eigenvalue decomposition of the channel frequency correlation (CFC). The eigen-decomposition will partition the signal into noise subspace and signal subspace. If the length of the multipath channel is known, which is estimated from the eigenvalues using minimum descriptive length (MDL) estimation method, one can get noise variance and channel power. SNR estimation for an OFDM system under AWGN channel is given in [163], where estimation is performed using the BPSK modulated preamble symbols of HiperLAN/2. In [164, 165], the assumption that the noise variance is constant over subcarriers is removed by calculating SNR values for each subcarrier. However, the correlation of the noise variance across subcarriers is not used in either paper as noise variance is calculated for each subcarrier separately. Blind (expectation maximization (EM)) and decision-directed noise variance estimation algorithms are given in [164]. The noise variances are calculated separately for each subcarrier by assuming they are constant over time. Therefore, the noise variance at each subcarrier is assumed to be independent of each other and the same algorithm is applied for each subcarrier. For the decision

directed approach, the distribution of error is obtained, and noise variance is calculated using the variance of estimated error values. A look-up table or the derived equations can be used for this transformation. SNR estimation for a 2×2 MIMO-OFDM system is presented in [165]. SNR is estimated using the preambles without the need for channel estimation. Two SNRs are defined, SNR per subcarrier and overall SNR. SNR per subcarrier is calculated using four neighboring subcarriers. However, the correlation of the noise variance across subcarriers is not used since noise variance is calculated for each subcarrier separately.

In this chapter, the white noise assumption is removed and variation of the noise power across OFDM sub-carriers as well as across OFDM symbols is considered. The noise variances at each subcarrier are estimated using a two dimensional MMSE filter whose coefficients are calculated using statistics of the noise. These estimates are especially useful for adaptive modulation, optimal soft value calculation for improving channel decoder performance, and for opportunistic spectrum usage for cognitive radios. Moreover, it can be used to detect and avoid narrowband interference. The chapter focuses more on estimation of noise power, and assumes that the signal power, and hence SNR, can be estimated from the channel estimates.

This chapter is organized as follows. In the next section, our system model is described. Section 5.3 explains the details of the proposed algorithms. Numerical results are presented in Section 5.4 and the conclusions are given in Section 5.5.

5.2 System Model

For the time and frequency domain OFDM symbols, the model given in Section 2.2 is used. At the receiver, the signal is received along with noise and interference. After synchronization and removal of the cyclic prefix (CP)[1], discrete Fourier transform (DFT) is applied to the received signal. The received signal at the kth subcarrier of the mth OFDM symbol can then be written as

$$Y_m(k) = X_m(k)H_m(k) + \underbrace{I_m(k) + W_m(k)}_{Z_m(k)} \qquad 0 \leq k \leq N-1, \tag{5.1}$$

where $I_m(k)$ is the colored noise caused by interferers or primary users. We assume that the impairments due to imperfect synchronization, transceiver non-linearities *etc.* are incorporated into $W_m(k)$ and the channel frequency response (CFR) does not change within the observation time.

[1]The length of the CP is assumed to be larger than the maximum excess delay of the channel.

The white noise is modeled as a zero-mean Gaussian random variable with variance σ_w^2, *i.e.* $W_m(k) = \mathcal{N}(0, \sigma_w^2)$. The interference term is also modeled as a zero-mean Gaussian variable whose variance is a function of the symbol and subcarrier indices, *i.e.* $I_m(k) = \mathcal{N}(0, \sigma_{m,k}^2)$, where $\sigma_{m,k}$ is the local standard deviation. Note that although the time-domain samples of the interference signal are correlated (colored), the frequency-domain samples $I_m(k)$ are not correlated, but their variances are correlated [166]. Assuming that the interference and white noise terms are uncorrelated, the overall noise term $Z_m(k)$ can be modeled as $Z_m(k) = \mathcal{N}(0, {\sigma'_{m,k}}^2)$, where ${\sigma'_{m,k}}^2 = \sigma_{m,k}^2 + \sigma_w^2$ is the effective noise variance. *The goal of this chapter is to estimate* ${\sigma'_{m,k}}^2$ *which can be used to find SNR or to measure the spectrum that the OFDM system is currently using.* Note that if $\sigma_w \gg \sigma_{m,k}$, the overall noise can be assumed to be white and it is colored otherwise.

The autocorrelation of the effective noise power is defined as

$$R_{\sigma'^2}(\tau, \Delta) = E_{m,k}\left[{\sigma'_{m,k}}^2 {\sigma'_{m+\tau,k+\Delta}}^2\right], \tag{5.2}$$

where $E_{m,k}[\cdot]$ represents expectation over OFDM symbols and subcarriers. When the time dependency is dropped, the correlation of variance in the frequency dimension can be expressed as

$$R_{\sigma'^2}(\Delta) = E_k\left[{\sigma'_k}^2 {\sigma'_{k+\Delta}}^2\right]. \tag{5.3}$$

5.3 Details of the Proposed Algorithm

In this chapter, three different scenarios for the noise process $Z_m(k)$ are considered: white noise, stationary[2] colored noise, and non-stationary colored noise. When the frequency direction is considered, the first scenario corresponds to the commonly assumed case, where the frequency spectrum of the noise is uniform. In the second scenario, the existence of a strong interferer which has larger bandwidth than the desired OFDM signal is addressed. A strong co-channel interferer is a good example for this case. In the third scenario, an interferer whose statistics are not stationary with respect to frequency is assumed to be present. Adjacent channel interference or a co-channel interference with a smaller bandwidth than the desired signal (narrowband interference) are examples of this type of interference. These three scenarios can also be applied to time domain where time-domain statistics of $Z_m(k)$ should be considered.

[2]Stationarity in both time and frequency domains are considered.

The commonly used approach for noise power estimation in OFDM systems is based on finding the difference between the noisy received sample in the frequency domain and the best hypothesis of the noiseless received sample [160]. It can be formulated as

$$\hat{Z}_m(k) = Y_m(k) - \hat{X}_m(k)\hat{H}_m(k), \tag{5.4}$$

where $\hat{X}_m(k)$ is the noiseless sample of the received symbol and $\hat{H}_m(k)$ is the channel estimate for the kth sub-carrier of nth OFDM symbol. The bias caused by incorrect hypothesis of data symbols $\hat{X}_m(k)$ can be removed by using a look-up table or statistical relation between the true and estimated SNR values [164].

We propose to filter the noise variance estimates calculated at each subcarrier $|\hat{Z}_m(k)|^2$ using a two dimensional filter. Filtering will remove the common assumption of having the noise to be white and it will take the colored interference (both in time and frequency) into account. Let us represent the weighting coefficient of the filter at each subcarrier with $\beta_{u,l}$. In this case, the estimate of the noise power at kth subcarrier of nth OFDM symbol can be written as

$$\hat{\sigma'}^2_{m,k} = \sum_{u=-U}^{U} \sum_{l=-L}^{L} \beta_{u,l} |\hat{Z}_{n+u,k+l}|^2, \tag{5.5}$$

where $2U+1$ and $2L+1$ are the dimensions of the filter in time and frequency directions respectively. The weighting coefficients should have a unity power, *i.e.* $\sum_u \sum_l \beta_{u,l} = 1$. The two dimensional filter given by (5.5) can be complex for practical implementation. To reduce the complexity, two cascaded one dimensional filters in time and frequency are used instead. This approach is valid as the variation of the noise variance in time and frequency dimensions are independent. For the rest of the chapter, filtering in the frequency direction will be considered and symbol index will be dropped for notational clarity. Time domain filtering is the dual of the frequency domain counterpart, and the same algorithm can be applied for filtering. The estimator in frequency domain only can be represented as

$$\hat{\sigma'}^2_{k} = \sum_{l=-L}^{L} \beta_l |\hat{Z}_{k+l}|^2, \tag{5.6}$$

where β_l satisfies $\sum_{l=-L}^{L} \beta_l = 1$. The filter coefficients β_l can be calculated using the statistics of the interference plus noise $Z(k)$. In this chapter, we use a minimum mean-square error (MMSE) approach for finding these coefficients.

Estimation error at the kth subcarrier can be written as

$$\varepsilon(k) = \hat{\sigma'}_k^2 - {\sigma'_k}^2 \tag{5.7}$$

$$= \sum_{l=-L}^{L} \beta_l |\hat{Z}(k+l)|^2 - {\sigma'_k}^2. \tag{5.8}$$

Note that the instantaneous errors (5.8) will be a function of the filter coefficients β_l, the interference statistics, average interference power, and average noise power. Hence, ideally the optimum values for weighting coefficients will be different for each subcarrier. However, this requires knowledge of local statistics and has a large complexity. In order to overcome these problems, we use the same coefficients for the whole subcarrier range.

The filter coefficients can be calculated by minimizing the mean-squared-error (MSE), *i.e* by minimizing the expected value of the square of (5.8). The MSE can be formulated as

$$\rho = E_k \left[\varepsilon(k)^2\right] \tag{5.9}$$

$$= E_k \left[\left(\sum_{l=-L}^{L} \beta_l |\hat{Z}(k+l)|^2 - {\sigma'_k}^2 \right)^2 \right] \tag{5.10}$$

$$= E_k \left[\sum_{l=-L}^{L} \sum_{u=-L}^{L} \beta_l \beta_u |\hat{Z}(k+l)|^2 |\hat{Z}_(k+u)|^2 - 2{\sigma'_k}^2 \sum_{l=-L}^{L} \beta_l |\hat{Z}(k+l)|^2 + {\sigma'_k}^4 \right], \tag{5.11}$$

where $E_k[\cdot]$ represents expectation over subcarriers. By further simplification, (5.11) can be written in terms of the auto-correlation of the variance of the noise component $R_{\sigma'^2}(\tau, \Delta)$ and the filter coefficients as

$$\rho = \left(1 + \sum_{l=-L}^{L} \beta_l^2\right) R_{\sigma'^2}(0) - 2 \sum_{l=-L}^{L} \beta_l R_{\sigma'^2}(l) + \sum_{l=-L}^{L} \sum_{u=-L}^{L} \beta_l \beta_u R_{\sigma'^2}(l-u). \tag{5.12}$$

The weighting coefficients that minimize (5.12) yield the MMSE solution. In order to find this solution, the derivative of MSE ρ with respect to filter coefficients can be set to zero. We can write (5.12) in matrix form for simplifying the calculations. Let $\boldsymbol{\beta} = [\beta_{-L} \cdots \beta_0 \cdots \beta_L]^T$ be the coefficient vector, $\boldsymbol{r} = [R_{\sigma'^2}(-L) \cdots R_{\sigma'^2}(0) \cdots R_{\sigma'^2}(L)]^T$ be the correlation vector, and $\boldsymbol{C}_{\sigma'^2}$ be the covariance matrix of size $(2L+1) \times (2L+1)$ with coefficients $\boldsymbol{C}_{\sigma'^2}(i,j) =_{\sigma'^2} (i-j)$. Using these

definitions, the MSE equation given in (5.12) can be represented in matrix form as

$$\rho = R_{\sigma'^2}(0)(1 + \boldsymbol{\beta}^T\boldsymbol{\beta}) - 2\boldsymbol{\beta}^T\boldsymbol{r} + \boldsymbol{\beta}^T\boldsymbol{C}_{\sigma'^2}\boldsymbol{\beta}. \tag{5.13}$$

The derivative of (5.13) with respect to the filter coefficients is

$$\frac{d}{d\boldsymbol{\beta}}\rho = 2R_{\sigma'^2}(0)\boldsymbol{\beta} - 2\boldsymbol{r} + 2\boldsymbol{C}_{\sigma'^2}\boldsymbol{\beta}. \tag{5.14}$$

By setting the derivative to zero, *i.e.* $d\rho/d\boldsymbol{\beta} = 0$, and arranging the terms, the coefficient vector can be calculated as

$$\boldsymbol{\beta} = (\boldsymbol{C}_{\sigma'^2} + R_{\sigma'^2}(0)\boldsymbol{I})^{-1}\boldsymbol{r}, \tag{5.15}$$

where $\boldsymbol{I}$ is $(2L+1)\times(2L+1)$ identity matrix. The variance of the proposed estimator can be found by inserting (5.15) into (5.13) as

$$\rho = R_{\sigma'^2}(0) - \boldsymbol{r}^T(\boldsymbol{C}_{\sigma'^2} + R_{\sigma'^2}(0)\boldsymbol{I})^{-1}\boldsymbol{r}. \tag{5.16}$$

Some example weighting factors[3] in the frequency domain are shown in Fig. 5.1 for different interference to white noise power ratios which is defined as

$$INR_{dB} \triangleq 10\log_{10}\frac{\sum_{k=0}^{N-1} E\left[|I(k)|^2\right]}{\sum_{k=0}^{N-1} E\left[|W(k)|^2\right]}. \tag{5.17}$$

As the noise becomes more colored (high decibel values in the figure), the filter becomes more localized in order to be able to capture the variation of noise variance. On the other hand, filter turns into a rectangular window when white noise becomes more dominant. Note that the weighting coefficients depend on the statistics of interference and white noise. These statistics can be obtained with averaging by assuming the noise process is time-stationary in a given interval. However, the statistics should be updated in time as they might be changing. In order to achieve this, a tracking method such as an alpha-tracker can be employed.

[3]See Section 5.4 for details of the considered system.

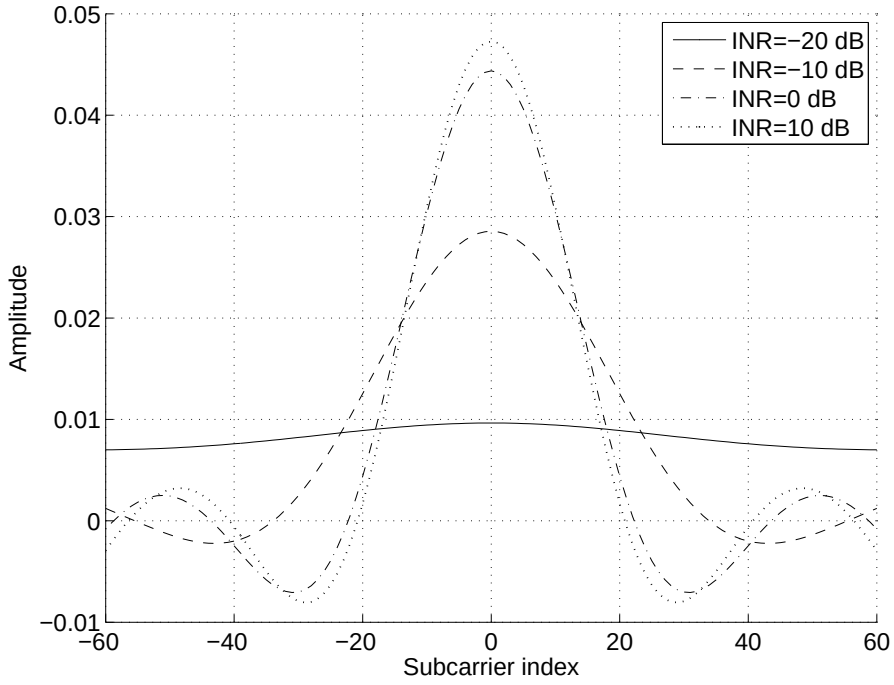

Figure 5.1 Weighting coefficients for different colored noise to white noise power ratios.

5.3.1 Rectangular Window

In order to decrease the computational complexity of the filtering algorithm, we propose an approximate method. Instead of using the weighting factor $\boldsymbol{\beta}$ for filtering, a simple rectangular window, *i.e.* a moving average, is used. The dimensions of this filter (as OFDM symbol and subcarrier number) can be calculated using the statistics of the received signal. The filter coefficients in rectangular window case can be written as

$$\beta_l' = \begin{cases} 1/L_w & -L_w \leq l \leq L_w \\ 0 & \text{otherwise} \end{cases} \tag{5.18}$$

where $2L_w + 1$ is the length of rectangular window. For calculating the optimum window size, the MSE given in (5.12) can be minimized by excessive searching [25]. Note that in this case β_l should be replaced with β_l'.

The window size can also be calculated using the weight β_l given in (5.15) by minimizing the squared error between the two coefficients as

$$L_w = \arg\min_{L_w} \left\{ \sum_{l=-L}^{L} (\beta_l - \beta'_l)^2 \right\}. \tag{5.19}$$

Our results show that both methods for calculating L_w yield very close results, and the second method, *i.e.* calculation using (5.19), is used in this chapter for finding the length of rectangular window.

For calculating the noise variance at one subcarrier, $2L$ multiplications and additions are required in the MMSE filtering algorithm. On the other hand, only $2L_w$ additions and 1 division is required in the rectangular window algorithm. Although, the reduction in the computational complexity is large, the performance loss due to the rectangular windowing is not very big as will be discussed later.

5.3.2 Edges and Time Averaging

The filtering method given by (5.6) requires the noise estimates at L-many left and right subcarriers for estimating the variance at current subcarrier. This might be a problem at the edges of the spectrum as the weights are calculated by assuming that averaging can be done on both sides of the current subcarrier. In order to find the weighing values at the edges, (5.6) is modified and (5.15) is derived again. In order to find the noise variance at the right edge of the spectrum, for example, (5.6) can be updated as

$$\hat{\sigma'}_k^2 = \sum_{l=-L}^{0} \beta_l |\hat{Z}(k+l)|^2. \tag{5.20}$$

In this case, the same formula for $\boldsymbol{\beta}$ given in (5.15) can be used for calculating the weighting coefficients. However, the definition of $\boldsymbol{\beta}$ and $\boldsymbol{r}$ should be updated as $\boldsymbol{\beta} = [\beta_{-L} \cdots \beta_0]^T$ and $\boldsymbol{r} = [R_{\sigma'^2}(-L) \cdots R_{\sigma'^2}(0)]^T$.

A similar problem to the edge problem in frequency domain is observed in the time domain filtering (across OFDM symbols) if the estimation is delay sensitive. In this case, the estimator might not have OFDM symbols after the current symbol and hence filtering should be applied as defined in (5.20). Therefore, the noise variance or other related parameters can be estimated using only the previous OFDM symbols.

5.4 Numerical Results

An OFDM system with 512 subcarriers and 20 MHz bandwidth is considered for testing the proposed algorithms. The stationary interference is assumed to be caused by a co-channel user transmitting in the same band with the desired user, and a co-channel signal with 3 MHz bandwidth centered in the middle of the 20 MHz band is used to simulate the non-stationary interference (please refer to Fig. 5.4). Filtering is performed in only frequency domain, *i.e.* $\beta_m(k) = w(k)$, and only one OFDM symbol is considered. However, the results can be generalized to the two dimensional case as mentioned earlier. The length of the MMSE filter is set to 120, *i.e.* $L = 60$. Normalized MSE is used as a performance measure of the estimator as it reflects both the bias and the variance of the estimation. The normalized MSE of σ'^2 is defined as

$$NMSE(\sigma'^2) \triangleq \frac{\sum_{k=0}^{N-1} E\left[\left(\hat{\sigma'}_k^2 - {\sigma'_k}^2\right)^2\right]}{\sum_{k=0}^{N-1} {\sigma'_k}^4}. \tag{5.21}$$

The MSE performances of the conventional, MMSE filtering, and rectangular window algorithms are given in Figs. 5.2 and 5.3. Fig. 5.2 gives the MSEs as a function of the stationary interference to white noise power ratio and Fig. 5.3 gives the MSEs as a function of the non-stationary interference to white noise power ratio. The interference to noise ratio is as defined in (5.17), and the total noise plus interference power is kept constant for both figures. When the ratio is very small (e.g. -20 dB), the total noise can be considered as white noise, and the conventional algorithm performs best because its inherent white noise assumption is valid. The estimation error increases as the total noise becomes more colored for all three methods. The proposed filtering algorithms have considerable performance gain over the conventional one. The rectangular window based algorithm has very close performance to the MSE filtering, and it may be preferable in practical applications because of its lower complexity. Note that Figs. 5.2 and 5.3 show the MSEs in logarithmic scale. The gain obtained by using the proposed algorithms at high power ratios is much larger than the MSE loss compared to conventional algorithm at low power ratios (white noise case).

Finally, the application of the proposed methods to narrowband interference detection is studied[4]. Fig. 5.4 shows the true and estimated power levels for a non-stationary interference/primary user. Figs. 5.5 and 5.6 show the probability of detection and probability of false alarm rates for a single

[4]Interference detection and primary user identification are the similar operations. Hence, the presented results are valid for primary user identification in cognitive radios.

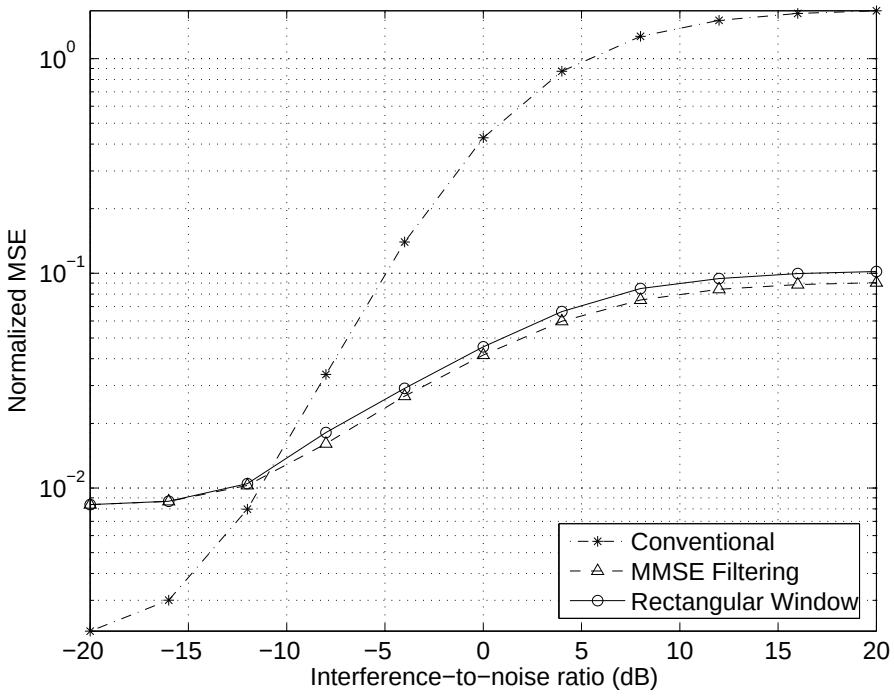

Figure 5.2 Mean squared error for different algorithms as a function of the stationary interference to white noise power ratios.

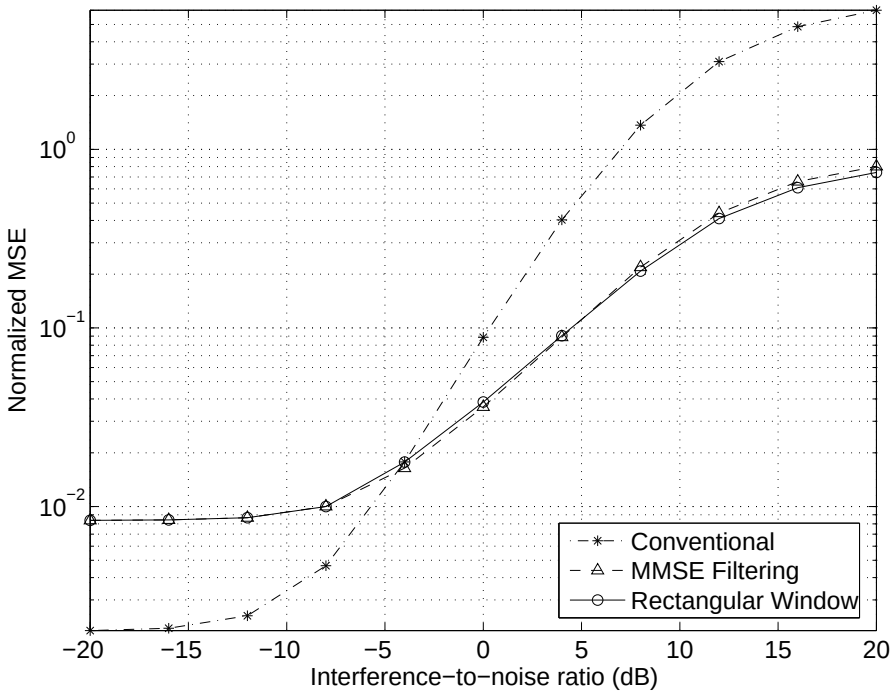

Figure 5.3 Mean squared error for different algorithms as a function of the non-stationary interference to white noise power ratios.

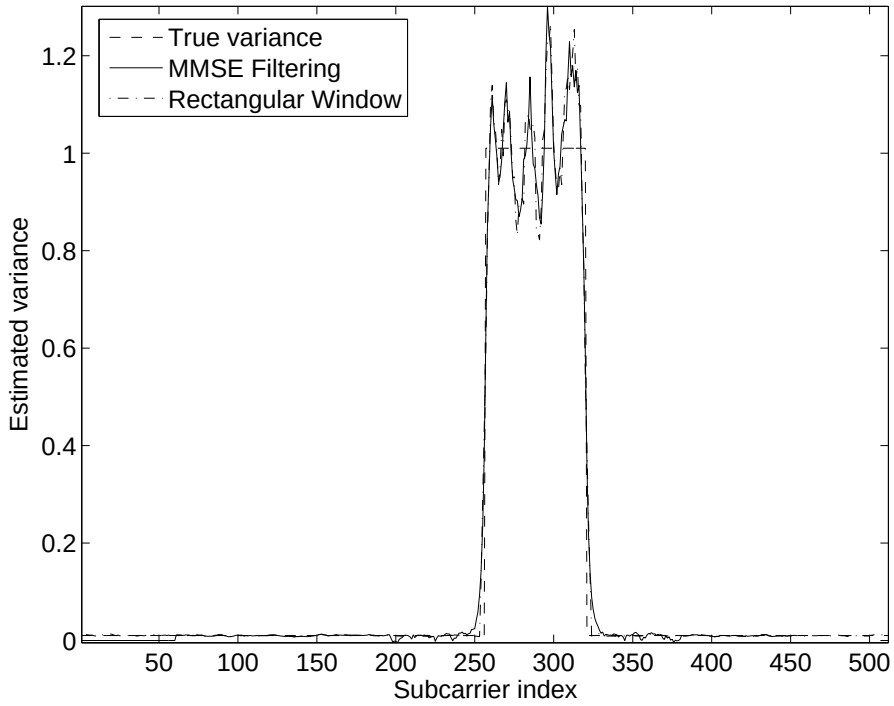

Figure 5.4 True and estimated noise variances in the presence of a narrowband interferer.

subcarrier. The output of the frequency domain filters (MMSE and rectangular) and the magnitude of the FFT output (no filtering) are passed through a threshold detector. The selection of threshold value can be performed in order to satisfy a target probability of detection or probability of false alarm [95]. However, it is out of the scope of this chapter and the threshold values are set equal to the white noise variance plus half of the interference variance, *i.e.* $\sigma_w^2 + \sigma_k^2/2$. Both the probability of detection and probability of false alarm performances are improved by application of the proposed MMSE and rectangular filtering which makes the energy detector based approach a better candidate for interference detection. Figs. 5.4, 5.5 and 5.6 show that the proposed methods can be used for identifying the subcarriers with interference and also for detecting the primary users in cognitive radios.

5.5 Conclusion

In this chapter, a new noise variance estimation algorithm for OFDM systems is proposed. The proposed method removes the common assumption of white Gaussian noise and considers colored noise. Noise variance, and hence SNR, is calculated by using two cascaded filters in time and fre-

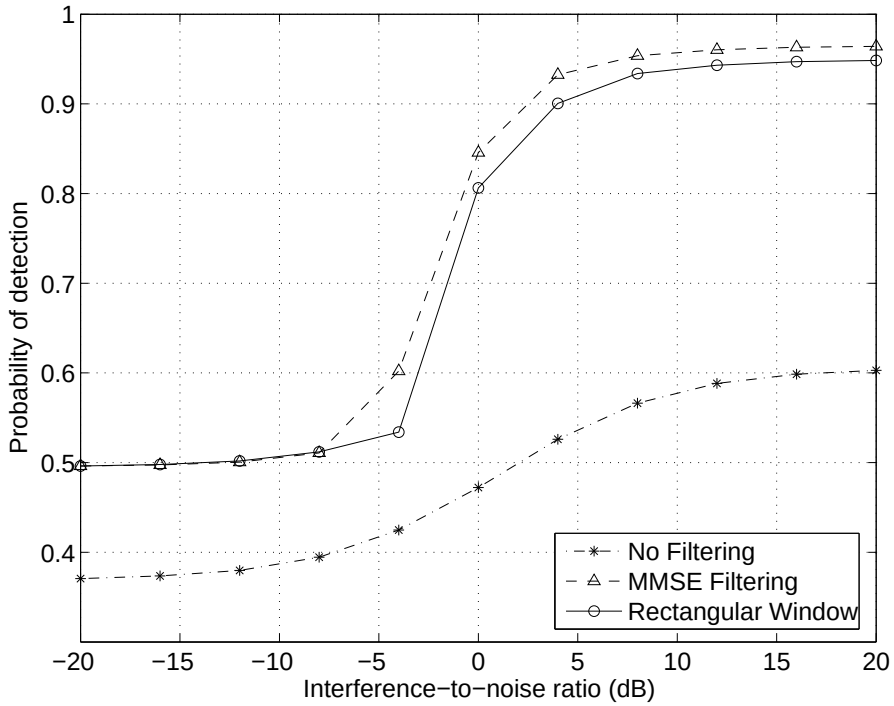

Figure 5.5 Probability of detection of interference as a function of interference to white noise power ratios.

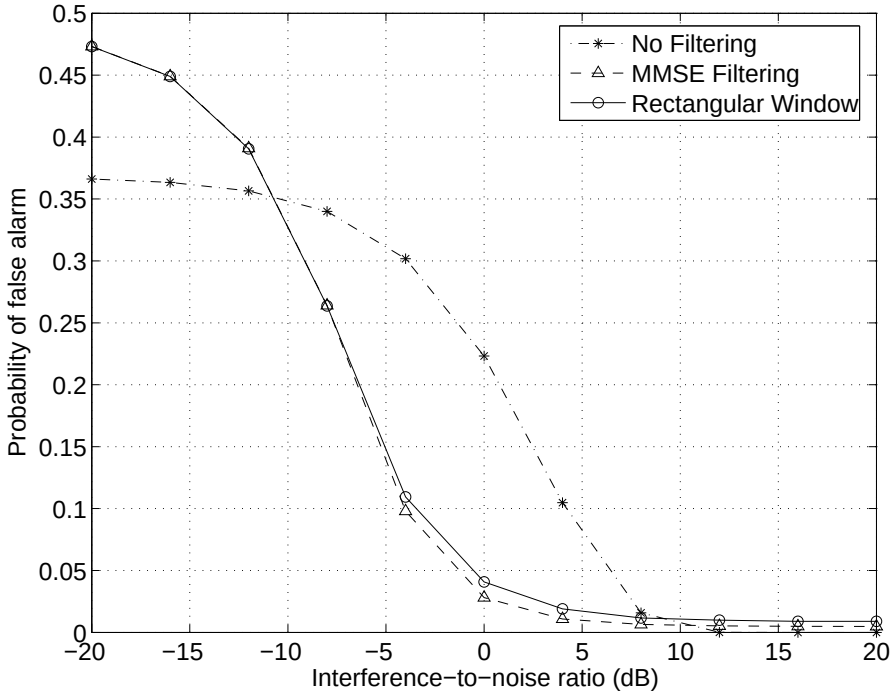

Figure 5.6 Probability of false alarm rates as a function of interference to white noise power ratios.

quency directions whose coefficients are calculated using the statistics of noise/interference variance. Simulation results show that the proposed algorithm out-performs conventional algorithm under colored noise cases and it can identify the presence of interference in the OFDM transmission band.

CHAPTER 6

SPECTRUM SENSING FOR COGNITIVE RADIO APPLICATIONS

6.1 Introduction

One of the most important components of cognitive radio concept is the ability to measure, sense, learn, and be aware of the parameters related to the radio channel characteristics, availability of spectrum and power, interference and noise temperature, radio's operating environment, user requirements and applications, available networks (infrastructures) and nodes, local policies and other operating restrictions. In cognitive radio terminology, *primary users* can be defined as the users who have higher priority or legacy rights on the usage of a specific part of the spectrum. On the other hand, *secondary users*, which have lower priority, exploit this spectrum in such a way that they do not cause interference to primary users. Therefore, secondary users need to have cognitive radio capabilities, such as sensing the spectrum reliably to check whether it is being used by a primary user, and to change the radio parameters to exploit the unused part of the spectrum.

Being the focus of this chapter, spectrum sensing by far is the most important task among others for the establishment of cognitive radio. Spectrum sensing includes awareness about the interference temperature and existence of primary users. As an alternative to spectrum sensing, geolocation and database or beacons[1] can be used for determining the current status of the spectrum usage [167, 168]. In this chapter, we focus on spectrum sensing performed by cognitive radios because of its broader application areas while referring other methods as needed. Although spectrum sensing is traditionally understood as measuring the spectral content, or measuring the interference temperature over the spectrum; when the ultimate cognitive radio is considered, it is a more general term that involves obtaining the spectrum usage characteristics across multiple dimensions such as time, space, frequency, and code. It also involves determining what type of signals are occupying

[1] When beacons are used, the transmitted information can be occupancy of a spectrum as well as other advanced features such as channel quality.

the spectrum (including the modulation, waveform, bandwidth, carrier frequency, *etc.*). However, this requires more powerful signal analysis techniques with additional computational complexity.

Various aspects of spectrum sensing task are illustrated in Fig. 6.1. The goal of this chapter is to point out several aspects of spectrum sensing as shown in this figure. These aspects will be discussed in the rest of this chapter. We start by explaining some challenges associated with spectrum sensing in Section 6.2. Section 6.3 explains the main spectrum sensing methods. Cooperative sensing concept and its various forms are introduced in Section 6.4, followed by a discussion of external sensing algorithms in Section 6.5. Statistical modeling of network traffic and utilization of these models for prediction of primary user behavior is studied in Section 6.6. Section 6.7 explains the factors on deciding the frequency of spectrum sensing. Hardware perspective of sensing problem is discussed in Section 6.8. We introduce the multi-dimensional spectrum sensing concept in Section 6.9. Finally, sensing features of some current wireless standards are explained in Section 6.10 and our conclusions are given in Section 6.11.

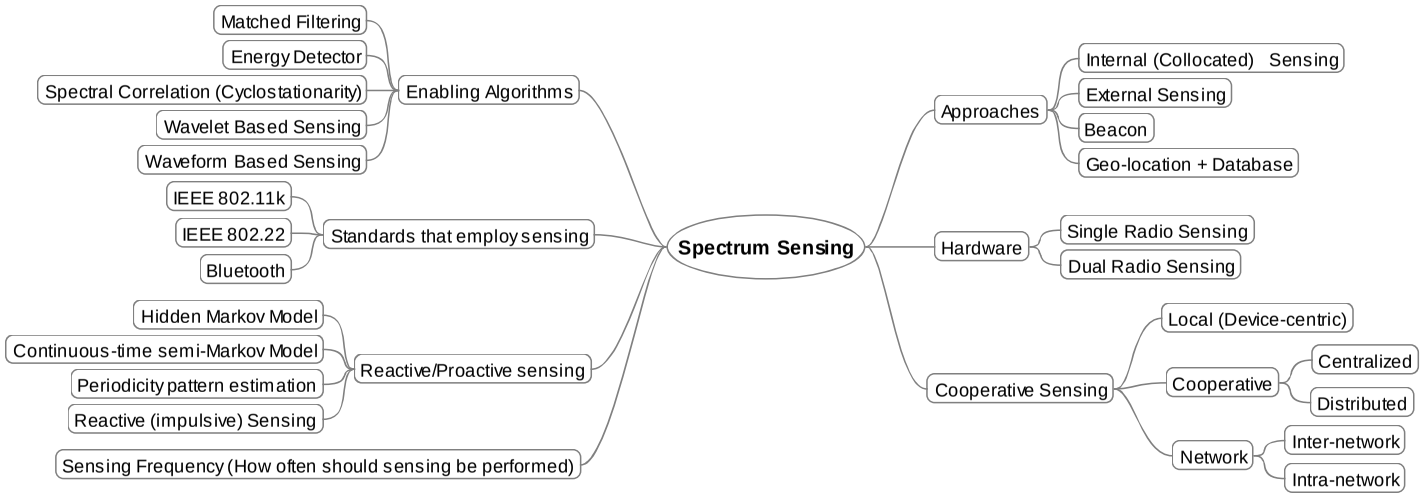

Figure 6.1 Various aspects of spectrum sensing for cognitive radio.

6.2 Challenges

Before getting into the details of spectrum sensing techniques, some challenges associated with the spectrum sensing for cognitive radio is given in this section.

6.2.1 Hardware Requirements

Spectrum sensing for cognitive radio applications requires high sampling rate, high resolution analog to digital converters (ADCs) with large dynamic range, multiple analog front end circuitry, and high speed signal processors. Estimating the noise variance or interference temperature over transmission of desired narrowband signals is not new. Such noise variance estimation techniques have been popularly used for optimal receiver designs like channel estimation, soft information generation *etc.*, as well as for improved hand-off, power control, and channel allocation techniques. The noise/interference estimation problem is easier for these purposes as receivers are tuned to receive signals that are transmitted over a desired bandwidth. Moreover, receivers are capable of processing the narrowband baseband signals with reasonably low complexity and low power processors. However, in cognitive radio, terminals are required to process transmission over a much wider band for sensing any opportunity.

6.2.2 Hidden Primary User Problem

Hidden primary user problem is similar to the hidden node problem in carrier sense multiple accessing (CSMA). This problem can be caused by many factors including severe multipath fading or shadowing that secondary users observe while scanning primary users' transmissions. Fig. 6.2 shows an illustration of hidden node problem. Here, cognitive radio device causes unwanted interference to the primary user (receiver) as the primary transmitters signal could not be detected because of the positioning of devices in space.

6.2.3 Spread Spectrum Primary Users

Primary users that use frequency hopping and spread spectrum signaling, where the power of the primary user signal is distributed over a wider frequency even though the actual information bandwidth is much narrower, are difficult to detect. Especially, frequency hopping based signaling creates significant problems regarding to spectrum sensing. This problem can be partially avoided if the hopping pattern is known and perfect synchronization to the signal can be achieved.

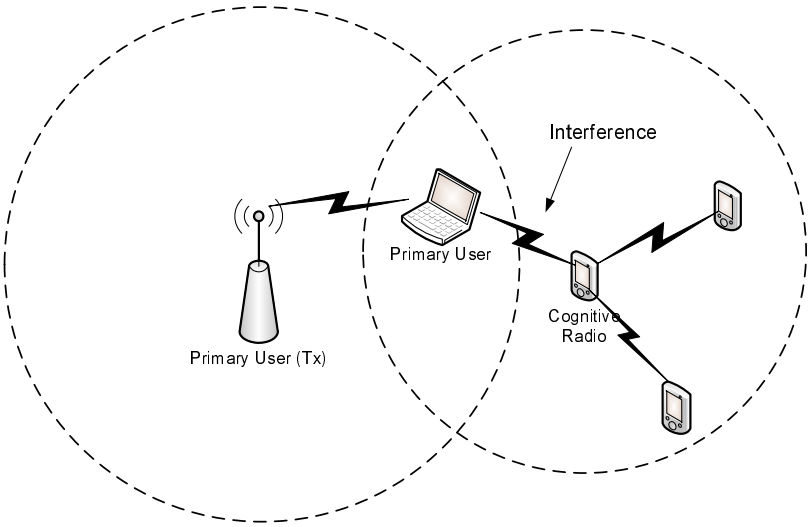

Figure 6.2 Illustration of hidden primary user problem in cognitive radio systems.

6.2.4 Sensing Time

Primary users can claim their frequency bands anytime while cognitive radio is operating at that band. In order to prevent interference to and from primary license owners, cognitive radio should be able to identify the presence of primary users as quickly as possible and should vacate the band immediately. Hence, sensing method should be able to identify the presence of primary user within a certain duration. This requirement possesses a limit on the performance of sensing algorithm and creates a challenge for cognitive radio design.

6.2.5 Other Challenges

Some other challenges that need to be considered while designing effective spectrum sensing algorithm include implementation complexity, presence of multiple secondary users, coherence times, multipath and shadowing, cooperation, competition, robustness, heterogeneous propagation losses, and power consumption.

6.3 Spectrum Sensing Methods for Cognitive Radio

The present literature for spectrum sensing is still in its early stages of development. A number of different methods are proposed for identifying the presence of signal transmission. In some approaches, characteristics of the identified transmission are detected for deciding the signal trans-

mission as well as identifying the signal type. In this section, some of the most common spectrum sensing techniques in the cognitive radio literature are explained.

6.3.1 Matched Filtering

Matched-filtering is known as the optimum method for detection of primary users when the transmitted signal is known [148]. The main advantage of matched filtering is the short time[2] to achieve a certain probability of false alarm or probability of miss detection [169] as compared to other methods that are discussed in this section. However, matched-filtering requires the cognitive radio to demodulate received signals. Hence, it requires perfect knowledge of the primary users signaling features such as bandwidth, operating frequency, modulation type and order, pulse shaping, frame format *etc.* Moreover, since cognitive radio needs receivers for all signal types, implementation complexity of sensing unit is impractically large [170]. Another disadvantage is large power consumption as various receiver algorithms need to be executed for detection.

6.3.2 Waveform Based Sensing

Known patterns are usually utilized in wireless systems to assist synchronization or for other purposes. Such patterns include preambles, midambles, regularly transmitted pilot patterns, spreading sequences *etc.* In the presence of a known pattern, sensing can be performed by correlating the received signal with a known copy of itself [171, 172]. This method is only applicable to systems with known signal patterns, and it is termed as waveform based sensing. In [171], it is shown that waveform-based sensing outperforms energy detector based sensing in reliability and convergence time. Furthermore, it is shown that the performance of the sensing algorithm increases as the length of the known signal pattern increases. As one of the methods for analyzing the wireless local area network (WLAN) channel usage characteristics, packet preambles of IEEE 802.11b [173] signals are exploited in [174, 175]. Measurement results presented in [176] show that waveform based sensing requires short measurements time. However, it is susceptible to synchronization errors.

Let us assume that the received signal has the following simple form

$$y(n) = s(n) + w(n), \tag{6.1}$$

[2]The required number of samples grows as $O(1/SNR)$ for a target probability of false alarm or miss detection at low signal-to-noise ratios (SNRs) [169].

where $s(n)$ is the signal to be detected, $w(n)$ is the additive white Gaussian noise (AWGN) sample, and n is the sample index. Note that $s(n) = 0$ when there is no transmission by primary user. The waveform based sensing metric[3] can be obtained as [171]

$$M = \mathrm{Re}\left[\sum_{n=1}^{N} y(n)s^*(n)\right], \tag{6.2}$$

where N is the length of known pattern. In the absence of the primary user, the metric value becomes

$$M = \mathrm{Re}\left[\sum_{n=1}^{N} w(n)s^*(n)\right]. \tag{6.3}$$

Similarly, in the presence of a primary user's signal, the sensing metric becomes

$$M = \sum_{n=1}^{N} |s(n)|^2 + \mathrm{Re}\left[\sum_{n=1}^{N} w(n)s^*(n)\right]. \tag{6.4}$$

The decision on the presence of a primary user signal can be made by comparing the decision metric M against a fixed threshold λ_W. This is equivalent to distinguishing between the following two hypotheses:

$$\mathcal{H}_0 \quad : \quad y(n) = w(n), \tag{6.5}$$

$$\mathcal{H}_1 \quad : \quad y(n) = s(n) + w(n). \tag{6.6}$$

The performance of the detection algorithm can be summarized with two probabilities: probability of detection P_D and probability of false alarm P_F. P_D is the probability of detecting a signal on the considered frequency when it truly is present, thus large detection probability is desired. It can be formulated as

$$P_D = \Pr\left(M > \lambda_W | \mathcal{H}_1\right), \tag{6.7}$$

where λ_W is the threshold value. P_F is the probability that the test incorrectly decides that the considered frequency is occupied when it actually is not, and it can be written as

$$P_F = \Pr\left(M > \lambda_W | \mathcal{H}_0\right). \tag{6.8}$$

[3]In this chapter, time-domain sampling is explained as an example. Modified versions of the method explained in this chapter can be used in frequency domain as well. Likewise, the method given in this chapter can be modified depending on the available pattern.

P_F should be kept as small as possible. The decision threshold λ_W can be selected for finding an optimum balance between P_D and P_F. However, this requires the knowledge of noise and detected signal powers. The noise power can be estimated, but the signal power is difficult to estimate as it changes depending on ongoing transmission characteristics and the distance between the cognitive radio and primary user. In practice, the threshold is chosen to obtain a certain false alarm rate. Hence, the knowledge of noise variance is enough for selection of a threshold.

6.3.3 Cyclostationarity Based Sensing

Cyclostationarity feature detection is a method for detecting primary user transmissions by exploiting the cyclostationarity features of the received signals [170,177–182]. Cyclostationary features are caused by the periodicity in the signal or in its statistics like mean and autocorrelation. Instead of power spectral density (PSD), cyclic correlation function is used for detecting signals present in a given spectrum. The cyclostationarity based detection algorithms can differentiate noise from primary users' signals. This is a result of the fact that noise is wide-sense stationary (WSS) with no correlation while modulated signals are cyclostationary with spectral correlation due to the redundancy of signal periodicities [179].

The cyclic spectral density (CSD) function of received signal (6.1) can be calculated as [183]

$$S(f,\alpha) = \sum_{\tau=-\infty}^{\infty} R_y^{\alpha}(\tau) e^{-j2\pi f\tau}, \tag{6.9}$$

where

$$R_y^{\alpha}(\tau) = E\left[y(n+\tau)y^*(n-\tau)e^{j2\pi\alpha n}\right] \tag{6.10}$$

is the cyclic autocorrelation function (CAF), and α is the cyclic frequency. The CSD function outputs peak values when the cyclic frequency is equal to the fundamental frequencies of transmitted signal $x(n)$. Cyclic frequencies can be assumed to be known [177, 182] or they can be extracted and used as features for identifying transmitted signals [180].

6.3.4 Energy Detector Based Sensing

Energy detector based approaches, also known as radiometry or periodogram, are the most common ways of spectrum sensing because of their low computational and implementation complexities [31, 96, 109, 170–172, 174, 175, 181, 184–190]. Moreover, they are more generic as receivers

do not need any knowledge on the primary users' signals. The signal is detected by comparing the output of energy detector with a threshold which depends on the noise floor [191]. Some of the challenges with energy detector based sensing include selection of the threshold for detecting primary users, inability to differentiate interference from primary users and noise, and poor performance under low SNR values [171]. Moreover, the energy detector does not work efficiently for detecting spread spectrum signals [170].

Using the same model given in (6.1), decision metric for energy detector can be written as

$$M = \sum_{n=0}^{N} |y(n)|^2. \tag{6.11}$$

The white noise can be modeled as a zero-mean Gaussian random variable with variance σ_w^2, *i.e.* $w(n) = \mathcal{N}(0, \sigma_w^2)$. For a simplified analysis, let us model the signal term as a zero-mean Gaussian variable as well[4], *i.e.* $s(n) = \mathcal{N}(0, \sigma_s^2)$. Because of these assumptions, the decision metric M follows chi-square distribution with $2N$ degrees freedom, χ_{2N}^2 and hence, it can be modeled as

$$M = \begin{cases} \frac{\sigma_w^2}{2}\chi_{2N}^2 & \mathcal{H}_0, \\ \frac{\sigma_w^2+\sigma_s^2}{2}\chi_{2N}^2 & \mathcal{H}_1. \end{cases} \tag{6.12}$$

For energy detector, the probabilities P_F and P_D can be calculated as [184][5]

$$P_F = 1 - \Gamma\left(L_f L_t, \frac{\lambda_E}{\sigma_w^2}\right), \tag{6.13}$$

$$P_D = 1 - \Gamma\left(L_f L_t, \frac{\lambda_E}{\sigma_w^2 + \sigma_s^2}\right), \tag{6.14}$$

where λ_E is the decision threshold, and $\Gamma(a, x)$ is the incomplete gamma function as given in [192] (see Equation 6.5.1). Fig. 6.3 shows the receiver operating characteristics (ROCs) for different SNR values. SNR is defined as the ratio of the primary user's signal power to noise power, *i.e.* SNR=σ_s^2/σ_w^2. The averaging size is set to 15 in this figure, $N = 15$. As this figure clearly shows, the performance of the threshold detector increases at high SNR values.

[4]In fact, the model for $s(n)$ is more complicated as fading should also be considered.

[5]Please note that the notation used in [184] is slightly different. Moreover, the noise power is normalized before it is fed into the threshold device in [184].

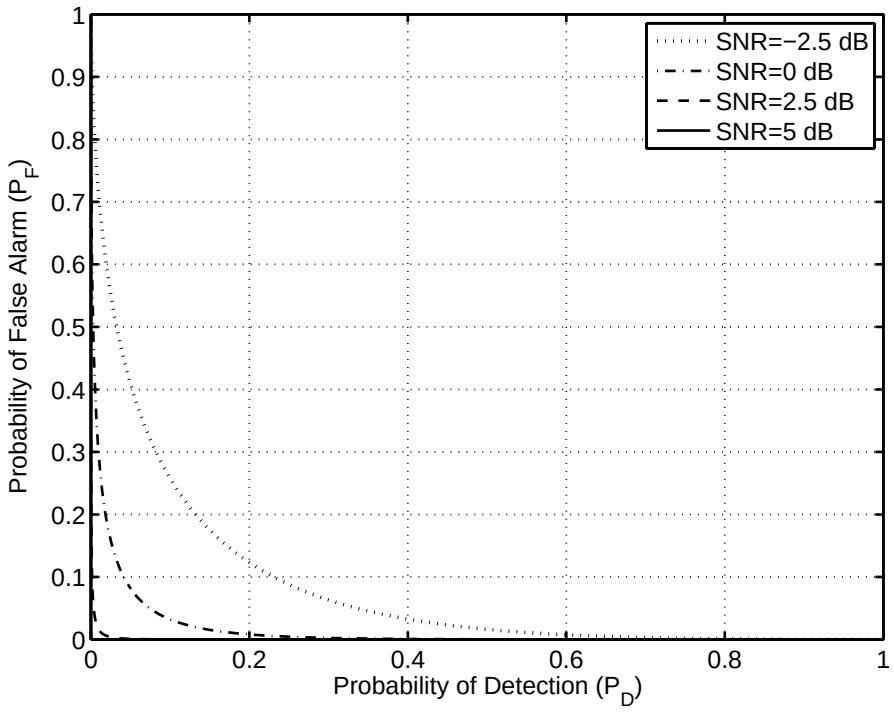

Figure 6.3 ROC curves for energy detector based spectrum sensing under different SNR values.

The threshold used in energy detector based sensing algorithms depends on the noise variance. Consequently, small noise power estimation errors cause significant performance loss [193]. As a solution to this problem, in [194], noise level is estimated dynamically by applying a reduced-rank eigenvalue decomposition to incoming signal's autocorrelation. Then, the estimated value is used to choose the threshold for satisfying a constant false alarm rate.

Measurement results are analyzed in [174, 175] using energy detector to identify the idle and busy periods of WLAN channels. Energy level for each GSM slot is measured and compared in [186] for identifying the idle slots for exploitation. The sensing task in this work is different in the sense that the cognitive radio has to be synchronized to the primary user network and the sensing time is limited to slot duration. A similar approach is used in [195] as well for opportunistic exploitation of unused cellular slots. In [187], power at the output of fast Fourier transform (FFT) of incoming signal is compared with a threshold value in order to identify the number of used TV channels. FFT is performed on the data sampled at 45 kHz around the centered TV carrier frequency for each TV channel. The performance of energy detector based sensing over various fading channels is investigated in [184]. Closed-form expressions for probability of detection under AWGN and

fading (Rayleigh, Nakagami, and Ricean) channels are derived. Average probability of detection for energy detector based sensing algorithms under log-normal shadowing and Rayleigh fading channels is derived in [95]. It is observed that the performance of energy-detector degrades considerably under Rayleigh fading. Forward methods based on energy measurements are studied for unknown noise power scenarios in [196]. The proposed method adaptively estimates the noise level, hence suitable for practical cases where noise variance is not known.

6.3.5 Radio Identification

A better knowledge about the spectrum characteristics can be obtained by identifying the transmission technology used by primary users. Such an identification enables cognitive radio with a higher dimensional knowledge as well as providing higher accuracy [31]. For example, assume that the primary user's technology is identified as a Bluetooth signal. Cognitive radio can use this information for extracting some useful information in space dimension as the range of Bluetooth signal is known to be around 10 meters[6]. Furthermore, cognitive radio may want to communicate with the identified communication systems in some applications. For radio identification, feature extraction and classification techniques are used in the context of European transparent ubiquitous terminal (TRUST) project [197]. The goal is to identify the presence of some known transmission technologies and achieve communication through them. The two main tasks are initial mode identification (IMI) and alternative mode monitoring (AMM). In IMI, the cognitive device searches for a possible transmission mode (network) following the power on. AMM is the task of monitoring other modes while cognitive device is having communication in a certain mode. Some of the proposed methods for blind radio identification are shown in Table 6.1. Several features are extracted from the received signal and they are used for selecting the most probable primary user technology by employing various classification methods.

6.3.6 Other Sensing Methods

Other alternative spectrum sensing methods include multitaper spectral estimation, wavelet transform based estimation, Hough transform, and time-frequency analysis. Multitaper spectrum estimation is proposed in [63]. The proposed algorithm is shown to be an approximation to maximum likelihood PSD estimator, and for wideband signals, it is nearly optimal. Although the complexity

[6]Please see Section 6.9 for more examples.

Table 6.1 Blind radio identification algorithms.

Article	Used Features	Classification Method
Mehta [198], Vardoulias [199]	Amount of energy detected, its distribution across the spectrum, and its correlation with some predefined functions (Briefly mentioned, not explained in detail).	-
Palicot [200]	Channel bandwidth and its shape: this feature is found to be the most discriminating parameter using tables and cross-tables, *i.e.* by comparing with other parameters.	Radial basis function (RBF) neural networks.
Gandetto [201]	The standard deviation of the instantaneous frequency and the maximum duration of a signal (Time-Frequency analysis).	Feed forward back-propagation neural networks (FFBPNNs) and support vector machines (SVMs) with RBF.
Fehske [180]	Spectral correlation density (SCD) and spectral coherence function (SCF).	Multilayer linear perception network (MLPN) neural networks.
Oner [177]	Spectral correlation density (SCD) and spectral coherence function (SCF).	Statistical tests for identifying the presence of cyclostationarity.

of this method is less than the maximum likelihood estimator, it is still computationally demanding. Random Hough transform of received signal is used in [202] for identifying the presence of radar pulses in the operating channels of IEEE 802.11 systems. This method can be used to detect any type of signals with periodic patterns as well. In [203], wavelets are used for detecting edges in the PSD of a wideband channel. Once the edges, which correspond to transitions from occupied band to empty band or vice versa, are detected, the power within bands between two edges are estimated. Using this information and edge positions, the PSD can be characterized as occupied or empty in a binary fashion. The assumptions made in [203], however, need to be relaxed for building a practical sensing algorithm.

6.4 Cooperative Sensing

The estimation of traffic in a specific geographic area can be done locally (by one cognitive radio only) or information from different cognitive radios can be combined. In the literature, cooperation is discussed as a solution to problems that arise in spectrum sensing due to noise uncertainty, fading, and shadowing. Cooperative sensing decreases the probability of mis-detections and the probability

Table 6.2 Local versus cooperative sensing.

Sensing Method	**Advantages**	**Disadvantages**
Non-cooperative sensing (Local sensing)	- Computational & implementation simplicity	- Hidden node problem - Multipath and shadowing
Cooperative sensing	- Higher accuracy (close to optimal) - Reduced sensing time [188] - Shadowing effect and hidden node problems can be prevented	- Complexity (complexity of sensor, complexity of within-system cooperation, complexity of among-system cooperation) - Traffic overhead - The need for a control channel

of false alarms considerably. In addition, cooperation can solve the hidden primary user problem and can decrease sensing time [176, 188, 189].

The interference to primary users caused by cognitive radio devices employing spectrum access mechanisms based on simple listen-before-talk (LBT) scheme is investigated in [190] via analysis and computer simulations. Results show that even simple local sensing can be used to explore the unused spectrum without causing interference to existing users. On the other hand, it is shown analytically and through numerical results that collaborative sensing provides significantly higher spectrum capacity gains than local sensing. The fact that cognitive radio acts without any knowledge about the location of the primary users in local sensing degrades the performance.

The challenges of cooperative sensing include developing efficient information sharing algorithms and increased complexity [204]. The advantages and disadvantages of local and cooperative (or collaborative) sensing methods are tabulated in Table 6.2.

In cooperative sensing architectures, the control channel can be implemented using different methodologies. These include a dedicated band, unlicensed band such as industrial, scientific and medical (ISM) band, and underlay ultra wide band (UWB) system [205]. Depending on the system requirements, one of these methods can be selected. The shared information can be soft or hard decisions made by each cognitive device [206]. Furthermore, various techniques for combining sensing results can be employed. The performances of equal gain-combining (EGC), selection combining (SC), and switch and stay combining (SSC) are investigated in [184] for energy detector based spectrum sensing under Rayleigh fading. The EGC method is found to have a gain of approximately two orders of magnitude while SC and SSC having one order of magnitude gain. As far as the

networking is concerned, the coordination algorithm should have reduced protocol overhead and it should be robust to changes and failures in the network. Moreover, the coordination algorithm should introduce minimum amount of delay.

Cooperative sensing can be implemented in two fashions: centralized or distributed [207]. These two methods will be explained in the following sections.

6.4.1 Centralized Sensing

In centralized sensing, a central unit collects sensing information from cognitive devices, identifies the available spectrum, and broadcasts this information to other cognitive radios or directly controls the cognitive radio traffic.

The hard (binary) sensing results are gathered at a central place which is known as access point (AP) in [109]. The goal is to mitigate the fading effects of the channel and increase detection performance. Resulting detection and false alarm rates are given in [208] for the sensing algorithm used in [109]. In [206], the sensing results are combined in a central node, termed as master node, for detecting TV channels. Hard and soft information combining methods are investigated for reducing the probability of missed opportunity. The results presented in [109,206] show that soft information-combining outperforms hard information-combining method in terms of the probability of missed opportunity.

6.4.2 Distributed Sensing

In the case of distributed sensing, cognitive nodes share information among each other but they make their own decisions as to which part of the spectrum they can use. Distributed sensing is more advantageous in the sense that there is no need for a backbone infrastructure.

An incremental gossiping approach termed as GUESS (gossiping updates for efficient spectrum sensing) is proposed in [209] for performing efficient coordination between cognitive radios in distributed collaborative sensing. The proposed algorithm is shown to have low-complexity with reduced protocol overhead. The GUESS algorithm has fast convergence and robust to network changes as it does not require a setup phase to generate the clusters. Incremental aggregation and randomized gossiping algorithms are also studied in [209] for efficient coordination within a cognitive radio network. A distributed collaboration algorithm is proposed in [189]. The collaboration is performed between two secondary users. The user closer to primary transmitter, which has a better change of

detecting the primary user transmission, cooperates with a far away user. An algorithm for pairing secondary users without a centralized mechanism is also proposed. A distributed sensing method is proposed in [95] where secondary users share their sensing information among themselves. Only final decisions are shared in order to minimize the network overhead due to collaboration. As secondary user receives decisions from other users and decides $\mathcal{H}_1$ if any of the received decisions plus its own is $\mathcal{H}_1$, a fusion rule known as OR-rule. The results presented in [95] clearly show the performance improvements achieved through collaborative sensing.

6.5 External Sensing

Another technique for obtaining spectrum information is the external sensing. In external sensing, an external agent performs the sensing and broadcasts the channel occupancy information to cognitive radios. External sensing algorithms solve some problems associated with the internal sensing, which is termed as collocated sensing in [181]. The main advantages are overcoming hidden primary user problem as well as the uncertainty due to shadowing and fading. Furthermore, as the cognitive radios do not spend time for sensing, spectrum efficiency is increased. The sensing network does not need to be mobile and not necessarily powered by batteries. Hence, power consumption problem of internal sensing can also be addressed.

A sensor node detector architecture is used in [210]. The presence of passive receivers, *viz.* television receivers, is detected by measuring the local oscillator (LO) power leakage. Once a receiver and the channel is detected, the sensor node notifies cognitive radios in the region of passive primary user via a control channel. Similar to [210], a sensor network based sensing architecture is proposed in [181]. A dedicated network composed of only spectrum sensing units is used to sense the spectrum continuously or periodically. The results are communicated to a sink (central) node which further processes the sensing data and shares the information about the spectrum occupancy in the sensed area with opportunistic radios. These opportunistic radios use the information obtained from sensing network for selecting the bands (and time durations) of their data transmissions. The sensing results can also be shared via a pilot channel similar to network access and connectivity channel (NACCH) [211]. External sensing is one of the methods proposed for identifying primary users in IEEE 802.22 standard as well (See Section 6.10).

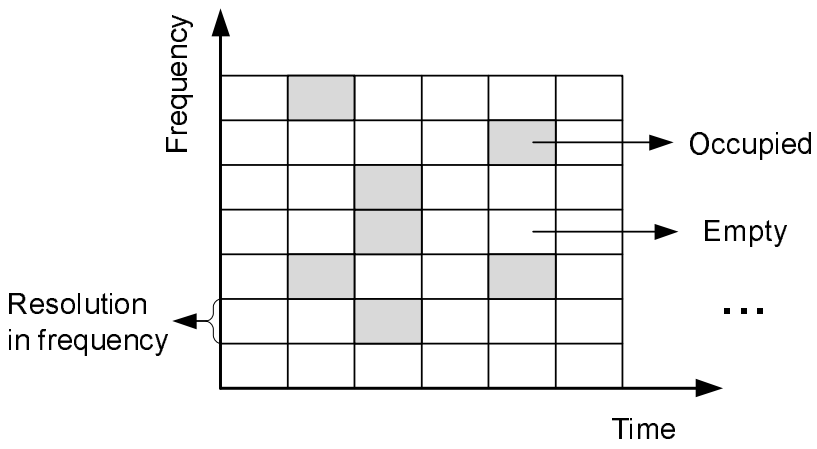

Figure 6.4 Binary scheme used for modeling spectrum occupation in [2].

6.6 Using History for Prediction

For minimizing interference to primary users while making the most out of the opportunities, cognitive radios should keep track of the variations in spectrum and should make predictions. Stemming from the fact that cognitive radio senses the spectrum steadily and has the ability of learning, the history of the spectrum usage information can be used for predicting the future profile of the spectrum. Towards this goal, knowledge about currently active devices or prediction algorithms based on statistical analysis can be used.

Channel access patterns of primary users are identified and used for predicting spectrum usage in [212]. Assuming a TDMA transmission, periodicity pattern of channel occupancy is extracted using cyclostationary detection. This parameter is then used to forecast the channel idle probability for a given channel. Furthermore, [212] proposes to use hidden Markov models (HMMs) in order to model the channel usage patterns of primary users. A multivariate time series approach is taken in [2] to be able to learn the primary user characteristics and predict the future occupancy of neighboring channels. A binary scheme (*empty* or *occupied*) is used to reduce the complexity and storage requirements as shown in Fig. 6.4. It is noted in [174] that the statistical model of primary users' behavior should be kept simple enough to be able to design optimal higher order protocols. On the other hand, it will be useless if the primary user's behavior could not be predicted well. In order to strike a balance between complexity and effectiveness, continuous-time semi-Markov process model is used to describe the statistical characteristics of WLAN channels that can be used by cognitive radio to predict transmission opportunities. The investigation of voice over Internet protocol (VoIP)

and file transfer protocol (FTP)-type traffic scenarios for semi-Markov model is performed in [175]. Pareto, phase-type (hyper-Erlang) and mixture distributions are used for fitting to the empirical data. Statistics of spectrum availability is employed in [185] for dynamically selecting the operating frequency, *i.e.* for identifying the spectrum holes. The statistics of the spectral occupancy of a bin (FFT output) is assumed to be at least piecewise stationary over the time at which they are observed in order to guarantee that these statistics are still reliable when a spectrum access request is received. Using the statistics, the likelihood that the spectral opportunity will remain available for at least the requested time duration is calculated for each bin. Then, these likelihood values are used to identify the range of frequencies which can be used for transmission.

6.7 Sensing Frequency

Sensing frequency, *i.e.* how often cognitive radio should perform spectrum sensing, is a design parameter that needs to be chosen carefully. The optimum value depends on the capabilities of cognitive radio itself and temporal characteristics of primary users in the environment. If the statuses of primary users are known to change slowly, sensing frequency can be relaxed. A good example for such a scenario is the detection of TV channels. The presence of a TV station usually does not change frequently in a geographical area unless a new station starts broadcasting or an existing station goes offline. Another factor that affects the sensing frequency is the interference tolerance of primary license owners. For example, when the cognitive radio is exploiting opportunities in public safety bands, sensing should be done as frequently as possible in order to prevent any interference. Cognitive radio should immediately vacate the band if it is needed by public safety units. In the IEEE 802.22 draft standard (see Section 6.10), the sensing period is defined as 30 seconds. In addition to these, the channel detection time, channel move time and some other timing related parameters are also defined [213].

6.8 Hardware Requirements and Approaches

In this section, several aspects of spectrum sensing from hardware perspective are investigated. As explained before, one of the main challenges lies on the requirements of high sampling rate, high resolution ADCs with large dynamic range. This requirement is a result of the need for a wideband sensing. Cognitive radio should be able to capture and analyze a relatively large band for identifying

Table 6.3 Comparison of single-radio and dual-radio sensing algorithms.

	Single-Radio Arch.	**Double-Radio Arch.**
Advantages	- Simplicity - Lower cost	- Higher spectrum efficiency - Better sensing accuracy
Disadvantages	- Lower spectrum efficiency - Poor sensing accuracy	- Higher cost - Higher power consumption - Higher complexity

spectrum opportunities. Moreover, high speed processing units (DSPs or FPGAs) are needed for performing computationally demanding signal processing tasks with relatively low delay.

Sensing can be performed via two different architectures: single-radio and dual-radio [181, 199]. In the single-radio architecture, only a specific time slot is allocated for spectrum sensing. As a result of this, only a certain accuracy can be guaranteed for spectrum sensing results. Moreover, the spectrum efficiency is decreased as some portion of the available time slot is used for sensing instead of data transmission. The obvious advantage of single-radio architecture is its simplicity and lower cost. In the dual-radio sensing architecture, one radio chain is dedicated for data transmission and reception while the other chain is dedicated for spectrum monitoring. The drawback of such an approach is the increased power consumption and hardware cost. Note that only one antenna would be sufficient for both chains as suggested in [199]. A comparison of advantages and disadvantages of single and dual-radio architectures is given in Table 6.3. In conclusion, one might prefer one architecture over the other depending on the available resources, and performance and/or data rate requirements.

6.9 Multi-Dimensional Spectrum Awareness

The definition of opportunity determines the ways of measuring and exploiting the spectrum space. The conventional definition of the spectrum opportunity which is often referred as "*band of frequencies that are not being used by the primary user of that band at a particular time in a particular geographic area*" [214] only exploits three dimensions of the spectrum space: frequency, time, and space. The problems stated in the previous section also relates to sensing the spectrum in these three dimensions. However, there are other dimensions that need to be explored further for spectrum opportunity. For example, the code dimension of the spectral space has not been explored well in the literature. Therefore, the conventional spectrum sensing algorithms do not

know how to deal with signals that use spread spectrum, time or frequency hopping codes. If the code dimension is interpreted as part of the spectrum space, this problem can be avoided, and new opportunities for spectrum usage can be created. Naturally, this will bring about other new challenges for detection and estimation of this new opportunity. Similarly, the angle dimension has not been exploited well enough for spectrum opportunity. It is assumed that the primary users and/or the secondary users are transmitting in all the directions. However, with the recent advances in multi-antenna technologies, *e.g.* beamforming, multiple users can be multiplexed into the same channel at the same time in the same geographical area. In other words, an additional dimension of spectral space can be created as opportunity. This will also create new opportunities for spectral estimation, where not only the frequency spectrum but also the angle of arrivals might need to be estimated. With these new dimensions, sensing only the frequency spectrum usage falls short. The radio space with the introduced dimensions can be defined as "*a theoretical hyperspace occupied by radio signals, which has dimensions of location, angle-of-arrival, frequency, time, and possibly others*" [215]. This hyperspace is called electrospace, transmission hyperspace, radio spectrum space, or simply spectrum space by various authors, and it can be used to describe how radio environment can be shared among multiple (primary and/or secondary) systems [216]. Various dimensions of this space and the corresponding measurement/sensing requirements are summarized in Table 6.4 along with some representative pictures. Each dimension has its own parameters that should be sensed for a complete spectrum awareness as indicated in the Table.

It is of crucial importance to define such an n-dimensional space for spectrum sensing. Spectrum sensing should include the process of identifying occupancy in all dimensions of the spectrum space and finding spectrum holes, or more precisely spectrum space holes. For example a certain frequency can be occupied for a given time, but it might be empty in another time. Hence, temporal dimension is as important as frequency dimension. This example can be extended to the other dimensions of spectrum space given in Table 6.4. As a result of this requirement, advanced spectrum sensing algorithms that offer awareness in multiple dimensions of the spectrum space should be developed.

6.10 Spectrum Sensing in Current Wireless Standards

Recently developed wireless standards have started to include cognitive features. Even though it is difficult to expect a wireless standard that is based on wideband spectrum sensing and opportunistic exploitation of spectrum, the trend is in this direction. In this section, wireless technologies

that require some sort of spectrum sensing for adaptation or for dynamic frequency selection (DFS) will be discussed. However, the spectrum knowledge can also be used to initiate advanced receiver algorithms such as adaptive interference cancellation [217].

6.10.1 IEEE 802.11k

A proposed extension to IEEE 802.11 specification is IEEE 802.11k which defines several types of measurements [218]. Some of the measurements include channel load report, noise histogram report and station statistic report. The noise histogram report provides methods to measure interference levels that display all non-802.11 energy on a channel as received by the subscriber unit. The AP collects channel information from each mobile unit and makes its own measurements. This data is then used by the AP to regulate access to a given channel.

The sensing (or measurement) information is used to improve the traffic distribution within a network as well. WLAN devices usually connect to the AP that has the strongest signal level. Sometimes, such an arrangement might not be the optimum and can cause overloading on one AP and underutilization of others. In 802.11k, when an AP with the strongest signal power is loaded to its full capacity, new subscriber units are assigned to one of the underutilized APs. Despite the fact that the received signal level is weaker, the overall system throughput is better thanks to more efficient utilization of network resources.

6.10.2 Bluetooth

A new feature, namely adaptive frequency hopping (AFH), is introduced to Bluetooth standard to reduce interference between wireless technologies sharing the 2.4 GHz unlicensed radio spectrum [219]. In this band IEEE 802.11b/g devices, cordless telephones, microwave ovens use the same wireless frequencies as Bluetooth. AFH identifies the transmissions in the ISM band and avoids their frequencies. Hence, narrow-band interference can be avoided and better bit-error-rate (BER) performance can be achieved as well as reducing the transmit power. Fig. 6.5 shows an illustrative Bluetooth transmission with and without AFH. By employing AFH, collusions with WLAN signals are avoided in this example.

AFH requires a sensing algorithm for determining whether there are other devices present in the ISM band and whether or not to avoid them. The sensing algorithm is based on statistics gathered to determine which channels are occupied and which channels are not occupied. Channel statistics

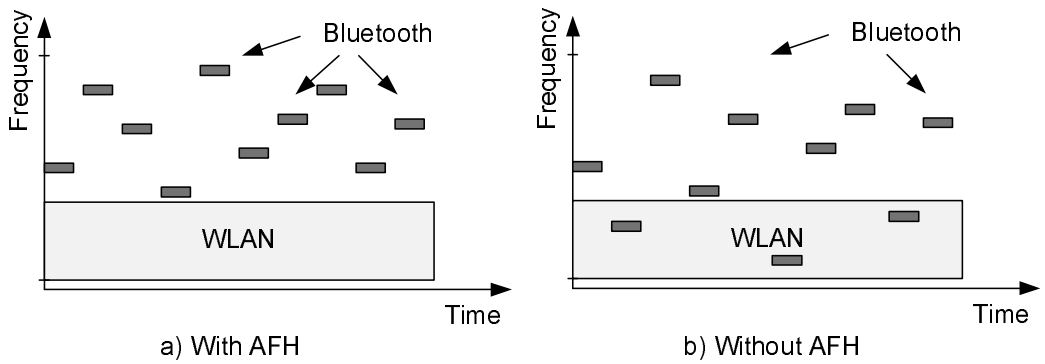

Figure 6.5 Bluetooth transmission with and without adaptive frequency hopping (AFH). AFH prevents collusions between WLAN and Bluetooth transmissions.

can be packet-error rate, BER, received signal strength indicator (RSSI), carrier-to-interference-plus-noise ratio (CINR) or other metrics [220]. The statistics are used to classify the channel as *good*, *bad*, or *unknown* [219].

6.10.3 IEEE 802.22

One of the most distinctive features of 802.22 standard is its sensing requirements [15]. IEEE 802.22 based wireless regional area network (WRAN) devices sense the TV channels and identify transmission opportunities. Sensing is envisioned to be based on two stages: fast and fine sensing [213]. In the fast sensing stage, a fast sensing algorithm is employed, *e.g.* energy detector. The fine sensing stage is initiated based on the fast sensing results. Fine sensing involves a more detailed sensing where more powerful methods are used. Several techniques that have been proposed and included in the draft standard include energy detection, waveform based sensing (PN511 or PN63 sequence detection and/or segment sync detection), cyclostationary feature detection, and matched filtering. A base station (BS) can distribute the sensing load among subscriber stations (SSs). The results are returned to BS which uses these results for managing the transmissions. Hence, it is a practical example of centralized collaborative sensing explained in Section 6.4.1.

Another approach for managing the spectrum in IEEE 802.22 devices is based on a centralized method for available spectrum discovery. The BSs would be equipped with a global positioning system (GPS) receiver which would allow its position to be reported. The location information would then be used to obtain the information about available TV channels through a central server. For low-power devices[7] operating in the TV bands, external sensing is proposed as an alternative

[7]These devices include wireless microphone, wireless camera etc.

technique. These devices periodically transmit beacons with a higher power level. These beacons are monitored by IEEE 802.22 devices to detect the presence of such low-power devices which are otherwise difficult to detect due to the low-power transmission.

6.11 Conclusions

One of the important elements of the cognitive radio is sensing the available spectrum opportunities. In this chapter, various aspects of spectrum sensing task are explained in detail. Several sensing methods are studied and collaborative sensing is considered as a solution to some common problems in spectrum sensing. Hardware aspects of spectrum sensing and pro-active approaches are given and sensing methods employed in current wireless systems are discussed. Furthermore, the spectrum opportunity and spectrum sensing concepts are re-evaluated by considering different dimensions of the spectrum space. The new interpretation of spectrum space will create new opportunities and challenges for spectrum sensing while it will solve some of the traditional problems. Estimating real levels of usage of the spectrum in multiple dimensions including time, frequency, space, angle, and code; identifying for opportunities in multiple dimensions including prediction into the future using past information and making reasoning can be considered some of these challenges for future research.

Table 6.4 Multi-dimensional radio spectrum space and transmission opportunities.

Dimension	What needs to be sensed?	Comments	Illustrations
Frequency	Opportunity in the frequency domain.	Availability in part of the frequency spectrum. The available spectrum is divided into narrower chunks of bands. Spectrum opportunity in this dimension means that all the bands are not used simultaneously at the same time, *i.e.* some bands might be available for opportunistic usage.	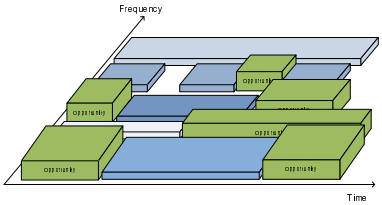
Time	Opportunity of a specific band in time.	This involves the availability of a specific part of the spectrum in time. In other words, the band is not continuously used. There will be times where it will be available for opportunistic usage.	
Geographical space	Location (latitude, longitude, and elevation) and distance of primary users.	The spectrum can be available in some parts of the geographical area while it is occupied in some other parts at a given time. This takes advantage of the propagation loss (path loss) in space. These measurements can be avoided by simply looking at the interference temperature. No interference means no primary user transmission in a local area. However, one needs to be careful because of hidden terminal problem.	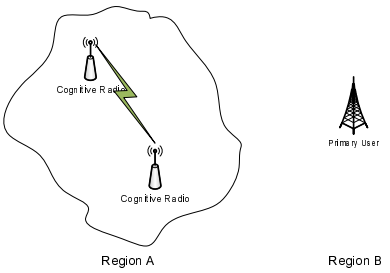
Code	The spreading code, time hopping (TH), or frequency hopping (FH) sequences used by the primary users. Timing information is also needed so that secondary users can synchronize their transmissions. The synchronization estimation can be avoided with long and random code usage. However, partial interference in this case is unavoidable.	The spectrum over a wideband might be used at a given time through spread spectrum or frequency hopping. This does not mean that there is no availability over this band. Simultaneous transmission without interfering with primary users would be possible in code domain with an orthogonal code with respect to codes that primary users are using. This requires the opportunity in code domain, *i.e.* not only detecting the usage of the spectrum, but also determining the used codes, and possibly multipath parameters as well.	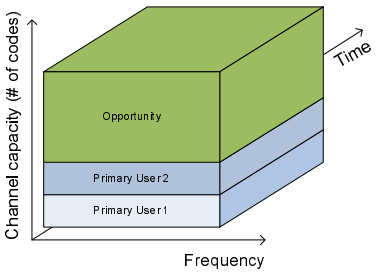
Angle	Directions of primary users' beam (azimuth and elevation angle) and locations of primary users.	Along with the knowledge of the location/position or direction of primary users, spectrum opportunities in angle dimension can be created. For example, if a primary user is transmitting in a specific direction, the secondary user can transmit in other directions without creating interference on the primary user.	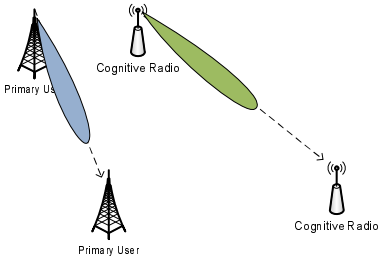
Signal	Signal polarization and waveforms of primary users.	Primary users and secondary users might be transmitting a waveform at a specific band for a given time in a geographical area in all the directions but secondary users can exploit the signal dimension to transmit an orthogonal waveform so that it does not create interference with primary users. This requires not only spectrum estimation but also waveform identification.	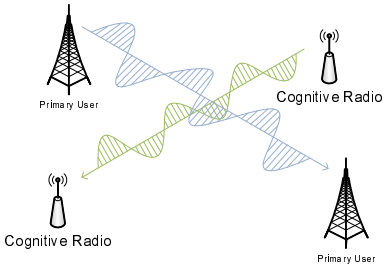

CHAPTER 7

SPECTRUM SENSING FOR COGNITIVE RADIO USING PARTIAL MATCH FILTERING

7.1 Introduction

Cognitive radio devices should be able to identify unused spectrum in a fast and efficient way. Conventional algorithms sense the spectrum without exploiting all the properties of primary users. In this chapter, we explore the *a priori* information about transmission properties of possible primary users for developing a framework for spectrum sensing. In this method, the parameters estimated from the received signal are matched to the possible transmission parameters for achieving a more robust and reliable sensing that covers multiple dimensions of the spectrum space. Furthermore, a case study, which uses energy detector based sensing and Bayesian classification, is presented and its performance is analyzed using computer simulations. Our contribution in this chapter can be summarized as following:

- A unification of various algorithms for spectrum sensing is presented by describing the essential steps in detail. The proposed framework is named as partial match-filtering (PMF).
- The most commonly used waveform identification features are summarized.
- A case study of energy-detector based PMF algorithm is provided. Bayesian classification is used for assigning the feature set to a radio access technology (RAT).
- Performance analysis of the energy-detector based PMF method is obtained using computer simulations.

This chapter is organized as follows. Proposed PMF algorithm is presented in Section 7.2. Section 7.3 discusses energy detector based PMF followed by numerical results in Section 7.4. Some discussions are presented in Section 7.5, and finally, the concluding remarks are given in Section 7.6.

7.2 Partial Match-Filtering

Spectrum estimation techniques given in the literature do not utilize most of the *a priori* knowledge about primary users. For example, IEEE 802.11a signal has a bandwidth of 20 MHz and operates at industrial, scientific and medical (ISM) or unlicensed national information infrastructure (U-NII) bands in the United States (US). This knowledge about center frequencies and bandwidth of this type of a signal along with other transmission characteristics can be exploited to identify the presence of an IEEE 802.11a transmission and thus to improve spectrum sensing accuracy. The features that describe certain type of devices can be obtained by investigating the received signal. These features then can be matched to the *a priori* sets of known parameters. By finding the exact transmission characteristics of primary users, possible estimation errors due to sensing algorithm and noise can be removed. We refer to this process as *partial match-filtering* as we are matching to the primary users' signal parameters instead of the signal itself. Once primary users or the occupied frequencies are detected, unused portion of the spectrum space can be identified for opportunistic exploitation. The PMF algorithm can be realized in three main steps:

1. Extraction of a predefined set of features from the received signal,

2. Using the extracted features for making decisions on the presence of an anticipated transmission,

3. Exploiting the gained knowledge about the active primary users for multi-dimensional spectrum characterization.

System model for PMF based cognitive radio is shown in Fig. 7.1. The blocks that represent the three main steps of PMF are marked with corresponding step numbers. Cognitive engine governs the selection of bands for transmission and communicates with radio, user, and open systems interconnection reference (OSI) layers. Radio identification is performed based on the extracted features of received signal, environmental information and cognitive radio's prior knowledge. The set of possible RATs and their transmission parameters can be collected by cognitive devices using previous decisions (blind) or they can be broadcasted by a central unit (assisted). Alternatively, these parameters can be pre-configured to cognitive radio during hardware design. Federal Communications Commission (FCC) Licensing and International Telecommunication Union (ITU) frequency alloca-

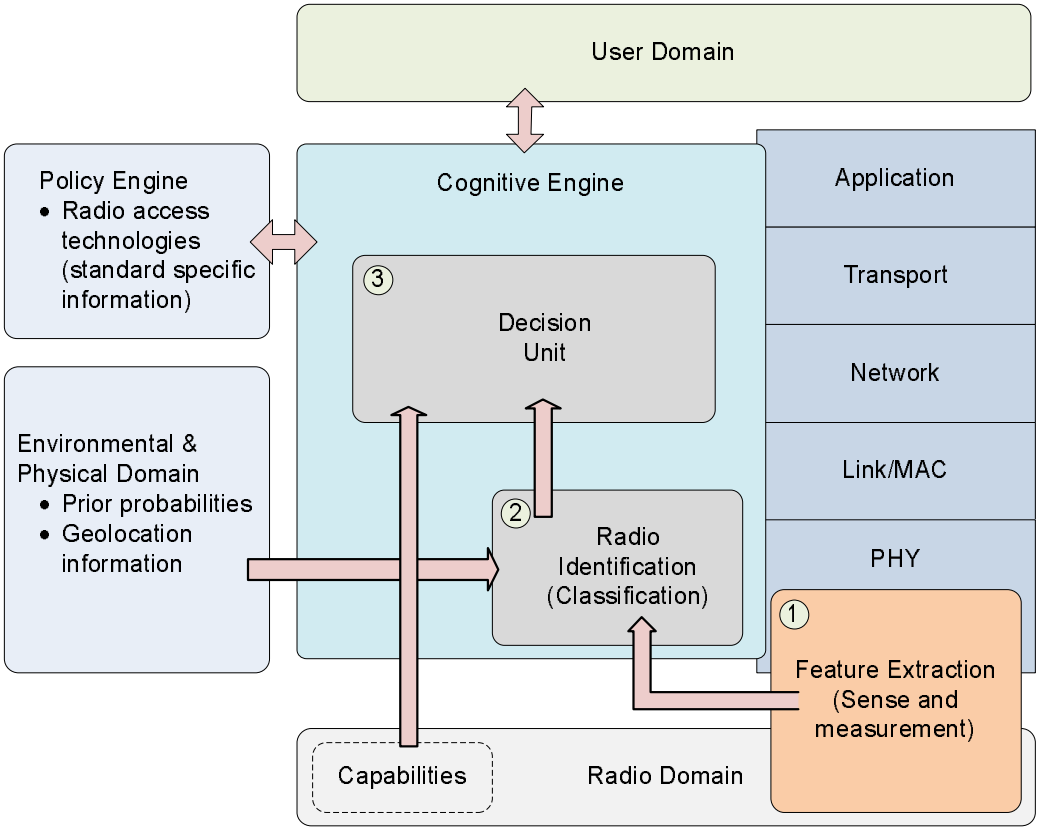

Figure 7.1 Block diagram of proposed algorithm.

tion rules are some example databases. The three steps that make PMF will be explained in detail in the rest of this section.

7.2.1 Feature Extraction

In this section, a comprehensive list of parameters that can be used to detect the presence of a particular type of primary user will be presented. These parameters can be extracted using a single algorithm or multiple algorithms such as energy detector, cyclostationarity based feature extraction *etc.* can be used together for estimating different parameters. Depending on the domain of estimation, the features are classified as time-domain or frequency-domain.

7.2.1.1 Frequency Domain Features

Bandwidth: Different wireless standards (licensed or unlicensed) utilize different transmission bandwidths depending on the data rate requirements. The bandwidth of a possible transmission can be

estimated and compared with the bandwidth of the expected transmissions in the considered frequency band [200]. Channel bandwidth and shape of the power spectral density (PSD) are found to the most discriminating features in [200] among other parameters.

Center frequency: Operating frequencies of different systems would be also a differentiating factor for detecting the presence of certain types of signals. It is especially useful for systems with large bandwidths such as wireless local area network (WLAN) where the transmission bands have large separation.

Single carrier versus multi-carrier: The knowledge of whether a particular signal is generated using single carrier or multi-carrier modulation can be used as a feature for classification. This knowledge is especially useful for reducing the size of the candidate set. In addition, cyclic prefix (CP) duration, symbol duration, fast Fourier transform (FFT) size and number of subcarriers can be used for further identifying the ongoing transmissions in the case of multi-carrier modulation [221].

7.2.1.2 Time Domain Features

Maximum duration of a signal: The maximum duration of a signal can also be used as a distinguishing parameter. This feature is used in [201] for discriminating WLAN and Bluetooth signals.

Multiple accessing: Multiple accessing method is another factor that can be used to differentiate distinct systems. A system employing time division multiple access (TDMA), for example, exhibits a pattern in time that does not exist in code division multiple access (CDMA) or carrier sense multiple accessing (CSMA) systems.

Duplexing method: The duplexing method refers to whether the transmission is half duplex or full duplex. For full duplexing, duplexing type, *i.e.*, time division duplexing (TDD) or frequency division duplexing (FDD), can be used as well.

Frame duration: Frame duration and/or the ratio of uplink (UL) and downlink (DL) frame lengths can be used as discriminating parameters for identifying different transmissions. Similarly time-slot and guard interval lengths can also be used.

Spreading codes - hopping pattern: In spread spectrum systems, the spreading codes assigned to a particular primary user could be beneficial for exploiting the opportunity in the code domain and for identifying primary users. Moreover, chip rate, spreading factor, hopping frequency *etc.* can also be extracted and used as discriminating parameters.

7.2.1.3 Other Features

The features given in this section are not meant to be a complete set, rather they are given as examples and the list can be extended. Some other discriminating features include cumulants, power moment matrices, and zero-crossing rate.

The dimension of the feature set is a design parameter. Some or all of the parameters can be extracted from the received data and used for classification. However, the larger the dimension of the feature set, the more complex the system, and the more reliable the classification results. Selection of the employed features can be performed by considering the characteristics of potential systems. The feature set can be represented as a vector $\boldsymbol{f}$ which is a point in multi-dimensional feature space. Then, this vector can be used for classifying the detected transmission into one of K candidate transmissions using a classifier that will be discussed in the next section.

7.2.2 Decision Making (Classification)

In this step, the measured signal is associated with a RAT. This process can be regarded as a classification problem. For this purpose, various classification methods can be used such as pattern recognition [201], neural networks [180, 200] or statistical classification. Selection of a classification method depends on the considered RATs and available features. Please note that the classification performed in this step is different from blind modulation classification task as not only the type of signaling but also some parameters of the transmission need to be identified.

Prior probabilities of different systems play an important role during classification. For example, we may have wireless universal serial bus (USB) with much less occurrence probability than WLANs. Similarly, Channels 1, 6, and 11 of WLAN systems are used more commonly then other bands. This prior information can be used during classification. Note that this parameter can not be obtained from received signals, but it is an *a priori* information that cognitive radio can collect after each classification.

The classification results can be further verified by using the structures of the anticipated signal such as preambles, pilots and spreading codes. For example, the repetition in the preamble of WLAN signals can be used to verify that indeed there is a WLAN transmission at the identified channel. The receiver does not need to actually synchronize with the WLAN signal in order to test the presence of WLAN packets.

7.2.3 Multi-Dimensional Spectrum Characterization

In this final step of PMF, the output of classification is used for obtaining a complete multi-dimensional spectrum awareness in cognitive radio. The knowledge of primary users can help identify the transmission opportunities across different dimensions. For example, if the identified signal is a cordless phone, the range is expected to be around 100 meters and for Bluetooth signals it is around 10 meters. This knowledge can be used in a cooperative sensing environment for gaining knowledge in the space dimension. The characterization in time, frequency, and code dimensions is straightforward once primary users are associated with a particular RAT.

7.3 Case Study: Energy Detector Based PMF

In this part of the chapter, we present a case study for the proposed PMF algorithm. Two features, namely bandwidth and center frequencies of primary users, are extracted using energy detector based algorithm. The feature extraction algorithm is based on FFT operation which is used to transform time-domain signal into frequency domain. In [109], FFT output samples are used for deciding whether an FFT frequency bin is occupied by a primary user or not. However, the primary users signal is usually spread over a group of FFT output samples as the bandwidth of primary user is expected to be larger than the considered bandwidth divided by the FFT size[1]. Using this fact, the FFT output is filtered for noise averaging in order to obtain a better performance.

The proposed algorithm is especially suitable for cognitive devices using OFDM as their transmission technology, such as systems similar to [97]. The availability of FFT circuitry in these systems eases the requirements on the hardware. Moreover, the computational requirement of the spectrum sensing algorithm is reduced as receiver needs to apply FFT for data detection.

[1]Making an analogy to orthogonal frequency division multiplexing (OFDM) systems, the primary users usually cover more than just one subcarrier.

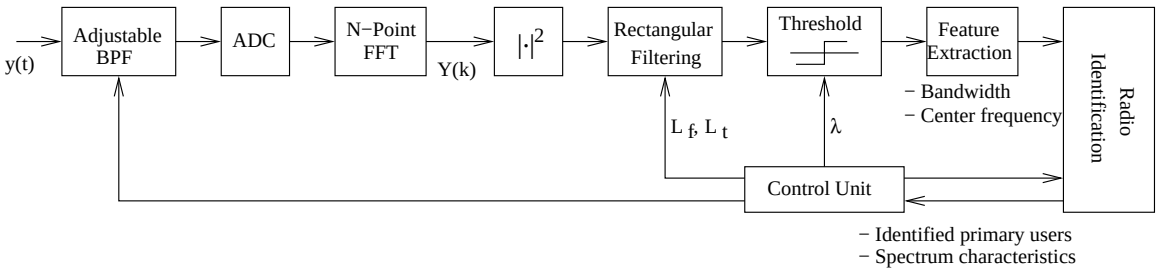

Figure 7.2 Block diagram of energy detector based partial match-filtering method.

The block diagram of the proposed algorithm is shown in Fig. 7.2. The signal that arrives to cognitive user $y(t)$ is first filtered with a band pass filter (BPF) to extract the signal in the frequencies of interest. This filter can be adjustable and controlled by a control unit in order to scan a wider range [222]. The output of the filter is sampled at Nyquist rate and N-point FFT is applied to obtain the frequency domain samples which can be modeled as

$$Y_m(k) = \begin{cases} W_m(k) & \mathcal{H}_0, \\ S_m(k) + W_m(k) & \mathcal{H}_1, \end{cases} \qquad k = 1, \cdots, N \tag{7.1}$$

where $S_m(k)$ is the transmitted signal by primary users at the output of mth FFT operation, $W_m(k)$ is the white noise sample at kth frequency sample, and N is the FFT size. $\mathcal{H}_0$ and $\mathcal{H}_1$ represent the null hypothesis and alternate hypothesis respectively. The white noise is modeled as a zero-mean Gaussian random variable with variance σ_w^2, *i.e.* $W(k) = \mathcal{N}(0, \sigma_w^2)$. The signal term is also modeled as a zero-mean Gaussian variable whose variance is a function of frequency, *i.e.* $S(k) = \mathcal{N}(0, \sigma_k^2)$, where σ_k is the local standard deviation. The variation of σ_k across frequency depends on the characteristics of primary users signals and operating frequency. Hence, by changing the signal variance across frequency, PSDs for various technologies can be represented.

Some critical blocks for the proposed energy detector based PMF algorithm will be discussed in the following.

7.3.1 Frequency Domain Filtering

The magnitude square of FFT output $|Y_m(k)|^2$ can be compared with a threshold value for detection of presence of transmission at a particular frequency. In order to smooth the FFT output, filtering is applied before applying the threshold detector. The optimum filter coefficients depend

on the statistics of primary user's signal as well as the noise power. In [27], minimum mean-square error (MMSE) filtering is applied for estimating the noise plus interference ratio for OFDM systems. The MMSE filter coefficients are derived as a function of the statistics of interference. As an approximation to MMSE filtering, a sliding rectangular window can also be applied for smoothing the spectrum estimates $Y(k)$. In this chapter, we use rectangular filter for its simplicity and lower computational complexity. In this case, the decision statistics at different frequencies can be calculated as

$$\tilde{Y}_m(k) = \sum_{l=k-\lfloor L_f/2 \rfloor}^{k+\lfloor L_f/2 \rfloor} \sum_{u=m-L_t+1}^{m} |Y_u(l)|^2 \tag{7.2}$$

where $\lfloor \cdot \rfloor$ represents the floor function, and L_t and L_f are the averaging filter lengths in time and frequency directions respectively.

7.3.2 Threshold Detector

The sensing time index m is dropped for simplicity in the rest of the chapter. The output of the rectangular filter $\tilde{Y}(k)$ is fed to a threshold device to identify the frequencies occupied by the primary users. This is equivalent to distinguishing between the following two hypotheses:

$$\mathcal{H}_0 \quad : \quad Y(k) = W(k), \tag{7.3}$$

$$\mathcal{H}_1 \quad : \quad Y(k) = S(k) + W(k). \tag{7.4}$$

As $Y(k)$ has Gaussian distribution, the decision statistics $\tilde{Y}(k)$ follows chi-square distribution with $2L_fL_t$ degrees freedom, $\chi^2_{2L_fL_t}$. Hence, $\tilde{Y}(k)$ can be modeled as

$$\tilde{Y}(k) = \begin{cases} \frac{\sigma_w^2}{2}\chi^2_{2L_fL_t} & \mathcal{H}_0, \\ \frac{\sigma_w^2+\sigma_k^2}{2}\chi^2_{2L_fL_t} & \mathcal{H}_1, \end{cases} \qquad k = 1, \cdots, N \tag{7.5}$$

where σ_w^2 and σ_k^2 are as defined before. The performance of the detection algorithm can be summarized with two probabilities: probability of detection P_D and probability of false alarm P_F. P_D is the probability of detecting a signal on the considered frequency when it is truly present, thus large detection probability is desired. It can be formulated as

$$P_D = \Pr\left(\tilde{Y} > \lambda | \mathcal{H}_1\right), \tag{7.6}$$

where λ is the threshold value. P_F is the probability that the test incorrectly decides that the considered frequency is occupied when it actually is not, and it can be written as

$$P_F = \Pr\left(\tilde{Y} > \lambda | \mathcal{H}_0\right). \tag{7.7}$$

P_F should be kept as small as possible. The probabilities P_F and P_D can be calculated as [184][2]

$$P_F = 1 - \Gamma\left(L_f L_t, \frac{\lambda}{\sigma_w^2}\right), \tag{7.8}$$

$$P_D = 1 - \Gamma\left(L_f L_t, \frac{\lambda}{\sigma_w^2 + \sigma_k^2}\right), \tag{7.9}$$

where $\Gamma(a, x)$ is the incomplete gamma function as given in [192] (see Equation 6.5.1). In general, P_D and P_F are inversely proportional. Fig. 7.3 shows the receiver operating characteristics (ROCs) for a single frequency sample at the output of threshold device (see Fig. 7.2) for different signal-to-noise ratio (SNR) values. SNR is defined as the ratio of the primary user's signal power to noise power, *i.e.* SNR=σ_k^2/σ_w^2. The averaging size is set to 15 in this figure. As this figure clearly shows, the performance of the threshold detector increases at high SNR values.

The decision threshold λ can be selected for finding an optimum balance between P_D and P_F. However, this requires the knowledge of noise and detected signal powers as seen in (7.8) and (7.9). Noise power can be estimated, but the signal power is difficult to estimate as it changes depending on the ongoing transmission characteristics and the distance between the cognitive radio and primary user. In this chapter, it is assumed that the noise variance is estimated and the threshold is chosen to obtain a false alarm rate of 0.1 percent.

7.3.3 Feature Extraction

In this stage, two features, bandwidth and center frequencies of primary users, are extracted by using the threshold detector output. In order to achieve this, the bins exceeding the threshold value are grouped together. In order to reject the erroneous bins, we apply a method similar to the initial stage of dynamic undersea detection extractor (DUDE) algorithm [223] by defining two parameters B_{min} and G_{max}. B_{min} is the minimum assumed bandwidth for the primary users and G_{max} is the maximum gap allowed between two frequency samples. The feature extraction algorithm searches for

[2]Please note that the notation used in [184] is different than the one used in this chapter. Moreover, the noise power is normalized before it is fed into the threshold device in [184].

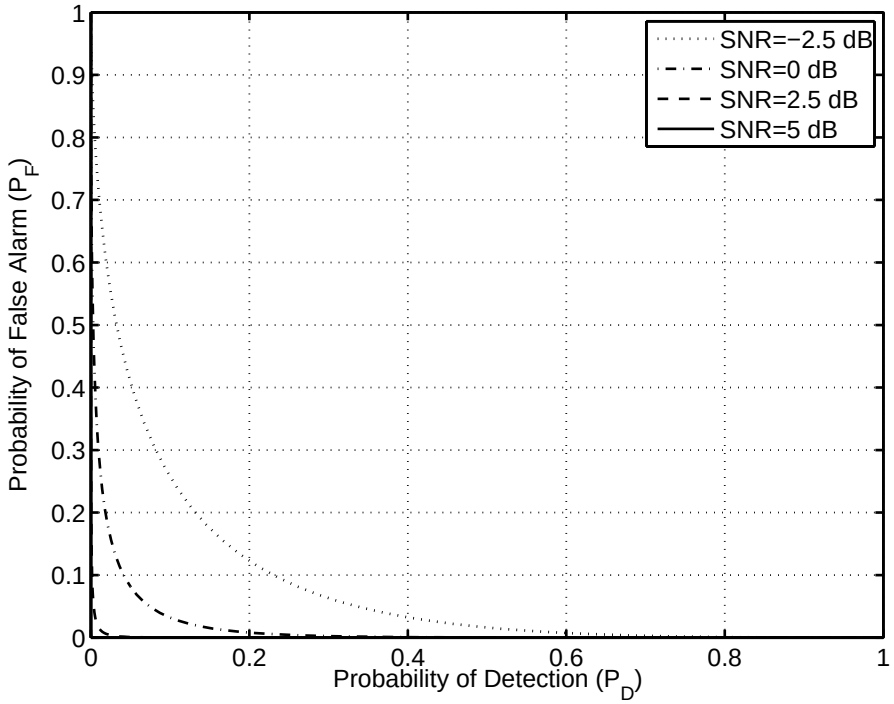

Figure 7.3 ROC curves for different SNR values.

continuous frequencies which are marked by threshold detector as having signal, not G_{max} samples away and with more adjacent frequency samples than B_{min} as illustrated in Fig. 7.4. Hence, using these two parameters, the occupied frequency band can be identified. It is then straightforward to estimate the bandwidth and the center frequency of transmission which make up the feature set $\boldsymbol{f}$. One drawback of this method, however, is that the cognitive radio may not differentiate between two (or more) superimposed primary user transmissions and threat them as a single transmission with a larger bandwidth.

7.3.4 Classification

In the final step, the primary users are identified by using the *a priori* information about their transmission parameters. Bayesian classifier is the optimum method from the statistical viewpoint and it will be used this chapter. By using Bayesian decision rule, we classify the feature set obtained using measurements in the previous section to systems or devices that has the highest *a posteriori* probability. The classifier can be represented in terms of a set of discriminant functions $g_i(\boldsymbol{f})$, $i = 1, \ldots, K$ where K is the total number of systems. Note that the same RATs operating at

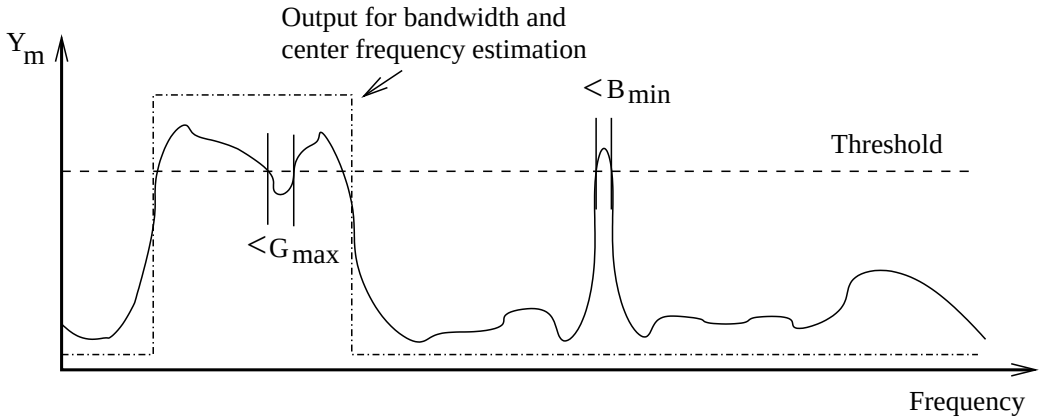

Figure 7.4 Illustration of DUDE algorithm for bandwidth and center frequency estimation.

different bands are regarded as different systems for the sake of classification. The transmission band of a system needs to be known for identifying the frequencies occupied by primary users. The discriminant functions are defined as

$$g_i(\boldsymbol{f}) \equiv \log P(\boldsymbol{f}|\omega_i) + \log P(\omega_i). \tag{7.10}$$

where $P(\omega_i)$ is the prior probability of class ω_i, and $P(\mathbf{x}|\omega_i)$ is the class conditional probability which is assumed to have multivariate normal distribution with mean vector $\boldsymbol{\mu}_i$ and covariance matrix $\boldsymbol{\Sigma}_i$. Under such an assumption, the discriminant functions can be obtained as [224]

$$g_i(\boldsymbol{f}) = -\frac{1}{2}(\boldsymbol{f} - \boldsymbol{\mu}_i)^T \boldsymbol{\Sigma}_i^{-1}(\boldsymbol{f} - \boldsymbol{\mu}_i) - \frac{1}{2}\log|\boldsymbol{\Sigma}_i| + \log P(\omega_i). \tag{7.11}$$

The classification regions defined by (7.11) are quadratic functions. Therefore, $g_i(\boldsymbol{x})$ is known as *normal-based quadratic discriminant function*. The classification rule can now be written as: assign a feature vector $\boldsymbol{f}$ to a system ω_i if $g_i(\boldsymbol{f}) > g_j(\boldsymbol{f})$ for all $j \neq i$.

The discriminant function $g_i(\boldsymbol{f})$ is locally estimated. When collaborative sensing is used, classification results can be shared among cognitive radios. Alternatively, instead of providing hard decisions cognitive radios can share the discriminant function values. Then, the central unit can combine these values and make a more optimum decision based on the discriminant function values from all cognitive radios present in the environment.

The mean vector $\boldsymbol{\mu}_i$ can be obtained by using the expected values of features, *e.g.* bandwidth and center frequency in this case. In practice, the covariance matrix $\boldsymbol{\Sigma}_i$ is unknown and can be

replaced with estimates based on the training data as

$$\hat{\boldsymbol{\Sigma}}_i = \frac{1}{D-1}\sum_{j=1}^{D}(\boldsymbol{f}_j - \boldsymbol{\mu}_i)(\boldsymbol{f}_j - \boldsymbol{\mu}_i)^T. \tag{7.12}$$

where D is the length of the training data. Furthermore, the covariance matrix can be assumed to be the same for all classes using the same RAT. For example, all the classes using WLAN are expected to have the same covariance matrix as only center frequency is changed. When the estimated features are not correlated to each other, the correlation matrix becomes a diagonal matrix. Different features will have different units and hence proper normalization of this features needs to be established. Moreover, the values of diagonal elements give the weights for each feature, and different weights can be assigned to different features.

7.4 Numerical Results

In order to test the proposed algorithm, we consider two RATs in 2.4 GHz ISM bands, namely WLAN and Bluetooth signals. Note that ISM band is an unlicensed band and there is no notion of primary users in this band. However, we have chosen this band for illustrative purposes as different types of devices can use this band. It is assumed that Bluetooth signal is not changing hopping frequency during the detection phase, *i.e.*, the detection process takes much less than 675 μs. Both WLAN and Bluetooth signals are assumed to have the same power and prior probabilities, and no overlap of spectrum between the two signals is allowed. The latter assumption can be justified by the adaptive frequency hopping (AFH) capability of Bluetooth. The spectrum of the ISM band is calculated using 1024-point FFT. Hence the frequency separation between two FFT output samples is 81.5 kHz, *i.e.* at least 12 frequency points will have Bluetooth signal and at least 246 frequency points will have WLAN signal. The length of the frequency domain filter is set to 5, *i.e.* $L_f = 5$. Fig. 7.5 shows the PSD of a WLAN signal operating at channel 5 (F_c=2.432 GHz) and a Bluetooth signal at frequency F_c=2.462 GHz. WLAN and Bluetooth signals are generated by transmitting random data modulated using OFDM and Gaussian frequency shift keying (GFSK) modulations as defined in their corresponding standards.

The features, transmission bandwidth and center frequency, are calculated as explained in Section 7.3 after passing the FFT output through a threshold device and finding continuous frequencies with power larger than the threshold. The threshold is chosen to have a low false alarm rate of 0.1

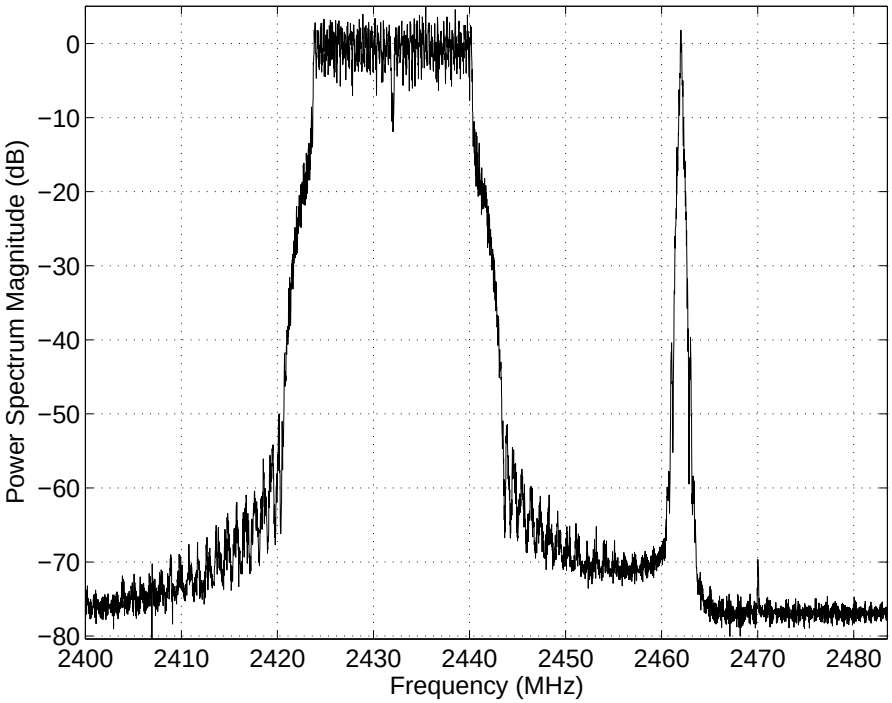

Figure 7.5 Power spectral density of tested WLAN and Bluetooth signals.

percent, *i.e.* $P_F = 0.001$. Note that while setting the threshold, the noise variance is assumed to be known. The feature extraction parameters are set as $G_{max} = 30$ and $B_{min} = 6$ which correspond to 2.44 MHz and 490 kHz respectively.

Figs. 7.6 and 7.7 show the error rates in detecting the WLAN and Bluetooth signals for additive white Gaussian noise (AWGN) channels. The error rate for identifying a non-existent system (or a system in another band) is shown as well. The time averaging L_t for Fig. 7.6 and Fig. 7.7 are set to be 15 and 30 respectively. Hence, sensing durations correspond to 184 μs and 368 μs. The classification is quite successful even at very low SNR scenarios and performance increases with increasing averaging duration. Note that the error rates for WLAN are smaller for a given SNR value. This is because of the large bandwidth and large separation of center frequencies of WLAN signals.

Fig. 7.8 shows the performance of energy detector based algorithm when the received signal is passed through a multipath channel with exponential delay power delay profile (PDP) with root-mean-squared (RMS) delay spread value of 50 ns. The performance of the Bluetooth signal detection is affected very little while the performance of WLAN detection is decreased. The power fluctuations

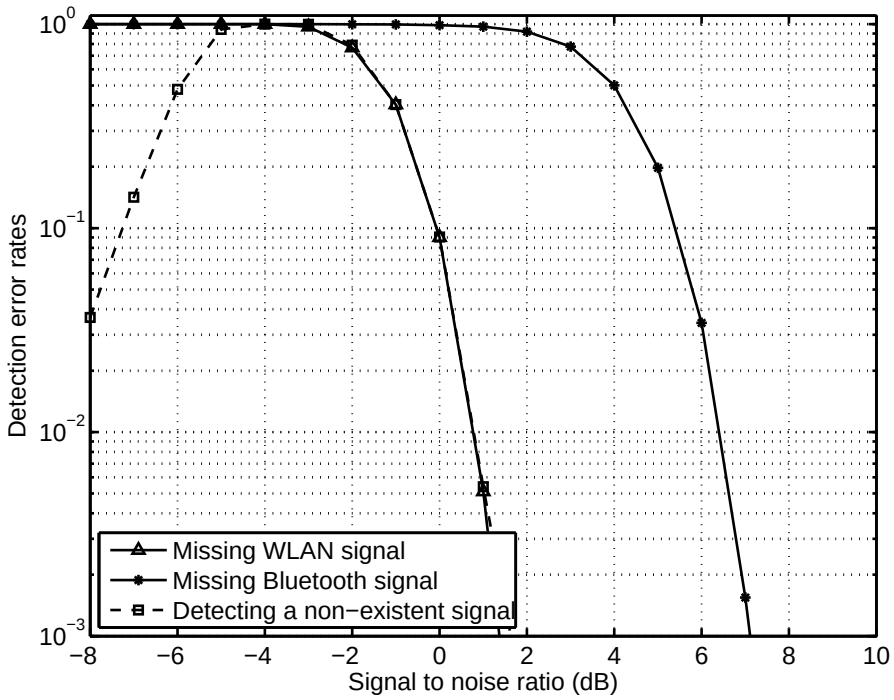

Figure 7.6 Detection error rates for the WLAN and Bluetooth systems at different SNR values for $L_t = 15$.

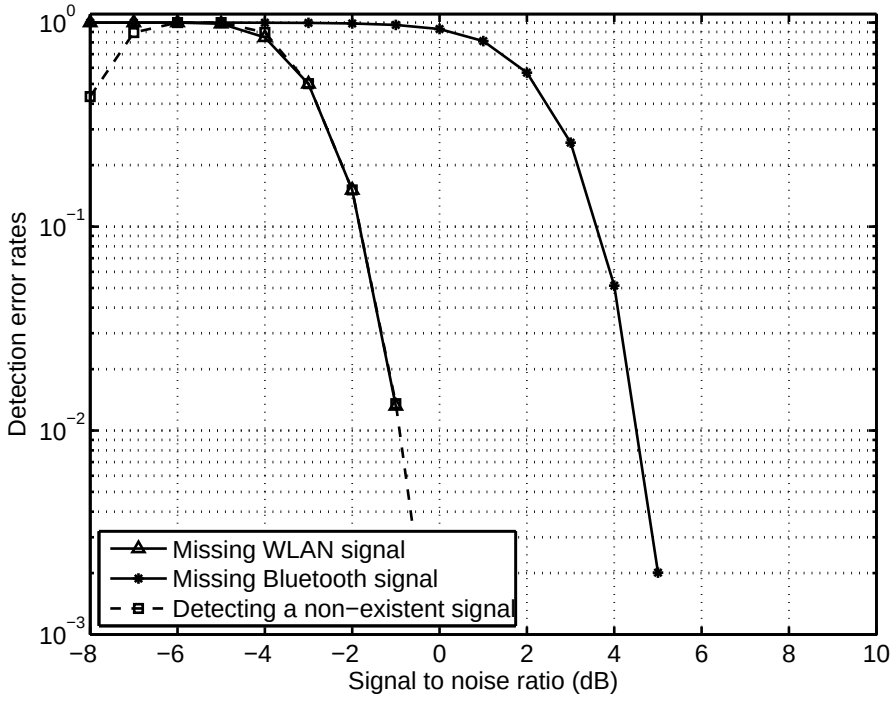

Figure 7.7 Detection error rates for the WLAN and Bluetooth systems at different SNR values for $L_t = 30$.

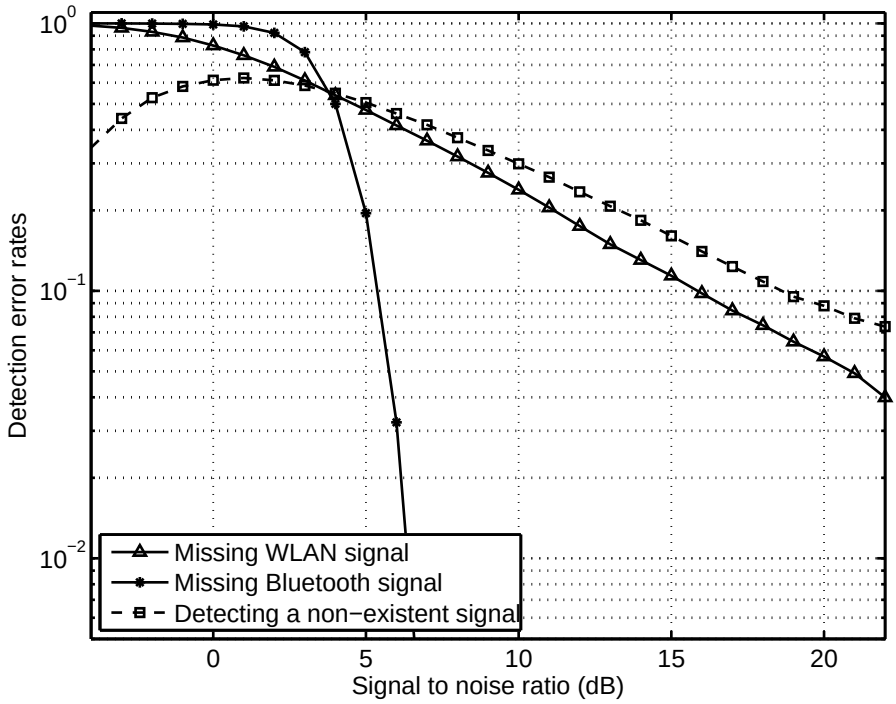

Figure 7.8 Detection error rates for the WLAN and Bluetooth systems at different SNR values for $L_t = 15$ under multi-path fading channel.

within the large bandwidth of the WLAN signal due to frequency selectivity and fading causes the performance degradation.

When the received signal is weak (low SNR values), the signal power falls below the noise floor. In such cases, the comparator yields zero output mostly due to the low P_F settings. Hence, no transmissions can be detected. As a result of this, the probability of missing ongoing transmissions becomes one and probability of detecting a non-existent signal approaches to zero.

7.5 Discussion

The energy detector based algorithm is presented as a case-study in the previous section. Even though energy detector based sensing has low complexity, it has some problems that need to be addressed. For commercially available devices, there are two main types of technologies: fixed frequency and spread spectrum. The two major spread spectrum technologies are frequency-hoping spread-spectrum (FHSS) and direct-sequence spread-spectrum (DSSS). Fixed frequency devices operate at a single frequency or *channel*. An example to such systems is IEEE 802.11a/g based WLAN. FHSS devices change their operational frequencies dynamically to multiple narrowband channels.

This is known as *hopping* and performed in a sequence that is known by both the transmitter and receiver. DSSS devices are similar to FHSS devices, however they use a single band to *spread* their energy. Bluetooth and IEEE 802.11b devices are examples to FHSS and DSSS respectively. Energy detector based algorithm works fine for fixed frequency signals. However, spread spectrum signals are very hard if not impossible to identify by using only energy detector based sensing as the energy is spread across the spectrum.

Another problem arises when the fixed frequency signals overlap in the frequency or when they are very close to each other. Energy detector based algorithm discussed in this chapter might not be able to differentiate the two transmissions and can regard the transmission as a single transmission with a wider bandwidth. This will in turn affect the classification output of PMF and yield inaccurate spectrum knowledge.

These problems can be solved by supporting the energy detector based algorithm with carefully designed signal processing techniques or extra features for PMF can be obtained using other signal processing tools such as cyclostationarity based or wavelet based methods. As explained in Section 7.2.1, the selection of features and algorithms for extracting these features should be done by considering the initial set of parameters and processing capabilities of cognitive radio. In this chapter, we have explored energy detector-based method as an example for PMF because of its simplicity.

7.6 Conclusions and Future Research

Transmissions within a given frequency band are identified by using PMF in this chapter. The characteristics of these transmissions are used for obtaining spectrum knowledge and finding spectrum holes. A simple feature extraction method is proposed for finding the transmission parameters using the energy detector output. By applying the partial match-filtering algorithm, the spectrum estimation can be improved significantly as not only the frequency spectrum but a multi-dimensional spectrum awareness can be obtained.

CHAPTER 8

OFDM SIGNAL IDENTIFICATION AND TRANSMISSION PARAMETER ESTIMATION FOR COGNITIVE RADIO APPLICATIONS

8.1 Introduction

Cognitive radios are expected to recognize different wireless networks and have capability to communicate with them. Multi-carrier techniques, specifically orthogonal frequency division multiplexing (OFDM), are commonly used in modern communications systems. For identification of active transmissions, signals can be classified as single-carrier and multi-carrier first. Hence, the size of candidate set can be reduced. Moreover, transmission parameters of an OFDM based system can be detected blindly if the system is not known to cognitive radio. Blind detection is also very helpful for reducing system signaling overhead in the case of adaptive transmission where transmission parameters are changed depending on the environmental characteristics or spectrum availability. The capability of identifying transmission parameters can be useful for spectrum survey for radio monitoring systems to discover enemy and illegal transmissions as well.

OFDM signals can be considered as a composition of large number of independent random signals. Hence, sampled OFDM signal can be assumed to have a Gaussian distribution thanks to central limit theorem. This observation is used in [221, 225, 226] for classification of signals as single-carrier or multi-carrier by applying normality tests to incoming signal. However, in the presence of multipath-fading and interference, single-carrier signals at the cognitive radio receiver can also have Gaussian distribution. This is especially true for low signal-to-noise ratio (SNR) scenarios. Furthermore, when power control is employed in time-multiplexed OFDM (such as IEEE 802.16), the Gaussian approximation does not hold anymore, and as a consequence, classification based on normality tests may fail.

Various parameter estimation algorithms for OFDM systems are developed in literature. Methods for finding the OFDM symbol and cyclic prefix (CP) durations are mostly based on exploitation of the cyclostationarity of OFDM signaling due to cyclic prefix extension [221, 226–230]. In [227],

symbol duration is estimated by finding the distance between the peaks at the correlation. In order to estimate the length of CP, time-frequency transform of the received signal is found and entropy is calculated which is then used to find the CP size. In [221], symbol duration is estimated using cyclic correlation based algorithm, and CP duration is estimated by performing a correlation test. A different approach is taken in [229] for finding the CP size when the data length is known. Auto-correlation of the received signal with its delayed copy is calculated and its magnitude is normalized with average signal power. As the auto-correlation has non-zero terms only for the part that falls into the guard time, power ratio of the guard time to the symbol duration can be used to find the CP length. However, SNR knowledge is required for a precise estimation.

Number of subcarriers or discrete Fourier transform (DFT) size is another key parameter for OFDM systems. An algorithm based on multiple signal classification (MUSIC) technique is used in [231] for finding the DFT size. Basically, eigen-decomposition is used to diagonalize the correlation matrix of the received signal. Then, using Akaike's criteria, number of sub-spaces or sub-carriers is estimated. However, zeros are used for generating OFDM signal instead of cyclic prefix in [231]. In [221], once CP and symbol durations are estimated, DFT size is found by testing all hypothesis DFT size values. The fact that the DFT output gives modulated data symbols, which do not have Gaussian properties, when DFT size is matched to correct one is explored. DFT outputs are tested for Gaussianity to find the correct DFT size. If not all of the subcarriers are employed for transmission, active subcarriers should be identified. This can be performed by analyzing the power level at the output of FFT [232]. However, such methods need the knowledge of FFT size and require synchronization to the received signal.

OFDM signal bandwidth can be a useful element for signal identification and finding white spaces in the spectrum. In literature, the brick-wall shape of the spectrum is used for estimating the OFDM bandwidth [233, 234]. Spectral breaking points are identified using edge detection algorithms and bandwidth information is extracted by using the spectral breaking points. These methods, however, are only effective when all of the subcarriers are employed.

In this chapter, classification of communications systems as single-carrier or multi-carrier is considered, and methods for estimation of fundamental transmission parameters in the case of multi-carrier transmission are proposed. Our contributions can be summarized as following:

- maximum likelihood (ML) and suboptimal ML algorithms are developed for estimating the OFDM symbol duration and CP size,

- a method for classifying unknown signals as OFDM or single-carrier is developed. This method is based on the likelihood function of the received signal evaluated at ML estimates of signal parameters,
- a new method based on estimation of signal parameters via rotational invariance techniques (ESPRIT) is developed to estimate the number and frequencies of subcarriers of the identified OFDM signals.

The chapter is organized as follows. Section 8.2 describes the system model. Proposed OFDM identification and parameter extraction algorithms are given in Section 8.3, followed by numerical results in Section 8.4. Finally, the chapter is concluded in Section 8.5.

8.2 System Model

OFDM converts serial data stream into parallel blocks of size N and modulates these blocks using inverse discrete Fourier transform (IDFT). The continuous-time OFDM signal in the baseband can be written as[1]

$$x_m(t) = \sum_{k=1}^{K} X_m(k) e^{j\frac{2\pi \mathbf{\Gamma}(k)t}{T_D}} \quad -T_G \leq t < T_D, \tag{8.1}$$

where $X_m(k)$ is the transmitted data symbol at kth (data) subcarrier of mth OFDM symbol and $\mathbf{\Gamma}$ denotes the set of K used subcarriers. Useful data duration and CP length are represented by T_D and T_G respectively and they make up the total duration of OFDM symbol T_S, *i.e.* $T_S = T_D + T_G$, as shown in Fig. 8.1. Transmitted signal can now be written as

$$x(t) = \sum_{m=-\infty}^{\infty} x_m(t - mT_S). \tag{8.2}$$

After D/A conversion and radio frequencies (RF) modulation, signal is passed through the mobile radio channel which can be modeled as a time-variant linear filter

$$h(t) = \sum_{l=1}^{L} h_l(t)\delta(t - \tau_l), \tag{8.3}$$

[1]Please note that in this chapter a continuous-time system model is used whereas in other parts of the dissertation discrete-time system model is used.

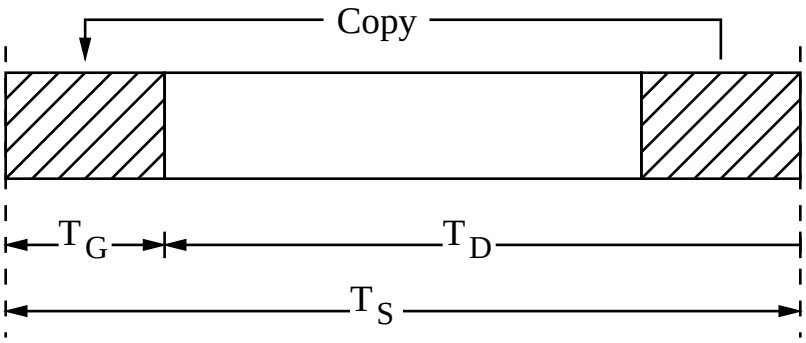

Figure 8.1 Illustration of cyclic prefix extension in OFDM systems.

where L is the number of sample-spaced channel taps and τ_l is the delay of lth tap. In this chapter, the channel is assumed to be constant over an OFDM symbol, but time-varying across OFDM symbols, which is a reasonable assumption for low and medium mobility.

At the receiver, the signal is received along with noise. After down-conversion, simplified base-band model of the received signal can be formulated as

$$y(t) = e^{j2\pi\xi t}\left[x(t) \star h(t)\right] + w(t) \tag{8.4}$$

$$= e^{j2\pi\xi t}\int x(\tau)h(t-\tau)d\tau + w(t) \tag{8.5}$$

$$= e^{j2\pi\xi t}\sum_{l=1}^{L} x(t-\tau_l)h_l(\tau_l) + w(t), \tag{8.6}$$

where ξ corresponds to the frequency offset due to inaccurate frequency synchronization with the received signal. The average received signal power is denoted by σ_s^2.

It is assumed that the receiver does not know the correct sampling rate[2] and samples the received signal with a sampling time of Δt. Now, the discrete-time received signal can be obtained from continuous time signal as

$$y[n] := y(n\Delta t). \tag{8.7}$$

In discrete-time representation, N_D, N_G and N_S are used to represent the number of samples corresponding to data, CP and total symbol durations respectively. The time durations can be calculated by multiplying these numbers with the sampling period, *e.g.* $T_S = N_S\Delta t$. The received signal is assumed to have D samples which contains an unknown single-carrier signal or unknown

[2]The Nyquist sampling period is $t_s = T_D/N$ where N is the DFT size used to generate the OFDM signal.

number of OFDM symbols. In vector notation the received signal can be represented as

$$\boldsymbol{y} = [y[1],\ y[2],\ \cdots\ y[D]]. \tag{8.8}$$

8.3 Proposed Algorithms

OFDM signaling is shown to be cyclostationary with period T_S in [235]. It is also known that cyclostationarity of a signal holds when it is passed through a linear time-invariant channel[3]. Hence, the received OFDM signal is also cyclostationary. In this section, detection algorithms are developed by exploring the cyclostationarity characteristics of the OFDM signaling in additive white Gaussian noise (AWGN) channel. The performance of developed methods under multipath fading channel is shown in Section 8.4. First, symbol duration and CP size are estimated by assuming an OFDM transmission. Then, the estimated parameters are used to decide on whether the received signal is OFDM signal or a single-carrier signal. Finally, we estimate the number and frequencies of active subcarriers by using the rotational invariance of OFDM signaling.

8.3.1 ML Estimation of OFDM Symbol Length and CP Size

For the observation vector $\boldsymbol{y}$, OFDM symbol duration N_D and CP size N_G are not known as well as the start time of each symbol, denoted by θ. Let us denote the set of samples that belong to CP with $\boldsymbol{\Omega}$. The samples in CP and in the last part of OFDM symbol are pairwise correlated (see Fig. 8.1). Using the structure of OFDM signaling, the correlation of the samples in observation vector can be written as

$$E\left[y[n]y^*[n+\Delta]\right] = \begin{cases} \sigma_s^2 + \sigma_w^2 & \Delta = 0, \\ \sigma_s^2 e^{-j2\pi\xi\Delta t N_D} & \Delta = N_D;\ n \in \boldsymbol{\Omega} \\ 0 & \text{otherwise.} \end{cases} \tag{8.9}$$

Maximum likelihood estimates of the unknown parameters N_D, N_G, and θ can be obtained by maximizing the log-likelihood function of the observations $\boldsymbol{y}$. Log-likelihood function can be

[3]In fact, for our application, it is enough that the channel is time-invariant for the duration of each OFDM symbol.

formulated as

$$\Lambda(\boldsymbol{y}; N_D, N_G, \theta) = \log\left(\prod_{n\in\boldsymbol{\Omega}} p(y[n], y[n+N_D]) \prod_{n\notin\boldsymbol{\Omega}\cup\boldsymbol{\Omega}'} p(y[n])\right) \tag{8.10}$$

$$= \log\left(\prod_{n\in\boldsymbol{\Omega}} \frac{p(y[n], y[n+N_D])}{p(y[n])p(y[n+N_D])} \prod_{n} p(y[n])\right) \tag{8.11}$$

where $p(\cdot)$ is the probability density function (PDF) of the observed samples and $p(\cdot,\cdot)$ is the joint PDF. The set $\boldsymbol{\Omega}'$ contains the samples of OFDM data that are copied to CP. Assuming that $\boldsymbol{y}$ has a jointly Gaussian distribution, it is shown in Appendix C that the log-likelihood function can be obtained as (C.5) where a and $\boldsymbol{\Omega}$ are as given in (C.4) and (C.6) respectively. Please note that, ML estimation obtained by maximizing the likelihood function given by (C.5) is asymptotically optimal when the following assumptions are satisfied:

1. Noise is white, Gaussian, and uncorrelated with the transmission signal.

2. $\boldsymbol{y}$ has a joint Gaussian distribution with correlation function given by (8.9).

Also note that, the ML estimation algorithm can be modified to estimate the frequency offset ξ as well.

The value of a, σ_s^2 and σ_w^2 are difficult to estimate in a non-cooperative scenario. At low SNR values, the second and third terms of (C.5) approaches to zero and can be dropped. Therefore, a suboptimal ML estimation is possible with less complexity and no need for the knowledge of noise and signal variances. Modified likelihood function can now be obtained from (C.5) as[4]

$$\tilde{\Lambda}(\boldsymbol{y}; N_D, N_G, \theta) = \left| \sum_{m=0}^{\left\lfloor \frac{D}{N_D+N_G} \right\rfloor} \sum_{p=1}^{N_G} y[m(N_D+N_G)+p+\theta] y^*[m(N_D+N_G)+N_D+p+\theta] \right|. \tag{8.12}$$

Hence, the proposed sub-obtimum ML estimation algorithm is

$$\hat{N}_D, \hat{N}_G, \hat{\theta} = \underset{N_D, N_G, \theta}{\arg\max} \left\{ \tilde{\Lambda}(\boldsymbol{y}; N_D, N_G, \theta) \right\} \tag{8.13}$$

$$= \underset{N_D, N_G, \theta}{\arg\max} \left\{ \left| \sum_{m=0}^{\left\lfloor \frac{D}{N_D+N_G} \right\rfloor} \sum_{p=1}^{N_G} y[m(N_D+N_G)+p+\theta] y^*[m(N_D+N_G)+N_D+p+\theta] \right| \right\}. \tag{8.14}$$

[4]Note that the likelihood function is independent of the frequency offset.

A method similar to (8.14) is used in [236] where the symbol duration and CP length have only a predetermined set of values as the underlying transmission was known.

Maximization given in (8.14) is a computationally demanding process. In order to reduce the complexity, maximization can be performed in two steps. First, OFDM symbol length N_D is estimated, and then the estimated N_D value is used to find CP duration N_G and timing offset θ in the second step. As will be shown later, the simplification on the computational complexity comes with the expense of performance degradation.

Step 1 The repetition due to CP is used to find the OFDM data duration T_D. As the receiver is assumed to have no prior information on the symbol duration, all expected values should be tested. The discrete correlation of the received signal can be written as

$$R_y(\Delta) = \frac{1}{D-\Delta} \sum_{n=1}^{D-\Delta} y[n] y^*[n+\Delta]. \tag{8.15}$$

Assuming enough statistical averaging, the correlation can be obtained as

$$R_y(\Delta) = \begin{cases} \sigma_s^2 + \sigma_w^2 & \Delta = 0, \\ \frac{N_G}{N_D+N_G} \sigma_s^2 e^{-j2\pi\xi\Delta t N_D} & \Delta = N_D, \\ 0 & \text{otherwise.} \end{cases} \tag{8.16}$$

Hence, the auto-correlation based estimation of N_D can be formulated as

$$\hat{N}_D = \arg\max_{\Delta} \{|R_y(\Delta)|\}, \quad \Delta > 0. \tag{8.17}$$

In order to simplify time and frequency synchronization, known sequences are transmitted in OFDM based systems. These sequences include preambles and pseudo-random pilot (data) symbols. OFDM preamble is usually composed of identical sequences that can be used to facilitate synchronization using auto-correlation. However, for the blind estimation method given by (8.17), the correlation peak due to repetition in the preamble cause ambiguity as the value of this peak can be larger than the peak generated by the cyclic prefix. Assume that the received signal has n_D OFDM data symbols, n_P preamble symbols, and power of the preamble is boosted by ζ. The worst case happens when the preamble has large number of identical parts. Assuming that the number of

identical parts is very large, the following inequality should be satisfied for correct detection

$$\zeta(n_P T_D + n_P T_G) < (n_D + \zeta n_P) T_G. \tag{8.18}$$

For IEEE 802.11a/g based wireless local area network (WLAN), for example, the minimum number of OFDM symbols for correct detection is 8. In order to remove this ambiguity in finding the symbol duration, we first find C peak values in the correlation and use the corresponding N_D values for ML estimation of CP duration. Then, the final value of N_D is selected in the second step.

Step 2 Once the OFDM symbol duration N_D is found, the CP duration can be estimated by testing for different N_G values as

$$\hat{N}_G, \hat{\theta} = \arg\max_{N_G, \theta} \left\{ \tilde{\Lambda}(\boldsymbol{y}; \hat{N}_D, N_G, \theta) \right\}. \tag{8.19}$$

Usually, the CP length is chosen as a multiple of OFDM symbol duration. In IEEE 802.16 systems, for example, available sizes are 1/4, 1/8, 1/16 and 1/32 [103]. Therefore, in order to further reduce the complexity, the CP size hypotheses can be limited to these ratios of the estimated N_D value from previous step.

A numerical comparison of ML, suboptimal ML, and two-step low-complexity algorithms is given in Fig. 8.2 which shows the normalized mean-squared-error (MSE) of OFDM data duration estimation for AWGN and multi-path fading channels for a WLAN system [10] (see Section 8.4 for more details of the used OFDM system and channel model). As can be seen from this figure, the performance loss for the suboptimal method is around 1 - 1.5 dB as compared to the ML method. Please note that for ML algorithm, perfect noise and signal variance knowledge is assumed; and the performance of ML algorithm is expected to decrease when these parameters are not perfectly known. Another 2 dB performance loss is observed when low-complexity two step method is used instead of calculating (8.14). In the rest of the chapter, we use two-step estimation algorithm based on modified likelihood function for obtaining performance results of the proposed method.

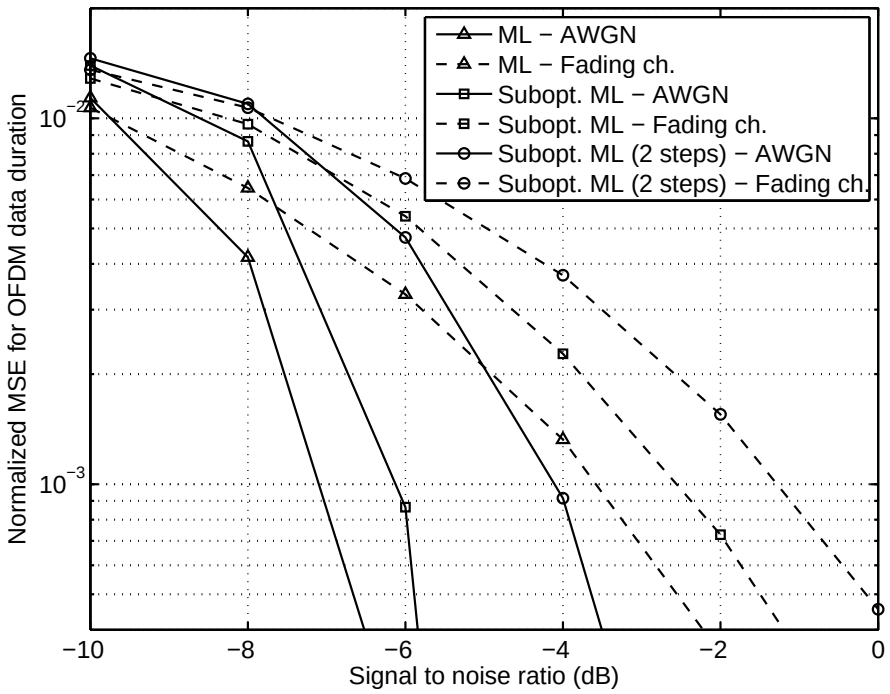

Figure 8.2 Numerical performance comparison of ML, suboptimal ML and two-step algorithms. Normalized MSE of OFDM symbol duration estimation versus SNR is presented.

8.3.2 OFDM Signal Identification

The modified likelihood function (8.12) evaluated at the estimated values can be written as

$$\gamma = \tilde{\Lambda}(\boldsymbol{y}; N_D, N_G, \theta)\Big|_{\hat{N}_D, \hat{N}_G, \hat{\theta}} = \tilde{\Lambda}(\boldsymbol{y}; \hat{N}_D, \hat{N}_G, \hat{\theta}). \tag{8.20}$$

Eqn. (8.20) gives us the likelihood of receiving $\boldsymbol{y}$ for an OFDM system which has the estimated parameters. For OFDM signals, as the number of samples increases, γ converges to $\left\lfloor \frac{D}{\hat{N}_D + \hat{N}_G} \right\rfloor \hat{N}_G \sigma_s^2$ and for non-OFDM signals, it becomes zero, *i.e.*

$$\gamma = \begin{cases} \left\lfloor \frac{D}{\hat{N}_D + \hat{N}_G} \right\rfloor \hat{N}_G \sigma_s^2 & \mathcal{H}_1 \\ 0 & \mathcal{H}_0, \end{cases} \tag{8.21}$$

where $\mathcal{H}_0$ and $\mathcal{H}_1$ represent the null hypothesis and alternate hypothesis, *i.e.* the received signal is not OFDM signal or it is an OFDM signal, respectively. This observation is used for classification of

a signal as single-carrier or multi-carrier (OFDM) by comparing γ to a threshold λ_{MC}. The received signal is classified as OFDM signal if $\gamma > \lambda_{MC}$.

The value of decision threshold depends on the incoming (OFDM) signal power and desired probability of false alarm (or probability of miss). Signal power can be found using the total signal if SNR is known. In non-cooperative environments, SNR knowledge is usually unavailable. In such a case, a low SNR value can be assumed. In Section 8.4, it is shown that such an approach gives robust results for a wide range of SNR values.

8.3.3 Estimation of Number and Frequencies of Active Subcarriers

Not all of the subcarriers carry data symbols in OFDM systems. Some subcarriers at the edges of the spectrum are not used to create guard bands which ease filter requirements. In addition, subcarriers might be turned off (unused) to prevent interference to relatively narrower-band primary users as done in spectrum pooling systems [97]. Moreover, in orthogonal frequency division multiple access (OFDMA) systems, subcarriers might be shared by different users. Knowledge of frequencies and number of active subcarriers can be used to find the FFT size and to blindly identify the deactivated subcarriers. The latter can be used in adaptive and cognitive radio systems to decrease the signaling overhead.

When only a single OFDM symbol is concerned, time domain signal can be considered as a sum of sinusoids whose number is equal to the number of active subcarriers. Hence, high-resolution methods can be used to estimate the number and positions (frequencies) of subcarriers. OFDM signals are inherently shift-invariant as time-shift causes only a subcarrier-dependent phase shift to the subcarriers. In OFDM, shift-invariance is caused by the addition of cyclic prefix. In this section, we exploit shift-invariance of signal subspaces of sinusoids using ESPRIT algorithm for estimating the number and frequencies of used subcarriers. Using the results of Section 8.3.1, observation vectors for each OFDM symbol can be constructed as

$$\boldsymbol{x}_m = [y_m[1]\ y_m[2] \cdots y_m[N_D]]^T \tag{8.22}$$

$$\boldsymbol{y}_m = [y_m[2]\ y_m[3] \cdots y_m[N_D+1]]^T, \tag{8.23}$$

where $y_m[1]$ is the first sample that belongs to data part of OFDM symbol. In order for $y_m[N_D+1]$ to stay within the mth symbol duration, start time can be shifted into CP portion as the phase shift between $\boldsymbol{x}_m$ and $\boldsymbol{y}_m$ is not affected.

Using (8.1) and (8.7), the observation vectors can be expressed in matrix notation as

$$\boldsymbol{x}_m = \boldsymbol{A}\boldsymbol{s}_m + \boldsymbol{w}_m, \tag{8.24}$$

$$\boldsymbol{y}_m = \boldsymbol{A}\boldsymbol{\Phi}\boldsymbol{s}_m + \boldsymbol{w}'_m, \tag{8.25}$$

where $\boldsymbol{A} = [\boldsymbol{a}_1\ \boldsymbol{a}_2\ \cdots\ \boldsymbol{a}_K]$ is $N_D \times K$ Vandermonde matrix whose columns are given as

$$\boldsymbol{a}_k = [1\ e^{j\omega_k}\ e^{j2\omega_k}\ \cdots\ e^{j(N_D-1)\omega_k}]^T. \tag{8.26}$$

The frequency of each subcarrier can be obtained using (8.1) as

$$\omega_k = \frac{2\pi\Delta t}{T_D}\boldsymbol{\Gamma}(k) \quad k = 1, 2\cdots K. \tag{8.27}$$

The $K \times K$ matrix $\boldsymbol{\Phi}$ contains the phase difference due to shifting and it is given by

$$\boldsymbol{\Phi} = \text{diag}\left[e^{j\omega_1},\ \cdots,\ e^{j\omega_K}\right]. \tag{8.28}$$

The column vector $\boldsymbol{s}_m$ is given as

$$\boldsymbol{s}_m = [H_m(1)X_m(1)\ H_m(2)X_m(2)\cdots H_m(K)X_m(K)]^T. \tag{8.29}$$

where $H_m(k)$ corresponds to the effect of multipath fading channel on the kth (active) subcarrier of mth OFDM symbol, *i.e.* the channel frequency response (CFR) at kth subcarrier position.

The auto-covariance matrix of $\boldsymbol{x}_m$ can be calculated as

$$\boldsymbol{R}_{\boldsymbol{xx}} = E_m\left[\boldsymbol{x}_m\boldsymbol{x}_m^H\right] = \boldsymbol{A}\boldsymbol{S}\boldsymbol{A}^H + \sigma_w^2\boldsymbol{I}. \tag{8.30}$$

Similarly cross-covariance matrix of $\boldsymbol{x}_m$ and $\boldsymbol{y}_m$ are obtained as

$$\boldsymbol{R}_{\boldsymbol{xy}} = E_m\left[\boldsymbol{x}_m\boldsymbol{y}_m^H\right] = \boldsymbol{A}\boldsymbol{S}\boldsymbol{\Phi}^H\boldsymbol{A}^H + \sigma_w^2\boldsymbol{L}, \tag{8.31}$$

where $\boldsymbol{L}$ is an $N_D \times N_D$ lower shift matrix. Assuming that the data symbols are normalized and symbols at different subcarriers are independent, *i.e.*

$$E\left[X_m(i)X_m^*(j)\right] = \begin{cases} 0 & i \neq j \\ 1 & i = j, \end{cases} \tag{8.32}$$

it can be shown that $\boldsymbol{S}$ becomes a diagonal matrix whose diagonal elements are equal to average channel power at each used subcarrier position. Hence $\boldsymbol{S}$ can be written as

$$\boldsymbol{S} = E_m\left[\boldsymbol{s}_m \boldsymbol{s}_m^H\right] = \text{diag}\left[\sigma_H^2(1),\ \sigma_H^2(2),\ \cdots,\ \sigma_H^2(K)\right]. \tag{8.33}$$

where $\sigma_H^2(k) = E\left[|H_m(k)|^2\right]$ is the average channel power at kth subcarriers.

In the following, we use auto-covariance and cross-covariance matices of observation vectors to estimate the number and frequencies of active subcarriers of received OFDM signal.

8.3.3.1 Number of Subcarriers

One critical parameter in high-resolution frequency estimation is the number of sinusoids that needs to be estimated using the received signal. In this chapter, we follow information theoretic approach developed in [237]. The number of active subcarriers K can be found as the value of k that minimizes the minimum descriptive length (MDL) criterion which is given as

$$\begin{aligned} MDL(k) = -D \log & \left(\frac{\prod_{i=k+1}^{N_D} \eta_i}{\left(\frac{1}{N_D-k}\sum_{k+1}^{N_D} \eta_i\right)^{N_D-k}} \right) \\ & + \frac{1}{2}k(2N_D - k)\log D, \end{aligned} \tag{8.34}$$

where $\eta_1 \geq \eta_2 \cdots \geq \eta_{N_D}$ denote the eigenvalues of $\boldsymbol{R}_{\boldsymbol{xx}}$. Hence, the estimator can be written as

$$\hat{K} = \arg\min_k \left\{MDL(k)\right\}. \tag{8.35}$$

In [237], it is shown that this estimator based on MDL criterion is consistent. Therefore, the value obtained using (8.35) converges to true value of number of signals as sample size grows. Simulation results presented in Section 8.4 are consistent with these conclusions as well.

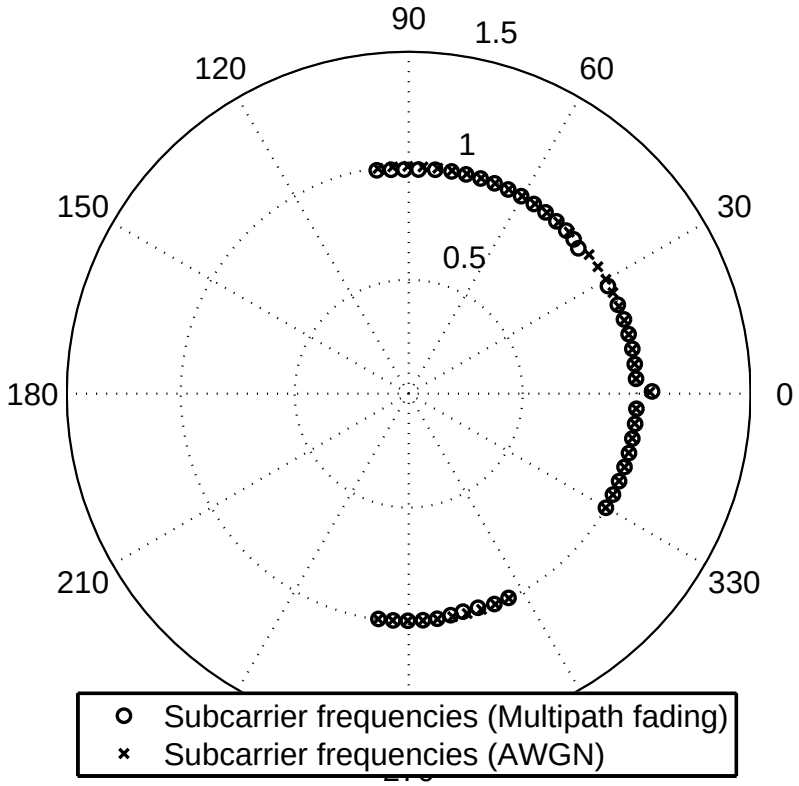

Figure 8.3 Illustration of ESPRIT based subcarrier estimation.

8.3.3.2 Frequencies of Subcarriers

Once the observation models are obtained, ESPRIT algorithm [238] can be used to estimate the frequencies of the subcarriers. Note that the formulation of (8.24) and (8.25) is different than the array problem given in [238]. In [238], the $\boldsymbol{s}_m$ vector was replaced by a constant vector, while in our problem $\boldsymbol{s}_m$ is varying for each observation as data symbols over each OFDM symbol are changed. However, the statistics such as auto or cross-covariance (ref. (8.30) and (8.31)) are independent of data symbols, which enables us to use ESPRIT method. Fig. 8.3 shows polar plot of generalized eigenvalues whose phase give the frequencies of subcarriers. The FFT size of the OFDM signal is 64 and 8 subcarriers are left deactivated in order to prevent interference to primary users (refer to Section 8.4 for more details). Mapping of these phases to frequencies, and power spectral density (PSD) of the signal in AWGN and fading channel is given in Fig. 8.4.

ESPRIT algorithm does not assume any prior knowledge about the (complex) sinusoids. By investigating (8.27), however, we see that the frequencies in our problem have a regular structure.

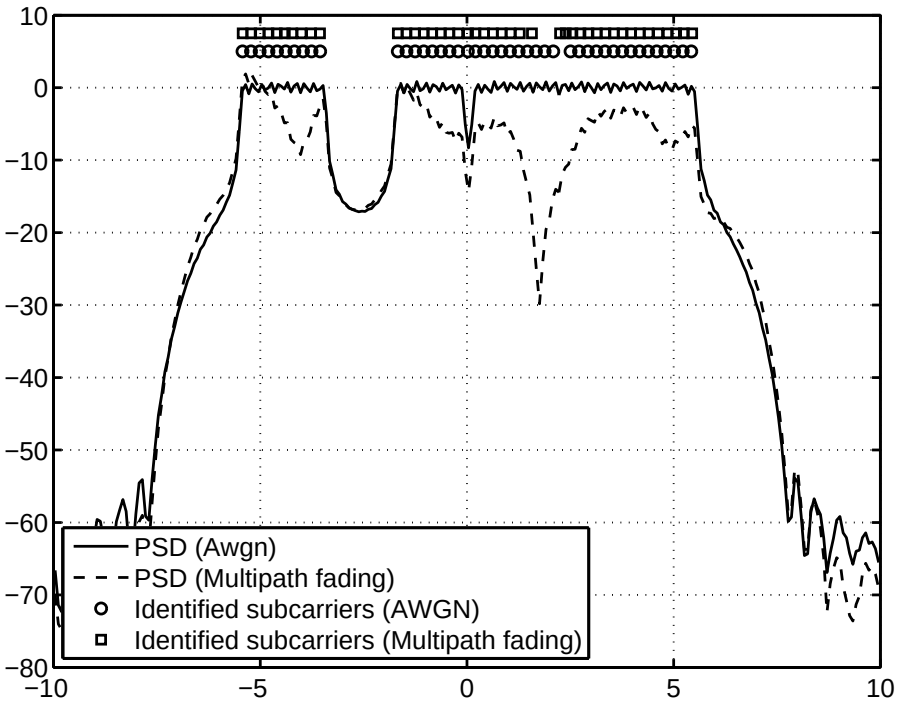

Figure 8.4 Subcarriers estimated by ESPRIT algorithm and power spectral density of received signal under AWGN and fading channels are illustrated.

This regular structure is used to develop a modified version of ESPRIT algorithm that suits well to the problem of estimating active subcarriers, *i.e.* $\mathbf{\Gamma}$. Using the same notation in [238], we define $\boldsymbol{C_{xx}}$ as

$$\boldsymbol{C_{xx}} = \boldsymbol{R_{xx}} - \hat{\sigma}_w^2 \boldsymbol{I} \approx \boldsymbol{A S A}^H, \tag{8.36}$$

where is $\hat{\sigma}_w^2$ the noise variance estimate which is estimated as

$$\hat{\sigma}_w^2 = \frac{1}{N_D - \hat{K}} \sum_{j=\hat{K}+1}^{N_D} \eta_j. \tag{8.37}$$

Similarly $\boldsymbol{C_{xy}}$ is defined as,

$$\boldsymbol{C_{xy}} = \boldsymbol{R_{xy}} - \hat{\sigma}_w^2 \boldsymbol{L} \approx \boldsymbol{A S \Phi}^H \boldsymbol{A}^H. \tag{8.38}$$

Now, let us consider the matrix pencil of the form

$$\boldsymbol{C_{xx}} - e^{-j\omega_i} \boldsymbol{C_{xy}} = \boldsymbol{AS}(\boldsymbol{I} - e^{-j\omega_i} \boldsymbol{\Phi}^H) \boldsymbol{A}^H \tag{8.39}$$

where $\omega_i = \frac{2\pi\Delta t}{T_D} i$. If $i \in \mathbf{\Gamma}$, one row of $\boldsymbol{I} - e^{-j\omega_i}\boldsymbol{\Phi}^H$ becomes zero. Consequently, the determinant of $\boldsymbol{I} - e^{-j\omega_i}\boldsymbol{\Phi}^H$ and hence the determinant of $\boldsymbol{C_{xx}} - e^{-j\omega_i}\boldsymbol{C_{xy}}$ become zero. Therefore, active subcarriers can be identified as the i values that makes the determinant of $\boldsymbol{C_{xx}} - e^{-j\omega_i}\boldsymbol{C_{xy}}$ zero and the frequencies of each subcarrier can be obtained as $\frac{2\pi\Delta t}{T_D} i$. Hence, the steps of proposed ESPRIT based subcarrier detection algorithm can be summarized as following:

1. Using received signal and synchronization knowledge, construct observation vectors $\boldsymbol{x}_m$ and $\boldsymbol{y}_m$.
2. Construct auto-correlation and cross-correlation matrices $\boldsymbol{R_{xx}}$ and $\boldsymbol{R_{xy}}$.
3. Compute the eigenvalues of $\boldsymbol{R_{xx}}$ and find number of subcarriers $\hat{K}$ using (8.35).
4. Compute $\boldsymbol{C_{xx}}$ $\boldsymbol{C_{xy}}$ using (8.36) and (8.38) respectively.
5. Calculate the determinant of $\boldsymbol{C_{xx}} - e^{-j\omega_i}\boldsymbol{C_{xy}}$ for $i = 0$ to $i = N_D$.
6. The i values which produce the $\hat{K}$ smallest determinants are selected as active subcarriers.

8.3.4 FFT Size and Communication Standard

If it is known that the received signal does not have any unused subcarriers (except guard bands and DC subcarrier), fast Fourier transform (FFT) size can be selected as the smallest integer larger than $\hat{K}$ and power of two. Otherwise, the gaps can be interleaved and $\hat{K}$ can be updated for calculating FFT size. Bandwidth of the received signal can easily be estimated by using knowledge of active subcarriers and their frequencies as well. In fact, actual bandwidth can easily be determined if the number of guard subcarriers is known which is possible when the underlying standard is identified.

It is straightforward to find the communication standard that the received signal belongs once its parameters are calculated. The estimated parameters can be compared with the *a priori* standard parameters. For this purpose, the most distinguishing parameters can be selected and based on these parameters a simple tree-based classification can be performed. In [226], for example, only the length of CP is used for finding which standard the received signal belongs. Alternatively, more complex and accurate methods such as statistical classification also be used [31].

8.4 Numerical Results

The proposed algorithms are tested using computer simulations. As for OFDM system, IEEE 802.11a based WLAN is used [10]. For this system, the transmission bandwidth is 20 MHz and number of subcarriers is 64, out of which 11 subcarriers are used as guard subcarriers and one as DC subcarrier. Furthermore, 8 subcarriers are deactivated in order to model a cognitive radio system. The spectrum of the transmitted signal can be seen in Fig. 8.4. CP contains 16 samples, hence, CP rate is 1/4. For this system, CP and total symbol durations correspond to 0.8 μs and 4 μs respectively. The sampling rate of received signal is assumed to be unknown to the cognitive radio and signal is assumed to be sampled at a rate 50% higher than Nyquist rate. An exponentially decaying power delay profile (PDP) with 90 ns root-mean-squared (RMS) delay spread is used for modeling wireless channel. Simulation results are obtained for 25, 50 and 100 consecutive OFDM symbols. The threshold for classifying signal as OFDM is chosen as $\lambda_{MC} = \frac{\sigma_s^2+\sigma_w^2}{2}\left\lfloor \frac{D}{\hat{N}_G+\hat{N}_D} \right\rfloor \hat{N}_G$. This value corresponds to a 0 dB SNR value. Normalized MSE is used as a performance measure of the estimation as it reflects both the bias and the variance of the estimation.

Fig. 8.5 shows the probability of incorrect classification of the simulated OFDM signal as single-carrier in AWGN and multi-path fading channels. As this figure shows, the classification is successful even at low SNR values and no error is observed for 10 dB or higher SNR values. Note that for AWGN channel, 0 dB is a decision boundary for classification. The reason for this boundary is the selected threshold λ_{MC} which corresponds to 0 dB SNR assumption for the received signal. If SNR information is available, the decision threshold λ_{MC} can be changed adaptively decreasing the false alarm and mis-detection rates. The normalized MSEs for T_D and T_G are given in Figs. 8.6 and 8.7 respectively. The estimation is more accurate for AWGN channel than multi-path fading channel as expected. It is noted that the number of available OFDM symbols used for estimation affects the performance of the estimation because of noise averaging.

For observing the performance of modified ESPRIT algorithm, knowledge of symbol and CP durations and perfect synchronization is assumed. The proposed method is applied to the same OFDM system whose parameters are given in this section. The probability of error for detecting the number of subcarriers is given in Fig. 8.8 for 100, 250 and 500 OFDM symbols. The probabilities of number of identified subcarriers for different SNR values in multipath fading channel are given in Fig. 8.9. The results are obtained for 250 OFDM symbols. Note that the total number of used

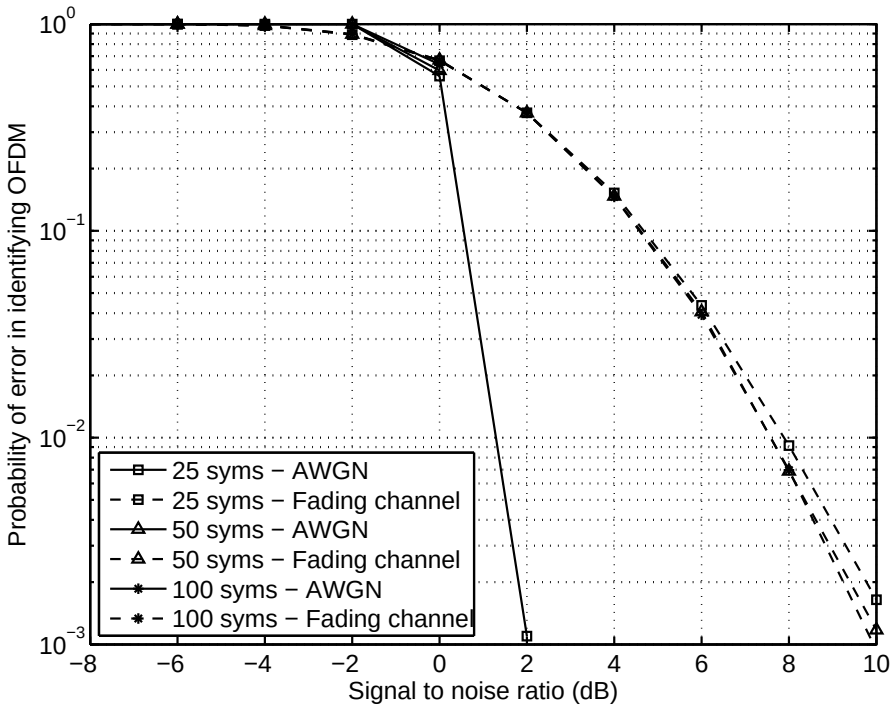

Figure 8.5 Probability of incorrect detection for OFDM signal for different number of symbols under AWGN and fading channels.

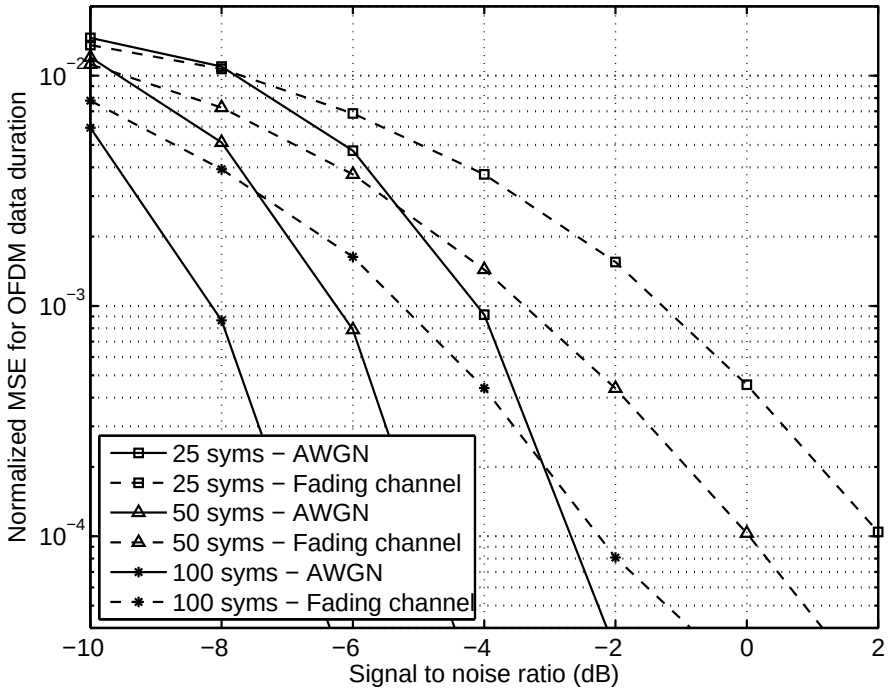

Figure 8.6 Normalized MSE of OFDM symbol duration as a function of SNR for different number of symbols under AWGN and fading channels.

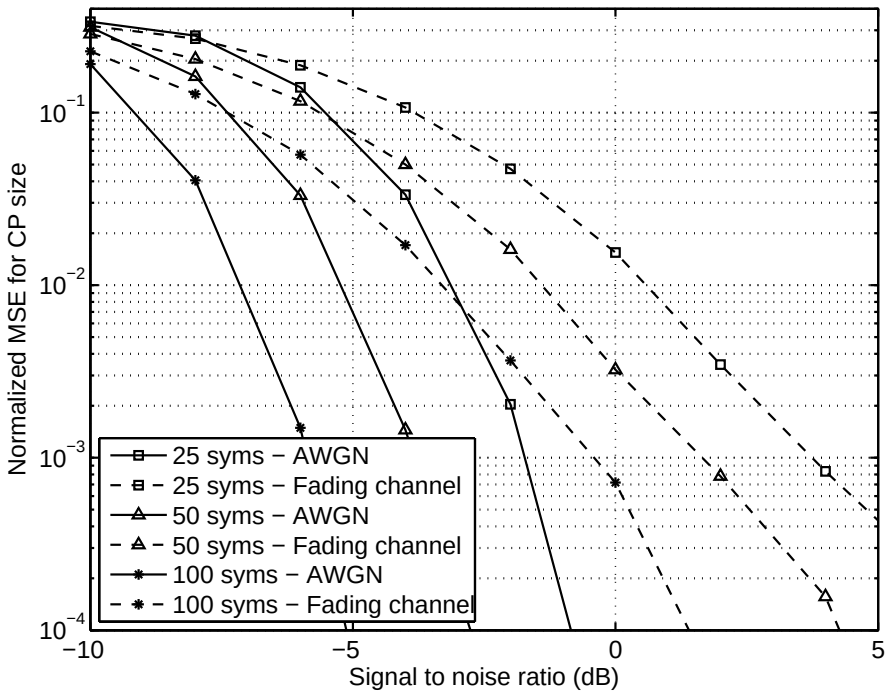

Figure 8.7 Normalized MSE of CP duration as a function of SNR for different number of symbols under AWGN and fading channels.

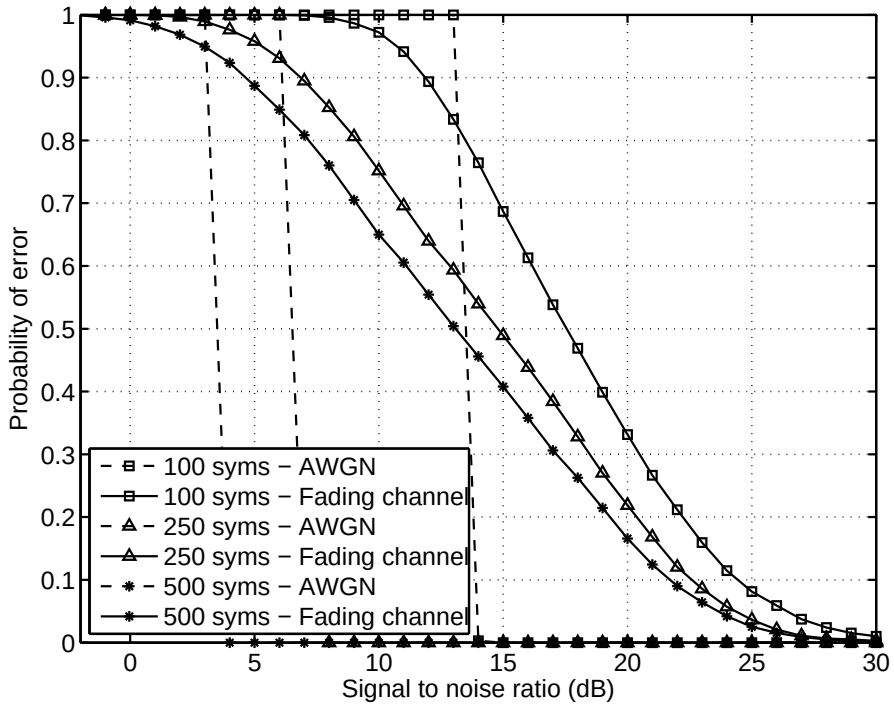

Figure 8.8 Probability of error for detecting number of active subcarriers for different number of symbols under AWGN and fading channels.

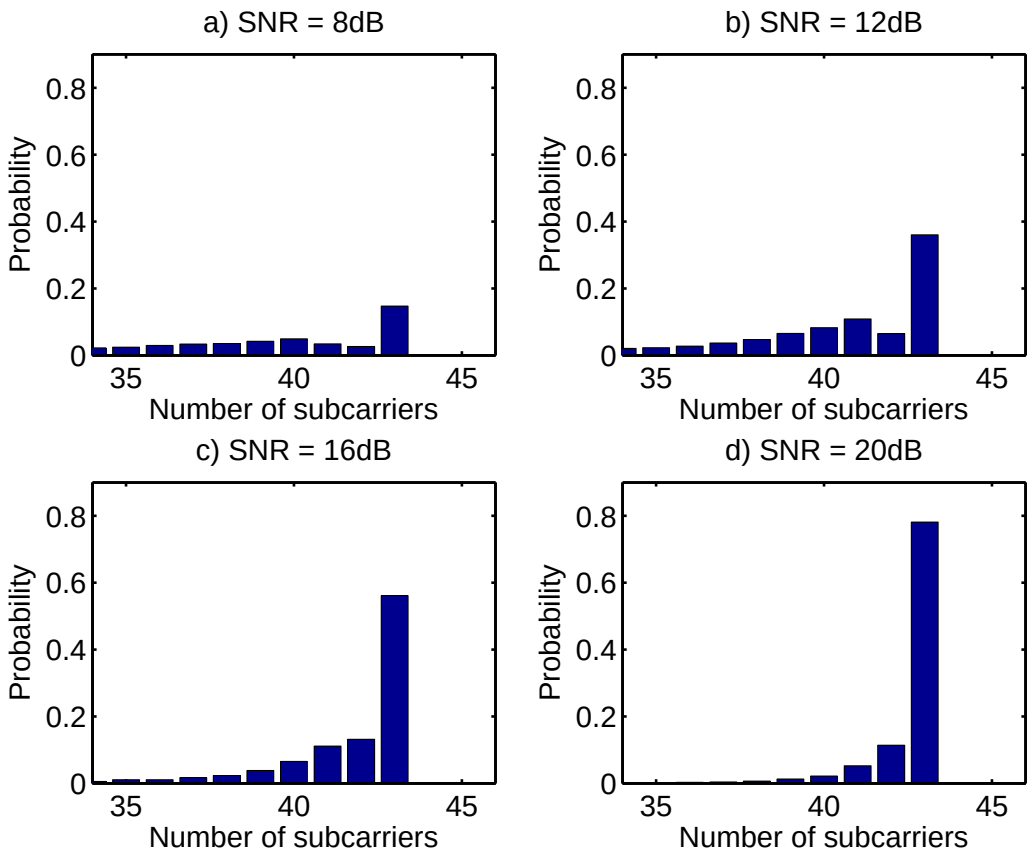

Figure 8.9 Histogram of number of detected subcarriers for different SNR values. The number of employed subcarriers is 44.

subcarriers is 44. The estimation of subcarriers is biased towards less number of subcarriers which can be explained by multipath fading of the channel. The performance of the subcarrier estimation algorithm under AWGN channel is found to be much better in the case of AWGN channel (not shown in figure). In the case of multipath fading, some subcarriers might be in deep fade and can be missed by the proposed algorithm.

While applying the modified ESPRIT algorithm, false alarms or miss detection can happen due to channel and noise. The former corresponds to identifying a deactivated subcarrier as active and latter means that an active subcarrier is missed by the algorithm. Fig. 8.10 shows the probability of errors for the subcarrier detection algorithm. Both false alarm and miss-detection are considered as errors.

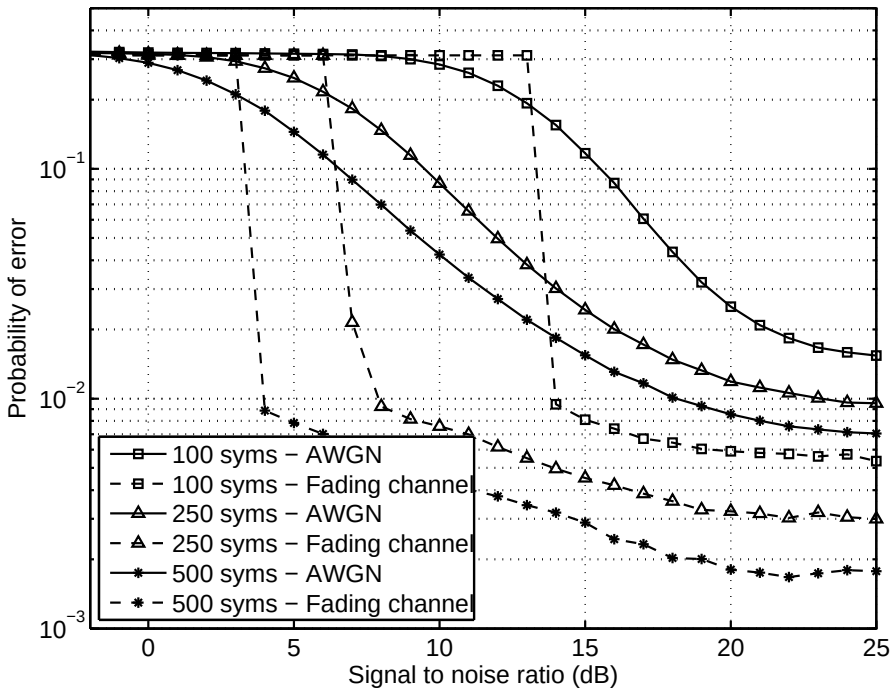

Figure 8.10 Probability of errors for proposed subcarrier detection algorithm. Errors include both false alarms and mis-detections of subcarriers.

8.5 Conclusion

It is shown in this chapter that most fundamental parameters of OFDM transmission can be blindly estimated and synchronization and demodulation is possible without any prior knowledge. Methods for identifying OFDM signals and their parameters are given. Furthermore, a method for identifying active subcarriers of an OFDM system is developed. This method is especially important for cognitive radio systems for reducing the signaling overhead that would otherwise be needed for transmitting spectrum shaping information. Simulation results show that proposed algorithms are capable of finding the transmission parameters under AWGN and multipath fading channels with only a limited amount of data.

CHAPTER 9

FEATURE SUPPRESSION FOR PHYSICAL-LAYER SECURITY IN OFDM SYSTEMS

9.1 Introduction

Security has always been an important requirement for military communication systems. With the increasing number of wireless devices and our dependence on these devices, security is becoming crucial for commercial systems as well. Bit-level security measures are commonly used in commercial and military applications for increasing security by encrypting data payloads. However, an eavesdropper can obtain the encrypted data and reverse engineer the encryption technique if synchronization is established to signal and data fields of the physical layer (PHY) data are identified. In order to achieve further security on top of encryption, the transmitted waveform can be altered according to an encryption technique. When this process is applied appropriately, eavesdroppers can not even obtain the transmitted signal in a meaningful way.

In orthogonal frequency division multiplexing (OFDM), linear convolution of the transmitted signal with the channel impulse response (CIR) is converted to circular convolution by cyclically extending the OFDM symbols. This way, transmitted data symbols can be recovered using a simple single-tap frequency domain equalizer. The redundancy introduced by the cyclic prefix (CP), however, can be used for detecting the transmission parameters [221, 226–229] as well as channel estimation [235, 239] and synchronization [240–242]. Hence, while having the aforementioned benefits, CP may be undesired for applications which require covertness. The periodicity introduced by the CP can be explored by undesired users to synchronize to transmitted signal. Note that the cyclic features in conventional OFDM systems are not suspended even when frequency hopping (FH) is used [243].

Various techniques are developed to achieve transmission-level security and covertness in OFDM systems. OFDM data symbols are embedded into a notched ultra wide band (UWB) noise signal in [244]. The aim is to design a spectrally undetectable system for building a network among

radars. However, sharp filters are required in the transmitter and receiver sides and there is a bit-error-rate (BER) gap (reliability gap) due to the added noise. UWB-OFDM is another method for achieving covertness thanks to its transmitted power which is below the noise level. Hence, UWB-OFDM can be used to facilitate covert and spectrally undetectable transmission. A random frequency jitter is applied to OFDM signals to mask OFDM signature in [243]. Time jitter can be used in frequency hopping OFDM (FH-OFDM) signals as well to remove the spectral lines at symbol and hopping periods [243]. In [245], CP and pilot tones are completely eliminated to suppress OFDM features. The inter-symbol interference (ISI) is removed using a decision feedback equalizer (DFE). However, the obvious disadvantage of such an approach is the increased complexity and loosing OFDM's advantage of handling multipath fading channel easily using CP. Pseudo-random sequences are used instead of preambles in [245] in order to facilitate time and frequency synchronization. A random frequency offset is added to each preamble to further mask the spectral lines. In addition to the aforementioned methods, power control, beamforming, and powerful channel coding can be used to obtain further PHY-layer security in any wireless system.

In this chapter, methods to prevent unwanted exploitation of the CP for eavesdropping to the transmitted signal, while maintaining the advantages of CP, are developed. This is achieved by suppressing the cyclic features of OFDM signals in order to 1) prevent identification of signaling parameters and 2) avoid undesired users to achieve synchronization to transmitted signal. Specifically, we propose to change the size of the CP size in a pseudo noise (PN) fashion and append random signals to some of the OFDM symbols to scramble the correlation peaks in time domain. These two methods prevent enemy detection of the transmitted signal even if an initial synchronization is achieved by undesired users.

The chapter is organized as follows. Section 9.2 explains the effects of short CP on the BER performance of the OFDM systems, followed by an overview of CP based (time and frequency) synchronization and parameter estimation algorithms in Section 9.3. The developed techniques are given in Section 9.4. Some numerical results are presented in Section 9.5 and conclusions are given in Section 9.6.

9.2 Effect of Cyclic Prefix on the BER

In order to remove the distortion due to multipath, the length of the CP should be larger than the maximum excess delay of the channel. Otherwise, previously transmitted OFDM symbol

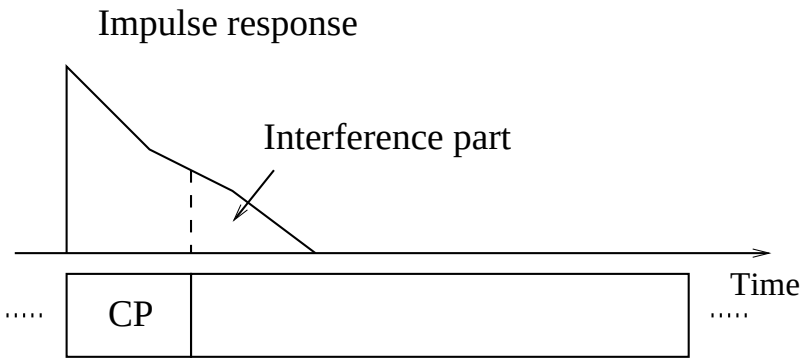

Figure 9.1 Illustration of inter-symbol interference due to multipath fading and short cyclic prefix size.

causes interference to the current OFDM symbol (see Fig. 9.1). This interference is called ISI and the performance degradation due to ISI is investigated in [76] and [44]. Assuming there is only post-cursors from the preceding symbol, signal-to-noise ratio (SNR) of the received signal at each subcarrier position can be written as

$$SNR(k) = \frac{1}{2} \frac{|H(k)|^2 N}{\sum_{l=N_G+1}^{L} |h_l|^2}, \tag{9.1}$$

where $H(k)$ is the channel frequency response (CFR) at kth subcarrier, N is the fast Fourier transform (FFT) size, L is the CIR length, and h_l is the lth tap of CIR. As can be seen in (9.1), the degradation depends on the ratio between the tail power of the CIR and total power of CIR. Unless equalization is used, short CP size causes performance degradation.

9.3 Blind Parameter Estimation and Synchronization

Various parameter estimation algorithms for OFDM systems are developed in literature. Methods for finding the OFDM symbol and CP duration are mostly based on exploitation of the cyclostationarity of OFDM signaling due to cyclic prefix extension [221, 226–229]. If cyclostationarity of the OFDM waveform is removed, *i.e.* cyclic features are suppressed, estimating parameters of OFDM signal becomes difficult and it can be prevented with proper system design.

The redundancy in the cyclic prefix of OFDM systems can also be exploited in order to obtain time and frequency synchronization once the symbol duration and CP size are estimated/known. Synchronization algorithms based on the maximum likelihood (ML) [240], minimum mean-square

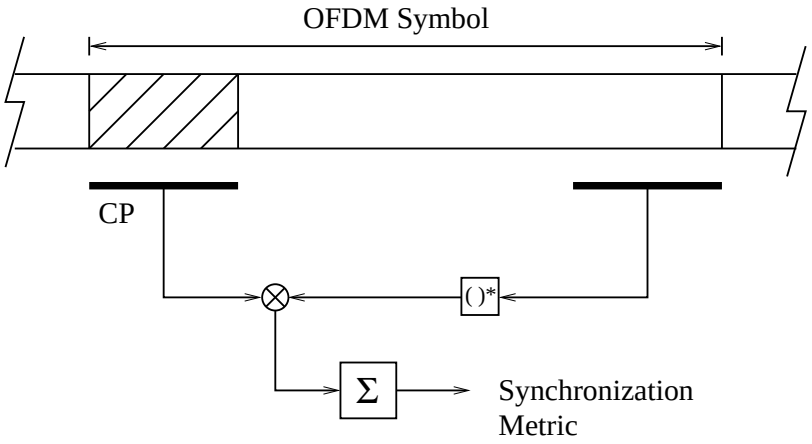

Figure 9.2 Illustration of cyclic prefix based maximum likelihood estimation.

error (MMSE) [241] and the maximum correlation (MC) [242] criteria can be used for this purpose. Moreover, it is possible to exploit the cyclostationarity for estimating channel state information [235].

The ML synchronization method is illustrated in Fig. 9.2 where only one OFDM symbol is shown. The synchronization metric obtained by one OFDM symbol can be written as

$$M(m) = \sum_{n=0}^{N_G-1} y(m-n)y^*(m-n+N_D), \tag{9.2}$$

where $y(n)$ is the received signal, N_G is the length of CP and N_D is the length of the useful data part. Using (9.2), the timing position can be found as

$$\hat{\theta} = \arg\max_m \{|M(m)|\}, \tag{9.3}$$

and frequency offset estimate is

$$\hat{\epsilon} = \frac{1}{2\pi}\angle M(\hat{\theta}). \tag{9.4}$$

In practical applications, extraction of the synchronization parameters by using the CP with only one OFDM symbol is very difficult if not impossible, since the CP is perturbed by multipath components and additive noise. Moreover, the presence of frequency offset decreases the correlation between the repeated parts. In order to overcome this problem, averaging over a number of OFDM symbols should be performed. Fig. 9.3 shows the noisy correlation outputs from different OFDM symbols and the resulting synchronization metric which is obtained by averaging these correlations. The results are obtained for an OFDM system with 64 subcarriers and 1/4 CP ratio. Please see

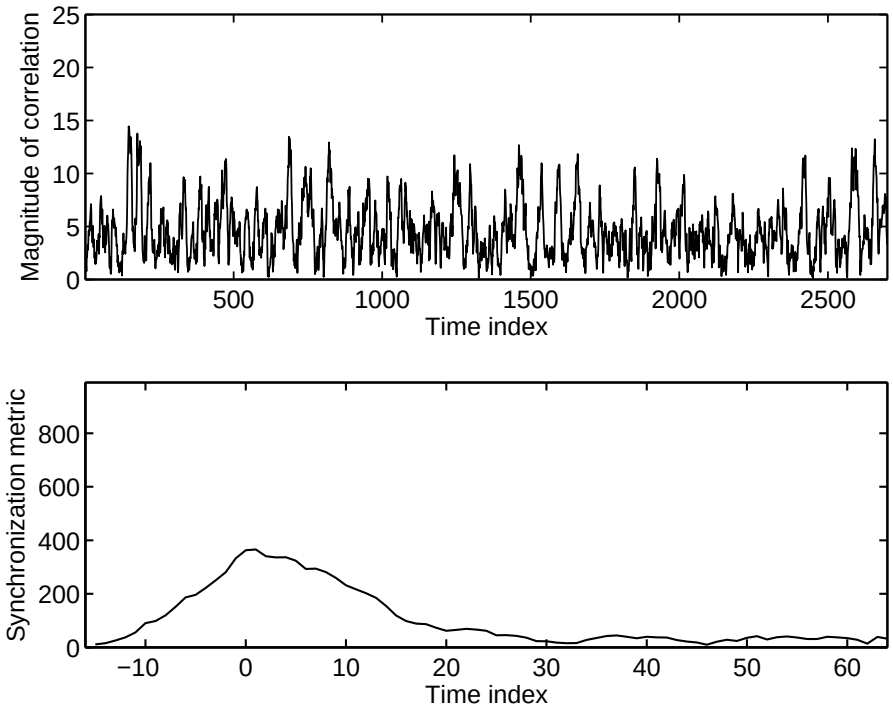

Figure 9.3 The correlations obtained by using the cyclic prefix and the resulting synchronization metric obtained by averaging.

Section 9.5 for more details on the considered system. As we can see, the instantaneous correlations are noisy and the resulting metric obtained by averaging has a peak around the correct timing point. As the number of available OFDM symbols increases, the estimates become more accurate. In the next section, we propose methods that prevent combining correlation information from different symbols and avoid synchronization by unwanted users.

9.4 Proposed Methods for Covert Transmission

As shown in the previous section, the periodicity introduced by usage of CP can be explored by undesired users to synchronize to and demodulate the transmitted signal. This problem leads us to find a technique which prevents enemy synchronization while maintaining the advantages of the CP. In the following, we propose new methods to prevent enemy exploitation of the CP for identification and synchronization purposes. These methods provide secure transmission, lower the requirements on coding by allowing CP usage, enable high data rate transmission and decrease the power consumption since equalizers are not required.

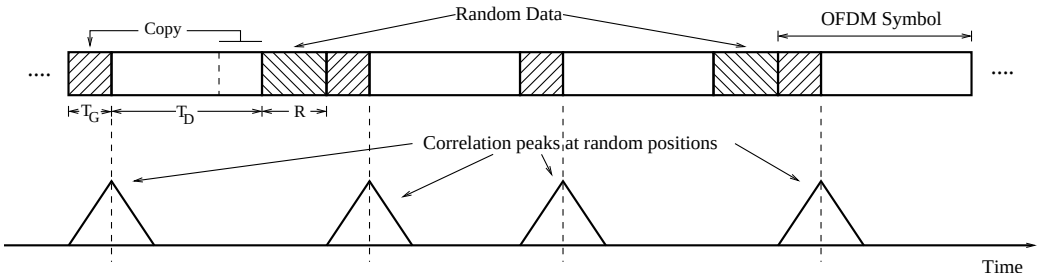

Figure 9.4 Illustration of the proposed transmission scheme. The resulting correlation peaks in the ideal case is shown as well.

9.4.1 Insertion of Random Signals

Averaging over different OFDM symbols can only be done if the length of each OFDM symbol is precisely known. We propose changing the length of OFDM symbols in a pseudo-random fashion by appending a totally random signal to some of the OFDM symbols. The resulting frame structure and correlation peaks in a noiseless static channel are illustrated in Fig. 9.4 where the length of CP is N_G, the length of the data is N_D, and the length of the appended random signal is R. Using this method, correlation peaks are scrambled in time (ref. Fig. 9.3). This prevents undesired users from using the CP for synchronization, since they can not combine the information from different symbols anymore. Note that even if an initial synchronization is obtained for the arriving frame, the receiver needs to know the exact start positions of individual OFDM symbols. This is only possible if the positions and length of the added random signals are known. The desired user, on the other hand, can extract the transmitted information since the pattern according to which the random signals are introduced is known. The proposed method prevents enemy from estimating the length of the CP and useful data by executive search method as well.

For synchronization, a PN-based preamble can be used as done in [245]. Since the transmitted signal is known only by the desired user, eavesdroppers can not synchronize to the transmitted signal. The desired users, however, can use the knowledge of scrambling pattern and the redundancy contained in the CP to obtain synchronization information by combining the correlation outputs from each OFDM symbol. Furthermore, synchronization information from the preamble and synchronization information from the CP can be combined using an appropriate method for increasing accuracy at the expense of increased numerical complexity.

The code sequence for prepending the random signal can be the same with the preamble sequence (if used) for decreasing signaling overhead. However, using the same sequence reduces the security

level and one might want to use different codes for this purpose. The sequence should be renewed and conveyed to receiver in a periodic fashion during transmission.

9.4.2 Adaptive Cyclic Prefix Size

The length of the CP is changed adaptively depending on the channel conditions. As it is shown in the previous section, insufficient CP causes performance degradation and not desired. On the other hand, it becomes easier for undesired users to synchronize to the transmitted signal with large CP sizes. Hence, the length of the CP should be just enough to prevent ISI. By changing the CP size, the total OFDM symbol duration is changed similar to the method given in Section 9.4.1. Therefore, undesired users can not achieve synchronization unless they know the duration of CP for each OFDM symbol. For decreasing the complexity and overhead, only a predefined set of CP sizes can be used.

Adaptive cyclic prefix method can be combined with channel coding and channel equalizer. The cyclic prefix does not have to be the same as the maximum excess delay of the channel; it can be smaller but not larger for security. If it is smaller, then the performance loss needs to be compensated by additional coding power or channel equalizers need to be used. In the limiting case, no CP is used and the ISI is compensated by using very high coding or channel equalizers as proposed in [245].

Adaptive cyclic prefix method requires the knowledge of the maximum excess delay of the wireless channel. Various algorithms are developed in literature for this purpose which uses CFR [128] or channel frequency correlation (CFC) [22]. Changing the length of the CP adaptively also provides efficient channel utilization since the overall CP time is minimized.

9.4.3 Possible Extensions

The followings are possible extensions that can be applied to increase effectiveness of the methods given in this section:

1. The size of the random signal inserted between OFDM symbols can be changed depending on a PN sequence. This provides extra scrambling of the correlation peaks.

2. For random data insertion, instead of using totally random signal, a known PN sequence can be used. The receiver can exploit the knowledge of used PN sequence for synchronization or channel estimation. This way, the bandwidth loss due to the transmission of the random signal can be reduced.

3. The FFT/IFFT sizes of each OFDM symbol can be changed based on a PN sequence. This provides two types of security by making synchronization and demodulation of received signal difficult for undesired users.

9.5 Numerical Results

Simulation results are obtained in order to show that the proposed methods remove cyclic features of OFDM signals. As for OFDM system, IEEE 802.11a based wireless local area network (WLAN) is used [10]. For this system, the transmission bandwidth is 20 MHz and number of subcarriers is 64, out of which 11 subcarriers are used as guard subcarriers and one as DC subcarrier. We use cyclic autocorrelation function (CAF) and cyclic spectral density (CSD) [183] for observing the cyclic features contained in the OFDM waveform. The CAF for 100 OFDM symbols in a noiseless scenario is given in Fig. 9.5. Fig. 9.6 shows the CSD for the same signal. These two figures clearly show the cyclic features that a conventional OFDM system exhibits. As explained in the text of the chapter, these features could be used for extracting the transmission parameters and for synchronization by undesired users.

The method given in Section 9.4.1 is realized by inserting random sequences of length 4, 8, and 12 samples or by not inserting any data. Each four case is assumed to have equal probability. The CAF for the transmitted signal with random signal insertion is given in Fig. 9.7. The cyclic frequencies are clearly removed from the correlation function. CSD is not presented because of space limitation. Please note that this information can be obtained from CAF.

Fig. 9.8 shows the CAF for the case where different CP sizes are used for each OFDM system. Four different CP sizes containing 8, 12, 16 and 20 samples are used randomly. The cyclic features are somewhat removed, but we can see that this method is not as effective as previous one in terms of removing cyclic features.

9.6 Conclusion

We have proposed new techniques for increasing the covertness and security of OFDM-based communication systems by altering the OFDM waveform. Variable cyclic prefix and random sequence addition to OFDM systems in a (pseudo) random fashion are investigated. Using these methods, synchronization to an OFDM system without the knowledge of used sequences is not possible if

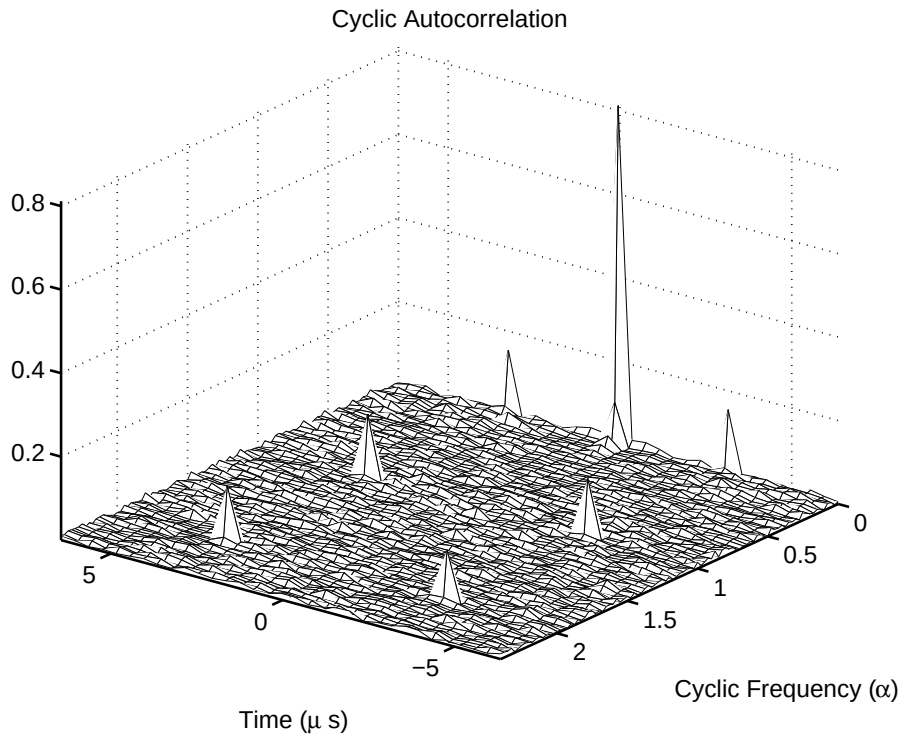

Figure 9.5 Cyclic auto correlation function (CAF) of a conventional OFDM system.

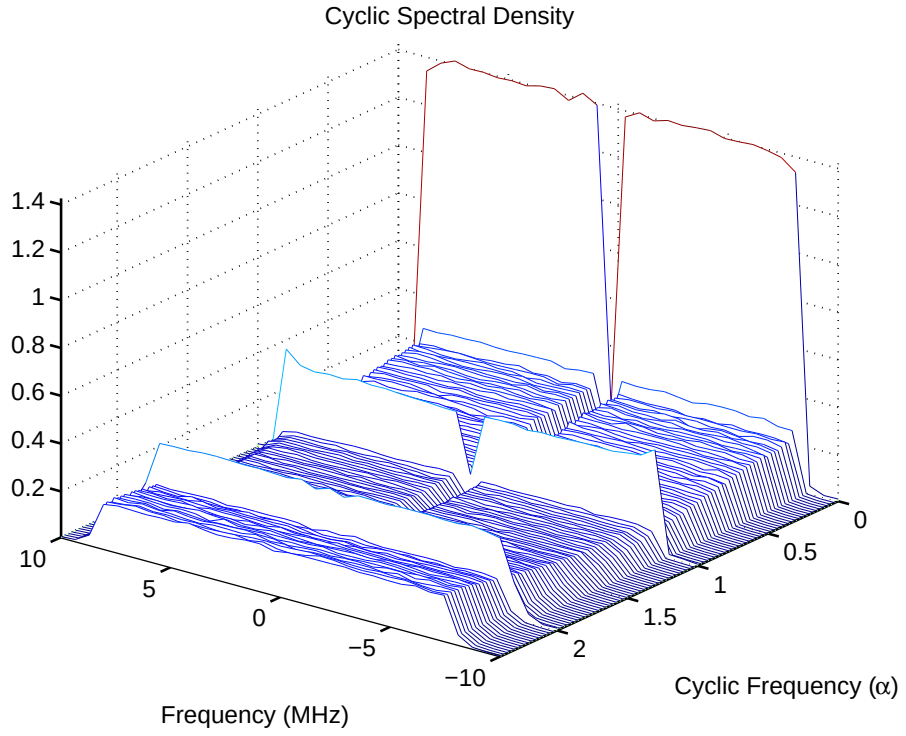

Figure 9.6 Cyclic frequency density (CFD) of a conventional OFDM system.

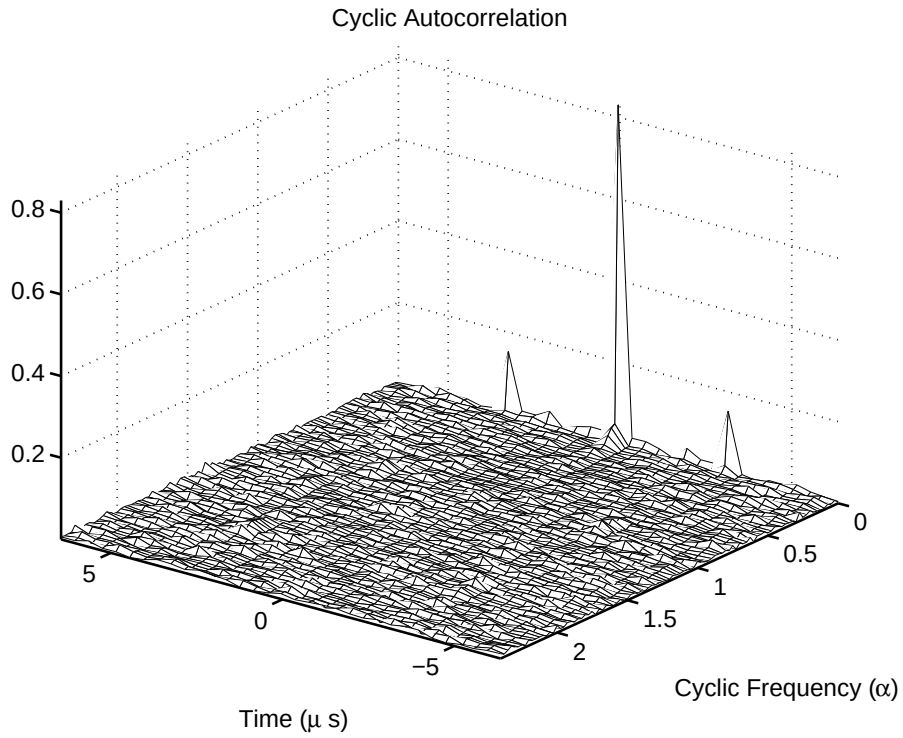

Figure 9.7 Cyclic auto correlation function (CAF) obtained by inserting random data with different lengths between OFDM symbols.

preambles and pilot tones are not used. Furthermore, the proposed methods suppress the cyclic features of OFDM waveform making blind estimation of transmission parameters difficult.

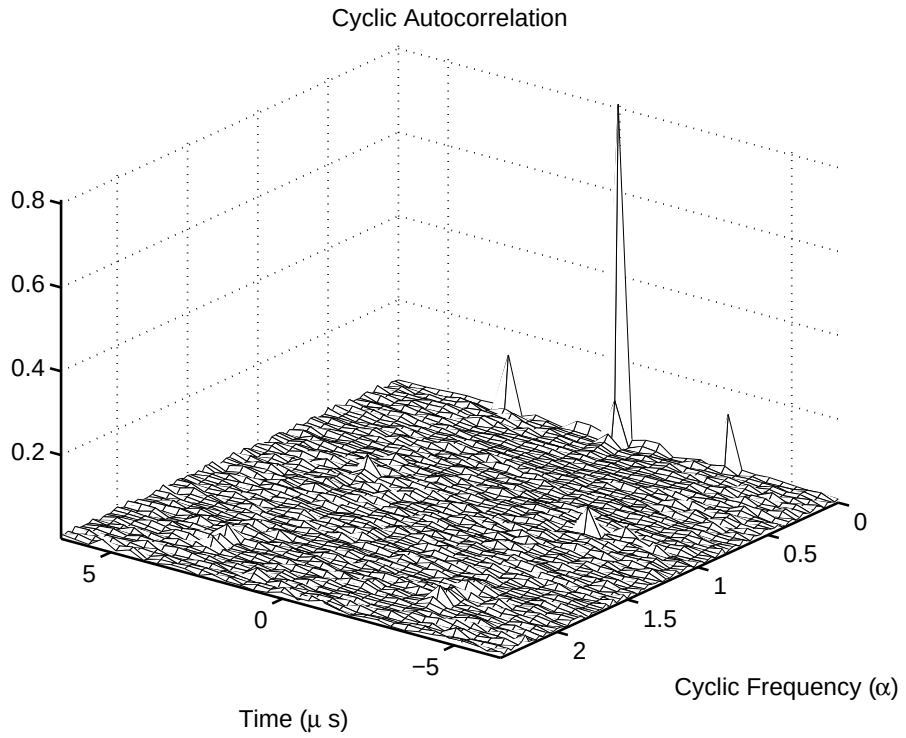

Figure 9.8 Cyclic auto correlation function (CAF) obtained by using different cyclic prefix lengths for each OFDM symbol.

CHAPTER 10

CONCLUSION AND FUTURE WORK

In this dissertation, we have addressed a number of transceiver design issues in multicarrier based cognitive radio. Adaptation and parameter estimation such as Doppler spread, delay spread, and noise variance estimations are considered in different chapters. Application of multicarrier techniques to cognitive radio is discussed. Furthermore, multi-dimensional spectrum space is studied and sensing methods for cognitive radios are developed. Some of the more significant issues that were reported (to our best knowledge) the first time in the literature are as follows:

- Effect of timing errors on delay spread estimation is investigated and methods robust to these errors are developed.
- White noise assumption is removed and variation of the noise power across OFDM sub-carriers as well as across OFDM symbols is considered.
- A detailed survey of spectrum sensing methods for cognitive radio applications is prepared.
- High-resolution frequency estimation techniques are used to identify active and idle subcarriers.
- OFDM waveform is altered by changing only the software to remove features and achieve covertness.

Below, we first present a list of specific contributions in different chapters of the dissertation. Then, possible extensions of the work done are discussed.

10.1 List of Specific Contributions

- Delay spread estimation
  - Synchronization errors are shown to bias the performance of estimators based on the channel correlation.

  - The bias due to timing errors is removed by obtaining the power delay profile (PDP) and root-mean-squared (RMS) delay spread using magnitude of the channel estimates.
  - The Cramér-Rao lower bound (CRLB) for estimation of RMS delay spread is derived and performances of the proposed algorithms are compared against this theoretical limit.

- Doppler spread estimation
  - Doppler spread is estimated using time domain channel estimates instead of frequency domain channel response. By using the CIR, the effect of noise and inter-carrier interference (ICI) on the frequency-domain channel is reduced.

- Noise plus interference power (SNR) estimation
  - A new noise variance estimation algorithm which uses MMSE filtering technique to estimate the noise power is developed. This method removes the common assumption of white Gaussian noise and considers colored noise.
  - The MMSE filter coefficients are obtained from the mean-squared-error (MSE) expression, which can be calculated using noise statistics.

- Spectrum sensing for dynamic spectrum access
  - A detailed survey of spectrum sensing methodologies for cognitive radio is presented.
  - Multi-dimensional spectrum sensing concept is explained and challenges this new concept brings about for cognitive radio are discussed.
  - Partial match-filtering (PMF) method is introduced where primary users are identified by matching the features extracted from received signal to the *a priori* information about primary users' transmission characteristics.
  - Energy detector based PMF method is developed and presented as a case study for PMF technique.

- OFDM signal identification and feature suppression
  - ML and suboptimal ML algorithms are developed for estimating OFDM symbol duration and CP size.

– A method for classifying unknown signals as OFDM or single-carrier is developed. This method is based on the likelihood function of the received signal evaluated at ML estimates of signal parameters.

– A new method based on estimation of signal parameters via rotational invariance techniques (ESPRIT) is developed to estimate the number and frequencies of subcarriers of identified OFDM signal.

– Transmission-level techniques for suppressing physical-layer features of OFDM waveform are proposed. Hence, a covert, secure, and reliable transmission based on OFDM technique can be achieved.

10.2 Final Comments and Future Work

Cognitive radio has recently become an exciting and promising concept. In parallel to this, OFDM technique has been used in many wireless systems and proven as a reliable and effective transmission method. OFDM can be used in realizing cognitive radio concept because of its inherent capabilities that are discussed in detail in Chapter 2. By employing OFDM transmission in cognitive radio systems; adaptive, aware, and flexible systems that can interoperate with current technologies can be realized. The adoption of OFDM in cognitive radios may happen in two ways: current wireless technologies might evolve to have more and more cognitive features or new systems might be developed that has full cognitive features. In either case, we foresee that OFDM will be the dominant physical layer technology for cognitive radio.

In this dissertation, we have discussed some challenges and developed methods for addressing those. Specifically, estimation algorithms for achieving awareness in cognitive radio are proposed. This awareness capability can be used for adaptation of OFDM systems and opportunistic spectrum access.

We have identified some of the open research areas for OFDM based cognitive radio systems in Chapter 2. These topics include spectrum shaping, effective pruning algorithm design, designing robust synchronization methods for cognitive radio applications, and reducing mutual interference due to power leakage to unused subcarriers. In addition to these general areas, the following extensions to the work in this dissertation are possible.

Partial match filtering: We have studied energy detector based spectrum sensing as a case study for partial match-filtering (PMF) algorithm developed in Chapter 7. The PMF framework can be used with different feature extraction algorithms as well, such as cyclostationarity-based or waveform-based sensing methods. Application of PMF with different feature extraction methods and performance comparison of these methods can be undertaken as a future research.

Interoperable cognitive radio: In order for cognitive radio to interoperate with existing devices, it needs to have the capability to generate all possible modulations. One method is to download the waveform from a centralized location. However, the file sizes can be very large and a total reconfiguration of physical layer may be necessary. Cognitive radio can be designed to use only OFDM waveform. In such a case, instead of whole waveform, cognitive radio can download (or even store) only the OFDM parameters such as CP size, FFT size, available symbol mappings and so on. Hence, the complexity of the reconfiguration is minimized and only a limited storage is necessary to store different waveforms. For identification of OFDM systems, methods developed in Chapter 8 can be used.

Covert OFDM system design: Analysis of a complete system which uses PN sequences for removing the OFDM cyclic features can be studied. Investigation of exploiting the PN sequences for channel estimation and synchronization can be done.

REFERENCES

[1] P. Dent, G. Bottomley, and T. Croft, "Jakes fading model revisited," *IEE Electron. Lett.*, vol. 29, no. 13, pp. 1162–1163, June 1993.

[2] S. Yarkan and H. Arslan, "Binary time series approach to spectrum prediction for cognitive radio," in *Proc. IEEE Veh. Technol. Conf.*, Baltimore, Maryland, USA, Sept./Oct. 2007.

[3] I. Mitola, J. and J. Maguire, G. Q., "Cognitive radio: making software radios more personal," *IEEE Personal Commun. Mag.*, vol. 6, no. 4, pp. 13–18, Aug. 1999.

[4] F. K. Jondral, "Software-defined radio–basics and evolution to cognitive radio," *Eurasip Journal on Wireless Comm. and Networking*, vol. 3, pp. 275–283, 2005.

[5] J. O. Neel, "Analysis and design of cognitive radio networks and distributed radio resource management algorithms," Ph.D. dissertation, Virginia Polytechnic Institute and State University, Sept. 2006.

[6] *Radio broadcasting systems; Digital Audio Broadcasting (DAB) to mobile, portable and fixed receivers*, ETSI – European Telecommunications Standards Institute Std. EN 300 401, Rev. 1.3.3, May 2001.

[7] *Digital Video Broadcasting (DVB); Framing structure, channel coding and modulation for digital terrestrial television*, ETSI – European Telecommunications Standards Institute Std. EN 300 744, Rev. 1.4.1, Jan. 2001.

[8] *Asymmetric Digital Subscriber Line (ADSL)*, ANSI – American National Standards Institute Std. T1.413, 1995.

[9] *Broadband Radio Access Networks (BRAN); HIPERLAN Type 2; Physical (PHY) layer*, ETSI – European Telecommunications Standards Institute Std. TS 101 475, Rev. 1.3.1, Dec. 2001.

[10] *Local and metropolitan area networks - specific requirements. Part 11: wireless LAN Medium Access Control (MAC) and Physical Layer (PHY) specifications: high-speed physical layer in the 5 GHz band*, The Institute of Electrical and Electronics Engineering, Inc. Std. IEEE 802.11a, Sept. 1999.

[11] *Broadband Mobile Access Communication System (HiSWANa)*, ARIB – Association of Radio Industries and Businesses Std. H14.11.27, Rev. 2.0, Nov. 2002.

[12] *IEEE Standard for Local and Metropolitan area networks Part 16: Air Interface for Fixed Broadband Wireless Access Systems*, The Institute of Electrical and Electronics Engineering, Inc. Std. IEEE 802.16-2004, 2004.

[13] "IEEE 802.15 WPAN high rate alternative PHY task group 3a (tg3a) website." [Online]. Available: http://www.ieee802.org/15/pub/TG3a.html.

[14] M. Sternad, T. Ottosson, A. Ahlén, and A. Svensson, "Attaining both coverage and high spectral efficiency with adaptive OFDM downlinks," in *Proc. IEEE Veh. Technol. Conf.*, Orlando, Florida, USA, Oct. 2003.

[15] *Standard for Wireless Regional Area Networks (WRAN) - Specific requirements - Part 22: Cognitive Wireless RAN Medium Access Control (MAC) and Physical Layer (PHY) Specifications: Policies and procedures for operation in the TV Bands*, The Institute of Electrical and Electronics Engineering, Inc. Std. IEEE 802.22.

[16] B. A. Fette, *Cognitive Radio Technology*. Newnes, 2006.

[17] H. Arslan and T. Yücek, *Adaptation Techniques in Wireless Multimedia Networks*. Nova Science Publishers, 2006, ch. Adaptation of Wireless Mobile Multi-carrier Systems.

[18] H. Mahmoud, T. Yücek, and H. Arslan, *Cognitive Radio, Software Defined Radio, and Adaptive Wireless Systems*. Springer, 2007, ch. OFDM for Cognitive Radio: Merits and Challenges.

[19] ——, "OFDM for cognitive radio: Merits and challenges," *submitted to IEEE Wireless Commun. Mag.*, 2007.

[20] H. Arslan and T. Yücek, "Delay spread estimation for wireless communication systems," in *Proc. IEEE Symposium on Computers and Commun.*, Antalya, Turkey, June/July 2003, pp. 282–287.

[21] ——, "Estimation of frequency selectivity for OFDM based new generation wireless communication systems," in *Proc. World Wireless Congress*, San Francisco, CA, USA, May 2003.

[22] T. Yücek and H. Arslan, "Delay spread and time dispersion estimation for adaptive OFDM systems," in *Proc. IEEE Wireless Commun. and Networking Conf.*, Las Vegas, Nevada, USA, Apr. 2006.

[23] ——, "Dispersion and delay spread estimation for adaptive OFDM systems," *submitted to IEEE Trans. Veh. Technol.*, 2006.

[24] T. Yücek, R. A. Tannious, and H. Arslan, "Doppler spread estimation for wireless OFDM systems," in *Proc. IEEE Sarnoff Symposium*, Princeton, New Jersey, USA, Apr. 2005, pp. 233–236.

[25] T. Yücek and H. Arslan, "Noise plus interference power estimation in adaptive OFDM systems," in *Proc. IEEE Veh. Technol. Conf.*, vol. 2, Stockholm, Sweden, May 2005, pp. 1278–1282.

[26] ——, "MMSE noise power and SNR estimation for OFDM systems," in *Proc. IEEE Sarnoff Symposium*, Princeton, New Jersey, USA, Mar. 2006.

[27] ——, "MMSE noise plus interference power estimation in adaptive OFDM systems," *IEEE Trans. Veh. Technol.*, 2007.

[28] ——, "Noise plus interference power estimation method for OFDM systems," U.S. U.S. Provisional Patent Application USF Ref. No. 05A011PR, 2005.

[29] H. Arslan and T. Yücek, *Cognitive Radio, Software Defined Radio, and Adaptive Wireless Systems*. Springer, 2007, ch. Spectrum Sensing for Cognitive Radio Applications.

[30] T. Yücek and H. Arslan, "A survey of spectrum sensing algorithms for cognitive radio applications," *submitted to IEEE Communications Surveys and Tutorials*, 2007.

[31] ——, "Spectrum characterization for opportunistic cognitive radio systems," in *Proc. IEEE Military Commun. Conf.*, Washington, D.C., USA, Oct. 2006, pp. 1–6.

[32] ——, "Spectrum sensing for cognitive radio using partial match filtering," *submitted to EURASIP Journal on Wireless Communications and Networking*, 2007.

[33] ——, "A method for spectrum sensing via radio identification," U.S. U.S. Provisional Patent Application, 2007.

[34] ——, "OFDM signal identification and transmission parameter estimation for cognitive radio applications," in *Proc. IEEE Global Telecomm. Conf. (Globecom)*, Washington, D.C., USA, Nov. 2007.

[35] ——, "OFDM signal identification and transmission parameter estimation for cognitive radio applications," *submitted to IEEE Trans. Wireless Commun.*, 2007.

[36] ——, "Feature suppression for physical-layer security in OFDM systems," in *submitted to Proc. IEEE Military Commun. Conf.*, 2007.

[37] ——, "Covert OFDM transmission using cyclic prefix," U.S. Patent application US2006/0 050 626, 2004.

[38] F. E. Retnasothie, M. K. Ozdemir, T. Yücek, J. Zhang, H. Celebi, and R. Muththaiah, "Wireless IPTV over WiMAX: Challenges and applications," in *Proc. IEEE Wamicon (invited paper)*, Clearwater, FL, Dec. 2006.

[39] T. Yücek, M. K. Ozdemir, H. Arslan, and F. E. Retnasothie, "A comparative study of initial downlink channel estimation algorithms for mobile WiMAX," in *Proc. IEEE Mobile WiMAX Symposium*, Orlando, Florida, USA, Mar. 2007, pp. 32–37.

[40] T. Yücek and H. Arslan, "Carrier frequency offset compensation with successive cancellation in uplink OFDMA systems," in *Proc. IEEE Veh. Technol. Conf.*, Montreal, Quebec French, Canada, Sept. 2006.

[41] ——, "Carrier frequency offset compensation with successive cancellation in uplink OFDMA systems," *IEEE Trans. Wireless Commun.*, 2007, to appear.

[42] S. K. Mitra, *Digital Signal Processing: A Computer-Based Approach*, 2nd ed. New York, NY, USA: McGraw-Hill, 2000.

[43] D. Huang and K. Letaief, "Carrier frequency offset estimation for OFDM systems using subcarriers," *IEEE Trans. Commun.*, vol. 54, no. 5, pp. 813–823, May 2006.

[44] W. Henkel, G. Taubock, P. Odling, P. Borjesson, and N. Petersson, "The cyclic prefix of OFDM/DMT - an analysis," in *International Zurich Seminar on Broadband Communications. Access, Transmission, Networking.*, Zurich, Switzerland, Feb. 2002, pp. 1–3.

[45] F. Tufvesson, "Design of wireless communication systems – issues on synchronization, channel estimation and multi-carrier systems," Ph.D. dissertation, Lund University, Aug. 2000.

[46] P. H. Moose, "A technique for orthogonal frequency division multiplexing frequency offset correction," *IEEE Trans. Commun.*, vol. 42, no. 10, pp. 2908–2914, Oct. 1994.

[47] P. Robertson and S. Kaiser, "The effect of Doppler spreads in OFDM(A) mobile radio systems," in *Proc. IEEE Veh. Technol. Conf.*, vol. 1, Amsterdam, The Netherlands, Sept. 1999, pp. 329–333.

[48] D. T. Harvatin and R. E. Ziemer, "Orthogonal frequency division multiplexing performance in delay and Doppler spread channels," in *Proc. IEEE Veh. Technol. Conf.*, vol. 3, no. 47, Phoenix, Arizona, USA, May 1997, pp. 1644–1647.

[49] A. Demir, A. Mehrotra, and J. Roychowdhury, "Phase noise in oscillators: A unifying theory and numerical methods for characterization," *IEEE Trans. Circuits Syst. IFundamental Theory and Applications*, vol. 47, no. 5, pp. 655–674, 2000.

[50] A. G. Armada, "Understanding the effects of phase noise in orthogonal frequency division multiplexing (OFDM)," *IEEE Trans. Broadcast.*, vol. 47, no. 2, pp. 153–159, June 2002.

[51] T. Pollet, M. Van Bladel, and M. Moeneclaey, "BER sensitivity of OFDM systems to carrier frequency offset and Wiener phase noise," *IEEE Trans. Commun.*, vol. 43, no. 234, pp. 191–193, Feb./Mar./Apr. 1995.

[52] K. Sathananthan and C. Tellambura, "Performance analysis of an OFDM system with carrier frequency offset and phase noise," in *Proc. IEEE Veh. Technol. Conf.*, vol. 4, Atlantic City, New Jersey, USA, Oct. 2001, pp. 2329–2332.

[53] L. Piazzo and P. Mandarini, "Analysis of phase noise effects in OFDM modems," *IEEE Trans. Commun.*, vol. 50, no. 10, pp. 1696–1705, Oct. 2002.

[54] E. P. Lawrey, "Adaptive techniques for multiuser OFDM," Ph.D. dissertation, James Cook University, Dec. 2001.

[55] T. May and H. Rohling, "Reducing the peak-to-average power ratio in OFDM radio transmission systems," in *Proc. IEEE Veh. Technol. Conf.*, vol. 3, Ottawa, Ont., Canada, May 1998, pp. 2474–2478.

[56] S. Muller and J. Huber, "A comparison of peak power reduction schemes for OFDM," in *Proc. IEEE Global Telecomm. Conf. (Globecom)*, vol. 1, Phoenix, Arizona, USA, Nov. 1997, pp. 1–5.

[57] H. Ochiai and H. Imai, "On the distribution of the peak-to-average power ratio in OFDM signals," *IEEE Trans. Commun.*, vol. 49, no. 2, Feb. 2001.

[58] S. Han and J. Lee, "An overview of peak-to-average power ratio reduction techniques for multicarrier transmission," *IEEE Wireless Commun. Mag.*, vol. 12, no. 2, pp. 56–65, Apr. 2005.

[59] H. Ochiai and H. Imai, "Performance of the deliberate clipping with adaptive symbol selection for strictly band-limited OFDM systems," *IEEE J. Select. Areas Commun.*, vol. 18, no. 11, pp. 2270–2277, Nov. 2000.

[60] P. Van Eetvelt, G. Wade, and M. Tomlinson, "Peak to average power reduction for OFDM schemes by selective scrambling," *IEE Electron. Lett.*, vol. 32, no. 21, pp. 1963–1964, Oct. 1996.

[61] A. Jones, T. Wilkinson, and S. Barton, "Block coding scheme for reduction of peak to mean envelope power ratio of multicarrier transmission schemes," *IEE Electron. Lett.*, vol. 30, no. 25, pp. 2098–2099, Dec. 1994.

[62] E. Lawrey and C. Kikkert, "Peak to average power ratio reduction of OFDM signals using peak reduction carriers," in *Signal Processing and Its Applications, 1999. ISSPA '99. Proceedings of the Fifth International Symposium on*, vol. 2, Brisbane, Qld., Australia, Aug. 1999, pp. 737–740.

[63] S. Haykin, "Cognitive radio: brain-empowered wireless communications," *IEEE J. Select. Areas Commun.*, vol. 3, no. 2, pp. 201–220, Feb. 2005.

[64] M. Uhm, "Making the adaptivity of SDR and cognitive radio affordable, going beyond flexibility to adaptivity in FPGAs." *Xcell DSP Magazine*, pp. 25–27, May 2006.

[65] Q. Zhang, F. Hoeksema, A. Kokkeler, and G. Smit, *Mobile Multimedia: Communication Engineering Perspective*. Nova Science Publishers, 2006, ch. Towards Cognitive Radio For Emergency Networks.

[66] M. Ahmed, H. Yanikomeroglu, and S. Mahmoud, "Fairness enhancement of link adaptation techniques in wireless access networks," in *Proc. IEEE Veh. Technol. Conf.*, vol. 3, Oct. 2003, pp. 1554–1557.

[67] M. Ahmed, H. Yanikomeroglu, D. Falconer, and S. Mahmoud, "Performance enhancement of joint adaptive modulation, coding and power control using cochannel-interferer assistance and channel reallocation," in *Proc. IEEE Wireless Commun. and Networking Conf.*, vol. 1, May 2003, pp. 306–310.

[68] T. Keller and L. Hanzo, "Adaptive modulation techiniques for duplex OFDM transmission," *IEEE Trans. Veh. Technol.*, vol. 49, no. 5, pp. 1893–1906, Sept. 2000.

[69] S. B. Reddy, T. Yücek, and H. Arslan, "An efficient blind modulation detection algorithm for adaptive OFDM systems," in *Proc. IEEE Veh. Technol. Conf.*, Orlando, Florida, USA, Oct. 2003.

[70] T. Yücek and H. Arslan, "A novel sub-optimum maximum-likelihood modulation classification algorithm for adaptive OFDM systems," in *Proc. IEEE Wireless Commun. and Networking Conf.*, Atlanta, Georgia, USA, Mar. 2004.

[71] S. Anderson, H. Dam, U. Forssen, J. Karlsson, F. Kronestedt, S. Mazur, and K.J. Molnar, "Adaptive antennas for GSM and TDMA systems," *IEEE Personal Commun. Mag.*, vol. 6, pp. 74–86, June 1999.

[72] L. M. Tuan, P. V. Su, J. Kim, and G. Yoon, "A new RLS-based adaptive beamforming algorithm for smart antennas applied to an OFDM system," in *Proc. Int. Conf. on Microwave and Millimeter Wave Technology*, Aug. 2002.

[73] E. Telatar, "Capacity of multiantenna Gaussian channels," AT&T Bell Laboratories, Tech. Rep., June 1995.

[74] G. J. Foschini and M. J. Gans, "On limits of wireless communications in a fading environment when using multiple antennas," *Wireless Personal Commun.*, vol. 6, no. 3, pp. 311–335, Mar. 1998.

[75] S. Catreux, V. Erceg, D. Gesbert, and J. Heath, R.W., "Adaptive modulation and MIMO coding for broadband wireless data networks," *IEEE Commun. Mag.*, vol. 40, no. 6, pp. 108–115, 2002.

[76] S. Celebi, "Interblock interference (IBI) and time of reference (TOR) computation in OFDM systems," *IEEE Trans. Commun.*, vol. 49, no. 11, pp. 1895–1900, Nov. 2001.

[77] Z.-Y. Zhang and L.-F. Lai, "A novel OFDM transmission scheme with length-adaptive cyclic prefix," *Journal of Zhejing University Science*, vol. 5, no. 11, pp. 1336–1342, 2004.

[78] S. Lei and V. Lau, "Adaptive interleaving for OFDM in TDD systems," *IEE Proc. Commun.*, vol. 48, no. 12, pp. 77–80, Apr. 2001.

[79] ——, "Performance analysis of adaptive interleaving for OFDM systems," *IEEE Trans. Veh. Technol.*, vol. 51, no. 3, pp. 435–444, May 2002.

[80] H. Steendam and M. Moeneclaey, "Analysis and optimization of the performance of OFDM on frequency-selective time-selective fading channels," *IEEE Trans. Commun.*, vol. 47, no. 12, pp. 1811–1819, Dec. 1999.

[81] F. Tufvesson and T. Maseng, *Multiaccess, mobility and teletraffic - advances in wireless networks*. Dordrecht, The Netherlands: Kluwer Academic Publishers, 1998, ch. Optimization of sub-channel bandwidth for mobile OFDM systems, pp. 103–114.

[82] H. Yaghoobi, "Scalable OFDMA physical layer in IEEE 802.16 WirelessMAN," *Intel Technology Journal*, vol. 8, no. 3, pp. 201–212, Aug. 2004.

[83] Y. Li, "Pilot-symbol-aided channel estimation for OFDM in wireless systems," *IEEE Trans. Veh. Technol.*, vol. 49, no. 4, pp. 1207–1215, July 2000.

[84] A. Dowler, A. Doufexi, and A. Nix, "Performance evaluation of channel estimation techniques for a mobile fourth generation wide area OFDM system," in *Proc. IEEE Veh. Technol. Conf.*, vol. 4, Vancouver, British Columbia, Canada, Sept. 2002, pp. 2036–2040.

[85] A. Dowler and A. Nix, "Performance evaluation of channel estimation techniques in a multiple antenna OFDM system," in *Proc. IEEE Veh. Technol. Conf.*, vol. 2, Orlando, Florida, USA, Oct. 2003, pp. 1214–1218.

[86] C. Hou, S. Song, , and D. Cao, "Channel estimation for adaptive OFDM system and effects of estimation error on system performance," in *Proc. IEEE Int. Workshop on Mobile and Wireless Commun. Network*, vol. 1, Stockholm, Sweden, Sept. 2002, pp. 200–204.

[87] X. Wang and K. J. R. Liu, "OFDM channel estimation based on time-frequency polynomial model of fading multipath channel," in *Proc. IEEE Veh. Technol. Conf.*, vol. 1, Atlantic City, New Jersey, USA, Oct. 2001, pp. 460–464.

[88] O. Simeone and U. Spagnolini, "Adaptive pilot pattern for OFDM systems," in *Proc. IEEE Int. Conf. Commun.*, vol. 2, Paris, France, June 2004, pp. 978–982.

[89] P. Robertson and S. Kaiser, "Analysis of the loss of orthogonality through Doppler spread in OFDM systems," in *Proc. IEEE Global Telecomm. Conf. (Globecom)*, vol. 1B, Rio de Janeireo, Brazil, 1999, pp. 701–706.

[90] J. Armstrong, P. M. Grant, and G. Povey, "Polynomial cancellation coding of OFDM to reduce intercarrier interference due to Doppler spread," in *Proc. IEEE Global Telecomm. Conf. (Globecom)*, vol. 5, Sydney, NSW, Australia, Nov. 1998, pp. 2771–2776.

[91] M. Russell and G. L. Stüber, "Interchannel interference analysis of OFDM in a mobile environment," in *Proc. IEEE Veh. Technol. Conf.*, vol. 2, Chicago, Illinois, USA, July 1995, pp. 820–824.

[92] Y. G. Li and L. J. C. Jr., "Bounds on the interchannel interference of OFDM in time-varying impairments," *IEEE Trans. Commun.*, vol. 49, no. 3, pp. 401–404, Mar. 2001.

[93] M. Sandell and O. Edfors, "A comparative study of pilot-based channel estimators for wireless OFDM," Lulea, Sept. 1996.

[94] T. Clancy and W. Arbaugh, "Measuring interference temperature," in *Virginia Tech Wireless Personal Communications Symposium*, June 2006.

[95] A. Ghasemi and E. Sousa, "Collaborative spectrum sensing for opportunistic access in fading environments," in *Proc. IEEE Int. Symposium on New Frontiers in Dynamic Spectrum Access Networks*, Baltimore, Maryland, USA, Nov. 2005, pp. 131–136.

[96] M. Wylie-Green, "Dynamic spectrum sensing by multiband OFDM radio for interference mitigation," in *Proc. IEEE Int. Symposium on New Frontiers in Dynamic Spectrum Access Networks*, Baltimore, Maryland, USA, Nov. 2005, pp. 619–625.

[97] T. Weiss and F. Jondral, "Spectrum pooling: an innovative strategy for the enhancement of spectrum efficiency," *IEEE Commun. Mag.*, vol. 42, no. 3, pp. 8–14, May 2004.

[98] F. Tufvesson, M. Faulkner, and T. Maseng, "Pre-compensation for Rayleigh fading channels in time division duplex OFDM systems," *Wireless Personal Communications*, vol. 16, no. 1, pp. 21–33, 2001.

[99] S. Haykin and M. Moher, *Modern Wireless Communications*. New York, NY, USA: Prentice-Hall Inc., 2004.

[100] Y. Li and N. Sollenberger, "Interference suppression in OFDM systems using adaptive antenna arrays," in *Proc. IEEE Global Telecomm. Conf. (Globecom)*, vol. 1, Sydney, NSW, Australia, Nov. 1998, pp. 213–218.

[101] G. Stuber, J. Barry, S. McLaughlin, Y. Li, M. Ingram, and T. Pratt, "Broadband MIMO-OFDM wireless communications," *Proc. IEEE*, vol. 92, no. 2, pp. 271–294, Feb. 2004.

[102] S. Hara and R. Prasad, "Overview of multicarrier CDMA," *IEEE Commun. Mag.*, vol. 35, no. 12, pp. 126–133, Dec. 1997.

[103] *IEEE Standard for Local and Metropolitan area networks Part 16: Air Interface for Fixed and Mobile Broadband Wireless Access Systems Amendment 2: Physical and Medium Access Control Layers for Combined Fixed and Mobile Operation in Licensed Bands and Corrigendum 1*, The Institute of Electrical and Electronics Engineering, Inc. Std. IEEE 802.16E-2005, 2005.

[104] Institute of Electrical and Electronics Engineers, "IEEE standard computer dictionary: A compilation of IEEE standard computer glossaries," New York, NY, USA, 1990.

[105] A. Meissner, T. Luckenbach, T. Risse, T. Kirste, and H. Kirchner, "Design challenges for an integrated disaster management communication and information system," in *Proc. 1st IEEE Workshop on Disaster Recovery Networks (DIREN '02) [co-located with IEEE INFOCOM 2002]*, New York City, June 24, 2002.

[106] National Task Force on Interoperability, "Why Can't We Talk? Working Together To Bridge the Communications Gap To Save Lives," Feb. 2003.

[107] K. J. Imel and J. W. Hart, *Understanding Wireless Communications in Public Safety: A Guidebook to Technology, Issues, Planning, and Management*, 2nd ed. National Institute of Justice, Jan. 2003.

[108] SDR Forum, "Software Defined Radio Technology for Public Safety," SDR Forum, Apr. 14, 2006, approved Document SDRF–06–A–0001–V0.00.

[109] T. Weiss, J. Hillenbrand, and F. Jondral, "A diversity approach for the detection of idle spectral resources in spectrum pooling systems," in *Proc. of the 48th Int. Scientific Colloquium*, Ilmenau, Germany, Sept. 2003, pp. 37–38.

[110] R. Rajbanshi, A. M. Wyglinski, , and G. J. Minden, "An efficient implementation of NC-OFDM transceivers for cognitive radios," in *Proc. IEEE Int. Conf. Cognitive Radio Oriented Wireless Networks and Commun. (Crowncom)*, Mykonos Island, Greece, June 2006.

[111] A. M. Wyglinski, "Effects of bit allocation on non-contiguous multicarrier-based cognitive radio transceivers," in *Proc. IEEE Veh. Technol. Conf.*, Sept. 2006.

[112] T. Weiss, A. Krohn, F. Capar, I. Martoyo, and F. Jondral, "Synchronization algorithms and preamble concepts for spectrum pooling systems," *IST Mobile & Wireless Telecommunications Summit*, June 2003.

[113] T. Weiss, J. Hillenbrand, A. Krohn, and F. Jondral, "Mutual interference in OFDM-based spectrum pooling systems," in *Proc. IEEE Veh. Technol. Conf.*, vol. 4, Milan, Italy, May 2004, pp. 1873–1877.

[114] C. Muschallik, "Improving an OFDM reception using an adaptive Nyquist windowing," *IEEE Trans. Consumer Electron.*, vol. 42, no. 3, pp. 259–269, Aug. 1996.

[115] S. H. Muller-Weinfurtner, "Optimum Nyquist windowing in OFDM receivers," *IEEE Trans. Commun.*, vol. 49, no. 3, pp. 417–420, Mar. 2001.

[116] H. Yamaguchi, "Active interference cancellation technique for MB-OFDM cognitive radio," in *Proc. IEEE European Microwave Conf.*, vol. 2, Amsterdam, The Netherlands, Oct. 2004, pp. 1105–1108.

[117] S. Brandes, I. Cosovic, and M. Schnell, "Sidelobe suppression in OFDM systems by insertion of cancellation carriers," in *Proc. IEEE Veh. Technol. Conf.*, vol. 1, Dallas, Texas, Sept. 2005, pp. 152–156.

[118] I. Cosovic, S. Brandes, and M. Schnell, "A technique for sidelobe suppression in OFDM systems," in *Proc. IEEE Global Telecomm. Conf. (Globecom)*, vol. 1, St. Louis, Missouri, USA, Nov./Dec. 2005, pp. 204–208.

[119] ——, "Subcarrier weighting: a method for sidelobe suppression in OFDM systems," *IEEE Commun. Lett.*, vol. 10, no. 6, pp. 444–446, June 2006.

[120] *Broadband Wireless Access: IEEE MAN standard*, IEEE LAN/MAN standards committee 802.16a, 2003.

[121] C. Cordeiro, K. Challapali, D. Birru, and S. Shankar, "IEEE 802.22: the first worldwide wireless standard based on cognitive radios," in *Proc. IEEE Int. Symposium on New Frontiers in Dynamic Spectrum Access Networks*, Baltimore, Maryland, USA, Nov. 2005, pp. 328–337.

[122] *IEEE standard for information technology- telecommunications and information exchange between systems- local and metropolitan area networks- specific requirements Part II: wireless LAN medium access control (MAC) and physical layer (PHY) specifications*, IEEE Std 802.11g-2003 (Amendment to IEEE Std 802.11, 1999 Edn. (Reaff 2003) as amended by IEEE Stds 802.11a-1999, 802.11b-1999, 802.11b-1999/Cor 1-2001, and 802.11d-2001) Std., 2003.

[123] *IEEE Std. 802.11h - 2003*, IEEE Std 802.11h-2003 (Amendment to IEEE Std 802.11, 1999 Edn. (Reaff 2003)) Std., 2003.

[124] R. Prasad and R. Van Nee, *OFDM for Wireless Multimedia Communications*. Boston, London: Artech House Publishers, 2000.

[125] F. Sanzi and J. Speidel, "An adaptive two-dimensional channel estimator for wireless OFDM with application to mobile DVB-T," *IEEE Trans. Broadcast.*, vol. 46, no. 2, pp. 128–133, June 2000.

[126] T. Onizawa, M. Mizoguchi, T. Sakata, and M. Morikura, "A simple adaptive channel estimation scheme for OFDM systems," in *Proc. IEEE Veh. Technol. Conf.*, vol. 1, Amsterdam, The Netherlands, 1999, pp. 279–283.

[127] K. Witrisal, Y.-H. Kim, and R. Prasad, "RMS delay spread estimation technique using non-coherent channel measurements," *IEE Electron. Lett.*, vol. 34, no. 20, pp. 1918–1919, Oct. 1998.

[128] ——, "A new method to measure parameters of frequency selective radio channel using power measurements," *IEEE Trans. Commun.*, vol. 49, pp. 1788–1800, Oct. 2001.

[129] K. Witrisal and A. Bohdanowicz, "Influence of noise on a novel RMS delay spread estimation method," in *Proc. IEEE Int. Symposium on Personal, Indoor and Mobile Radio Commun.*, vol. 1, London, UK, Sept. 2000, pp. 560–566.

[130] H. Schober and F. Jondral, "Delay spread estimation for OFDM based mobile communication systems," in *Proc. European Wireless Conf.*, Florence, Italy, Feb. 2002, pp. 625–628.

[131] C. Athaudage and A. Jayalath, "Delay-spread estimation using cyclic-prefix in wireless OFDM systems," *IEE Proc. Commun.*, vol. 151, no. 6, pp. 559–566, Dec. 2004.

[132] K. Ramasubramanian and K. Baum, "An OFDM timing recovery scheme with inherent delay-spread estimation," in *Proc. IEEE Global Telecomm. Conf. (Globecom)*, vol. 5, San Antonio, TX, Nov. 2001, pp. 3111–3115.

[133] H. Minn, V. Bhargava, and K. Letaief, "A robust timing and frequency synchronization for OFDM systems," *IEEE Trans. Wireless Commun.*, vol. 2, no. 4, pp. 822–839, July 2003.

[134] C. Athaudage, "BER sensitivity of OFDM systems to time synchronization error," in *Proc. IEEE Int. Conf. Commun. Systems*, vol. 1, Nov. 2002, pp. 42–46.

[135] C. Tepedelenlioğlu and G. B. Giannakis, "On velocity estimation and correlation properties of narrow-band mobile communication channels," *IEEE Trans. Veh. Technol.*, vol. 50, no. 4, pp. 1039–1052, July 2001.

[136] T. S. Rappaport, *Wireless Communications, Principles and Practice*, 2nd ed. Upper Saddle River, New Jersey, USA: Prentice-Hall Inc., 2002.

[137] "Guidelines for evaluation of radio transmission technologies for IMT-2000," Recommendation ITU-R M.1225, International Telecommunication Union, 1997.

[138] Y. R. Zheng and C. Xiao, "Improved models for the generation of multiple uncorrelated Rayleigh fading waveforms," *IEEE Commun. Lett.*, vol. 6, no. 5, June 2002.

[139] R. Prasad, *OFDM for Wireless Communication Systems.* Artech House Publishers, 2004.

[140] C. Tepedelenlioğlu, A. Abdi, G. Giannakis, and M. Kaveh, "Estimation of Doppler spread and signal strength in mobile communications with applications to handoff and adaptive transmission," *Wireless Communications and Mobile Computing*, vol. 1, pp. 221–242, March. 2001.

[141] J. Cai, W. Song, and Z. Li, "Doppler spread estimation for mobile OFDM systems in Rayleigh fading channels," *IEEE Trans. Consumer Electron.*, vol. 49, pp. 973–977, Nov. 2003.

[142] H. Schober and F. Jondral, "Velocity estimation for OFDM based communication systems," in *Proc. IEEE Veh. Technol. Conf.*, Kyoto, Japan, May 2002, pp. 715–718.

[143] W. Jakes, *Microwave Mobile Communications*, 1st ed. Piscataway, NJ: IEEE Press, 1993.

[144] Y. Choi, P. Voltz, and F. Cassara, "On channel estimation and detection for multicarrier signals in fast and selective Rayleigh fading channels," *IEEE Trans. Commun.*, vol. 49, pp. 1375–1387, Aug. 2001.

[145] Y. Zhao and A. Huang, "A novel channel estimation method for OFDM mobile communication systems based on pilot signals and transform-domain processing," in *Proc. IEEE Veh. Technol. Conf.*, Phoenix, Arizona, USA, May 1997, pp. 2089–2093.

[146] L. Krasny, H. Arslan, D. Koilpillai, and S. Chennakeshu, "Doppler spread estimation in mobile radio systems," *IEEE Commun. Lett.*, vol. 5, no. 5, pp. 197–199, May 2001.

[147] H. Schober, F. Jondral, R. Stirling-Gallacher, and Z. Wang, "Adaptive channel estimation for OFDM based high speed mobile communication systems," in *Proc. 3rd Generation Wireless and Beyond Conf.*, San Francisco, CA, USA, May/June 2001, pp. 392–397.

[148] J. G. Proakis, *Digital Communications*, 4th ed. McGraw-Hill, 2001.

[149] K. Fazel and S. Kaiser, *Multi-Carrier and Spread Spectrum Systems.* John Wiley & Sons Ltd., 2003.

[150] J. Balakrishnan, A. Batra, and A. Dabak, "A multi-band OFDM system for UWB communication," in *Proc. IEEE Conference on Ultra Wideband Systems and Technologies*, Nov. 2003, pp. 354–358.

[151] *IEEE Standard for Local and Metropolitan area networks Part 16: Air Interface for Fixed Broadband Wireless Access Systems*, The Institute of Electrical and Electronics Engineering, Inc. Std. IEEE 802.16-2001, 2001.

[152] P. Chow, J. Cioffi, and J. Bingham, "A practical discrete multitone transceiver loading algorithm for data transmission over spectrally shaped channels," *IEEE Trans. Commun.*, vol. 43, no. 234, pp. 773–775, Feb./Mar./Apr. 1995.

[153] J. Kim, J.-T. Chen, and J. Cioffi, "Low complexity bit mapping algorithm for multi-carrier communication systems with fading channels," in *Proc. IEEE International Conf. on Universal Personal Commun.*, vol. 2, Florence, Italy, Oct. 1998, pp. 927–931.

[154] B. Krongold, K. Ramchandran, and D. Jones, "Computationally efficient optimal power allocation algorithms for multicarrier communication systems," *IEEE Trans. Commun.*, vol. 48, no. 1, pp. 23–27, Jan. 2000.

[155] L. van der Perre, S. Thoen, P. Vandenameele, B. Gyselinckx, and M. Engels, "Adaptive loading strategy for a high speed OFDM-based WLAN," in *Proc. IEEE Global Telecomm. Conf. (Globecom)*, vol. 4, Sydney, NSW, Australia, Nov. 1998, pp. 1936–1940.

[156] S. Thoen, L. Van der Perre, M. Engels, and H. De Man, "Adaptive loading for OFDM/SDMA-based wireless networks," *IEEE Trans. Commun.*, vol. 50, no. 11, pp. 1798–1810, Nov. 2002.

[157] A. Wyglinski, F. Labeau, and P. Kabal, "Effects of imperfect subcarrier SNR information on adaptive bit loading algorithms for multicarrier systems," in *Proc. IEEE Global Telecomm. Conf. (Globecom)*, vol. 6, Nov./Dec. 2004, pp. 3835–3839.

[158] D. Pauluzzi and N. Beaulieu, "A comparison of SNR estimation techniques for the AWGN channel," *IEEE Trans. Commun.*, vol. 48, no. 10, pp. 1681–1691, Oct. 2000.

[159] M. Türkboylari and G.-L. Stüber, "An efficient algorithm for estimating the signal-to-interference ratio in TDMA cellular systems," *IEEE Trans. Commun.*, vol. 46, no. 6, pp. 728–731, June 1998.

[160] S. He and M. Torkelson, "Effective SNR estimation in OFDM system simulation," in *Proc. IEEE Global Telecomm. Conf. (Globecom)*, vol. 2, Sydney, NSW, Australia, Nov. 1998, pp. 945–950.

[161] A. N. Mody and G. L. Stüber, "Parameter estimation for OFDM with transmit receive diversity," in *Proc. IEEE Veh. Technol. Conf.*, vol. 2, Rhodes, May 2001, pp. 820–824.

[162] X. Xu, Y. Jing, and X. Yu, "Subspace-based noise variance and SNR estimation for OFDM systems," in *Proc. IEEE Wireless Commun. and Networking Conf.*, vol. 1, New Orleans, Louisiana, USA, Mar. 2005, pp. 23–26.

[163] D. Athanasios and K. Grigorios, "SNR estimation algorithms in AWGN for HiperLAN/2 transceiver," in *Proc. Int. Conf. on Mobile and Wireless Comm. Networks*, Marrakech, Morocco, Sept. 2005.

[164] C. Aldana, A. Salvekar, J. Tallado, and J. Cioffi, "Accurate noise estimates in multicarrier systems," in *Proc. IEEE Veh. Technol. Conf.*, vol. 1, Boston, Massachusetts, USA, Sept. 2000, pp. 434–438.

[165] S. Boumard, "Novel noise variance and SNR estimation algorithm for wireless MIMO OFDM systems," in *Proc. IEEE Global Telecomm. Conf. (Globecom)*, vol. 3, Dec. 2003, pp. 1330–1334.

[166] M. Ghosh and V. Gadam, "Bluetooth interference cancellation for 802.11g WLAN receivers," in *Proc. IEEE Int. Conf. Commun.*, vol. 2, Seattle, Washington, USA, May 2003, pp. 1169–1173.

[167] Federal Communications Commission, "In the matter of unlicensed operation in the TV broadcast bands," Notice of proposed rule making ET Docket No. 04-186 (FCC 04-113), May 2004.

[168] M. Marcus, "Unlicensed cognitive sharing of TV spectrum: the controversy at the federal communications commission," *IEEE Commun. Mag.*, vol. 43, no. 5, pp. 24–25, 2005.

[169] R. Tandra and A. Sahai, "Fundamental limits on detection in low SNR under noise uncertainty," in *Proc. IEEE Int. Conf. Wireless Networks, Commun. and Mobile Computing*, vol. 1, Maui, HI, June 2005, pp. 464–469.

[170] D. Cabric, S. Mishra, and R. Brodersen, "Implementation issues in spectrum sensing for cognitive radios," in *Proc. Asilomar Conf. on Signals, Systems and Computers*, vol. 1, Pacific Grove, California, USA, Nov. 2004, pp. 772–776.

[171] H. Tang, "Some physical layer issues of wide-band cognitive radio systems," in *Proc. IEEE Int. Symposium on New Frontiers in Dynamic Spectrum Access Networks*, Baltimore, Maryland, USA, Nov. 2005, pp. 151–159.

[172] A. Sahai, R. Tandra, S. M. Mishra, and N. Hoven, "Fundamental design tradeoffs in cognitive radio systems," in *Proc. of Int. Workshop on Technology and Policy for Accessing Spectrum*, Aug. 2006.

[173] *Supplement to IEEE standard for information technology telecommunications and information exchange between systems - local and metropolitan area networks - specific requirements. Part 11: wireless LAN Medium Access Control (MAC) and Physical Layer (PHY) specifications: high-speed physical layer externsion in the 2.4 GHz band*, The Institute of Electrical and Electronics Engineering, Inc. Std. IEEE 802.11b, Sept. 1999.

[174] S. Geirhofer, L. Tong, and B. Sadler, "A measurement-based model for dynamic spectrum access in WLAN channels," in *Proc. IEEE Military Commun. Conf.*, Washington, D.C., USA, Oct. 2006.

[175] S. Geirhofer, B. Sadler, and L. Tong, "Dynamic spectrum access in WLAN channels: Empirical model and its stochastic analysis," in *Proc. of Int. Workshop on Technology and Policy for Accessing Spectrum*, Boston, Massachusetts, USA, Aug. 2006.

[176] D. Cabric, A. Tkachenko, and R. Brodersen, "Spectrum sensing measurements of pilot, energy, and collaborative detection," in *Proc. IEEE Military Commun. Conf.*, Washington, D.C., USA, Oct. 2006, pp. 1–7.

[177] M. Oner and F. Jondral, "Cyclostationarity based air interface recognition for software radio systems," in *Proc. IEEE Radio and Wireless Conf.*, Atlanta, Georgia, USA, Sept. 2004, pp. 263–266.

[178] ——, "Cyclostationarity-based methods for the extraction of the channel allocation information in a spectrum pooling system," in *Proc. IEEE Radio and Wireless Conf.*, Atlanta, Georgia, USA, Sept. 2004, pp. 279–282.

[179] D. Cabric and R. W. Brodersen, "Physical layer design issues unique to cognitive radio systems," in *Proc. IEEE Int. Symposium on Personal, Indoor and Mobile Radio Commun.*, vol. 2, Berlin, Germany, Sept. 2005, pp. 759–763.

[180] A. Fehske, J. Gaeddert, and J. Reed, "A new approach to signal classification using spectral correlation and neural networks," in *Proc. IEEE Int. Symposium on New Frontiers in Dynamic Spectrum Access Networks*, Baltimore, Maryland, USA, Nov. 2005, pp. 144–150.

[181] S. S. N, C. Cordeiro, and K. Challapali, "Spectrum agile radios: utilization and sensing architectures," in *Proc. IEEE Int. Symposium on New Frontiers in Dynamic Spectrum Access Networks*, Baltimore, Maryland, USA, Nov. 2005, pp. 160–169.

[182] M. Ghozzi, F. Marx, M. Dohler, and J. Palicot, "Cyclostationarity-based test for detection of vacant frequency bands," in *Proc. IEEE Int. Conf. Cognitive Radio Oriented Wireless Networks and Commun. (Crowncom)*, Mykonos Island, Greece, June 2006.

[183] U. Gardner, WA, "Exploitation of spectral redundancy in cyclostationary signals," *IEEE Signal Processing Mag.*, vol. 8, no. 2, pp. 14–36, 1991.

[184] F. Digham, M. Alouini, and M. Simon, "On the energy detection of unknown signals over fading channels," in *Proc. IEEE Int. Conf. Commun.*, vol. 5, Seattle, Washington, USA, May 2003, pp. 3575–3579.

[185] S. Jones and N. Wang, "An experiment for sensing-based opportunistic spectrum access in CSMA/CA networks," in *Proc. IEEE Int. Symposium on New Frontiers in Dynamic Spectrum Access Networks*, Baltimore, Maryland, USA, Nov. 2005, pp. 593–596.

[186] P. Papadimitratos, S. Sankaranarayanan, and A. Mishra, "A bandwidth sharing approach to improve licensed spectrum utilization," *IEEE Commun. Mag.*, vol. 43, no. 12, pp. 10–14, Dec. 2005.

[187] A. Leu, K. Steadman, M. McHenry, and J. Bates, "Ultra sensitive TV detector measurements," in *Proc. IEEE Int. Symposium on New Frontiers in Dynamic Spectrum Access Networks*, Baltimore, Maryland, USA, Nov. 2005, pp. 30–36.

[188] G. Ganesan and Y. Li, "Agility improvement through cooperative diversity in cognitive radio," in *Proc. IEEE Global Telecomm. Conf. (Globecom)*, vol. 5, St. Louis, Missouri, USA, Nov./Dec. 2005, pp. 2505–2509.

[189] ——, "Cooperative spectrum sensing in cognitive radio networks," in *Proc. IEEE Int. Symposium on New Frontiers in Dynamic Spectrum Access Networks*, Baltimore, Maryland, USA, Nov. 2005, pp. 137–143.

[190] A. Leu, M. McHenry, and B. Mark, "Modeling and analysis of interference in listen-before-talk spectrum access schemes," *Int. Journal of Network Management*, vol. 16, pp. 131–147, 2006.

[191] H. Urkowitz, "Energy detection of unknown deterministic signals," *Proc. IEEE*, vol. 55, pp. 523–531, Apr. 1967.

[192] M. Abramowitz and I. Stegun, Eds., *Handbook of Mathematical Functions With Formulas, Graphs, and Mathematical Tables*, 9th ed. National Bureau of Standards, 1970.

[193] A. Sahai, N. Hoven, and R. Tandra, "Some fundamental limits on cognitive radio," in *Proc. Allerton Conf. on Commun., Control, and Computing*, Monticello, Illinois, Oct. 2004.

[194] M. Olivieri, G. Barnett, A. Lackpour, and A. Davis, "A scalable dynamic spectrum allocation system with interference mitigation for teams of spectrally agile software defined radios," in *Proc. IEEE Int. Symposium on New Frontiers in Dynamic Spectrum Access Networks*, Baltimore, Maryland, USA, Nov. 2005, pp. 170–179.

[195] S. Lal and A. Mishra, "A look ahead scheme for adaptive spectrum utilization," in *Proc. IEEE Radio and Wireless Conf.*, Boston, Massachusetts, USA, Aug. 2003, pp. 83–86.

[196] J. Lehtomaki, J. Vartiainen, M. Juntti, and H. Saarnisaari, "Spectrum sensingwith forward methods," in *Proc. IEEE Military Commun. Conf.*, Washington, D.C., USA, Oct. 2006, pp. 1–7.

[197] T. Farnham, G. Clemo, R. Haines, E. Seidel, A. Benamar, S. Billington, N. Greco, N. Drew, T. Le, B. Arram, and P. Mangold, "IST-TRUST: A perspective on the reconfiguration of future mobile terminals using software download," in *Proc. IEEE Int. Symposium on Personal, Indoor and Mobile Radio Commun.*, London, UK, Sept. 2000, pp. 1054–1059.

[198] M. Mehta, N. Drew, G. Vardoulias, N. Greco, and C. Niedermeier, "Reconfigurable terminals: an overview of architectural solutions," *IEEE Commun. Mag.*, vol. 39, no. 8, pp. 82– 89, 2001.

[199] G. Vardoulias, J. Faroughi-Esfahani, G. Clemo, and R. Haines, "Blind radio access technology discovery and monitoring for softwaredefined radio communication systems: problems and techniques," in *Proc. Int. Conf. 3G Mobile Communication Technologies*, London, UK, Mar. 2001, pp. 306–310.

[200] J. Palicot and C. Roland, "A new concept for wireless reconfigurable receivers," *IEEE Commun. Mag.*, vol. 41, no. 7, pp. 124–132, 2003.

[201] M. Gandetto, M. Guainazzo, and C. S. Regazzoni, "Use of time-frequency analysis and neural networks for mode identification in a wireless software-defined radio approach," *EURASIP Journal on Applied Signal Processing*, vol. 2004, pp. 1778–1790, 2004.

[202] K. Challapali, S. Mangold, and Z. Zhong, "Spectrum agile radio: Detecting spectrum opportunities," in *Proc. Int. Symposium on Advanced Radio Technologies*, Boulder, Colorado, USA, Mar. 2004.

[203] Z. Tian and G. B. Giannakis, "A wavelet approach to wideband spectrum sensing for cognitive radios," in *Proc. IEEE Int. Conf. Cognitive Radio Oriented Wireless Networks and Commun. (Crowncom)*, Mykonos Island, Greece, June 2006.

[204] T. Weiss, J. Hillenbrand, A. Krohn, and F. Jondral, "Efficient signaling of spectral resources in spectrum pooling systems," in *Proc. IEEE Symposium on Commun. and Veh. Technol.*, Eindhoven, Netherlands, Nov. 2003.

[205] D. Čabrić, S. Mishra, D. Willkomm, R. Brodersen, and A. Wolisz, "A cognitive radio approach for usage of virtual unlicensed spectrum," in *Proc. IST Mobile and Wireless Communications Summit*, Dresden, Germany, June 2005.

[206] E. Visotsky, S. Kuffner, and R. Peterson, "On collaborative detection of TV transmissions in support of dynamic spectrum sharing," in *Proc. IEEE Int. Symposium on New Frontiers in Dynamic Spectrum Access Networks*, Baltimore, Maryland, USA, Nov. 2005, pp. 338–345.

[207] I. F. Akyildiz, W. Y. Lee, M. C. Vuran, and S. Mohanty, "NeXt generation / dynamic spectrum access / cognitive radio wireless networks: A survey," *Computer Networks Journal (Elsevier)*, Sept. 2006.

[208] J. Hillenbrand, T. Weiss, and F. Jondral, "Calculation of detection and false alarm probabilities in spectrum pooling systems," *IEEE Commun. Lett.*, vol. 9, no. 4, pp. 349–351, Apr. 2005.

[209] N. Ahmed, D. Hadaller, and S. Keshav, "GUESS: gossiping updates for efficient spectrum sensing," in *Proc. International workshop on Decentralized resource sharing in mobile computing and networking*, Los Angeles, California, USA, 2006, pp. 12–17.

[210] B. Wild and K. Ramchandran, "Detecting primary receivers for cognitive radio applications," in *Proc. IEEE Int. Symposium on New Frontiers in Dynamic Spectrum Access Networks*, Baltimore, Maryland, USA, Nov. 2005, pp. 124–130.

[211] D. Hunold, A. Barreto, G. Fettweis, and M. Mecking, "Concept for universal access and connectivity in mobile radionetworks," in *Proc. IEEE Int. Symposium on Personal, Indoor and Mobile Radio Commun.*, vol. 2, London, UK, Sept. 2000, pp. 847–851.

[212] T. Clancy and B. Walker, "Predictive dynamic spectrum access," in *Proc. SDR Forum Technical Conference*, Orlando, Florida, USA, Nov. 2006.

[213] C. Cordeiro, K. Challapali, and D. Birru, "IEEE 802.22: An introduction to the first wireless standard based on cognitive radios," *Journal of communications*, vol. 1, no. 1, Apr. 2006.

[214] P. Kolodzy et al., "Next generation communications: Kickoff meeting," in *Proc. DARPA*, Oct. 2001.

[215] R. Matheson, "The electrospace model as a frequency management tool," in *Int. Symposium On Advanced Radio Technologies*, Boulder, Colorado, USA, Mar. 2003, pp. 126–132.

[216] W. D. Horne, "Adaptive spectrum access: Using the full spectrum space," in *Proc. Annual Telecommunications Policy Research Conf.*, Arlington, Virginia, Oct. 2003.

[217] J. Andrews, "Interference cancellation for cellular systems: a contemporary overview," *IEEE Wireless Commun. Mag.*, vol. 12, no. 2, pp. 19–29, 2005.

[218] *Draft Supplement to STANDARD FOR Telecommunications and Information Exchange Between Systems - LAN/MAN Specific Requirements - Part 11: Wireless Medium Access Control (MAC) and physical layer (PHY) specifications: Specification for Radio Resource Measurement*, The Institute of Electrical and Electronics Engineering, Inc. Std. IEEE 802.11k/D0.7, Oct. 2003.

[219] *Specification of the Bluetooth system, Master Table of Contents & Compliance Requirements*, Bluetooth, SIG Std. Bluetooth Standard, Nov. 2004.

[220] N. Golmie, N. Chevrollier, and O. Rebala, "Bluetooth and WLAN coexistence: challenges and solutions," *IEEE Wireless Commun. Mag.*, vol. 10, no. 6, pp. 22–29, Dec. 2003.

[221] H. Li, Y. Bar-Ness, A. Abdi, O. Somekh, and W. Su, "OFDM modulation classification and parameters extraction," in *Proc. IEEE Int. Conf. Cognitive Radio Oriented Wireless Networks and Commun. (Crowncom)*, Mykonos Island, Greece, June 2006, pp. 1–6.

[222] M. Rahman and K. Shamsaifar, "Electronically tunable LTCC based multi-layer filter for mobile handset application," in *Proc. IEEE MTT-S Inter. Microwave Symposium Digest*, vol. 3, Philadelphia, Pennsylvania, USA, June 2003, pp. 1767–1770.

[223] H. G. Keane, "A new approach to frequency line tracking," in *Proc. Asilomar Conf. on Signals, Systems and Computers*, vol. 2, Pacific Grove, California, USA, Nov. 1991, pp. 808–812.

[224] A. Webb, *Statistical Pattern Recognition*. England: John Wiley & Sons Ltd., 1999.

[225] W. Akmouche, "Detection of multicarrier modulations using 4th-order cumulants," in *Proc. IEEE Military Commun. Conf.*, vol. 1, Atlantic City, New Jersey, USA, Oct./Nov. 1999, pp. 432–436.

[226] D. Grimaldi, S. Rapuano, and G. Truglia, "An automatic digital modulation classifier for measurement on telecommunication networks," in *Proc. IEEE Instrumentation and Measurement Technology Conference*, Anchorage, AK, May 2002, pp. 957–962.

[227] W. Akmouche, E. Kerherve, and A. Quinquis, "OFDM parameters estimation a time approach," in *Proc. Asilomar Conf. on Signals, Systems and Computers*, vol. 1, Pacific Grove, California, USA, Oct./Nov. 2000, pp. 142–146.

[228] H. Ishii and G. W. Wornell, "OFDM blind parameter identification in cognitive radios," in *Proc. IEEE Int. Symposium on Personal, Indoor and Mobile Radio Commun.*, vol. 1, Berlin, Germany, Sept. 2005, pp. 700–705.

[229] L. Zou, "Detection of the guard interval length in OFDM systems," in *Proc. IEEE Consumer Commun. and Networking Conf.*, vol. 2, Las Vegas, Nevada, USA, Jan. 2006, pp. 1048–1051.

[230] M. Shi, Y. Bar-Ness, and W. Su, "Blind OFDM systems parameters estimation for software defined radio," in *Proc. IEEE Int. Symposium on New Frontiers in Dynamic Spectrum Access Networks*, Dublin, Ireland, Apr. 2007, pp. 119–122.

[231] W. Akmouche, E. Kerherve, and A. Quinquis, "OFDM spectral characterization: estimation of the bandwidth and the number of sub-carriers," in *Proc. IEEE Workshop on Statistical Signal and Array Processing*, Pocono Manor, PA, USA, Aug. 2000, pp. 48–52.

[232] Y. Kiong and M. Motani, "On implementation of link adaptation in OFDM wireless networks," in *Proc. IEEE Int. Conf. Commun.*, Paris, France, June 2004, pp. 195–199.

[233] E. Kerherve, W. Akmouche, and A. Quinquis, "OFDM bandwidth estimation using Morlet's wavelet decomposition," in *Proc. IEEE/AFCEA Inf. Systems for Enhanced Public Safety and Security*, Munich, Germany, May 2000, pp. 62–66.

[234] P. Liu, B. Li, Z. Lu, and F. Gong, "An OFDM bandwidth estimation scheme for spectrum monitoring," in *Proc. Int. Conf. Wireless Commun., Networking and Mobile Computing*, vol. 1, Maui, Hawaii, USA, Sept. 2005, pp. 248–251.

[235] R. Heath Jr and G. Giannakis, "Exploiting input cyclostationarity for blind channel identification in OFDM systems," *IEEE Trans. Signal Processing*, vol. 47, no. 3, pp. 848–856, Mar. 1999.

[236] H. Nogami, S. Tsuruga, and N. Morinaga, "A transmission mode detector for OFDM systems," *Electronics and Communications in Japan (Part I Communications)*, vol. 86, no. 8, pp. 79–94, Mar. 2003.

[237] M. Wax and T. Kailath, "Detection of signals by information theoretic criteria," *IEEE Trans. Acoust., Speech, Signal Processing*, vol. 33, no. 2, pp. 387–392, Apr. 1985.

[238] R. Roy, A. Paulraj, and T. Kailath, "ESPRIT–a subspace rotation approach to estimation of parameters of cisoids in noise," *IEEE Trans. Acoust., Speech, Signal Processing*, vol. 34, no. 5, pp. 1340–1342, Oct. 1986.

[239] B. Muquet, M. de Courville, P. Duhamel, and B. Stepmind, "Subspace-based blind and semi-blind channel estimation for OFDM systems," *IEEE Trans. Signal Processing*, vol. 50, no. 7, pp. 1699–1712, July 2002.

[240] J. van de Beek, M. Sandell, and P. Börjesson, "ML estimation of time and frequency offset in OFDM systems," *IEEE Trans. Signal Processing*, vol. 45, no. 7, pp. 1800–1805, July 1997.

[241] M. Speth, F. Classen, and H. Meyr, "Frame synchronization of OFDM systems in frequency selective fading channels," in *Proc. IEEE Veh. Technol. Conf.*, vol. 3, Phoenix, Arizona, USA, May 1997, pp. 1807–1811.

[242] T. Keller, L. Piazzo, P. Mandarini, and L. Hanzo, "Orthogonal frequency division multiplex synchronization techniques for frequency-selective fading channels," *IEEE J. Select. Areas Commun.*, vol. 19, no. 6, pp. 999–1008, June 2001.

[243] R. Meyer and M. Newhouse, "OFDM waveform feature suppression," in *Proc. IEEE Military Commun. Conf.*, vol. 1, Anaheim, California, USA, Oct. 2002, pp. 582–586.

[244] S. C. Surender and R. M. Narayanan, "Synchronization for wireless multi-radar covert communication networks," in *Proceedings of SPIE Defense Transformation and Net-Centric Systems*, Orlando, Florida, USA, Apr. 2007.

[245] X. Wang, P. Ho, and Y. Wu, "Robust channel estimation and ISI cancellation for OFDM systems with suppressed features," *IEEE J. Select. Areas Commun.*, vol. 23, no. 5, pp. 963–972, May 2005.

[246] I. Reed, "On a moment theorem for complex Gaussian processes," *IEEE Trans. Inform. Theory*, vol. 8, no. 3, pp. 194–195, Apr. 1962.

[247] S. Kay, *Fundamentals of statistical signal processing: estimation theory.* Upper Saddle River, New Jersey, USA: Prentice-Hall Inc., 1993.

APPENDICES

Appendix A Derivation of Channel Magnitude Correlation

The frequency domain channel frequency response (CFR) can be obtained as

$$H(k) = \frac{1}{\sqrt{N}} \sum_{l} h_l e^{-j2\pi lk/N}. \tag{A.1}$$

Using (A.1) and definition of correlation, the correlation of CFR magnitude can be formulated as

$$R_{|H|^2}(\Delta) = E_{m,k}\left[|H_m(k)|^2 |H_m(k+\Delta)|^2\right] \tag{A.2}$$

$$= \frac{1}{N^2} \sum_{l} \sum_{l'} \sum_{u} \sum_{u'} E\left[h_l h_{l'}^* h_u h_{u'}^* e^{-j2\pi[k(l-l')+(k+\Delta)(u-u')]}\right]. \tag{A.3}$$

The summands in (A.3) equate to zero except for the following cases

1. $l = l' = u = u'$, in this case
   - $E\left[h_l h^* l' h_u h^* u'\right] = E\left[|h_l|^4\right]$ [1] $= 2P_l^2$
   - $E\left[e^{-j2\pi[k(l-l')+(k+\Delta)(u-u')]}\right] = 1$
2. $l = l'$, $u = u'$, $l \neq u$, in this case
   - $E\left[h_l h_{l'}^* h_u h_{u'}^*\right] = P_l P_u$
   - $E\left[e^{-j2\pi[k(l-l')+(k+\Delta)(u-u')]}\right] = 1$
3. $l = u'$, $u = l'$, $l \neq u$, in this case
   - $E\left[h_l h_{l'}^* h_u h_{u'}^*\right] = P_l P_u$
   - $E\left[e^{-j2\pi[k(l-l')+(k+\Delta)(u-u')]}\right] = e^{-j2\pi\Delta(l-u)}$

Using these results, (A.3) can be written as

$$R_{|H|^2}(\Delta) = \frac{1}{N^2}\left[\sum_{l} 2P_l^2 + \sum_{l} \sum_{u;u\neq l} P_l P_m + \sum_{l} \sum_{u;u\neq l} P_l P_u \cos 2\pi\Delta(l-u)/N\right] \tag{A.4}$$

$$= \frac{1}{N^2} \sum_{l} \sum_{u} P_l P_m \left(1 + \cos(2\pi\Delta(l-u)/N)\right) \tag{A.5}$$

$$= \frac{2}{N^2} \sum_{l} \sum_{u} P_l P_m \cos^2(\pi\Delta(l-u)/N). \tag{A.6}$$

[1] The fourth order moment of a complex Gaussian variable [246].

Appendix B Derivation of Cramér-Rao Bound

The root-mean-squared (RMS) delay spread is a function of power delay profile (PDP) as given in (3.22). Let $\boldsymbol{P} = [P_1 P_2 \cdots P_L]$, then τ_{rms} can be written as a function of $\boldsymbol{P}$ as $\tau_{rms} = g(\boldsymbol{P})$. In this case, the Cramér-Rao lower bound (CRLB) for τ_{rms} can be obtained as [247]

$$CRLB(\tau_{rms}) = \frac{\partial g(\boldsymbol{P})}{\partial \boldsymbol{P}} \boldsymbol{I}^{-1}(\boldsymbol{P}) \frac{\partial g(\boldsymbol{P})}{\partial \boldsymbol{P}}^T, \tag{B.1}$$

where $(\cdot)^T$ denotes the transpose and $\partial g(\boldsymbol{P})/\partial \boldsymbol{P}$ is defined as

$$\frac{\partial g(\boldsymbol{P})}{\partial \boldsymbol{P}} = \left[\frac{\partial g(\boldsymbol{P})}{\partial P_1} \frac{\partial g(\boldsymbol{P})}{\partial P_2} \cdots \frac{\partial g(\boldsymbol{P})}{\partial P_L} \right]. \tag{B.2}$$

Using the definition of RMS delay spread (3.22), the partials with respect to each tap can be obtained as

$$\frac{\partial g(\boldsymbol{P})}{\partial P_i} = \frac{1}{2\tau_{rms}} \left[\frac{\tau_i^2}{\sum_l P_l} + \frac{\sum_l P_l \tau_l^2}{(\sum_l P_l)^2} + \frac{\sum_l P_l \tau_l}{(\sum_l P_l)^3} \left(\tau_i \sum_l P_l - \sum_l P_l \tau_l \right) \right]. \tag{B.3}$$

The $L \times L$ matrix $\boldsymbol{I}(\boldsymbol{P})$ is the Fisher information matrix and it is defined by

$$[\boldsymbol{I}(\boldsymbol{P})]_{ij} = -E \left[\frac{\partial^2 \ln p(\boldsymbol{h}; \boldsymbol{P})}{\partial P_i \partial P_j} \right], \tag{B.4}$$

where $p(\boldsymbol{h}; \boldsymbol{P})$ is the likelihood function of channel impulse response (CIR) vector $\boldsymbol{h} = [h_1 h_2 \cdots h_L]$ conditioned on $\boldsymbol{P}$. We model channel taps h_i as independent complex Gaussian random variables. Hence, $p(\boldsymbol{h}; \boldsymbol{P})$ can be easily formulated. When each channel tap is assumed to be independent of each other, the Fisher matrix becomes a diagonal matrix whose diagonal entries can be calculated as

$$[\boldsymbol{I}(\boldsymbol{P})]_{ii} = \frac{N_f}{P_i^2}, \tag{B.5}$$

where N_f is the number of available CIRs, i.e. number of frames over which the estimation is performed. Consequently, the inverse of $\boldsymbol{I}(\boldsymbol{P})$ can easily be obtained as

$$\left[\boldsymbol{I}^{-1}(\boldsymbol{P})\right]_{ii} = \frac{P_i^2}{N_f}. \tag{B.6}$$

Appendix B (Continued)

Please note that the diagonal entries of $\boldsymbol{I}^{-1}(\boldsymbol{P})$ gives the lower bound on the estimation error of each tap's power, *i.e.* $E\left[(\hat{P}_i - P_i)^2\right] \leq P_i^2/N_f$, where $\hat{P}_i$ is the estimate of ith tap. Finally, By inserting (B.2) and (B.6) into (B.1), the CRLB for the RMS delay spread can be obtained as

$$CRLB(\tau_{rms}) = \frac{1}{N_f} \sum_{i=0}^{L-1} \frac{P_i^2}{4\tau_{rms}^2} \left[\frac{\tau_i^2}{\sum_l P_l} + \frac{\sum_l P_l \tau_l^2}{(\sum_l P_l)^2} + \frac{\sum_l P_l \tau_l}{(\sum_l P_l)^3} \left(\tau_i \sum_l P_l - \sum_l P_l \tau_l \right) \right]^2 . \quad \text{(B.7)}$$

Appendix C Log-Likelihood Function for OFDM Parameter Estimation

The probability density function (PDF) of one-dimensional complex Gaussian sample can be written as

$$p(y[n]) = \frac{1}{\pi(\sigma_s^2 + \sigma_w^2)} \exp\left(\frac{-|y[n]|^2}{\sigma_s^2 + \sigma_w^2}\right). \tag{C.1}$$

It follows from (C.1) that the second product term in (8.11) can be dropped as $p(y[n])$ is not a function of unknown parameters set. Then, the log-likelihood function can be written as

$$\Lambda(\boldsymbol{y}; N_D, N_G, \theta) = \sum_{n \in \boldsymbol{\Omega}} \log\left(\frac{p(y[n], y[n+N_D])}{p(y[n])p(y[n+N_D])}\right). \tag{C.2}$$

The numerator of (C.2) has a bivariate complex Gaussian distribution, whose PDF can be found using (8.9) as [240].

$$p\left(r[n], r[n+N_D]\right) = \frac{1}{\pi^2(\sigma_y^2 + \sigma_w^2)^2(1-a^2)} \exp\left(-\frac{|r[n]|^2 - 2a\Re\{e^{j2\pi} r[n] r^*[n+N_D]\} + |r[n+N_D]|^2}{(\sigma_y^2 + \sigma_w^2)(1-a^2)}\right) \tag{C.3}$$

where the variable a is given as

$$a = \frac{\sigma_s^2}{\sigma_s^2 + \sigma_w^2}. \tag{C.4}$$

By inserting (C.1) and (C.3) into (C.2), and after some simplifications, the log-likelihood function can be found as

$$\begin{aligned}\Lambda(\boldsymbol{y}; N_D, N_G, \theta) = &\left|\sum_{n \in \boldsymbol{\Omega}} y(n) y^*(n+N_D)\right| \\ &- \sum_{n \in \boldsymbol{\Omega}} \left(\frac{a}{2}\left(|y[n]|^2 + |y[n+N_D|^2\right) + \frac{1}{2a}(\sigma_s^2 + \sigma_w^2)(1-a^2)\log(1-a^2)\right).\end{aligned} \tag{C.5}$$

Please note that the CP set $\boldsymbol{\Omega}$ is not known and depends on the symbol and cyclic prefix (CP) durations. This set is defined as following

$$\begin{aligned}\boldsymbol{\Omega} := \Big\{ n \;\Big|\; & m(N_D + N_G) + p + \theta, m = \{0,\ 1,\ \cdots, \left\lfloor \frac{D}{N_D + N_G} \right\rfloor - 1\}, \\ & p = \{1,\ 2,\ \cdots,\ N_G\},\ \theta = \{0,\ 1,\ \cdots,\ N_D - 1\}\Big\}.\end{aligned} \tag{C.6}$$

ABOUT THE AUTHOR

Tevfik Yücek received his B.S. degree in Electrical and Electronics Engineering from Middle East Technical University, Ankara, Turkey, in 2001, and his M.S. degree in Electrical Engineering from University of South Florida in 2003. Currently, he is working toward his Ph.D. degree in Electrical Engineering at University of South Florida. During his graduate studies, he has worked as teaching assistant for numerous graduate and undergraduate level courses and taught a senior-level undergraduate course on wireless communications. His research interests are in signal processing techniques for wireless multi-carrier systems and cognitive radio. Mr. Yücek is student member of Institute of Electrical and Electronics Engineers (IEEE).